Mechanistic Investigation of an Anticancer Agent that Damages DNA and Interacts with the Androgen Receptor

by

Kyle David Proffitt

B.S. Chemistry
University of South Carolina, 2002

Submitted to the Department of Chemistry in
Partial Fulfillment of the Requirements
for the Degree of

Doctor of Philosophy in Biological Chemistry
at the

Massachusetts Institute of Technology

June 2009

Signature of Author: _____
Department of Chemistry
May 7, 2009

Certified By: _____
John Martin Essigmann
William R. and Betsy P. Leitch Professor of Chemistry and Biological Engineering
Thesis Supervisor

Accepted By: _____
Robert Warren Field
Robert T. Haslam and Bradley Dewey Professor of Chemistry
Chairman, Departmental Committee on Graduate Students

Committee

This doctoral thesis has been examined by a committee of the Department of Chemistry as follows:

Steven R. Tannenbaum
Underwood-Prescott Professor of Toxicology and Chemistry

John Martin Essigmann
William R. and Betsy P. Leitch Professor of Chemistry and Biological Engineering

Alexander M. Klibanov
Novartis Professor of Chemistry and Bioengineering

Mechanistic Investigation of an Anticancer Agent that Damages DNA and Interacts with the Androgen Receptor

by

Kyle David Proffitt

Submitted to the Department of Chemistry on May 7, 2009
in Partial Fulfillment of the Requirements for the Degree of Doctor of Philosophy in Biological Chemistry

Abstract

The 11β molecule comprises a ligand for the androgen receptor (AR), which is crucial to progression and survival of many prostate cancers, tethered to a DNA-damaging aniline mustard. The compound was designed to exhibit selective toxicity toward prostate cancer cells by forming sites of 11β-DNA damage to which AR binds, physically blocking access of repair enzymes while becoming unavailable to activate transcription of pro-survival genes. Previous studies have demonstrated the ability of 11β to damage DNA, retain affinity for AR when covalently adducted to DNA, and prevent selectively the growth of prostate xenograft tumors implanted in mice.

Here we demonstrate that 11β promotes phosphorylation and nuclear localization of AR, resulting in receptor association with androgen response elements. However, 11β only weakly drives AR transcriptional activity, and instead moderately antagonizes AR-mediated transcription elicited by natural androgens. Furthermore, 11β dramatically decreases steady-state levels of AR protein. Collectively, these activities limit the expression of androgen-regulated genes and could control toxicity in AR-expressing prostate cancers.

Despite possessing an ability to modulate AR transcriptional activity, 11β is not selectively toxic toward the AR-positive member of an otherwise isogenic pair of prostate cancer cell lines derived from PC3 cells, which do not depend on AR-mediated gene expression for growth or survival. Therefore, the extraneous presence of AR does not increase 11β toxicity. LNCaP cells are not rescued from toxicity by addition of high-affinity AR ligand, raising doubts about AR involvement in the mechanism of toxicity in these cells as well.

To further assess AR involvement in 11β toxicity, an analogue with ~10-fold lower affinity for AR, 17α-OH-11β, was synthesized and shown to produce measurably reduced AR-driven transcription compared with 11β. 17α-OH-11β is less toxic to AR-positive cell lines; however, this differential toxicity persists in an AR-null cell line, further suggesting that AR is uninvolved in 11β toxicity.

Global transcriptional profiling has been conducted to assess other potential mechanisims for 11β toxicity and has uncovered an ability of 11β to activate cholesterol/lipid biosynthetic pathways and a response to unfolded protein while down-regulating genes related to DNA damage repair. The unfolded protein response represents an attractive potential mechanistic explanation for selective toxicity toward

cancerous cells, which may be related to an ability of 11β to perturb biological membranes.

Thesis Supervisor: John M. Essigmann
Title: William R. and Betsy P. Leitch Professor of Chemistry and Biological Engineering

Acknowledgments

I have to thank several people for their assistance in getting me here. I'll start with John Essigmann. I thank John for accepting me into his lab, for being the kind of scientist that understands there is more to life than science, and for gently nudging me toward the goal of bettering myself (and graduating) without any real micro-management. John has always maintained optimism and creativity as he assessed results, considering them on a practical and global scale. He is also a fantastic teacher and it has been a pleasure to learn from him. I also need to thank Bob Croy, who has been just as much my boss and mentor for a significant percentage of my time here. While John often considered results on this global scale, Bob would address the intricate details and ensure that appropriate controls were conducted. Bob's wealth of knowledge, especially with respect to the details, has been invaluable.

Thanks are due to Steve Tannenbaum for serving as chair of my committee, meeting with me annually, and challenging me to reconsider the hypotheses about how these compounds work. Also, thanks to Alex Klibanov for serving on my committee. His efficiency in e-mail reply and scheduling meetings along with his ability to cut to the heart of an important question without any dancing around the issue are traits I consider exemplary.

The Essigmann lab has been a great place to work. This is largely due to the native population. The fatal engineering team is and always has been a great group of people to work with, and the relationships always extend outside of the lab. I need to give special thanks to John Marquis for being my most immediate mentor in the first few years, teaching me the methods of tissue culture, how to design and run experiments, and other aspects of what it means to be a good scientist. John was always willing to listen to my problems, both those related to experimental difficulties as well as the ones of a much more personal nature. Shawn Hillier also spent a decent amount of time teaching me, but primarily with respect to the methods of handling and treating mice. Unfortunately, these projects did not become a focus of my research, but I value what I learned from them. Alfio Fichera gets special credit in the last year as I tried to relearn the details of organic chemistry. He was very patient, helpful, and practical in all aspects. Jim Delaney also

gets my appreciation for his help in identifying the different DNA adduction caused by the 17α-OH compound.

To fully express appreciation for each of the relationships that I have had with other members of the Essigmann lab would require a treatise of its own. Just let it be known that I have made great friends, had excellent scientific discussions, and have reaped rewards from this wonderful group of people. I only hope that as many of these relationships as possible persist and continue to deepen.

I'm also very appreciative of what Kim does for the Essigmann lab to keep things running. She has been patient with me each time I've asked her to remind me how to fill out a certain form, or of course when she sends the e-mail asking who hasn't filed their requisition forms (me).

Outside of the Essigmann lab, there are many who have been partially responsible for my successes. In the realm of gene chip analysis, I must thank Mayuree Fuangthong, Rebecca Fry, Sanchita Bhattacharya, and Jadwiga Bienkowska. Jadwiga also deserves special praise for quickly re-performing analyses for me just one month ago, despite my not having contacted her in months and the collaboration that initially brought us in contact having ended much earlier. Shao-Yong Chen and Howie Shen of the laboratory of Steven Balk have been tremendously helpful in the last several months with all aspects of androgen receptor study. Numerous plasmids and cell lines along with immeasurable e-mail support have been provided. Rosa Liberman and Paul Skipper have assisted with all accelerator mass spectrometry experiments. Jeff Simpson deserves full credit for all two-dimensional NMR experiments for the differentiation of 17α-OH from 17β-OH dienone steroids.

My editors—Alli Proffitt, Leslie Woo, Jeannette Fiala, and Lauren Frick, have all greatly improved the final state of my dissertation. Special credit also goes to Lauren for editing my thesis, despite this "duty" no longer existing since she has been out of the lab for over a year now. Yet she was willing to quickly provide priceless editing advice over e-mail.

Alli gets her own section. She has been a treasure always, but in the last year has shined. I spent less time and directed less energy toward her as this project became all-consuming, but she stood beside me and has been the most understanding person that I

could hope for. When I did take breaks, spending time with her was refreshing and I quickly remembered each time that I desperately needed to interact with her. The only down side is that spending time with her will always be more fun than writing a thesis. She has kept me fed and has encouraged and praised me constantly. I've hardly washed a dish in months. She has remained calm and steady even when the defense date kept changing and the future job situation hung in the balance. As such, I will spend a significant portion of the remnant of our lives showing her how grateful I am for her support in these past months, and the rest of my life showing her that I love her as much as she loves me. I give her approximately half of the credit in completing this journey. Thank you, Alli.

Thanks to my parents for regularly checking on me and listening to my efforts to explain the most recent difficulties, for always reminding me that I'd get there and that they believed in me. The same goes for my sister, Kenda. And the rest of my family, my in-laws, and many friends. Thanks to everyone who has been praying for me or pulling for me in your own way. I needed it.

Table of Contents

Figures and Tables

Chapter One

Chapter Two

Chapter Three

Chapter Four

Abbreviations

11β	2-(6-((8S,11S,13S,14S,17S)-17-hydroxy-13-methyl-3-oxo-2,3,6,7,8,11,12,13,14,15,16,17 dodecahydro-1H-cyclopenta[a]phenanthren-11-yl)hexylamino)ethyl 3-(4-(bis(2-chloroethyl)amino)phenyl)propylcarbamate
17α-OH-11β	2-(6-((8S,11S,13S,14S,17R)-17-hydroxy-13-methyl-3-oxo-2,3,6,7,8,11,12,13,14,15,16,17-dodecahydro-1H-cyclopenta[a]phenanthren-11-yl)hexylamino)ethyl 3-(4-(bis(2-chloroethyl)amino)phenyl)propylcarbamate
2PI	2-(4'-hydroxyphenyl)-3-methyl-5-hydroxy-indole
AF-1	Activation Function 1
AF-5	Activation Function 5
AMS	Accelerator mass spectrometry
APC	Annual percentage change
AR	Androgen receptor
ARE	Androgen response element
ATC	Anatomical therapeutic chemical
BCNU	Bis-chloronitrosourea
Bic	Bicalutamide (Casodex)
Cbl	Chlorambucil
CDK	Cyclin-dependent kinase
CDTFBS	Charcoal/dextran treated fetal bovine serum
Cisplatin	*cis*-diamminedichloroplatinum(II)
Cm	centimeters
CMAP	Connectivity map
CMV	Cytomegalovirus
Cpm	Counts per minute
Cyc	Cycloheximide
DBD	DNA binding domain
DHT	Dihydrotestosterone
Di	11β-dimethoxy; 2-(6-((11S,13S,17S)-17-hydroxy-13-methyl-3-oxo-2,3,6,7,8,11,12,13,14,15,16,17-dodecahydro-1H-cyclopenta[a]phenanthren-11-yl)hexylamino)ethyl 3-(4-(bis(2-methoxyethyl)amino)phenyl)propylcarbamate
DI H_2O	Deionized water
DIAD	Diisopropyl azodicarboxylate
DMF	Dimethyl formamide
DMSO	Dimethyl sulfoxide
DNA	Deoxyribonucleic acid
DRE	Digital Rectal Examination
E2	Estradiol
E2-7α	2-(6-((7R,8R,13S,14S,17S)-3,17-dihydroxy-13-methyl-7,8,9,11,12,13,14,15,16,17-decahydro-6H-cyclopenta[a]phenanthren-7-yl)hexylamino)ethyl 3-(4-(bis(2-chloroethyl)amino)phenyl)propylcarbamate

EDTA.....Ethylenediaminetetraacetic acid
EGF.....Epidermal growth factor
ER.....Estrogen Receptor (Chapter 1), Endoplasmic Reticulum (Chapter 4)
ESI-MS.....Electrospray ionization mass spectrometry
ESI-TOF.....Electrospray ionization time-of-flight mass spectrometry
EtOAc.....Ethyl acetate
EtOH.....Ethanol
FBS.....Fetal bovine serum
FDG-PET.....^{18}F-fluorodeoxyglucose positron emission tomography
Flut.....Flutamide
gCOSY.....Gradient-selected correlation spectroscopy
GCRMA.....GC Robust multi-array average
GO.....Gene ontology
gHMBC.....Gradient-selected heteronuclear multiple bond correlation
GR.....Glucocorticoid receptor
HAP.....Hydroxyapatite
HEPES.....4-(2-hydroxyethyl)-1-piperazineethanesulfonic acid)
HMG.....High mobility group
HPLC.....High performance liquid chromatography
HRP.....Horseradish peroxidase
HRPC.....Hormone refractory prostate cancer
Hr.....Hour
Hrs.....Hours
HSP.....Heat-shock protein
hUBF.....Human Upstream Binding Factor
HSQC.....Heteronuclear single quantum coherence
INSIG.....Insulin induced gene
IP.....Intraperitoneal
Kd.....Equilibrium binding dissociation constant
kDa.....Kilodalton
KLK3.....Kallikrein 3; prostate specific antigen
LBD.....Ligand binding domain
LFC.....Log_2 fold change; LFC of 1 = 2-fold change
LH.....luteinizing hormone
LHRH.....luteinizing hormone releasing hormone
LNCaP.....Lymph node carcinoma of the prostate; specific cell line
mRNA.....Messenger ribonucleic acid
MeOH.....Methanol
MR.....Mineralocorticoid receptor
MRM.....Multiple reaction monitoring
NMR.....Nuclear magnetic resonance
NaOAc.....Sodium Acetate
NTD.....N-terminal domain
PARP.....Poly-(ADP-ribose) polymerase
PBS.....Phosphate buffered saline
PCR.....Polymerase chain reaction

PIN .....Prostatic intraepithelial neoplasia
PMSF .....Phenylmethylsulfonyl fluoride
PPh_3.....Triphenylphosphine
PSA .....Prostate specific antigen; classical androgen-regulated gene
PR.....Progesterone Receptor
PVDF .....Polyvinylidene fluoride
QQQ.....Tandem mass spectrometry
rRNA.....Ribosomal RNA
RBA .....Relative binding affinity
ROS.....Reactive oxygen species
RNA .....Ribonucleic acid
RNAi.....RNA interference
RPM .....Revolutions per minute
RT .....Room temperature
RT-PCR.....Reverse transcription polymerase chain reaction
SCAP.....SREBP cleavage activating protein
SDS .....Sodium dodecyl sulfate
SDS-PAGE .....Sodium dodecyl sulfate polyacrylamide gel electrophoresis
SEM .....Standard error of the mean
siRNA .....Small interfering RNA
SREBP .....Sterol regulatory element binding protein
$t_{1/2}$.....Half-life
trans-DDP.....trans-diamminedichloroplatinum(II)
THF .....Tetrahydrofuran
Tris .....Tris(hydroxymethyl)aminomethane
Unt.....Untreated
UPR.....Unfolded protein response
UV.....Ultraviolet light (λ 10-400 nm)

Chapter 1: Introduction

Cancer

Cancer is a conglomerate of multiple and varied diseases, each sharing the common characteristics of uncontrolled, invasive cell growth. Together, this group of diseases accounts for 13% of current annual human mortality (Boyle and Levin, 2008), or even as much as 25% of all deaths in the U.S. (Jemal et al. 2008). It is a disease that affects both genders, all races, and all levels of income. It is, however, a disease that predominantly affects the aged. Cancers are now understood to be diseases of the genetic material, our DNA, and it is generally agreed that mutation of this genetic material is at the heart of cancer development. Mutation can occur through single base substitution resulting in coding for an alternate amino acid, or through larger scale chromosomal rearrangements. Epigenetic mechanisms are increasingly being appreciated. Such mechanisms could involve differential placement of 5-methylcytosine in regulatory regions (Jones and Baylin, 2002), or by way of post-translational modification of structural proteins involved in chromatin packaging (Herranz and Esteller, 2007). In most cases in which gene mutations are involved, several mutations are required to convert a normal cell into a malignant neoplasm. The mutations are necessary in order for cells to gain the now well-accepted "hallmarks" of cancer: limitless replicative potential (immortality), autonomy in growth signals, insensitivity to anti-growth signals, resistance to apoptosis (cell suicide), sustained angiogenesis (coercion of neighboring cells to reroute blood supply to the expanding tumor), and ultimately, invasive, metastatic capacity (ability to break off from a primary tumor, enter the bloodstream, establish a new clone elsewhere and take up root) (Hanahan and Weinberg, 2000). An additional noteworthy hallmark of cancer has been proposed—a metabolic switch from oxidative phosphorylation to glycolytic metabolism (Warburg, 1930), which has important implications in cancer detection and treatment. A common method for detection of tumors is use of ^{18}F fluorodeoxyglucose positron emission tomography (FDG-PET), which is successful due to the increased rate of glucose utilization by solid tumors.

It is due to this need (Hanahan and Weinberg, 2000) for several successive mutations that cancer is primarily a disease of the aged, although unique cases exist that create a predisposition to the childhood cancers, due to their development from cell types that reach maximum numbers at this stage (Stiller, 2004). Also, osteosarcomas peak in

adolescence due to rapid long bone growth during this stage of development (Miller et al. 1996). Any individual mutation may allow for gain of more than one function and is likely to be selected for by providing a competitive advantage over neighboring cells. The individual genes that become mutated in the progression of cancer can be divided into two categories: recessive loss of function tumor suppressor genes, which normally function to keep cell growth in check, and dominant gain of function oncogenes, which normally function in promoting cell growth and survival. By reducing the activity of tumor suppressor genes and increasing the activity of oncogenes, cells can gain the requisite hallmarks and fully transition into the potentially lethal neoplasms of cancer.

Genetic mutation can take place naturally through background rates of DNA replication errors, but it has been proposed that this background rate is not enough to account for the heterogeneity present in advanced cancers. It is then necessary to invoke a "mutator" phenotype, which would significantly decrease the fidelity of replication and allow for mutations to accumulate more quickly than they would otherwise (Loeb et al., 2008). It is unknown at what stage of cancer progression such a mutator phenotype might arise. In addition to underlying heredity, epidemiological studies highlight several additional factors that can increase the collective risk of developing cancer, notably tobacco use, prolonged exposure to sunlight without adequate UV protection, exposure to chemical carcinogens, ionizing radiation, obesity and high fat diets, excessive alcohol use, some hormones, and exposure to certain infectious pathogens. It is not always well understood whether these risk factors serve to increase rates of mutation or promote tumors by enhancing growth rates; both routes are likely involved.

While cancers have been associated with thousands of different individual mutations, there are a few common genes that are found to be mutated in multiple different cancers of distinct lineage. At the forefront of this list is the tumor suppressor gene *TP53*, mutated in more than 50% of cancers (Hollstein et al., 1994). This gene codes for the protein p53, which is involved in maintenance of genomic integrity, cellular senescence, and also induction of apoptosis. *RB1* is a tumor suppressor gene coding for the retinoblastoma protein, which functions in normal cells to hinder cell cycle progression and is found altered in 5-10% of cancers (Boyle et al., 2008). *CDKN2A* is the gene coding for p16, another tumor suppressor and cell cycle regulator, and is found

mutated in 30-60% of cancers. Additional tumor suppressor genes commonly mutated include *APC* (especially in colon cancers) *PTEN* (in several cancers), and the breast cancer associated genes *BRCA1* and *BRCA2*.

There are also several oncogenes commonly altered by mutation or amplification in cancers, most notably *KRAS*, coding for the Ras protein and mutated in 20-30% of cancers (Bos, 1989). Additionally important oncogenes include *ERBB2* (gene for epidermal growth factor receptor, HER2, especially important in breast cancer), *MYC* (involved in cell proliferation and survival), *BCL2* (inhibitor of apoptosis), *CCND1* (coding for cyclin D1, promoting cell cycle progression), *CTNNB1* (encoding the protein beta-catenin), and *MDM2* (encoding protein of the same name, which is a ubiquitin ligase most notable for its role in targeting p53 for proteasomal degradation). It is noteworthy that while these genes are overrepresented in the development of cancer, each individual cancer often has its signature of more and less commonly mutated genes. For instance, while *KRAS* is mutated in 20-30% of cancers, its mutation is very rare in breast cancers (Bos, 1989).

Treatment of cancers follows three primary routes. First, solid tumors will be removed by surgical excision if possible. In the same manner, directed radiotherapy can be used with the goal of killing what is still a locally confined neoplasm. There is an obvious difference in the case of the hematological malignancies which do not form primary tumors and thus cannot be removed surgically. The second route of cancer treatment is chemotherapy, in which a drug is given to a patient systemically. This route can be used concurrently with surgery or radiation to kill micrometastases (adjuvant therapy) or to increase effectiveness of radiotherapy. Additionally, chemotherapy is useful or necessary in treatment of hematological cancers and advanced metastatic cancers since they are systemic or difficult to locate and remove individually.

Chemotherapy historically involves the use of agents that target rapidly dividing cells by interfering with DNA replication or the processes of cellular division (Hurley, 2002). Agents that target DNA include antimetabolites such as methotrexate, which inhibits the enzyme dihydrofolate reductase and is necessary for DNA synthesis, and the largest class of anticancer drugs, the DNA damaging agents. These include compounds which form covalent damage to DNA, such as cisplatin, mitomycin C,

cyclophosphamide, BCNU, chlorambucil, and melphalan. There are also agents which do not directly damage DNA, but intercalate between stacked DNA bases and often interfere with the unwinding action of topoisomerases. These include doxorubicin, etoposide, mitoxantrone, and topotecan. Other chemotherapeutics interfere with cell division by preventing mitosis, usually by inhibiting microtubule activity. Examples of this class are paclitaxel, vincristine, and the epothilones. In addition to the historical chemotherapeutic agents, other, newer strategies are proving successful. Monoclonal antibodies against specific oncogenes have been used with some success, such as trastuzumab (Herceptin) in the case of breast cancer, which targets the *HER2* protein product epidermal growth factor receptor 2. In combination with chemotherapeutics, Herceptin has been shown to improve median survival time of breast cancer by 25% compared with chemotherapy alone (Baselga, 2001). Angiogenesis inhibitors such as bevacizumab (Avastin) are approved and in clinical use, and in the case of Avastin have been shown to increase median survival time of colon cancer by 30% (Hurwitz et al., 2004). Other small compound treatments have been developed to target cancer specific proteins. The targets are often kinases, and the best example is imatinib (Gleevec), which was developed to inhibit specifically the tyrosine kinase domain of the novel Bcr-Abl fusion protein created in chronic myelogenous leukemia (CML). Gleevec has proven much more effective than the previous standard treatment of interferon α in combination with cytarabine (O'Brien et al., 2003). Finally, anti-hormonal treatment is commonly used to counteract tumor progression, especially of breast and prostate cancers which depend on hormone receptor signaling for growth and survival. This method will be discussed in detail with reference to prostate cancer later. Due to the heterogeneity of advanced cancers, chemotherapy treatments are usually given in combination, under the rationale that multiple compounds with different mechanisms will achieve the most toxicity. It is also due to this heterogeneity that cancer treatment is more effective when detection, diagnosis, and treatment occur sooner.

In 2007, estimates of the five most common cancers diagnosed worldwide (excepting nonmelanoma skin cancers) were lung (1,549,121), breast (1,301,867), colon/rectum (1,167,020), stomach (1,066,543), and prostate (782,647), while the five most lethal cancers were lung (1,351,034), stomach (800,230), liver (679,871),

colon/rectum (602,967), and breast (464,854) (Garcia et al., 2007). In the U.S., the story is slightly different. In 2008, the estimated most prominent new cases were cancers of the lung (215,020), prostate (186,320), breast (184,450), colon/rectum (148,810), and lymphoma (74,320), while most deaths were from lung (161,840), colon/rectum (49,960), breast (40,930), prostate (28,660), and pancreatic (34,290) cancers (Jemal et al. 2008). This exemplifies the different cancer burden profiles affecting the developed and developing world. As further testament, the developing world was estimated to have 725,230 new cases and 569,549 deaths from stomach cancer, second only to lung cancer, while in the U.S. stomach cancer does not make the top five list in either incidence or deaths.

It is welcome news that cancer treatment is effective. In the U.S., the 5-year median survival rate for all cancers has increased from 50% from 1975-1977 to 66% in the years 1996-2002 (American Cancer Society, 2007). This increased survival is the result of combined efforts for better and earlier screening and detection, along with improvements in treatment ranging from more sophisticated combinations and dosing regimens with existing therapeutics to the development of entirely new and more effective therapeutics. Despite these advances, it hardly needs stating that cancer remains a deadly disease with a continued need for newer, better treatments in addition to the effective public campaigns increasing awareness of the dangers of tobacco, poor diet, and poor hygiene. This work will highlight efforts toward development of a new treatment for prostate cancer.

Prostate Cancer

Prostate cancer is the most frequently diagnosed non-skin cancer among males in the U.S., with an estimated 186,320 new cases leading to 28,660 deaths in 2008 (Jemal et al. 2008). While reported incidence of prostate cancer is subject to variable trends in screening for prostate specific antigen (PSA), which increased from 1995 through 2002 before finally leveling off, mortality estimates are true judges of the advances being made in detection and treatment. Prostate cancer mortality was increasing in the U.S. from the years 1987-1991 by an annual percentage change (APC) of 3.0. However, incidence began to decrease from 1991-1994 by an APC of -0.6, and from 1994-2005 the mortality

has been steadily decreasing, by a -4.1 APC (Jemal et al. 2008). While it was anticipated that these kinds of improvements in overall survival might occur as a result of increased testing for PSA, studies have dismissed increased testing as significantly extending overall survival (U.S. Preventive Services Task Force, 2002; Concato et al., 2006). The reason that increased PSA screening does not necessarily translate into increased survival is probably the combined effects of late age at diagnosis and the inherent slow growth of prostate tumors. Thus, while increased testing will lead to many more diagnoses of prostate cancer, patients will often die with, rather than from, this disease. It remains to be determined what the exact causes for recent decreasing mortality from prostate cancer are, whether indicative of better treatment or other as yet undiscovered factors such as changes in diet (Oliver et al., 2001). One very intriguing possibility is that accelerated use of statins in controlling cholesterol is actually shown to have an inverse relationship with advanced prostate cancer (Platz et al., 2006), thus potentially providing a fortuitous and unintentional effect on prostate cancer survival.

Despite PSA screening not necessarily resulting in increased overall survival of prostate cancer, its utility in detecting cancer is undisputed. In fact, a recent study demonstrates the potential that a single PSA test given to men aged 44 to 50 could accurately predict prostate cancer incidence up to 25 years later (Lilja et al. 2007). PSA is a 34 kDa glycoprotein produced almost exclusively by the prostate. Its normal function is as a serine protease, fragmenting fibronectin and seminogelin and resulting in the liquefaction of semen, allowing sperm to swim freely and achieve successful fertilization (Lilja et al. 1987). The prostate gland is composed of a layer of secretory epithelial cells, surrounded by basal cells and a basement membrane. PSA is produced by the epithelial cells, from which it is secreted into the lumen and becomes part of seminal fluid. Disruption of the basal cells and basement membrane is a common occurrence in prostate cancer, and this disruption allows PSA to enter the circulation where it can be detected by a routine blood test (Balk et al., 2003). Even in healthy males, PSA is normally present in blood, albeit at very low levels. Any disruption to the architecture of the prostate can result in a significant increase in the serum concentration (Bostwick 1994), which can unfortunately lead to many unnecessary biopsies in conditions such as benign prostatic hyperplasia or local infection. Additionally, it is not

altogether uncommon for prostate tumors to develop significantly without circulating PSA levels reaching the accepted high-risk cutoff of 4.0 ng/mL. In one study, 449 of 2950 men (15.2%) with PSA readings below 4.0 ng/mL were diagnosed with prostate cancer following biopsy (Thompson et al., 2004). However, circulating PSA levels above 10 ng/mL are very predictive of prostate cancer (Catalona et al., 1991). Therefore, while PSA testing as a gauge of prostate cancer is subject to significant levels of both false positives and false negatives that must be eliminated, its utility remains. PSA is also quite valuable for following disease progression. Monitoring of serum PSA levels can be helpful in detecting effectiveness of primary surgery and radiation (Hudson et al., 1989), disease relapse after primary treatment (Killian et al., 1985), and the utility of anti-hormonal therapy and predicted duration of remission in advanced stages (Miller et al. 1992). Finally, constant efforts are being made to use PSA detection in more sophisticated ways such as monitoring the relative change over time rather than use of a single reading.

Prostate Cancer Risk Factors

The underlying causes of prostate cancer are not very well understood. The only well established risk factors are age, race, and family history. Old age is the most predictive factor for prostate cancer, with a mean patient age of 72-74, and 85% of diagnoses occurring after age 65 (Grönberg 2003). However, preneoplastic lesions have been detected in men in their twenties and are frequent for men in their fifties (Sakr et al., 1993). There is wide variation among different ethnic and geographical populations, with extremes of 70-fold different risk between Chinese of the Tianjin region (1.9 per 100,000) and African-Americans (137 per 100,000) (Parkin et al., 1997). The reduced risk to Asians is widely recognized and has been attributed to differences of lifestyle and the Asian diet's inclusion of phytoestrogens contained in soy products and general exclusion of more fatty foods (Adlercreutz and Mazur, 1997). Migration studies have shown that Japanese men (low incidence), having moved to the U.S., increase their risk of developing clinical stage cancer. Yet, the increased risk is not on par with those of Caucasians or African Americans, both demonstrating an environmental effect and at the same time implicating genetics as a significant factor. However, it has also been shown

that the rates of histological presentation of prostate cancer (upon autopsy) are much more similar in these different populations than clinical presentation, suggesting that some of these factors may have more to do with disease progression than incidence (Breslow et al., 1977).

Family history is a strong risk factor. Men with an affected father or brother are twice as likely to develop prostate cancer (Steinberg et al., 1990). Put another way, 10-15% of prostate cancer patients have at least one affected relative (Hayes et al., 1995; Whittemore et al., 1995). This familial association has been mapped to several gene loci, leading to identification of many genes with potential association, including *ELAC2* (Tavtigian et al., 2001), *RNASEL* (Carpten et al. 2002), *MSR1* (Xu et al. 2002), *CHEK2* (Chk2 checkpoint homolog (*S. pombe*)) (Wu et al. 2006), *CAPZB* (Berry et al., 2000), *VDR* (Vitamin D Receptor), and *PON1* (Deutsch et al., 2004). More research is warranted to clarify further each of these genes' impacts upon prostate cancer susceptibility, in addition to biochemical studies to uncover potential mechanistic explanations in most cases.

Certain genes are commonly mutated during disease progression of both familial and sporadic prostate cancers. Inactivation of the tumor suppressor gene *PTEN* has been associated with prostate cancer. One study found that 23% of first time diagnosis patients have lost this gene, increasing to 59% of advanced metastatic disease cases (Schmitz et al., 2007). These data implicate PTEN inactivation as a potential early event in progression to more advanced stage of disease. PTEN (phosphatase and tensin homolog) functions in negative regulation of the Akt signaling pathway, thus serving as a cell cycle control, with additional functions related to apoptosis and angiogenesis. An additional factor that may be involved in early stages of prostate cancer progression is the loss of tumor suppressor *CDKN2A* (p16). p16 is also a cell-cycle regulating protein, functioning to inhibit cyclin dependent kinase 4, thus preventing progression from G1 to S in the cell cycle. It is frequently inactivated in numerous cancers, and finds inactivation by homozygous deletion or promoter methylation at a low frequency in prostate cancer (Rocco and Sidransky, 2001). *RB1* is also inactivated in over 30% of localized prostate cancers (Ittmann and Wieczorek, 1996).

The best correlation between inactivation of a single gene and prostate cancer exists for glutathione S-transferase pi 1 (*GSTP1*), which is silenced by promoter hypermethylation in greater than 90% of diseased patients (Meiers et al., 2007). Furthermore, this hypermethylation already exists in a vast majority of pre-cancerous prostatic intraepithelial neoplasia (PIN), despite no detection of hypermethylation in normal tissue samples. GSTP1 functions in the detoxification of reactive oxygen species (ROS) and other electrophilic toxins. A full understanding of how this protein influences prostate cancer progression is currently lacking, but this gene is a good candidate as a forebear to the mutator phenotype. Finally, a fusion between the androgen responsive gene *TMPRSS2* and the ETS oncogenes *ERG*, *ETV1*, or *ETV4* occurs in a majority of prostate cancers (Tomlins et al., 2007). ERG or ETV1 are found overexpressed in 57% of prostate cancers, and in greater than 90% of these cases, a TMPRSS2 fusion is concurrent (Tomlins et al., 2005). The fusion is not found in benign prostatic tissue.

Another handful of genes are commonly mutated in advanced prostate cancer, but detected primarily following progression to a hormone refractory state. These include recognizable examples such as amplification of *MYC* (Emmert-Buck et al., 1995), *BCL2* (McDonnell et al. 1992), *ERBB2* (Ross et al. 1997), and the androgen receptor (*AR*) (Abate-Shen & Shen 2000), and inactivation or mutation of *TP53* (Hall et al. 1995) and *CDKN1B* (p27) (Fernández et al., 1999).

Prostate Cancer Treatment

The five-year survival rate of prostate cancer in the U.S. has improved from 69% to nearly 100% within the past twenty-five years, demonstrating improvements made in disease management (American Cancer Society, 2007). Treatment of prostate cancer often begins with detection of an elevated PSA count or an irregularity of size, shape, or texture of the prostate gland detected by digital rectal examination (DRE). Subsequently, a tumor biopsy is usually performed in order to assign a stage and prognosis. The most important parameter of staging is whether or not the tumor is still confined to the prostate. Prognosis is good with progression-free cure rates exceeding 90% for locally confined prostate adenocarcinoma. When a tumor is locally confined, treatment consists of primarily three options. One option is to do nothing at all, in what is termed "watchful

waiting." Due to the inherently slow growth of prostate cancers and taking into account the elderly average age at diagnosis, treatment with intent to cure is not always warranted. In this case, monitoring of PSA levels would continue as a metric of disease progression, and a re-evaluation would take place in the event of a sudden spike. The second option is complete removal of the prostate gland by radical prostatectomy, while the third option seeks to destroy the cancerous tissue by directed radiation. It has long been recognized that prostate cancer is fueled by androgens (Huggins and Hodges, 1941), and another option, which in locally confined cancer, is generally only used in conjunction with prostatectomy or radiation therapy, is anti-hormonal therapy. Additionally, if the cancer has already spread outside of the prostatic boundary, or if there is an increase in PSA level following initial prostatectomy or radiotherapy indicative of relapse, anti-hormonal therapy is likely to be the next standard treatment.

Anti-hormonal therapy encompasses all efforts to reduce the circulating concentration of androgens that fuel prostate cancer growth. The first method widely used was orchiectomy, or surgical removal of the testicles. Surgical castration gave way to "chemical castration," which encompasses a few different strategies. The first of these involves interfering with the luteinizing hormone releasing hormone (LHRH) system. The hypothalamus responds to the presence of various steroids by producing LHRH. LHRH then travels to the pituitary gland where it binds to its receptor and induces release of luteinizing hormone (LH), which then travels to the testes and increases production of testosterone. By interfering with this cascade at any level, the circulating level of androgens can be reduced. LHRH agonists were developed to interfere with this process, and in use initially cause a spike of testosterone production (and associated flare of symptoms), but in prolonged use lead to lower LH release and resultant serum testosterone levels. Newer LHRH antagonists perform the same function while eliminating the initial flare that increases symptoms. Despite the development of these new agents, LHRH agonists have become the preferred method of androgen ablation in the United States. In addition to the testes, the adrenal gland produces low levels of androgen and can provide some fuel to hormone-starved prostate cells. Adrenalectomy was initially attempted as corollary treatment with some success, but compounds have

since been developed to prevent adrenal steroid synthesis, with ketoconazole serving as the current standard (Pont et al., 1982).

While these efforts all aim at reducing circulating androgen levels, the ultimate target of any of these treatments is a reduction of signaling mediated by the androgen receptor. This has also been achieved more directly, by creating antagonists of AR activity that bind directly to AR in target prostate cancer cells and disrupt normal signaling. This class includes the steroidal cyproterone acetate, as well as non-steroidal anti-androgens flutamide (Eulexin) and bicalutamide (Casodex). Total androgen blockade involves the concurrent use of AR antagonists along with surgical or medical castration. While these efforts at interfering with AR signaling are all effective at reducing pain and other symptoms, it is inevitable that prostate cancer not eradicated by prostatectomy or radiation will progress through anti-hormonal therapy to an androgen independent state termed hormone refractory prostate cancer (HRPC). At this stage of prostate cancer progression, treatments generally involve more traditional cytotoxic chemotherapy. The only current FDA-approved treatments for advanced hormone-refractory prostate cancer are therapies of mitoxantrone, docetaxel, and estramustine, often in conjunction with prednisone, but there are several new treatments being developed. The most successful of these treatments, docetaxel, provides less than 2.5 months of extended survival (Mike et al., 2006). Many elderly patients at this stage of disease choose not to undergo cytotoxic chemotherapy merely to gain two months of quality minimized life. It is clear that better treatments are needed in the management of HRPC, and the work described herein represents one such approach to a new potential treatment.

The Androgen Receptor

The androgen receptor is a type I ligand-activated member of the steroid receptor family of nuclear receptors. This family also includes the estrogen receptor (ER), glucocorticoid receptor (GR), progesterone receptor (PR), and mineralocorticoid receptor (MR). Only one *AR* gene has been discovered, located in single copy on the X chromosome at Xq11.2-q12 (Trapman et al. 1988; Chang et al. 1988; Lubahn et al. 1988). The complete gene is over 90 kb long, spanning 8 exons and coding for a protein

of 910-920 amino acids. Two variable-length stretches within the N-terminal domain (NTD) resulting from trinucleotide repeats of glutamine (CAG) and glycine (GGN) in the *AR* gene account for the different protein lengths observed. Reports have demonstrated that shorter CAG repeats correlate with higher AR transcriptional activity and increased risk of prostate cancer (Giovannucci et al., 1997).

The primary function of the AR is as a transcription factor mediating expression of a select set of genes. Its function is crucial in development and maintenance of the male sexual phenotype, and its involvement in prostate cancer progression is also well studied and established. AR is primarily expressed as an apparent 110 kDa protein (AR-B), which is post-translationally modified by immediate phosphorylation to yield a protein running as 112 kDa by sodium dodecyl sulfate polyacrylamide gel electrophoresis (SDS-PAGE) (Wong et al. 2004). An additional 87 kDa protein (AR-A), created from truncation of the NTD resulting from loss of the first 187 amino acids, has been detected in several tissues, but is less thoroughly studied, and its importance is unknown (Wilson & McPhaul 1996). Any mention of the AR to follow refers to AR-B, the more well understood full-length form.

AR Structure and Organization

The AR protein, like all steroid receptors, is composed primarily of three separate modular domains—the N-terminal domain, DNA binding domain (DBD), and ligand-binding domain (LBD). Within the NTD, Activation Function 1 (AF-1) located between amino acids 101 and 370, is necessary for greatest transcriptional activation following hormonal exposure, while a second Activation Function 5 (AF-5), located between amino acids 360 and 485, allows for constitutive receptor activity in absence of ligand (Jenster et al., 1995) (Figure 1.1). In fact, LBD deletion results in constitutive activity of the receptor that does not depend on AF-1 activity but requires AF-5, implicating the LBD in a functional repression of AF-1 in a full length receptor lacking ligand, and repression of AF-5 once ligand is present. Additionally, the NTD contains a dimerization surface composed of amino acids 1-36 which includes the ^{23}FQNLF^{27} motif, involved in intra- and inter-molecular interaction with the C-terminus that is elicited by androgen stimulation (Schaufele et al., 2005). The region from 370-494 within AF-5 is also

required for the interaction between the N and C termini resulting in transcriptional activation (Brinkmann et al. 1999). The DNA binding domain, spanning amino acids 559-624, is the most conserved domain among steroid receptors and consists of two zinc fingers, each having four cysteine residues bound to a zinc ion and responsible for binding to androgen response elements (ARE's) present in target gene promoters. A small hinge region from amino acids 624-676 contains the nuclear localization sequence responsible for redistribution of AR from cytoplasm into the nucleus upon hormonal stimulation. Amino acids 676-919 compose the LBD, containing Activation Function 2 (AF-2), which, during hormone stimulation, interacts with either the ^{23}FQNLF^{27} motif of the NTD or with a co-activator protein carrying a similar LXXLF or FXXLF motif (Dubbink et al., 2004). A distinct second region outside of AF-2 but within the LBD is involved in interaction with ^{433}WHTLF^{437} within AF-5. The LBD, as its name portends, also contains the binding pocket which receives either testosterone or the more potent androgen 5α-dihydrotestosterone (DHT). Finally, a nuclear export signal is also located in this LBD region (Saporita et al., 2003).

To date, no crystal structures of full length steroid receptors have been solved. However, several structures have been solved for the LBD portions of these proteins. All of the steroid receptors' LBDs display a very similar three-dimensional structure, composed of 10-12 alpha helices arranged in an anti-parallel, three-layered "alpha-helical sandwich". The AR LBD shares the most sequence identity with PR, GR, and MR (all around 50%) (Marhefka et al., 2001), and is actually composed of 11 helices, lacking H2 present in other nuclear steroid receptors (numbering remains the same for the other complementary helices so that comparison is easier). Together, H5, the N-terminal portion of H3, and the C-terminal regions of H10 and H11 form the bulk of the hydrophobic binding pocket (Figure 1.2). Upon androgen binding, H12 shifts and closes over the binding pocket, assisting in ligand retention (Zhou et al. 1995). Additionally, the conformational changes that take place upon ligand binding allow formation of the functional AF-2 surface, necessary for binding of co-activator proteins and for amino/carboxyl terminal (N/C) interaction.

The DNA binding domain structures of several steroid receptors have also been solved. The DBD of all steroid receptors is a well-conserved region consisting of three

alpha-helices containing two zinc-fingers, in addition to a C-terminal extension (CTE). The first zinc finger contains a stretch of five amino acids called the P-box, which directly interacts with the major groove of DNA and provides the majority of sequence discrimination. The second zinc finger contains another stretch of five amino acids called the D-box, containing the major residues involved in DNA-dependent receptor dimerization (Umesono and Evans, 1989). Amino acids within the CTE also confer DNA-dependent DBD dimerization for the AR (Schoenmakers et al., 1999, 2000; Haelens et al., 2001). The AR, PR, GR, and MR all recognize very similar or identical DNA sequences, raising the long-standing questions of how these receptors elicit specific responses with such degeneracy in response elements. Definitive answers are still lacking, but it is believed that specificity comes from differences in steroid metabolism, receptor expression (Strähle et al., 1989), chromatin structure (List et al., 1999), and cofactor expression and recruitment to active transcriptional complexes (Müller et al., 2000). The AR is unique in that it binds to the consensus inverted repeat sequence AGAACAnnnTGTTCT (classical ARE) (Nelson et al., 2002), in addition to direct repeat sequence AGAACAnnnAGAACA (selective ARE) (Shaffer et al., 2004), allowing an extra level of potential specificity. For the GR (Luisi et al., 1991) and ER (Schwabe et al., 1993), crystal structures show that the respective DBD's bind to an inverted repeat hormone response element in a head-to-head fashion. As such, it is assumed that the AR DBD also dimerizes in a head-to-head fashion on classical inverted repeat response elements. It was further surmised that binding to the selective ARE's would be in a head-to-tail fashion, matching the underlying response element arrangement. However, the structure of a crystallized AR DBD bound to a selective ARE demonstrates that even when bound to a direct repeat response element, dimerization is in a head-to-head fashion (Shaffer et al., 2004). In this binding mode, one AR monomer binds to its respective hexameric half site response element with high affinity while the other binds with lower affinity, demonstrating the importance of the DBD dimerization interface in AR-specific DNA binding.

Finally, the NTD of steroid receptors are not amenable to crystal structure analysis, presumably due to structural flexibility in this region. The NTD is the least

conserved among the steroid receptor domains, and as such, is likely to be heavily involved in receptor-specific effects.

AR Transcriptional Activation

AR binds to both T and DHT with Kd's of ~1nM and 0.1nM respectively. Testosterone is reduced by the enzyme 5α-reductase in some target tissues including the prostate to convert it to the more potent androgen DHT. In absence of androgen, the AR resides predominantly in the cytoplasm in a large complex of heat shock proteins including Hsp90, Hsp70, and Hsp56 (Veldscholte et al., 1992), immunophilins such as FKBP52 (Cheung-Flynn et al., 2005), co-chaperones, and tetratricopeptide repeat-containing proteins (Buchanan et al., 2007). However, ligand binding induces conformational changes in the LBD that allow AR to be released from chaperone proteins, become phosphorylated, translocate into the nucleus, auto-dimerize, interact with co-activator proteins, bind to androgen response elements (ARE's) in the promoters of target androgen genes, and recruit machinery to induce transcription of these genes (Brinkmann et al., 1999). Additionally, ligand binding is essential for nuclear retention of AR, as the transfer of cells into a medium lacking androgen allows for export of AR to the cytoplasm. Up to four rounds of cycling from cytoplasmic to nuclear location has been demonstrated for the AR prior to receptor degradation (Roy et al. 2001).

Several phosphorylation sites have been established in the AR, including serines 16, 81, 94, 256, 308, 424, and 650 (Gioeli et al., 2002). Serine 94 is constitutively phosphorylated, while each of the others display elevated phosphorylation upon androgen exposure. Serine 650 phosphorylation was also stimulated by protein kinase A, protein kinase C, and epidermal growth factor signaling, while serine 81 was shown to have the highest stoichiometric phosphorylation in response to hormone (Gioeli et al., 2002).

Another unique and incompletely understood feature of AR activation is the N/C terminal interaction that occurs upon androgen stimulation. This interaction was first established through use of mammalian two-hybrid assays (Langley et al., 1995). More recent fluorescence resonance energy transfer (FRET) studies have shown convincingly that intramolecular N/C interaction occurs within ~3.5 minutes of androgen addition, followed 6 minutes later by intermolecular interaction of N and C termini (dimerization).

Furthermore, these results showed that no receptor dimerization occurred in the cytoplasm, while N/C interaction occurred equally in cytoplasmic and nuclear compartments (Schaufele et al., 2005). These results suggest that dimerization requires nuclear compartment-specific events to occur. The active AF-2 region of the LBD created by addition of androgen has posed somewhat of a conundrum, because this region interacts with either the ^{23}FQNLF^{27} motif of the NTD, or with co-activator proteins containing LXXLF motifs, suggesting these two activities compete. In fact, experiments have shown that the active AF-2 prefers interaction with FXXLF over LXXLF motifs (He et al. 2000). Additional experiments demonstrate that N/C interaction occurs predominantly in mobile receptors, while co-activator binding occurs preferentially once AR is bound to DNA (van Royen et al., 2007). This result suggests that the N/C terminal interaction may serve to stabilize the receptor and maintain androgen binding until DNA binding occurs, at which time association of co-activator proteins can take over and assist in transcriptional activation.

The activation functions within the AR interact with co-activator and co-repressor proteins, assisting in the recruitment of chromatin remodeling enzymes as well as providing additional levels of transcriptional regulation. The most widely understood co-activator proteins are those of the p160 family, including steroid receptor coactivator 1 (SRC1) (Oñate et al., 1995), transcriptional intermediary factor 2 (TIF2) (also known as glucocorticoid receptor interacting protein 1 (GRIP1) (Voegel et al., 1996), and amplified in breast cancer 1 (AIB1/SRC3) (Anzick et al., 1997). Recruitment of these factors influences transcription directly via histone acetyltransferase (HAT) activity and indirectly by creating a platform for recruitment of secondary co-activators with chromatin remodeling activities. Alternatively, recruitment of co-repressor proteins including nuclear receptor co-repressor 1 (NCoR1) (Cheng et al., 2002) and the silencing mediator of retinoic and thyroid hormone receptor (SMRT) (Liao et al. 2003), which both inhibit transcription, occurs in the presence of androgens and is increased in the presence of AR antagonists or partial agonists. Co-repressor binding requires extension of the p160 co-activator protein binding LXXLL-like motif to an LXX-I/H-IXXX-L/I motif, known as a CoRNR box (Hu & Lazar 1999). Re-positioning of helix 12 away from helices 3-5 is believed to allow for the larger CoRNR box containing three helical turns

instead of the two turns seen in LXXLL-like motifs. Presumed helix 12 displacement and additional conformational changes in the LBD are involved in increased association of co-repressor proteins with mifepristone (RU-486) bound AR (Hodgson et al., 2008). Several other co-regulators of transcriptional activity have been studied and catalogued and exemplify the complex regulatory mechanisms driving transcription through the AR (Chmelar et al., 2007).

AR Regulation

AR is eventually degraded via the ubiquitin-proteasome pathway after an unknown number of transcriptional events. A conserved PEST sequence thought to be important for protein tagging by ubiquitylation is present within the hinge region of AR, and use of proteasome inhibitors increases steady-state AR protein levels (Sheflin et al., 2000). It has been further demonstrated that AR can form a complex with Akt and Mdm2, which promote phosphorylation-dependent AR ubiquitylation (Lin et al. 2002). However, it is also well established that proteasome activity is necessary for AR transcriptional activity (Lin et al. 2002). One study has shown that the S1 subunit of the 19S proteasomal cap interacts with the PSA promoter, and that proteasome inhibition prevents release of the receptor from the PSA promoter (Kang et al., 2002). Combined with the finding that consecutive rounds of nucleocytoplasmic shuttling of receptor lead to less effective nuclear translocation of AR (Tyagi et al. 2000), it is likely that proteasome activity modulates the number of transcriptional events in which one receptor may participate. The ability for a single AR to undergo multiple rounds of transcription once again makes it unique relative to the other steroid receptors which typically are degraded by the proteasome after a single round of replication.

AR Involvement in Prostate Cancer

The AR is involved in prostate cancer development at every stage. AR turns on the expression of several genes involved in promotion of growth and survival. As such, cells which maintain AR signaling have a slight growth advantage over neighboring cells and will persist. Men who were castrated at a young age, or who have deficiency in 5α-

reductase or other androgen insensitivity syndrome mutations do not develop prostate cancer. Men with shorter CAG repeats in the AR gene corresponding to shorter polyglutamine tracts have higher AR transcriptional activity (Chamberlain et al., 1994), which corresponds to an increased risk and a statistically earlier onset of prostate cancer (Giovannucci et al., 1997). Thus, expression of genes mediated by AR is a causal factor in prostate cancer. Several androgen-regulated genes have been identified, with PSA the most thoroughly studied due to its utility in detection of prostate cancer and monitoring of progression. However, while some theorize that PSA plays a causal role in prostate cancer progression (Williams et al. 2007), it is not a good candidate for a pro-growth or pro-survival gene.

AR acts as a master regulator of the G1-S cell cycle phase progression, increasing expression of cyclin-dependent kinases (CDK) 2 and 4, as well as down regulating expression of p16 (Lu et al. 1997). Androgens also induce expression of cyclins D1, D2, and D3 and phosphorylation and inactivation of RB (Xu et al. 2006). These transcriptional and translational changes mediated by the AR promote cells into the S phase of replication and enhance proliferation. Due to the dependence on AR signaling for prostate cancer progression, the first line therapy in metastatic prostate cancer treatment is inhibition of AR signaling by lowering circulating androgen levels and/or the use of AR antagonists. However, it is a certainty that prostate cancer will progress from an androgen-dependent stage into hormone-refractory disease. The progression to HRPC can take several routes, including mutations within the AR LBD that allow promiscuity for other ligands, amplification and over-expression of AR that increases transcription from low levels of circulating androgen, increased expression of co-activator proteins and increased local production of androgens. So-called 'outlaw' pathways can also take over, in which case growth factors such as insulin-like growth-factor-1 (IGF-1), keratinocyte growth factor (KGF), and epidermal growth factor (EGF) are able to promote AR activation in absence of any androgen (Culig et al., 1994). HER-2 overexpression is also able to activate AR in the absence of AR ligand, but requires AR protein expression (Craft, Shostak, et al., 1999). In each of these mechanisms of androgen independence, AR presence is required despite ability of prostate cancers to progress in absence of normal levels of circulating androgen.

Other mechanisms exist that can allow progression in complete absence of AR, known as bypass pathways. Effective bypass involves the use of other signaling pathways to stimulate androgen-independent cells to proliferate. *BCL2* is a gene thought to be involved in bypass pathways, as it is not normally expressed in prostate epithelial cells, but is commonly expressed in PIN and in HRPC (Colombel et al., 1993). Because BCL2 is anti-apoptotic, its overexpression could allow prostate cancer cells to proliferate despite lacking AR signaling. In fact, it is thought that BCL2 overexpression, along with family members BCL-X and MCL-1 (Krajewska et al., 1996), is partially responsible for the low success rate in treatment of prostate cancer with traditional cytotoxic chemotherapy regimens (Osborne et al. 1992; Smith et al. 1993; Williamson et al. 1996; van Brussel et al. 2000).

A final hypothesis to consider in the progression to HRPC is that there are "lurker" cells present which do not depend on androgens for growth (Isaacs 1999). This hypothesis presupposes the development of prostate cancer from an epithelial prostate stem cell. In such a scenario, most of the cells descending from these stem cells would differentiate into androgen-dependent cells and comprise the majority of a tumor, while androgen-independent progenitor cells remained present at low levels. Androgen deprivation therapy would provide a selective pressure that increases the proportion of cells having independence from androgen signaling and ultimately lead to clinical presentation of HRPC. Support for this hypothesis is provided by experimental evidence of clonal expansion of androgen independent cells within an androgen-dependent tumor (Craft, Chhor, et al., 1999). Despite progression of prostate cancer to a hormone refractory state, a majority of prostate cancers continue to express and depend on AR signaling (van der Kwast et al. 1991; Visakorpi et al. 1995; Gregory et al. 1998; Holzbeierlein et al. 2004; Mohler et al. 2004). The AR therefore remains an excellent target of new therapeutics, but these therapeutics need to be designed such that they inhibit AR signaling in novel ways. Our work described herein will discuss the use of cytotoxic chemotherapeutics designed to utilize the ubiquitous expression of AR in prostate cancers as a mechanism of enhanced toxicity.

Cisplatin

The use of DNA damaging agents is historically verified as one of the most successful cancer treatment strategies. However, there are two primary shortcomings to this therapy: 1) Toxicity to healthy somatic cells is high, and 2) resistance can be achieved by increased DNA repair activity in cancerous cells, rendering them less sensitive to alkylation damage (Harris 1985; Masuda et al. 1988; Andrews 1994; T. Fojo 2001; Wang et al. 2001). One chemotherapeutic DNA damaging agent that appears to have overcome these limitations is *cis*-diamminedichloroplatinum(II) (cisplatin). Cisplatin is one of few true success stories in the chemotherapeutic field, as its use in combination therapy of testicular cancer affords 5-year survival rates of greater than 95% (Horner et al., 2009). This rate represents a dramatic improvement from just three and a half decades ago when, prior to the introduction of cisplatin, the cure rate for testicular cancer was only 23% (Huang et al. 2008). It is well established that the anticancer activity of cisplatin comes from its ability to modify DNA covalently. Studies have shown that *E. coli* and eukaryotic cells lacking crucial DNA repair enzymes are 3-10 fold more sensitive to cisplatin than their wild-type counterparts (Kartalou & Essigmann 2001). The levels of cisplatin-DNA adducts formed in blood cells of ovarian and testicular cancer patients are directly correlated with clinical response (Reed et al. 1986). Finally, while cisplatin can react with other cellular macromolecules, it is believed that the level of adduction to these molecules is too low to be of importance at therapeutically relevant doses (Pascoe & Roberts 1974; Akaboshi et al. 1992).

Cisplatin is a neutral, square planar molecule composed of a central Pt(II) coordinated to two chloride and two ammonia groups, with the chloride ligands in the cis configuration (Figure 1.3). Interestingly, when the chloride ligands are coordinated in the trans geometry (*trans*-diamminedichloroplatinum(II), or *trans*-DDP), the resulting compound is ineffective as a chemotherapeutic agent. Cisplatin is administered intravenously and remains coordinated to its chloride ligands in the blood, where the free chloride concentration is ~100 mM. However, upon entry into a tumor cell where the chloride concentration is ~4 mM, water is able to replace chloride ligands relatively rapidly ($t_{1/2}$ = 2 hrs for substitution of the first chloride ligand by water) (Johnson et al. 1980; Bancroft et al. 1990). It is this cationic aquated species which can more easily

undergo nucleophilic attack by DNA, forming N7 adducts with guanine and adenine ($t_{1/2}$ = 0.1 hr) along with intra- and inter-strand crosslinks between these bases ($t_{1/2}$ = 2.1 hrs) (Bancroft et al., 1990). Studies performed *in vitro* demonstrate that the majority of adducts created are 1,2-d(GpG) intrastrand crosslinks (65%), followed by 25% intrastrand 1,2-d(ApG), 5-10% intrastrand 1,3-d(GpG), and a minor quantity of interstrand crosslinks and monoadducts (Kartalou & Essigmann 2001). Importantly, a similar profile is observed in cancer patient samples (Fichtinger-Schepman et al., 1987). Therapeutically inactive *trans*-DDP is incapable of forming 1,2-d(GpG) or 1,2-d(ApG) adducts due to its geometry, instead favoring formation of intrastrand crosslinks between N7 of guanines or between guanine and N3 of cytosine, always separated by at least one base (Kartalou & Essigmann 2001). In addition, *trans*-DDP forms significantly more interstrand crosslinks than cisplatin, as much as 20% of all adducts, primarily between complementary guanine and cytosine residues (Brabec and Leng, 1993).

The structure of the major 1,2-d(GpG) cisplatin adduct has been solved, demonstrating that this adduct causes bending of the DNA helix toward the major groove by 50° or more along with unwinding by more than 20° (Takahara et al. 1995; Takahara et al. 1996; Gelasco & Lippard 1998). This bending narrows the major groove and widens and flattens the minor groove. Structures of 1,2-d(ApG) (Fouchet et al., 1997) and 1,3-d(GpG) (van Garderen and van Houte, 1994) adducts have also been obtained, demonstrating that 1,2-d(ApG) is very similar to 1,2-d(GpG), while 1,3-d(GpG) causes slightly more helical distortion. The crystal structure of a single interstrand G-G crosslink has been solved, and in this case bending is toward the minor groove by 47° along with unwinding by 70°, while cytosine bases complementary to adducted guanines are extruded from the helix (Coste et al., 1999).

Cisplatin Forms DNA Adducts That Attract Specific Binding of Several Proteins

It was quickly recognized that cisplatin adducted DNA was able to recruit the association of a variety of proteins to its sites of damage. Several of these containing a high-mobility group (HMG) domain have been shown to display affinity specifically toward clinically useful cisplatin adducts while displaying negligible affinity for *trans*-DDP adducts. These proteins bind specifically to the 1,2-d(GpG) and 1,2-d(ApG), but

not the 1,3 adducts of cisplatin, thus providing explanation for why *trans*-DDP adducts do not recruit them (Toney et al. 1989; Pil & Lippard 1992). Within this class of proteins, human upstream binding factor (hUBF) is most notable due to its exceptional affinity for 1,2-d(GpG) adducts of cisplatin. The equilibrium dissociation constant (Kd) of hUBF for cisplatin adducts is 60 pM, while the Kd of hUBF for its natural response element, in the promoters of ribosomal RNA (rRNA) is 18 pM, making a cisplatin adduct an attractive and likely important binding site (Treiber et al., 1994). These observations have elicited two potential mechanistic explanations for the efficacy of cisplatin: 1) cisplatin adducts recruit proteins including those possessing an HMG domain, which bind with enough affinity to interfere with DNA repair processes, and 2) because hUBF is a transcription factor that is responsible for regulating the transcription of rRNA, titrating this transcription factor from its normal promoter sites results in less rRNA being transcribed, and the cell is rendered more sensitive. These two mechanistic explanations will hereafter be referred to by the terms "repair shielding" and "transcription factor hijacking," respectively (Figure 1.3).

Evidence supporting the repair shielding hypothesis is provided by experiments that demonstrate inhibited *in vitro* excision repair by cell extracts when the HMG proteins HMG1, mtTFA, tsHMG, or SRY are added (Huang et al., 1994; Zamble et al., 1996; Trimmer et al., 1998). Furthermore, addition of steroidal hormones to breast cancer cells expressing corresponding steroid receptors increases expression of HMG1 protein and in so doing increases cisplatin sensitivity (He et al. 2000). Additionally, *S. cerevisiae* cells knocked out for Ixr1 protein (a member of the HMG family) are 2-6 fold less sensitive to cisplatin and are found to maintain fewer adducts (Brown et al. 1993; McA'Nulty & Lippard 1996).

Evidence for the transcription factor hijacking hypothesis is provided by the finding that cisplatin adducts, at levels lower than those detected in cancer patients, can effectively compete with ribosomal promoter sites for binding to hUBF (Treiber et al., 1994). Reconstituted *in vitro* transcriptional assays demonstrate that cisplatin adducts can hinder rRNA transcription, and that addition of excess hUBF can counteract this inhibition (Zhai et al. 1998). Even more impressive, this same inhibited ribosomal RNA transcription occurs *in vivo* (Jordan and Carmo-Fonseca, 1998). Thus, while there are

many more hypotheses and potential explanations for the impressive anticancer activity of cisplatin, there is good evidence that transcription factor hijacking and/or repair shielding are important factors that can collectively influence toxicity.

Fatal Engineering

Unfortunately, despite the stellar success of cisplatin in combination treatment of testicular cancers, it is less effective for treatment of other tumors. As such, an endeavor was undertaken to re-engineer DNA damaging agents using the lessons learned from cisplatin, rationally incorporating features that would allow them to work by the mechanisms of repair shielding and transcription factor hijacking. We proposed that by chemically tethering a nitrogen mustard DNA damaging moiety to a steroid receptor ligand, the mechanisms responsible for toxicity of cisplatin could be recapitulated and expanded into other cancers. It is important to address the novelty of this idea, as the connection of a DNA damaging agent to a steroid is not a new idea (Fredholm et al. 1978; Leclercq et al. 1983; Lam et al. 1987; Knebel & von Angerer 1988; Kubota et al. 1988; Eisenbrand et al. 1989; Brix et al. 1990; Roth et al. 1995; Hannon et al. 2006). In most of these cases, the goal is to achieve selective delivery and accumulation of a toxic agent in cells expressing the target protein; in fact, the tether is often intentionally designed to be labile. Our strategy is unique in its maintenance of a stable linkage between the DNA damaging region and the protein recognition domain, thus maintaining high affinity for a steroid receptor even when covalently bound to DNA. In this way it is thought that repair shielding can occur through tight binding of steroid receptors to sites of damage and associated hindrance of repair enzymes. Additionally, by recruiting these receptors away from their normal transcription response elements in the promoters of genes often involved in proliferation and survival, transcription factor hijacking would occur and increase cytotoxicity.

Design of Agents that form DNA Damage that Recruits the Estrogen Receptor

The first attempt at achieving these goals was aimed at gaining selective toxicity toward cells expressing high levels of the estrogen receptor (ER), a situation occurring in breast and ovarian cancers (Slotman and Rao, 1988; Fernö et al., 1990) To this end, 2-

(4'-hydroxyphenyl)-3-methyl-5-hydroxy-indole (2PI) ligand for the ER was tethered through an alkylaminocarbamate chain to a 4-(3-aminopropyl)-N,N-(2-chloroethyl)-aniline group (Rink et al., 1996) (Figure 1.4). An aniline nitrogen mustard was chosen as the DNA damaging agent because of its lower reactivity than alkyl mustards, making it more selective for DNA, in addition to its proven clinical use in anticancer agents such as chlorambucil (Figure 1.4) and melphalan. Furthermore, nitrogen mustards form DNA adducts which are easily repaired, yet are more toxic to cells incapable of repairing them (De Silva et al., 2000; Panasci et al., 2002), affording the opportunity to enhance this form of DNA damage by limiting its repair. The linkage between these two functional groups was designed in order to permit DNA damage to occur while maintaining high affinity to the ER through the 2PI group. A secondary amine assists in solubility, and as it is expected to bear a positive charge at physiological pH (pKa 2° amine ~9-10), is thought to assist in association with the polyanionic phosphate backbone of DNA. Additionally, a carbamate was chosen to link the two halves of the molecule synthetically, due to its resistance to cellular enzymatic activity which could otherwise cleave the molecule in two (Cho et al., 1993).

A series of compounds was synthesized with variation in linker lengths in order to optimize dual capacities of DNA damage and ER affinity (Figure 1.5). An additional control molecule was made by incorporation of a 2-(4'-hydroxyphenyl)-3-methyl-indole as the protein recognition domain (2PI(OH)-C6NC2, Figure 1.5), due to this modification significantly decreasing ER affinity (von Angerer et al., 1984). All molecules were tested for affinity to ER by measuring their ability to compete with [^{3}H]-estradiol binding to full-length ER in calf uterine extracts (Rink et al., 1996). Results are expressed as relative binding affinity (RBA), defined as the molar ratio of unlabeled estradiol (E2) to test compound necessary to reduce [^{3}H]-estradiol occupancy by 50%. The molecule 2PI-C6NC2 had the highest affinity to ER of the molecules tested (RBA = 7.1). As expected, removal of the –OH group crucial to ER binding in the 2PI portion of the molecule reduced affinity by 70-fold. Molecules were next tested for their abilities to damage self-complementary 16-mer oligonucleotide 5'-d(ATTATTGGCCAATAAT) containing a central GGCC, optimal for formation of preferred GNC interstrand crosslinks (Rink et al., 1993). Overall reactivity followed a trend from 2PI-C3NC3 > 2PI-C5NC3 > 2PI-

C6NC2 > chlorambucil > 2PI(OH)-C6NC2. Chemical fragmentation analysis demonstrated that guanine, likely N7 (Singer, 1975; Lawley and Phillips, 1996), was the primary site of attack, followed by adenine, likely at N3 (Pieper et al., 1989). Rink et al. also demonstrated that DNA adducted by 2PI-C6NC2 maintained affinity for ER, albeit significantly less affinity than the free compound (RBA ~0.5), demonstrating that adducted DNA could potentially act as a decoy binding site for ER.

Most importantly, molecules were tested for their ability to kill breast cancer cells. An ER positive line (MCF-7) and an ER null line (MDA-MB-231) were compared to determine if ER was a toxicity enhancing factor. Treatments were performed for two hours before replenishing fresh media in order to minimize antagonistic effects, and after recovery for 24 hrs, cells were re-plated at clonal density to measure survival following several days growth (Rink et al., 1996). General toxicity followed the trend of compound DNA damaging abilities. Importantly, the molecules with higher affinity for ER displayed greater toxicity toward MCF-7 than MDA-MB-231 cells, whereas 2PI-C3NC3 or chlorambucil showed comparable toxicity in each cell line. Furthermore, the 2PI(OH)-C6NC2 compound with much lower affinity to ER showed no enhanced toxicity toward cells expressing the ER. The absence of differential sensitivity for compounds with poor affinity to the ER is strong evidence that the differences seen with 2PI-C6NC2 and 2PI-C5NC3 are not due to inherent differences in sensitivity to DNA damaging agents between MCF-7 and MDA-MB-231 cells.

The combination of results with the 2PI series of compounds showed that a 6-carbon linker between the PI portion of the molecule and the secondary amine yielded the best affinity for ER. It is believed that this distance is optimal for the molecule to reach into the ligand binding pocket of ER through a primarily hydrophobic patch and still maintain the ability to modify DNA covalently. The crystal structure of ER-LBD complexed with the antagonist ICI 164384 gives the best support to this hypothesis (Pike et al. 2001) (Fig. 1.6). ICI 164384 is based on the core steroidal structure of estradiol, but with a 16-atom straight chain linkage from the 7α position. As such, the steroid portion of ICI 164384 binds upside down from the manner in which E2 is seen in crystal structures of ER-LBD (Tanenbaum et al., 1998; Brzozowski et al., 1997). The structure seen in Figure 1.6 gives a good clue to explain this observation, as there is no other

obvious path of entry into the ligand binding pocket. Approximately six carbon units are necessary in order to reach the surface of this ligand binding domain, and it is likely that placement of a secondary amine closer to the steroid nucleus interacts unfavorably with the hydrophobic pore of ligand binding pocket access.

Refinement of DNA Damaging Agents with Selective Toxicity Toward ER (+) Cells

A next generation ER-specific toxin was created by redesigning the ligand portion of the ER recognition domain, in hopes of further increasing toxicity in favor of killing ER (+) cancer cells. Toward this end, a new molecule was synthesized by maintaining the optimized C6NC2 linker from 2PI-C6NC2, but replacing the 2PI group with E2. Attachment was made in the 7α position of E2, based on reports that large alkyl groups could be attached here with minimal disruption of ER affinity (Bucourt et al., 1978; Bowler et al., 1989; DaSilva and van Lier, 1990). The completed compound, E2-7α (Figure 1.4), was shown to have an improved affinity for ER compared with the 2PI-C6NC2 compound (RBA = 30) (Mitra et al., 2002). Again it was demonstrated that this compound could successfully modify DNA, making 50% of a self-complementary 16-mer piperidine labile, and that this modified 16-mer could associate with ER-LBD as determined by gel shift studies. Furthermore, this shift could be competed away with an excess of E2. E2-7α also demonstrated enhanced toxicity toward ER(+) MCF-7 cells as compared with ER(-) MDA-MB-231 in a clonogenic survival assay performed as with the 2PI compounds.

The next steps toward improving these compounds involved a more systematic investigation into linker modification for the E2-7α compound (Sharma et al., 2004). Figure 1.7 shows the structures of these compounds. In all cases, a six-carbon linker was maintained between the steroid and first heteroatom (nitrogen in all cases except for the carbamate), employing lessons learned from the 2PI compounds. Further modifications were made beyond this point, incorporating a single amide bond, a single secondary amine, a single carbamate, a guanidine, an amide combined with a guanidine, an amide combined with a carbamate (E2-7α), two amide bonds, or two secondary amines, with associated variation in overall linker length from 11 to 16 atoms between the steroid and the aromatic ring of the aniline mustard (Figure 1.7). These compounds were all tested

for their abilities to compete with E2 for binding to ER from calf uterine extracts. The parent E2-7α compound proved to have the highest affinity for ER of the compounds tested (RBA = 46 in this assay). However, all compounds maintained reasonably high affinity binding to ER, with the amine, diamine, diamide, and guanidine compounds all having RBAs of 28 and higher (Sharma et al., 2004). Next, it was shown that most of these compounds maintained significant DNA damaging ability, with the amide and carbamate being the exceptions. This result lends support to the hypothesis that a formal positive charge assists in DNA adduction. In fact, the diamine compound, which would be doubly charged, shows the greatest DNA damaging ability, modifying 79% of the 16-mer tested (Sharma et al., 2004).

The most important measure for our designed mechanism of action is provided by testing the adducted oligos for their ability to interact with the ER. Here it was once again determined that E2-7α was most successful at causing a band shift (93%) indicative of ER-LBD association with the adducted oligo (Sharma et al., 2004). The amine compound was next best (67%), followed by the diamine and guanidine (both 38%). Surprisingly, the amine-guanidine, despite having one of the lowest RBA's for ER, was also able to form adducts that presumably interact with ER, producing a 93% band shift. This result is unexplained, but is likely an experimental artifact. Unsurprisingly, the amide and carbamate are unable to form adducts that interact appreciably with ER-LBD. It is unclear, however, why the diamide adducts are not band shifted upon addition of ER-LBD, as this compound maintains high affinity for ER and similar DNA damaging ability as E2-7α. This is perhaps due to unforeseen structural variations that occur upon DNA adduction that are specific to this compound and prevent its association with ER. Finally, all compounds were tested for their toxicity in the ER(+) MCF-7 and ER(-) MDA-MB-231 cells. Only E2-7α, amine, and diamine compounds maintained significant toxicity (Sharma et al., 2004). Furthermore, each of these compounds is selectively more toxic toward the MCF-7 cells, with E2-7α ultimately showing the greatest efficacy.

Design of Agents that Form Sites of DNA Damage that Maintain Affinity for the Androgen Receptor

We next expanded the scope of original design to include an additional target: the androgen receptor. The majority of work presented here will focus primarily on the compound produced as a result of these efforts. As discussed previously, the AR is a crucial protein involved in the progression of prostate cancer and it is involved at all stages of disease, representing a valuable target. For this molecule, the chosen protein recognition domain with specificity for AR was based on the steroid structure of RU-486, which was demonstrated to possess significant affinity for the AR (Fuhrmann et al., 2000). The steroid used was a 17β-hydroxy-estra$^{\Delta 4(5),\ 9(10)}$-3-one, with linker-mustard attachment at the 11β position, following the example of RU-486 (Marquis et al. 2005). The accumulation of information learned from molecular optimization of the 2PI and E2-7α series of compounds was applied toward synthesis of an AR-specific toxicant, employing the same six-carbon chain extension from the steroid nucleus, a secondary amine, and a carbamate linkage in the C6NC2 fashion of 2PI and E2-7α, creating the molecule 11β[1] (Figure 1.4). In addition to 11β, a control molecule was synthesized by replacement of chlorine atoms within the chloroethyl arms of the aniline mustard with –OCH_3 groups to create 11β-dimethoxy (Figure 1.4). The mechanism of nitrogen mustard mediated DNA damage first requires the formation of an aziridinium ion by donation of electron density from nitrogen to the carbon alpha to chlorine, removing this electronegative atom (Colvin et al., 1976; Wilman and Conners, 1980). However, when the more electropositive and poor leaving group –OCH_3 is present, no aziridinium ion formation can occur, thus rendering the 11β-dimethoxy molecule incapable of DNA damage and providing a useful control compound to test effects independent of DNA damage.

Both 11β and 11β-dimethoxy were tested for their binding affinity to AR. In this assay, [^{3}H]-R1881 and test compound are allowed to compete for binding to AR in

[1] 2-(6-((8S,11S,13S,14S,17S)-17-hydroxy-13-methyl-3-oxo-2,3,6,7,8,11,12,13,14,15,16,17 dodecahydro-1H-cyclopenta[a]phenanthren-11-yl)hexylamino)ethyl 3-(4-(bis(2-chloroethyl)amino)phenyl)propylcarbamate

LNCaP whole cell extracts under equilibrium conditions. RBA is the molar ratio of unlabeled R1881 vs. test compound able to compete away 50% of [^{3}H]-R1881 binding. 11β and 11β-dimethoxy each display similar affinities to AR (RBA = 11.3 and 18.1, respectively, Fig. 1.8). R1881 is a synthetic androgen with two to three fold greater affinity for AR than the most potent natural androgen, DHT (Zhao et al., 1999). Therefore, the RBA of 11β for AR with respect to DHT is ~20, meaning 11β binds 1/5 as well as DHT. Having shown that 11β possesses significant affinity for AR, experiments were performed to test DNA damaging ability. As in the cases of 2PI and E2-7α, 11β displayed significant DNA damage capacity, modifying 75% of the self-complementary 16-mer as determined by piperidine cleavage. Importantly, 11β-dimethoxy did not modify this oligonucleotide, demonstrating its inability to damage DNA. Next, adducted oligo was purified and used in a competitive binding assay to determine affinity for 11β-DNA adducts, with a resulting RBA of 0.2. Due to similarity of receptor structure, 11β, 11β-dimethoxy and 11β-DNA adducts were all tested for competitive binding with ^{3}H-progesterone to the PR. These all demonstrated a reduced but significant affinity for the PR, with RBA's of 4.2, 3.6, and 0.04, respectively.

Compounds were tested for toxicity toward AR positive LNCaP cells. Results showed that 11β, at concentrations > 5 μM, was able to induce LNCaP cells to undergo a contraction, or rounding, and subsequent detachment from tissue culture dishes within ~6 hrs. Treatment with 11β-dimethoxy caused similar morphological changes to cells initially, but rather than detaching like 11β treated cells, the cells recovered their normal morphology, appearing similar to untreated cells by 24 hrs post treatment. Several lines of evidence demonstrated that 11β was able to induce an apoptotic program in LNCaP cells; treatment with concentrations > 5 μM induced annexin-V staining, laddering of DNA indicative of internucleosomal fragmentation, and poly-ADP-ribose polymerase (PARP) cleavage, starting as early as 9 hrs post treatment (Marquis et al. 2005). 11β-dimethoxy was unable to cause any changes associated with apoptosis. However, cell cycle analysis demonstrated that 11β-dimethoxy caused a strong block in the G1 phase of the cell cycle, while 11β showed no redistribution of cell cycle phasing, but only an increase in sub-G1 population cells consistent with apoptosis (Marquis et al. 2005). Due

to the G1 block caused by 11β-dimethoxy, both compounds were tested for their effects on the cell cycle regulating proteins p21 and p27. Each compound caused an increase in the levels of p27 that was not seen with the DNA damaging agent chlorambucil. In the case of p21, both 11β and 11β-dimethoxy initially caused a decrease of p21. However, p21 levels in 11β-dimethoxy treated cells recovered to pre-treatment levels, while in 11β treated cells they continued to increase to several fold above untreated levels (Marquis et al. 2005). Chlorambucil at equivalent concentrations also caused an increase in p21 levels, but without any initial drop, suggesting that the initial decrease may be a factor in avoidance of cell cycle arrest that leads to apoptosis in cells treated with 11β. The levels of p27 protein can be modulated by the ubiquitin-proteasome system in a reaction requiring ubiquitylation by the E3 ligase SCF^{Skp2} (Carrano et al. 1999; Lu et al. 2002). As such, Skp2 protein levels were also monitored following treatment with these compounds and shown to display a reciprocal relationship with p27 expression in all cases (Marquis et al. 2005).

It has been shown that high concentrations of androgens can induce p27 accumulation associated with Skp2 degradation in LNCaP cells, and this provides a reasonable explanation for the effects on these two proteins (Tsihlias et al. 2000; Lu et al. 2002). However, there may be something unique either about the linkage between an androgen and a DNA damaging agent, or about this particular steroid structure, because RU-486, either alone or in combination with chlorambucil, is unable to elicit an increase in p27 levels.

11β Has Impressive Ability to Prevent Growth of LNCaP Xenograft Tumors

It was next demonstrated that 11β possesses impressive activity in preventing growth of LNCaP xenograft tumors implanted in NIH Swiss *nu/nu* mice, while demonstrating minimal side effects of toxicity (~10% weight loss) (Figure 1.9) (Marquis et al. 2005). Treatment consisted of a 45-day, seven course regimen of five-day cycles, with a daily dose of 30 mg/kg injected intraperitoneally. Compared to vehicle, this treatment regimen resulted in a 90% inhibition of growth on the final day of study ($p < 0.0001$) and provides a solid foundation for continued studies into the mechanisms responsible for tumor-specific growth inhibition.

An additional study was performed to determine the nature and quantity of DNA adducts formed by 11β, both in tissue culture cells, as well as in tumors and livers of mice treated with this compound (Hillier et al. 2006). First, [^{14}C]-11β was used to measure bio-distribution in treated mice. 11β was shown to reach concentrations as high as 128 μM in the blood within 15 minutes before quickly decreasing with a $t_{1/2}$ of 1.3 hrs, but remained above 10 μM even 24 hrs after treatment. It was also shown that the compound remained primarily intact for at least 4 hrs following treatment, though products eluting more quickly from HPLC consistent with metabolites do appear. The compound was well distributed, appearing most concentrated in the liver, intestine, spleen, lung, and fat. It began to accumulate rapidly in feces after 4 hrs, consistent with biliary excretion (Hillier et al., 2006).

11β-DNA adducts were detected and quantified *in vitro*, in cell culture, and *in vivo*. First, 11β was allowed to react with salmon sperm DNA, which was then subjected to acid hydrolysis and analyzed by HPLC. A single peak eluting earlier than parent compound was isolated and analyzed by electrospray-ionization mass spectrometry (ESI-MS), finding a molecule with *m/z* of 813.5, consistent with a structure of 11β having one chloroethyl arm adducted to guanine and the other hydrolyzed by water (Hillier et al. 2006). Next, 11β was used to treat LNCaP cells growing in culture. After 6 hrs of incubation, DNA was isolated, hydrolyzed, and analyzed by ESI-MS, finding the same 813.5 *m/z* molecular species. Different concentrations of [^{14}C]-11β were then used to treat LNCaP cells for various periods of time before isolating DNA. This DNA was analyzed by accelerator mass spectrometry (AMS), allowing several orders of magnitude better sensitivity than traditional scintillation counting. Adduct quantities detected were directly proportional to concentration of [^{14}C]-11β in tissue culture media, producing from 0.3 to 1.0 adducts per 10^6 bases within 4 hrs (Hillier et al. 2006). Furthermore, these adducts continued to accumulate after 10 μM treatment at a rate of 0.25 adducts per 10^6 base pairs per hour.

Adduct formation in liver and xenografted LNCaP tumors was also assessed. First, unlabeled 11β was used in a 45 mg/kg single intraperitoneal (IP) dose before isolating liver sample four hrs later. DNA was isolated, hydrolyzed, and analyzed by

ESI-MS as with *in vitro* samples, once again detecting a species of m/z 813.5 consistent with a guanine mono-adduct (Hillier et al. 2006). [^{14}C]-11β was next used to treat tumor bearing mice at a concentration of 50 mg/kg for 4 hrs. Liver and tumor were both isolated before purifying DNA and analyzing by AMS. Adduct levels were determined to be ~10x higher in liver than tumor. However, the level of adducts detected in LNCaP tumors was determined to be ~0.2 adducts per 10^6 base pairs, similar to the quantity produced in cultured cells treated with 2.5 μM 11β for the same duration (Hillier et al. 2006).

Finally, due to the significantly higher level of adduct formation occurring in mouse liver, blood serum levels of four markers of hepatotoxicity were measured. At the therapeutically effective dose of 30 mg/kg, none of these markers was affected, although higher doses did cause changes consistent with hepatotoxicity. Due to the low overt toxicity seen over a 45-day seven-course regimen of treatment with 30 mg/kg (Marquis et al. 2005), there is little collective cause for concern that hepatotoxicity is problematic.

Based on these studies, the important conclusions to be drawn are that: 1) 11β has good bioavailability, reaching concentrations in blood even greater than those toxic to LNCaP cells in culture, 2) 11β forms adducts with guanine both in cultured cells and *in vivo* and to a similar extent in each, demonstrating relatively similar levels of compound getting to cells in each scenario, and most importantly 3) 11β is selectively toxic to the LNCaP tumor cells growing in the mouse, and not the mouse itself.

No extensive testing was conducted with the 11β compounds in order to determine the level of involvement of AR, as was performed with the 2PI and E2-7α compounds. However, unpublished results from Dr. Robert Croy (Figure 1.10) demonstrate that among three cell lines (LNCaP, AR(+); PC3, AR(-); DU145, AR(-)), there is enhanced toxicity toward the AR positive LNCaP cells.

My work presented here will more rigorously address the involvement of AR in the mechanism of toxicity of 11β, by using isogenic cell lines altered only in expression of AR, by experiments using competition for binding to AR with a high-affinity ligand for the AR, and by synthesis of an 11β analogue with reduced affinity to AR. The work explores the nature of interaction between 11β and AR within tissue culture cells, finding

that 11β causes AR redistribution to a nuclear compartment and binding at promoters of AR target genes, but also antagonizes AR mediated transcription and enhances receptor degradation. This work will also address potential explanations for the toxicity caused by 11β that is clearly independent of AR status, by way of gene expression microarray profiling of LNCaP cells treated with 11β, 11β-dimethoxy, and other control compounds.

Androgen Receptor Structural Organization

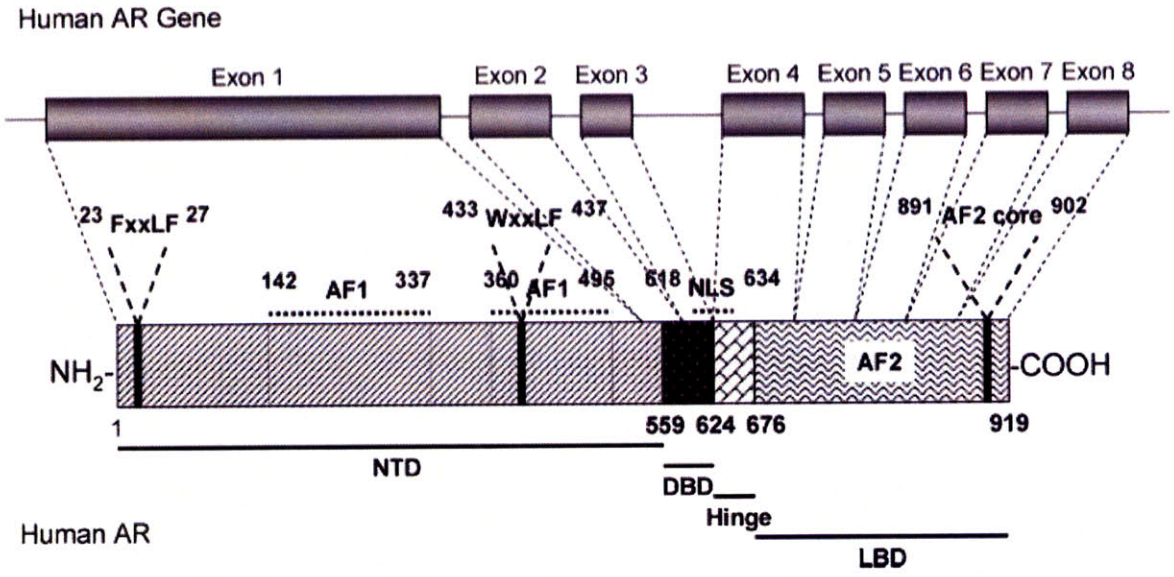

Fig 1.1 Organization and Structure of the Androgen Receptor. Schematic organization of the AR gene and protein showing functional domains (reprinted with permission from Gao et al. 2005, Chem. Rev. 105, 3352).

Androgen Receptor Ligand Binding Domain Structure

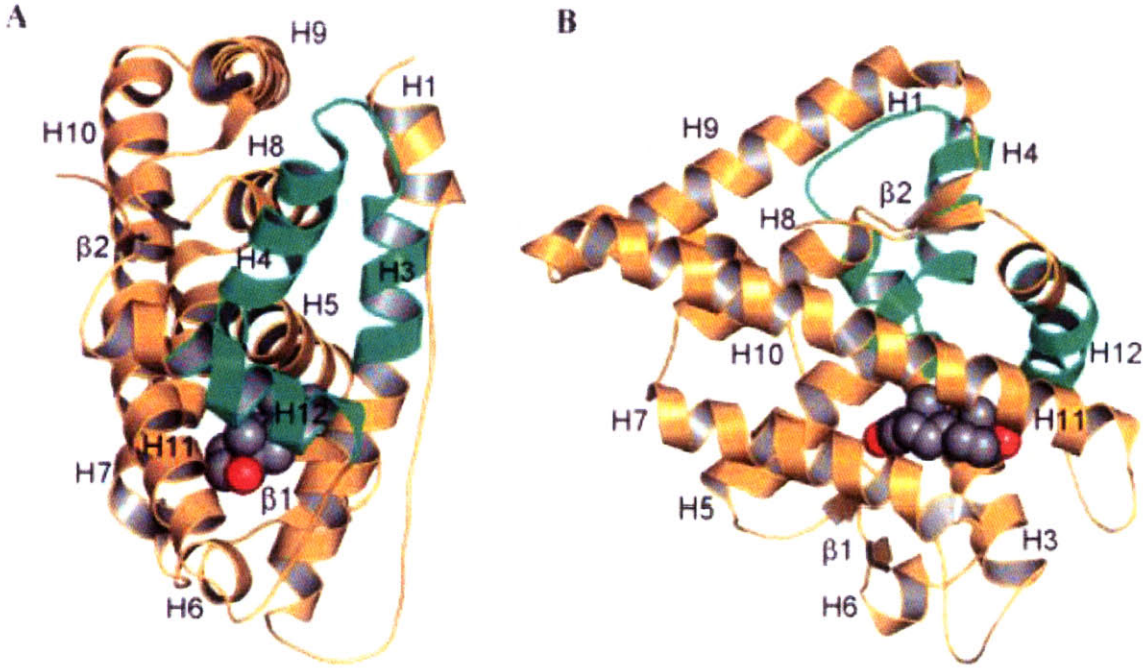

Fig 1.2 Crystal structure of AR ligand binding domain with DHT bound. Structure is based on 1I37.pdb **A.** Front view; **B.** Ligand view (reprinted with permission from Gao et al. 2005, Chem. Rev. 105, 3352)

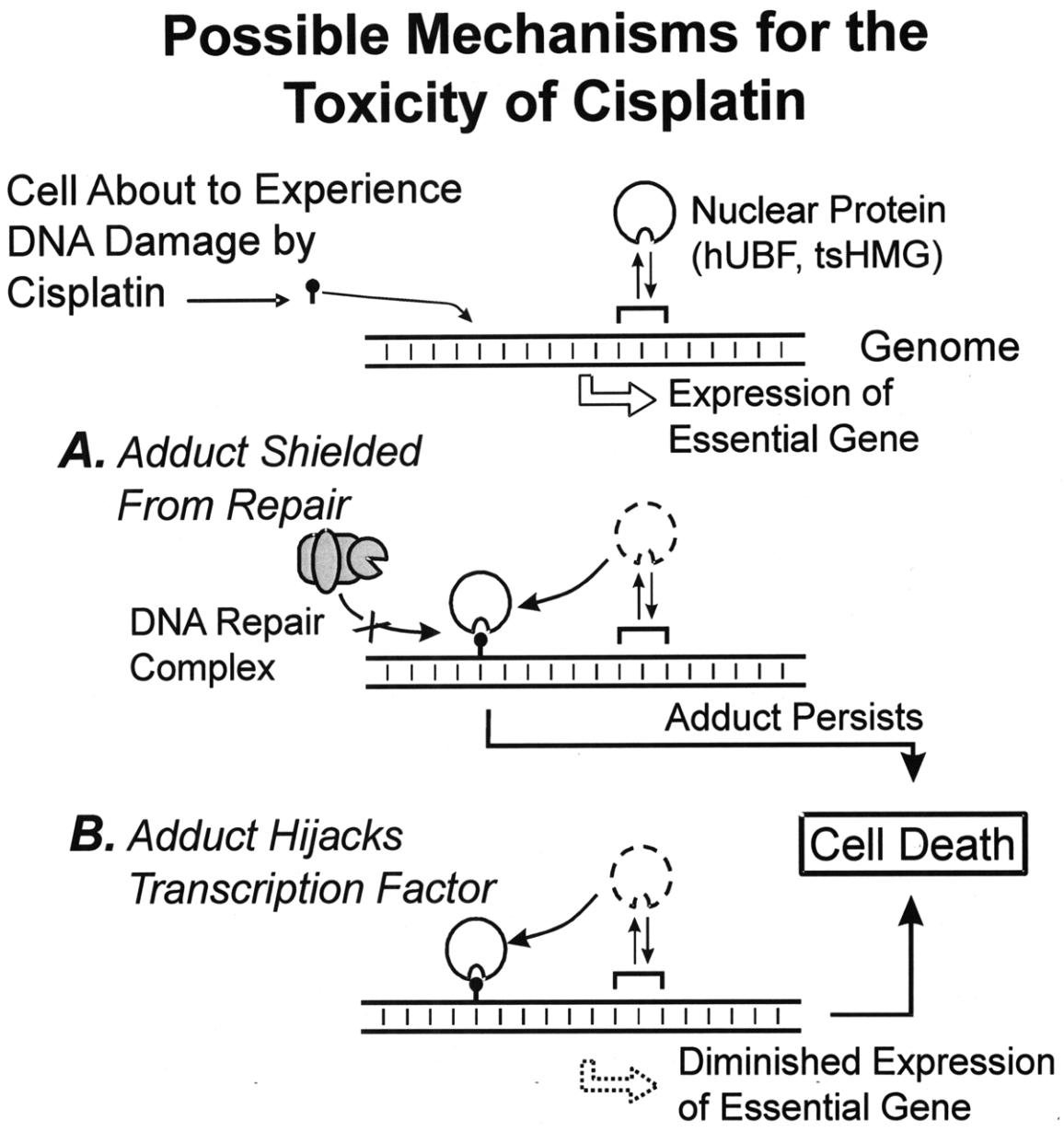

Fig 1.3 The impressive toxicity of cisplatin towards testicular cancer may be explained by the mechanisms shown. **A.** Repair shielding: Cisplatin forms sites of DNA damage which are capable of recruiting binding of specific proteins. In this manner, a damage site will be less accessible by DNA repair enzymes. **B.** Transcription factor hijacking: In some cases (i.e. hUBF), the protein which binds to sites of DNA damage is a transcription factor. When affinity of DNA adducts is similar to the affinity of this transcription factor for its response element (hUBF Kd is 60 pM and 18 pM, respectively), there will be diminution in its ability to drive transcription, and this can increase toxicity. Figure reprinted with permission from Rink et al. 1996.

Relevant Structures

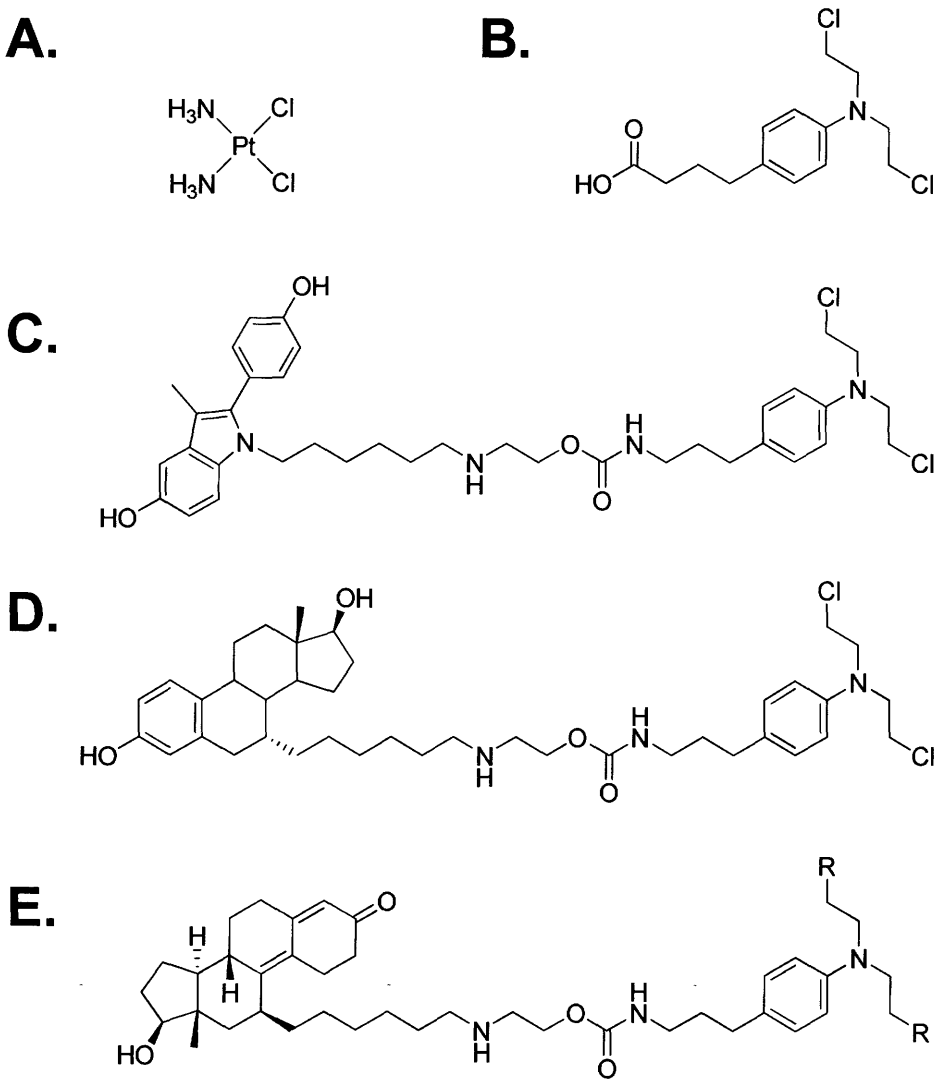

Fig 1.4 Structures of compounds relevant to text
A. *cis*-Diamminedichloroplatinum (II) (cisplatin) **B.** Chlorambucil **C.** 2PI-C6NC2-mustard (2PI) **D.** E2-7α-C6NC2-mustard (E2-7α) **E.** 11β-Compounds; 11β, R=Cl; 11β-Dimethoxy, R=OCH_3

Structure and Binding Affinity for the Estrogen Receptor of 2-Phenyl-Indole Derivatives

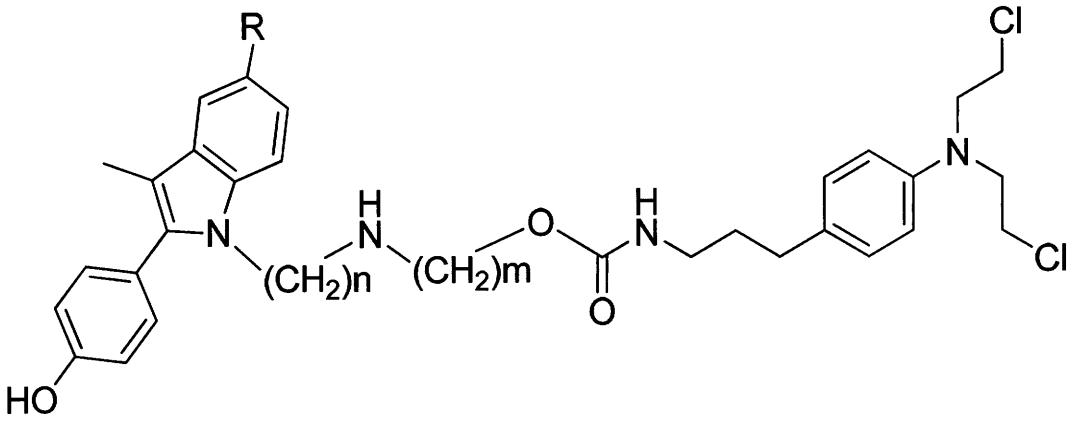

Mustard	m	n	R	RBA
2PI-C3NC3	3	3	OH	0
2PI-C5-NC3	3	5	OH	0.6
2PI-C6NC2	2	6	OH	7.1
2PI(OH)-C6NC2	2	6	H	0.1

Fig 1.5 Structures of 2-phenyl-indole aniline mustard conjugates and their corresponding relative binding affinities (RBA) for the ER.

Structure of Estrogen Receptor Ligand Binding Domain Complexed with Antagonist ICI 164384

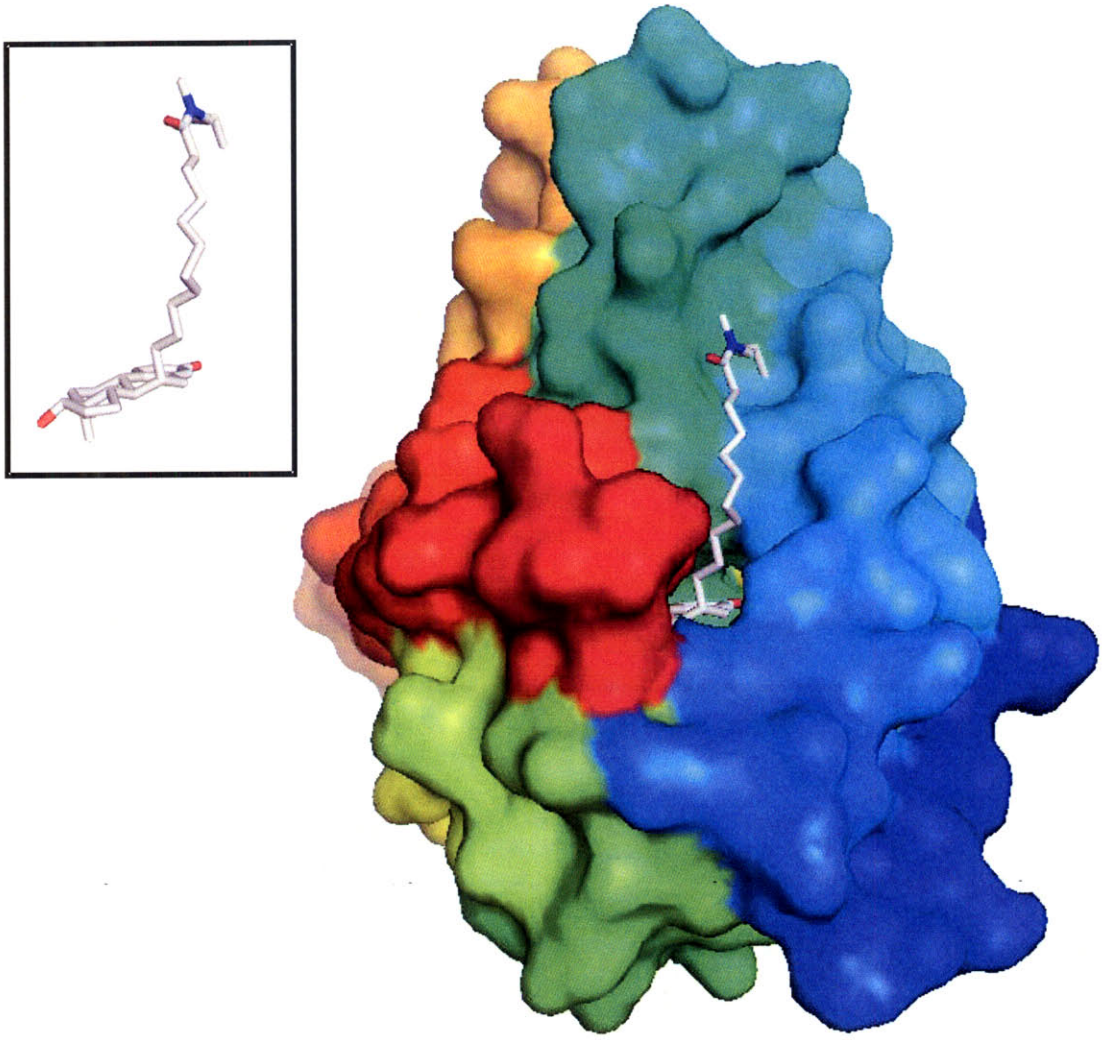

Fig 1.6 Surface representation of ER-LBD complexed with ICI 164384, colored by helix. The 7α linkage and steric bulk forces it to bind in an "upside-down" configuration from estradiol and displaces helix 12, making it invisible in the structure. (Based on 1HJ1.pdb, Pike et al. 2001 Structure 9, 145-153)

Chemical Structures of E2-7α Derivatives

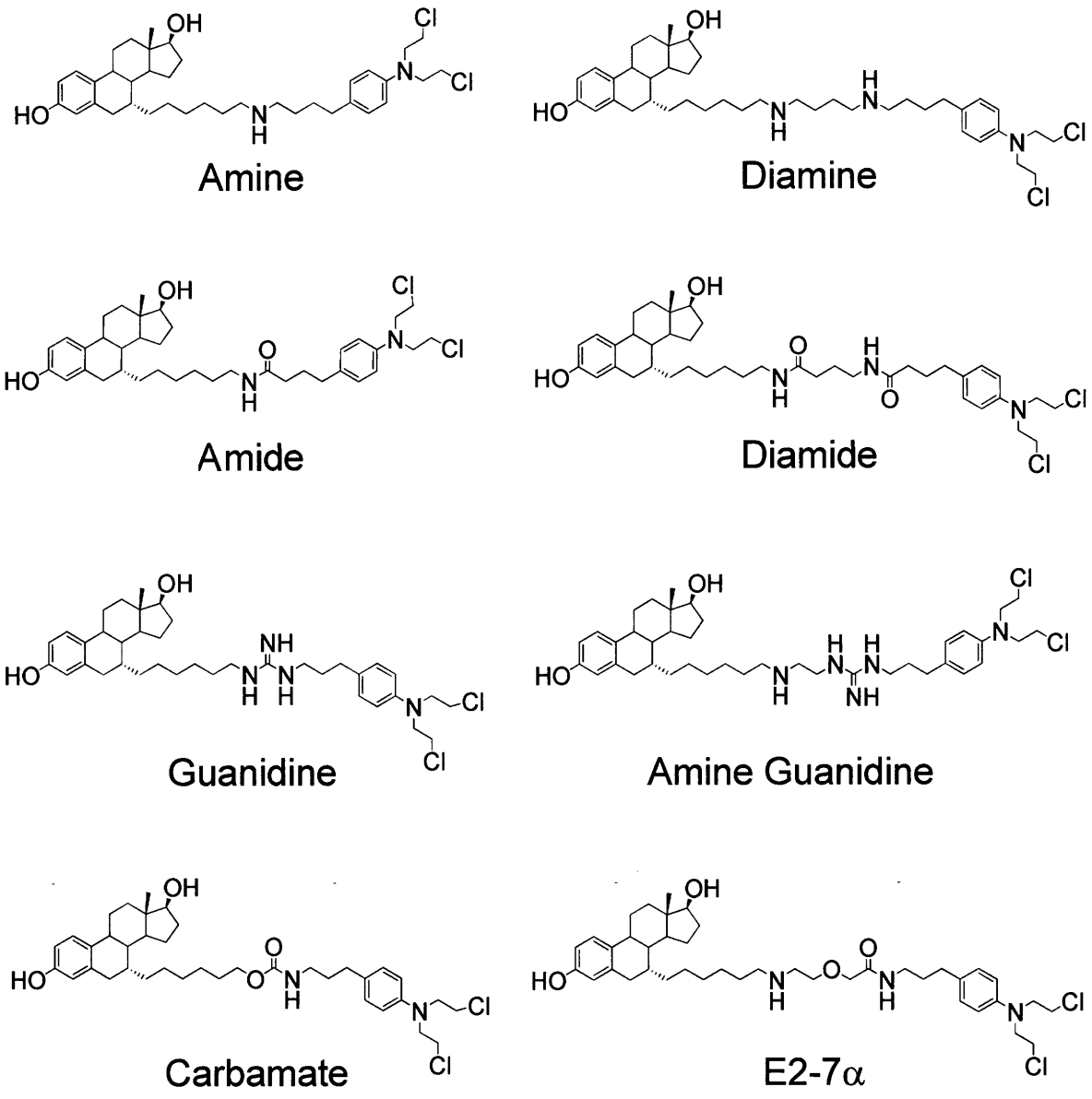

Fig 1.7 Chemical structures of E2-7α derivatives (Sharma et al. 2004).

11β and 11β-dimethoxy have High Affinity for the Androgen Receptor

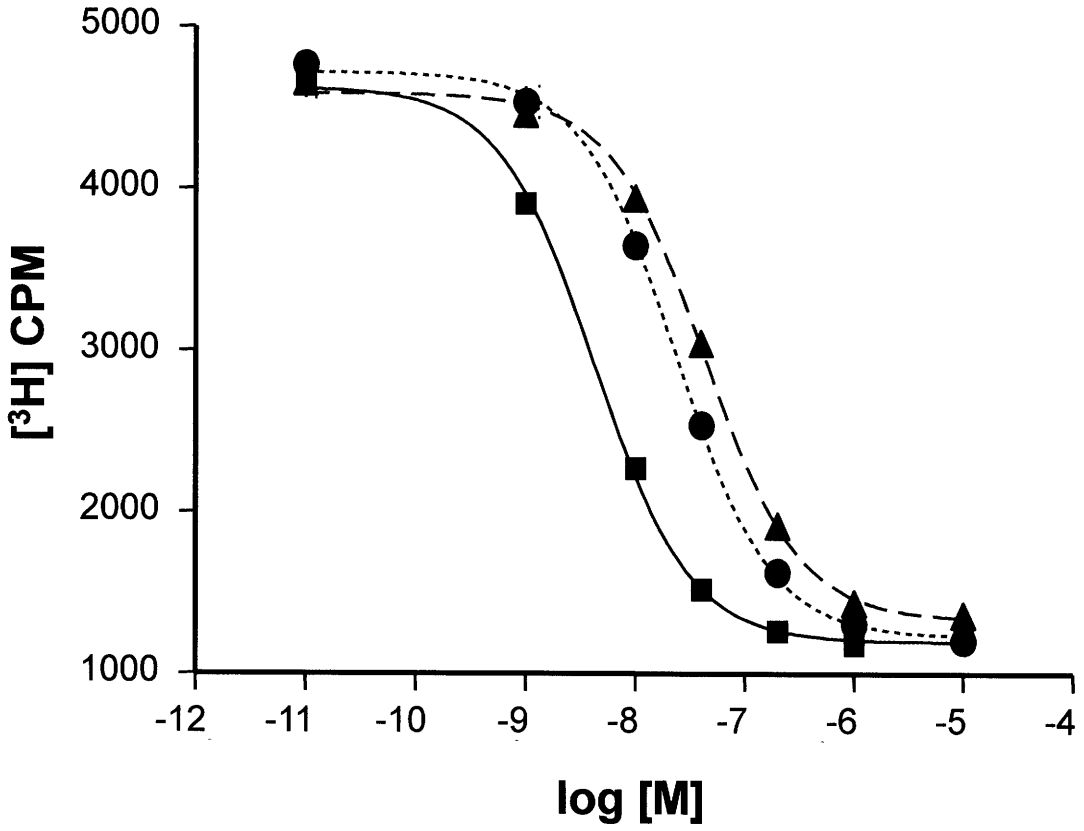

Fig 1.8 Relative binding affinity of 11β compounds for the AR. The affinity of 11β (–▲–) and 11β-dimethoxy (··●··) are compared to the synthetic androgen R1881 (–■–). Both 11β compounds have similar affinity for the receptor. Figure courtesy of Dr. Shawn Hillier.

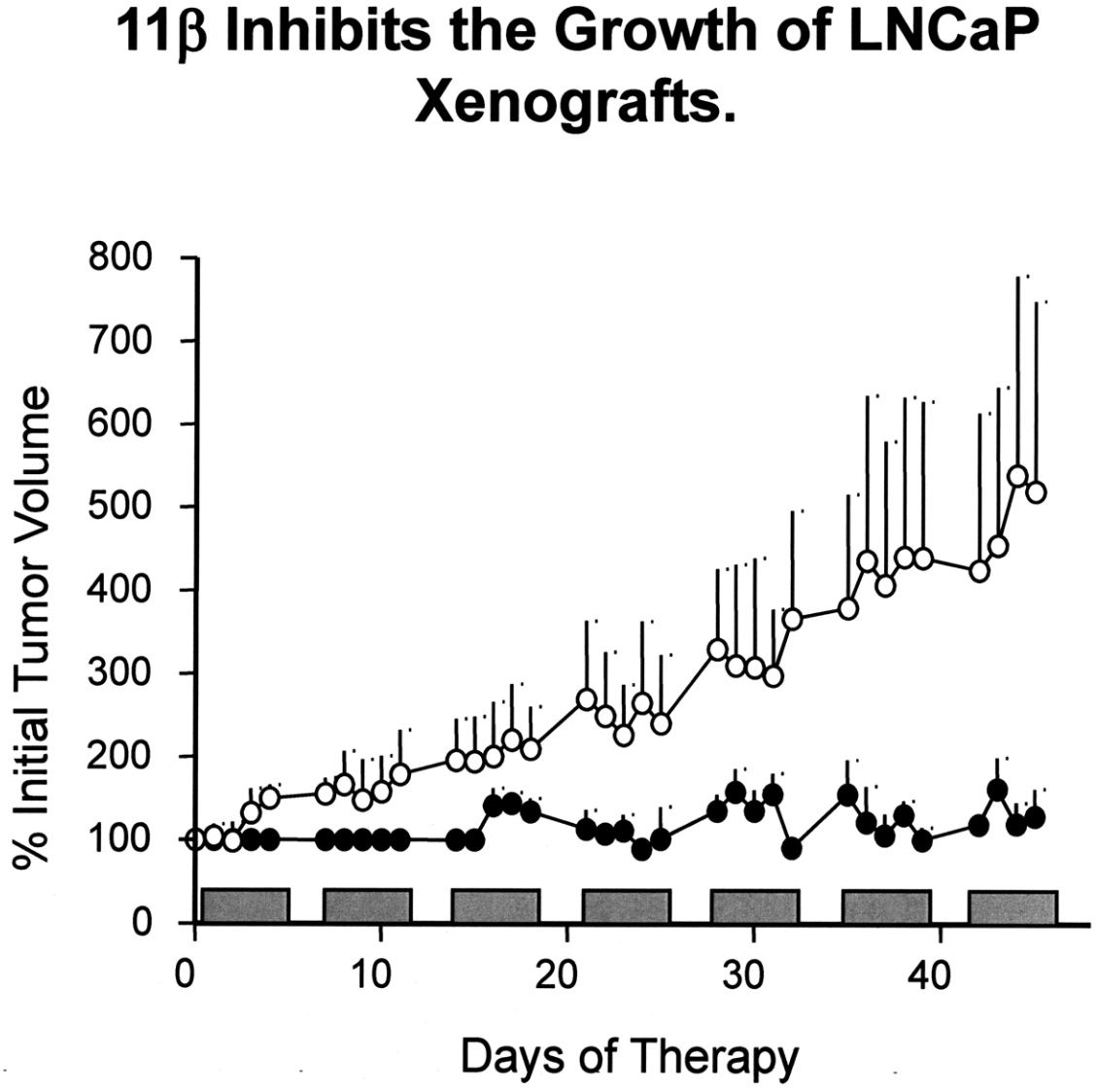

Fig 1.9 11β therapy of LNCaP xenografts in mice. Groups of 5 mice in each group were treated with either 11β (●)or with vehicle (○). A paired t-test provided a p-value < 0.0001. Gray bars indicate treatment times (5 days on, 2 days off). Figure courtesy of Dr. Shawn Hillier.

AR (+) LNCaP Cells are More Sensitive to 11β than AR (-) Cell Lines

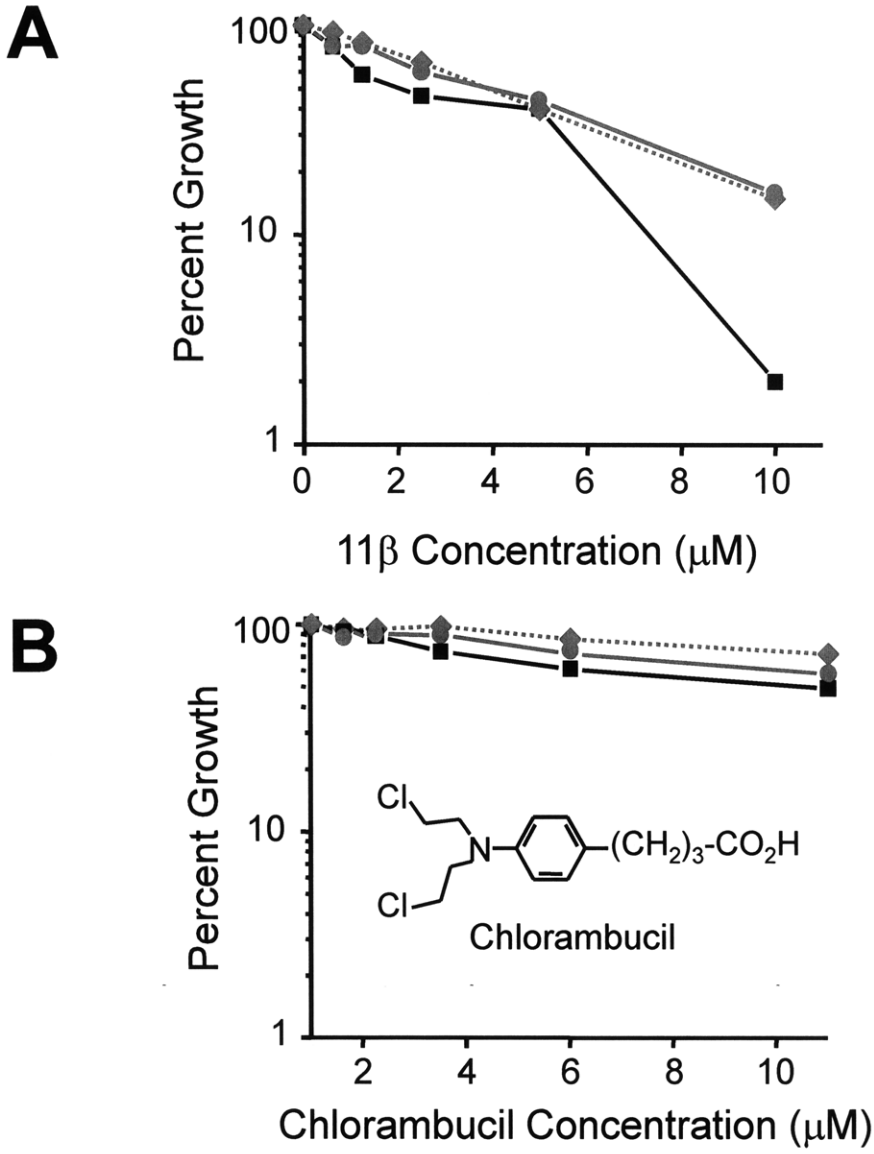

Fig 1.10 Prostate cancer cells exposed to 11β **(A)** or chlorambucil **(B)** at concentrations shown. The AR (+) LNCaP cell line (—■—) shows greatest sensitivity to 11β, while PC-3 (—●—) and DU-145 (···◆···), AR (-) cell lines, are less sensitive. Each cell line shows similar sensitivity to the DNA damaging agent, chlorambucil. Figure courtesy of Dr. Robert Croy.

References

Abate-Shen, C., and Shen, M. M. (2000). Molecular genetics of prostate cancer. Genes Dev *14*, 2410-34.

Adlercreutz, H., and Mazur, W. (1997). Phyto-oestrogens and Western diseases. Ann Med *29*, 95-120.

Akaboshi, M., Kawai, K., Maki, H., Akuta, K., Ujeno, Y., and Miyahara, T. (1992). The number of platinum atoms binding to DNA, RNA and protein molecules of HeLa cells treated with cisplatin at its mean lethal concentration. Jpn J Cancer Res *83*, 522-6.

American Cancer Society (2007). Cancer Facts and Figures 2007 (Atlanta, GA: American Cancer Society).

Andrews, P. A. (1994). Mechanisms of acquired resistance to cisplatin. Cancer Treat Res *73*, 217-48.

von Angerer, E., Prekajac, J., and Strohmeier, J. (1984). 2-Phenylindoles. Relationship between structure, estrogen receptor affinity, and mammary tumor inhibiting activity in the rat. J Med Chem *27*, 1439-47.

Anzick, S. L., Kononen, J., Walker, R. L., Azorsa, D. O., Tanner, M. M., Guan, X. Y., Sauter, G., Kallioniemi, O. P., Trent, J. M., and Meltzer, P. S. (1997). AIB1, a steroid receptor coactivator amplified in breast and ovarian cancer. Science *277*, 965-8.

Balk, S. P., Ko, Y., and Bubley, G. J. (2003). Biology of Prostate-Specific Antigen. J Clin Oncol *21*, 383-391.

Bancroft, D. P., Lepre, C. A., and Lippard, S. J. (1990). Platinum-195 NMR kinetic and mechanistic studies of cis- and trans-diamminedichloroplatinum(II) binding to DNA. Journal of the American Chemical Society *112*, 6860-6871.

Baselga, J. (2001). Clinical trials of Herceptin(trastuzumab). Eur J Cancer *37 Suppl 1*, S18-24.

Berry, R., Schaid, D. J., Smith, J. R., French, A. J., Schroeder, J. J., McDonnell, S. K., Peterson, B. J., Wang, Z. Y., Carpten, J. D., Roberts, S. G., et al. (2000). Linkage analyses at the chromosome 1 loci 1q24-25 (HPC1), 1q42.2-43 (PCAP), and 1p36 (CAPB) in families with hereditary prostate cancer. Am J Hum Genet *66*, 539-46.

Bos, J. L. (1989). ras oncogenes in human cancer: a review. Cancer Res *49*, 4682-9.

Bostwick, D. G. (1994). Prostate-specific antigen. Current role in diagnostic pathology of prostate cancer. Am J Clin Pathol *102*, S31-7.

Bowler, J., Lilley, T. J., Pittam, J. D., and Wakeling, A. E. (1989). Novel steroidal pure antiestrogens. Steroids *54*, 71-99.

Boyle, P., and Levin, B. eds. (2008). World Cancer Report 2008 (WHO-IARC).

Brabec, V., and Leng, M. (1993). DNA interstrand cross-links of trans-diamminedichloroplatinum(II) are preferentially formed between guanine and complementary cytosine residues. Proceedings of the National Academy of Sciences of the United States of America *90*, 5345-5349.

Breslow, N., Chan, C. W., Dhom, G., Drury, R. A., Franks, L. M., Gellei, B., Lee, Y. S., Lundberg, S., Sparke, B., Sternby, N. H., et al. (1977). Latent carcinoma of prostate at autopsy in seven areas. The International Agency for Research on Cancer, Lyons, France. Int J Cancer *20*, 680-8.

Brinkmann, A. O., Blok, L. J., de Ruiter, P. E., Doesburg, P., Steketee, K., Berrevoets, C. A., and Trapman, J. (1999). Mechanisms of androgen receptor activation and function. The Journal of Steroid Biochemistry and Molecular Biology *69*, 307-313.

Brix, H. P., Berger, M. R., Schneider, M. R., Tang, W. C., and Eisenbrand, G. (1990). Androgen-linked alkylating agents: biological activity in methylnitrosourea-induced rat mammary carcinoma. J Cancer Res Clin Oncol *116*, 538-49.

Brown, S. J., Kellett, P. J., and Lippard, S. J. (1993). Ixr1, a yeast protein that binds to platinated DNA and confers sensitivity to cisplatin. Science *261*, 603-5.

van Brussel, J. P., Busstra, M. B., Lang, M. S., Catsburg, T., Schröder, F. H., and Mickisch, G. H. (2000). A phase II study of temozolomide in hormone-refractory prostate cancer. Cancer Chemother Pharmacol *45*, 509-12.

Brzozowski, A. M., Pike, A. C., Dauter, Z., Hubbard, R. E., Bonn, T., Engström, O., Ohman, L., Greene, G. L., Gustafsson, J. A., and Carlquist, M. (1997). Molecular basis of agonism and antagonism in the oestrogen receptor. Nature *389*, 753-8.

Buchanan, G., Ricciardelli, C., Harris, J. M., Prescott, J., Yu, Z. C., Jia, L., Butler, L. M., Marshall, V. R., Scher, H. I., Gerald, W. L., et al. (2007). Control of Androgen Receptor Signaling in Prostate Cancer by the Cochaperone Small Glutamine Rich Tetratricopeptide Repeat Containing Protein {alpha}. Cancer Res *67*, 10087-10096.

Bucourt, R., Vignau, M., and Torelli, V. (1978). New biospecific adsorbents for the purification of estradiol receptor. J Biol Chem *253*, 8221-8.

Carpten, J., Nupponen, N., Isaacs, S., Sood, R., Robbins, C., Xu, J., Faruque, M., Moses, T., Ewing, C., Gillanders, E., et al. (2002). Germline mutations in the ribonuclease L gene in families showing linkage with HPC1. Nat Genet *30*, 181-4.

Carrano, A. C., Eytan, E., Hershko, A., and Pagano, M. (1999). SKP2 is required for ubiquitin-mediated degradation of the CDK inhibitor p27. Nat Cell Biol *1*, 193-199.

Catalona, W. J., Smith, D. S., Ratliff, T. L., Dodds, K. M., Coplen, D. E., Yuan, J. J., Petros, J. A., and Andriole, G. L. (1991). Measurement of prostate-specific antigen in serum as a screening test for prostate cancer. N Engl J Med *324*, 1156-61.

Chamberlain, N. L., Driver, E. D., and Miesfeld, R. L. (1994). The length and location of CAG trinucleotide repeats in the androgen receptor N-terminal domain affect transactivation function. Nucleic Acids Res *22*, 3181-6.

Chang, C. S., Kokontis, J., and Liao, S. T. (1988). Molecular cloning of human and rat complementary DNA encoding androgen receptors. Science *240*, 324-6.

Cheng, S., Brzostek, S., Lee, S. R., Hollenberg, A. N., and Balk, S. P. (2002). Inhibition of the Dihydrotestosterone-Activated Androgen Receptor by Nuclear Receptor Corepressor. Mol Endocrinol *16*, 1492-1501.

Cheung-Flynn, J., Prapapanich, V., Cox, M. B., Riggs, D. L., Suarez-Quian, C., and Smith, D. F. (2005). Physiological role for the cochaperone FKBP52 in androgen receptor signaling. Mol Endocrinol *19*, 1654-66.

Chmelar, R., Buchanan, G., Need, E. F., Tilley, W., and Greenberg, N. M. (2007). Androgen receptor coregulators and their involvement in the development and progression of prostate cancer. International Journal of Cancer *120*, 719-733.

Cho, C. Y., Moran, E. J., Cherry, S. R., Stephans, J. C., Fodor, S. P., Adams, C. L., Sundaram, A., Jacobs, J. W., and Schultz, P. G. (1993). An unnatural biopolymer. Science *261*, 1303-5.

Colombel, M., Symmans, F., Gil, S., O'Toole, K. M., Chopin, D., Benson, M., Olsson, C. A., Korsmeyer, S., and Buttyan, R. (1993). Detection of the apoptosis-suppressing oncoprotein bc1-2 in hormone-refractory human prostate cancers. Am J Pathol *143*, 390-400.

Colvin, M., Brundrett, R. B., Kan, M. N., Jardine, I., and Fenselau, C. (1976). Alkylating properties of phosphoramide mustard. Cancer Res *36*, 1121-6.

Concato, J., Wells, C. K., Horwitz, R. I., Penson, D., Fincke, G., Berlowitz, D. R., Froehlich, G., Blake, D., Vickers, M. A., Gehr, G. A., et al. (2006). The Effectiveness of Screening for Prostate Cancer: A Nested Case-Control Study. Arch Intern Med *166*, 38-43.

Coste, F., Malinge, J. M., Serre, L., Shepard, W., Roth, M., Leng, M., and Zelwer, C. (1999). Crystal structure of a double-stranded DNA containing a cisplatin interstrand cross-link at 1.63 A resolution: hydration at the platinated site. Nucleic Acids Res *27*, 1837-46.

Craft, N., Chhor, C., Tran, C., Belldegrun, A., DeKernion, J., Witte, O. N., Said, J., Reiter, R. E., and Sawyers, C. L. (1999). Evidence for clonal outgrowth of androgen-independent prostate cancer cells from androgen-dependent tumors through a two-step process. Cancer Res *59*, 5030-6.

Craft, N., Shostak, Y., Carey, M., and Sawyers, C. L. (1999). A mechanism for hormone-independent prostate cancer through modulation of androgen receptor signaling by the HER-2/neu tyrosine kinase. Nat Med *5*, 280-5.

Craig Hall, M., Navone, N. M., Troncoso, P., Pollack, A., Zagars, G. K., von Eschenbach, A. C., Conti, C. J., and Chung, L. W. (1995). Frequency and characterization of p53 mutations in clinically localized prostate cancer. Urology *45*, 470-475.

Culig, Z., Hobisch, A., Cronauer, M. V., Radmayr, C., Trapman, J., Hittmair, A., Bartsch, G., and Klocker, H. (1994). Androgen receptor activation in prostatic tumor cell lines by insulin-like growth factor-I, keratinocyte growth factor, and epidermal growth factor. Cancer Res *54*, 5474-8.

DaSilva, J. N., and van Lier, J. E. (1990). Synthesis and structure-affinity of a series of 7 alpha-undecylestradiol derivatives: a potential vector for therapy and imaging of estrogen-receptor-positive cancers. J Med Chem *33*, 430-4.

De Silva, I. U., McHugh, P. J., Clingen, P. H., and Hartley, J. A. (2000). Defining the roles of nucleotide excision repair and recombination in the repair of DNA interstrand cross-links in mammalian cells. Mol Cell Biol *20*, 7980-90.

Deutsch, E., Maggiorella, L., Eschwege, P., Bourhis, J., Soria, J. C., and Abdulkarim, B. (2004). Environmental, genetic, and molecular features of prostate cancer. Lancet Oncol *5*, 303-13.

Dubbink, H. J., Hersmus, R., Verma, C. S., van der Korput, H. A. G. M., Berrevoets, C. A., van Tol, J., Ziel-van der Made, A. C. J., Brinkmann, A. O., Pike, A. C. W., and Trapman, J. (2004). Distinct recognition modes of FXXLF and LXXLL motifs by the androgen receptor. Mol Endocrinol *18*, 2132-50.

Eisenbrand, G., Berger, M. R., Brix, H. P., Fischer, J. E., Mühlbauer, K., Nowrousian, M. R., Przybilski, M., Schneider, M. R., Stahl, W., and Tang, W. (1989). Nitrosoureas. Modes of action and perspectives in the use of hormone receptor affinity carrier molecules. Acta Oncol *28*, 203-11.

Emmert-Buck, M. R., Vocke, C. D., Pozzatti, R. O., Duray, P. H., Jennings, S. B., Florence, C. D., Zhuang, Z., Bostwick, D. G., Liotta, L. A., and Linehan, W. M. (1995). Allelic loss on chromosome 8p12-21 in microdissected prostatic intraepithelial neoplasia. Cancer Res *55*, 2959-62.

Fernández, P. L., Arce, Y., Farré, X., Martínez, A., Nadal, A., Rey, M. J., Peiró, N., Campo, E., and Cardesa, A. (1999). Expression of p27/Kip1 is down-regulated in human prostate carcinoma progression. J. Pathol *187*, 563-566.

Fernö, M., Borg, A., Johansson, U., Norgren, A., Olsson, H., Rydén, S., and Sellberg, G. (1990). Estrogen and progesterone receptor analyses in more than 4,000 human breast cancer samples. A study with special reference to age at diagnosis and stability of analyses. Southern Swedish Breast Cancer Study Group. Acta Oncol *29*, 129-35.

Fichtinger-Schepman, A. M., van Oosterom, A. T., Lohman, P. H., and Berends, F. (1987). cis-Diamminedichloroplatinum(II)-induced DNA adducts in peripheral leukocytes from seven cancer patients: quantitative immunochemical detection of the adduct induction and removal after a single dose of cis-diamminedichloroplatinum(II). Cancer Res *47*, 3000-4.

Fojo, T. (2001). Cancer, DNA Repair Mechanisms, and Resistance to Chemotherapy. J. Natl. Cancer Inst. *93*, 1434-1436.

Fouchet, M., Guittet, E., Cognet, J. A. H., Kozelka, J., Gauthier, C., Bret, M. L., Zimmermann, K., and Chottard, J. (1997). Structure of a nonanucleotide duplex cross-linked by cisplatin at an ApG sequence. Journal of Biological Inorganic Chemistry *2*, 83-92.

Fredholm, B., Gunnarsson, K., Jensen, G., and Müntzing, J. (1978). Mammary tumour inhibition and subacute toxicity in rats of prednimustine and of its molecular components chlorambucil and prednisolone. Acta Pharmacol Toxicol (Copenh) *42*, 159-63.

Fuhrmann, U., Hess-Stumpp, H., Cleve, A., Neef, G., Schwede, W., Hoffmann, J., Fritzemeier, K., and Chwalisz, K. (2000). Synthesis and Biological Activity of a Novel, Highly Potent Progesterone Receptor Antagonist. Journal of Medicinal Chemistry *43*, 5010-5016.

Garcia, M., Jemal, A., Ward, E., Center, M., Hao, Y., Siegel, R., and Thun, M. (2007). Global Cancer Facts and Figures 2007 (Atlanta, GA: American Cancer Society).

van Garderen, C. J., and van Houte, L. P. (1994). The solution structure of a DNA duplex containing the cis-Pt(NH3)2[d(-GTG-)-N7(G),N7(G)] adduct, as determined with high-field NMR and molecular mechanics/dynamics. Eur J Biochem *225*, 1169-79.

Gelasco, A., and Lippard, S. J. (1998). NMR solution structure of a DNA dodecamer duplex containing a cis-diammineplatinum(II) d(GpG) intrastrand cross-link, the major adduct of the anticancer drug cisplatin. Biochemistry *37*, 9230-9.

Gioeli, D., Ficarro, S. B., Kwiek, J. J., Aaronson, D., Hancock, M., Catling, A. D., White, F. M., Christian, R. E., Settlage, R. E., Shabanowitz, J., et al. (2002). Androgen Receptor Phosphorylation. Regulation and Identification of the Phosphorylation Sites. J. Biol. Chem. *277*, 29304-29314.

Giovannucci, E., Stampfer, M. J., Krithivas, K., Brown, M., Brufsky, A., Talcott, J., Hennekens, C. H., and Kantoff, P. W. (1997). The CAG repeat within the androgen receptor gene and its relationship to prostate cancer. Proceedings of the National Academy of Sciences of the United States of America *94*, 3320-3323.

Gregory, C. W., Hamil, K. G., Kim, D., Hall, S. H., Pretlow, T. G., Mohler, J. L., and French, F. S. (1998). Androgen receptor expression in androgen-independent prostate cancer is associated with increased expression of androgen-regulated genes. Cancer Res *58*, 5718-24.

Grönberg, H. (2003). Prostate cancer epidemiology. The Lancet *361*, 859-864.

Haelens, A., Verrijdt, G., Callewaert, L., Peeters, B., Rombauts, W., and Claessens, F. (2001). Androgen-receptor-specific DNA binding to an element in the first exon of the human secretory component gene. Biochem J *353*, 611-20.

Hanahan, D., and Weinberg, R. A. (2000). The hallmarks of cancer. Cell *100*, 57-70.

Hannon, M. J., Green, P. S., Fisher, D. M., Derrick, P. J., Beck, J. L., Watt, S. J., Ralph, S. F., Sheil, M. M., Barker, P. R., Alcock, N. W., et al. (2006). An estrogen-platinum terpyridine conjugate: DNA and protein binding and cellular delivery. Chemistry *12*, 8000-13.

Harris, A. L. (1985). DNA repair and resistance to chemotherapy. Cancer Surv *4*, 601-24.

Hayes, R. B., Liff, J. M., Pottern, L. M., Greenberg, R. S., Schoenberg, J. B., Schwartz, A. G., Swanson, G. M., Silverman, D. T., Brown, L. M., Hoover, R. N., et al. (1995). Prostate cancer risk in U.S. blacks and whites with a family history of cancer. International Journal of Cancer *60*, 361-364.

He, B., Kemppainen, J. A., and Wilson, E. M. (2000). FXXLF and WXXLF Sequences Mediate the NH2-terminal Interaction with the Ligand Binding Domain of the Androgen Receptor. J. Biol. Chem. *275*, 22986-22994.

He, Q., Liang, C. H., and Lippard, S. J. (2000). Steroid hormones induce HMG1 overexpression and sensitize breast cancer cells to cisplatin and carboplatin. Proceedings of the National Academy of Sciences of the United States of America *97*, 5768-5772.

Herranz, M., and Esteller, M. (2007). DNA methylation and histone modifications in patients with cancer: potential prognostic and therapeutic targets. Methods Mol Biol *361*, 25-62.

Hillier, S. M., Marquis, J. C., Zayas, B., Wishnok, J. S., Liberman, R. G., Skipper, P. L., Tannenbaum, S. R., Essigmann, J. M., and Croy, R. G. (2006). DNA adducts formed by a novel antitumor agent 11{beta}-dichloro in vitro and in vivo. Mol Cancer Ther *5*, 977-984.

Hodgson, M. C., Shen, H. C., Hollenberg, A. N., and Balk, S. P. (2008). Structural basis for nuclear receptor corepressor recruitment by antagonist-liganded androgen receptor. Mol Cancer Ther *7*, 3187-3194.

Hollstein, M., Rice, K., Greenblatt, M. S., Soussi, T., Fuchs, R., Sørlie, T., Hovig, E., Smith-Sørensen, B., Montesano, R., and Harris, C. C. (1994). Database of p53 gene somatic mutations in human tumors and cell lines. Nucleic Acids Res. *22*, 3551–3555.

Holzbeierlein, J., Lal, P., LaTulippe, E., Smith, A., Satagopan, J., Zhang, L., Ryan, C., Smith, S., Scher, H., Scardino, P., et al. (2004). Gene expression analysis of human prostate carcinoma during hormonal therapy identifies androgen-responsive genes and mechanisms of therapy resistance. Am J Pathol *164*, 217-27.

Horner, M., Ries, L., Krapcho, M., Neyman, N., Aminou, R., Howlader, N., Altekruse, S., Feuer, E., Huang, L., Mariotto, A., et al. eds. (2009). SEER Cancer Statistics Review, 1975-2006 (Bethesda, MD: National Cancer Institute).

Hu, X., Li, Y., and Lazar, M. A. (2001). Determinants of CoRNR-Dependent Repression Complex Assembly on Nuclear Hormone Receptors. Mol Cell Biol. *21*, 1747–1758.

Huang, J. C., Zamble, D. B., Reardon, J. T., Lippard, S. J., and Sancar, A. (1994). HMG-domain proteins specifically inhibit the repair of the major DNA adduct of the anticancer drug cisplatin by human excision nuclease. Proceedings of the National Academy of Sciences of the United States of America *91*, 10394-10398.

Huang, L., Cronin, K. A., Johnson, K. A., Mariotto, A. B., and Feuer, E. J. (2008). Improved survival time: What can survival cure models tell us about population-based survival improvements in late-stage colorectal, ovarian, and testicular cancer? Cancer *112*, 2289-2300.

Hudson, M. A., Bahnson, R. R., and Catalona, W. J. (1989). Clinical use of prostate specific antigen in patients with prostate cancer. J Urol *142*, 1011-7.

Huggins, C., and Hodges, C. (1941). Studies on Prostatic Cancer I: The Effect of Castration, of Estrogen and of Androgen Injection on Serum Phosphatases in Metastatic Carcinoma of the Prostate. Cancer Res, 293-297.

Hurley, L. H. (2002). DNA and its associated processes as targets for cancer therapy. Nat Rev Cancer *2*, 188-200.

Hurwitz, H., Fehrenbacher, L., Novotny, W., Cartwright, T., Hainsworth, J., Heim, W., Berlin, J., Baron, A., Griffing, S., Holmgren, E., et al. (2004). Bevacizumab plus irinotecan, fluorouracil, and leucovorin for metastatic colorectal cancer. N Engl J Med *350*, 2335-42.

Isaacs, J. T. (1999). The biology of hormone refractory prostate cancer. Why does it develop? Urol Clin North Am *26*, 263-73.

Ittmann, M. M., and Wieczorek, R. (1996). Alterations of the retinoblastoma gene in clinically localized, stage B prostate adenocarcinomas. Human Pathology *27*, 28-34.

Jemal, A., Thun, M. J., et al. (2008). Annual Report to the Nation on the Status of Cancer, 1975-2005, Featuring Trends in Lung Cancer, Tobacco Use, and Tobacco Control. J. Natl. Cancer Inst. *100*, 1672-1694.

Jemal, A., Siegel, R., Ward, E., Hao, Y., Xu, J., Murray, T., and Thun, M. J. (2008). Cancer statistics, 2008. CA Cancer J Clin *58*, 71-96.

Jenster, G., van der Korput, H. A. G. M., and Trapman, J. (1995). Identification of Two Transcription Activation Units in the N-terminal Domain of the Human Androgen Receptor. J. Biol. Chem. *270*, 7341-7346.

Johnson, N. P., Hoeschele, J. D., and Rahn, R. O. (1980). Kinetic analysis of the in vitro binding of radioactive cis- and trans-dichlorodiammineplatinum(II) to DNA. Chem Biol Interact *30*, 151-69.

Jones, P. A., and Baylin, S. B. (2002). The fundamental role of epigenetic events in cancer. Nat Rev Genet *3*, 415-28.

Jordan, P., and Carmo-Fonseca, M. (1998). Cisplatin inhibits synthesis of ribosomal RNA in vivo. Nucl. Acids Res. *26*, 2831-2836.

Kang, Z., Pirskanen, A., Jänne, O. A., and Palvimo, J. J. (2002). Involvement of proteasome in the dynamic assembly of the androgen receptor transcription complex. J Biol Chem *277*, 48366-71.

Kartalou, M., and Essigmann, J. M. (2001). Recognition of cisplatin adducts by cellular proteins. Mutation Research/Fundamental and Molecular Mechanisms of Mutagenesis *478*, 1-21.

Killian, C. S., Yang, N., Emrich, L. J., Vargas, F. P., Kuriyama, M., Wang, M. C., Slack, N. H., Papsidero, L. D., Murphy, G. P., Chu, T. M., et al. (1985). Prognostic Importance of Prostate-specific Antigen for Monitoring Patients with Stages B2 to D1 Prostate Cancer. Cancer Res *45*, 886-891.

Knebel, N., and von Angerer, E. (1988). Platinum complexes with binding affinity for the estrogen receptor. J Med Chem *31*, 1675-9.

Krajewska, M., Krajewski, S., Epstein, J. I., Shabaik, A., Sauvageot, J., Song, K., Kitada, S., and Reed, J. C. (1996). Immunohistochemical analysis of bcl-2, bax, bcl-X, and mcl-1 expression in prostate cancers. Am J Pathol. *148*, 1567–1576.

Kubota, T., Koh, J., Yamada, Y., Oka, S., Enomoto, K., Ishibiki, K., Abe, O., Masui, O., and Asano, K. (1988). Mode of action of estra-1,3,5(10)-triene-3,17 beta-diol 3-benzoate 17-[4-(4-bis(2-chloroethyl)amino)phenyl)-1-oxobutoxy)acet ate) on human breast carcinoma xenografts in nude mice. Jpn J Cancer Res *79*, 1224-9.

van der Kwast, T. H., Schalken, J., Ruizeveld de Winter, J. A., van Vroonhoven, C. C., Mulder, E., Boersma, W., and Trapman, J. (1991). Androgen receptors in endocrine-therapy-resistant human prostate cancer. Int J Cancer *48*, 189-93.

Lam, H. Y., Ng, P. K., Goldenberg, G. J., and Wong, C. M. (1987). Estrogen receptor-binding affinity and cytotoxic activity of three new estrogen-nitrosourea conjugates in human breast cancer cell lines in vitro. Cancer Treat Rep *71*, 901-6.

Langley, E., Zhou, Z. X., and Wilson, E. M. (1995). Evidence for an anti-parallel orientation of the ligand-activated human androgen receptor dimer. J Biol Chem *270*, 29983-90.

Lawley, P. D., and Phillips, D. H. (1996). DNA adducts from chemotherapeutic agents. Mutat Res *355*, 13-40.

Leclercq, G., Devleeschouwer, N., and Heuson, J. C. (1983). Guide-lines in the design of new antiestrogens and cytotoxic-linked estrogens for the treatment of breast cancer. J Steroid Biochem *19*, 75-85.

Liao, G., Chen, L., Zhang, A., Godavarthy, A., Xia, F., Ghosh, J. C., Li, H., and Chen, J. D. (2003). Regulation of Androgen Receptor Activity by the Nuclear Receptor Corepressor SMRT. J. Biol. Chem. *278*, 5052-5061.

Lilja, H., Oldbring, J., Rannevik, G., and Laurell, C. B. (1987). Seminal vesicle-secreted proteins and their reactions during gelation and liquefaction of human semen. J Clin Invest. *80*, 281–285.

Lilja, H., Ulmert, D., Bjork, T., Becker, C., Serio, A. M., Nilsson, J., Abrahamsson, P., Vickers, A. J., and Berglund, G. (2007). Long-Term Prediction of Prostate Cancer Up to 25 Years Before Diagnosis of Prostate Cancer Using Prostate Kallikreins Measured at Age 44 to 50 Years. J Clin Oncol *25*, 431-436.

Lin, H., Altuwaijri, S., Lin, W., Kan, P., Collins, L. L., and Chang, C. (2002). Proteasome activity is required for androgen receptor transcriptional activity via regulation of androgen receptor nuclear translocation and interaction with coregulators in prostate cancer cells. J Biol Chem *277*, 36570-6.

Lin, H., Wang, L., Hu, Y., Altuwaijri, S., and Chang, C. (2002). Phosphorylation-dependent ubiquitylation and degradation of androgen receptor by Akt require Mdm2 E3 ligase. EMBO J *21*, 4037-48.

List, H. J., Lozano, C., Lu, J., Danielsen, M., Wellstein, A., and Riegel, A. T. (1999). Comparison of chromatin remodeling and transcriptional activation of the mouse mammary tumor virus promoter by the androgen and glucocorticoid receptor. Exp Cell Res *250*, 414-22.

Loeb, L. A., Bielas, J. H., Beckman, R. A., and Bodmer, I. W. (2008). Cancers Exhibit a Mutator Phenotype: Clinical Implications. Cancer Res *68*, 3551-3557.

Lu, L., Schulz, H., and Wolf, D. (2002). The F-box protein SKP2 mediates androgen control of p27 stability in LNCaP human prostate cancer cells. BMC Cell Biology *3*, 22.

Lu, S., Tsai, S. Y., and Tsai, M. J. (1997). Regulation of androgen-dependent prostatic cancer cell growth: androgen regulation of CDK2, CDK4, and CKI p16 genes. Cancer Res *57*, 4511-6.

Lubahn, D. B., Joseph, D. R., Sullivan, P. M., Willard, H. F., French, F. S., and Wilson, E. M. (1988). Cloning of human androgen receptor complementary DNA and localization to the X chromosome. Science *240*, 327-30.

Luisi, B. F., Xu, W. X., Otwinowski, Z., Freedman, L. P., Yamamoto, K. R., and Sigler, P. B. (1991). Crystallographic analysis of the interaction of the glucocorticoid receptor with DNA. Nature *352*, 497-505.

Marhefka, C. A., Moore, B. M., Bishop, T. C., Kirkovsky, L., Mukherjee, A., Dalton, J. T., and Miller, D. D. (2001). Homology Modeling Using Multiple Molecular Dynamics Simulations and Docking Studies of the Human Androgen Receptor Ligand Binding Domain Bound to Testosterone and Nonsteroidal Ligands†. Journal of Medicinal Chemistry *44*, 1729-1740.

Marquis, J. C., Hillier, S. M., Dinaut, A. N., Rodrigues, D., Mitra, K., Essigmann, J. M., and Croy, R. G. (2005a). Disruption of gene expression and induction of apoptosis in prostate cancer cells by a DNA-damaging agent tethered to an androgen receptor ligand. Chem Biol *12*, 779-87.

Marquis, J. C., Hillier, S. M., Dinaut, A. N., Rodrigues, D., Mitra, K., Essigmann, J. M., and Croy, R. G. (2005b). Disruption of Gene Expression and Induction of Apoptosis in Prostate Cancer Cells by a DNA-Damaging Agent Tethered to an Androgen Receptor Ligand. Chemistry & Biology *12*, 779-787.

Masuda, H., Ozols, R. F., Lai, G., Fojo, A., Rothenberg, M., and Hamilton, T. C. (1988). Increased DNA Repair as a Mechanism of Acquired Resistance to cis-Diamminedichloroplatinum(II) in Human Ovarian Cancer Cell Lines. Cancer Res *48*, 5713-5716.

McA'Nulty, M. M., and Lippard, S. J. (1996). The HMG-domain protein Ixr1 blocks excision repair of cisplatin-DNA adducts in yeast. Mutat Res *362*, 75-86.

McDonnell, T. J., Troncoso, P., Brisbay, S. M., Logothetis, C., Chung, L. W. K., Hsieh, J., Tu, S., and Campbell, M. L. (1992). Expression of the Protooncogene bcl-2 in the Prostate and Its Association with Emergence of Androgen-independent Prostate Cancer. Cancer Res *52*, 6940-6944.

Meiers, I., Shanks, J. H., and Bostwick, D. G. (2007). Glutathione S-transferase pi (GSTP1) hypermethylation in prostate cancer: review 2007. Pathology *39*, 299-304.

Mike, S., Harrison, C., Coles, B., Staffurth, J., Wilt, T. J., and Mason, M. D. (2006). Chemotherapy for hormone-refractory prostate cancer. Cochrane Database Syst Rev, CD005247.

Miller, J. I., Ahmann, F. R., Drach, G. W., Emerson, S. S., and Bottaccini, M. R. (1992). The clinical usefulness of serum prostate specific antigen after hormonal therapy of metastatic prostate cancer. J Urol *147*, 956-61.

Miller, R., Boice, J. J., and Curtis, R. (1996). Bone Cancer. In Cancer Epidemiology and Prevention, D. Schottenfeld and J. Fraumeni, eds. (New York: Oxford University Press), pp. 971-983.

Mitra, K., Marquis, J. C., Hillier, S. M., Rye, P. T., Zayas, B., Lee, A. S., Essigmann, J. M., and Croy, R. G. (2002). A rationally designed genotoxin that selectively destroys estrogen receptor-positive breast cancer cells. J Am Chem Soc *124*, 1862-3.

Mohler, J. L., Gregory, C. W., Ford, O. H., Kim, D., Weaver, C. M., Petrusz, P., Wilson, E. M., and French, F. S. (2004). The androgen axis in recurrent prostate cancer. Clin Cancer Res *10*, 440-8.

Müller, J. M., Isele, U., Metzger, E., Rempel, A., Moser, M., Pscherer, A., Breyer, T., Holubarsch, C., Buettner, R., and Schüle, R. (2000). FHL2, a novel tissue-specific coactivator of the androgen receptor. EMBO J *19*, 359-69.

Nelson, P. S., Clegg, N., Arnold, H., Ferguson, C., Bonham, M., White, J., Hood, L., and Lin, B. (2002). The program of androgen-responsive genes in neoplastic prostate epithelium. Proceedings of the National Academy of Sciences of the United States of America *99*, 11890-11895.

O'Brien, S. G., Guilhot, F., Larson, R. A., Gathmann, I., Baccarani, M., Cervantes, F., Cornelissen, J. J., Fischer, T., Hochhaus, A., Hughes, T., et al. (2003). Imatinib Compared with Interferon and Low-Dose Cytarabine for Newly Diagnosed Chronic-Phase Chronic Myeloid Leukemia. N Engl J Med *348*, 994-1004.

Oliver, S. E., May, M. T., and Gunnell, D. (2001). International trends in prostate-cancer mortality in the "PSA era". International Journal of Cancer *92*, 893-898.

Oñate, S. A., Tsai, S. Y., Tsai, M. J., and O'Malley, B. W. (1995). Sequence and characterization of a coactivator for the steroid hormone receptor superfamily. Science *270*, 1354-7.

Osborne, C. K., Blumenstein, B. A., Crawford, E. D., Weiss, G. R., Bukowski, R. M., and Larrimer, N. R. (1992). Phase II study of platinum and mitoxantrone in metastatic prostate cancer: a Southwest Oncology Group Study. Eur J Cancer *28*, 477-8.

Panasci, L., Xu, Z., Bello, V., and Aloyz, R. (2002). The role of DNA repair in nitrogen mustard drug resistance. Anticancer Drugs *13*, 211-20.

Parkin, D. M., Whelan, S. L., Ferlay, J., and Raymond Land Young, J. (1997). Cancer Incidence in Five Continents, vol VII. IARC Scientific Publication No 143. Lyon: International Agency for Research on Cancer.

Pascoe, J. M., and Roberts, J. J. (1974). Interactions between mammalian cell DNA and inorganic platinum compounds. II. Interstrand cross-linking of isolated and cellular DNA by platinum(IV) compounds. Biochem Pharmacol *23*, 1345-57.

Pieper, R. O., Futscher, B. W., and Erickson, L. C. (1989). Transcription-terminating lesions induced by bifunctional alkylating agents in vitro. Carcinogenesis *10*, 1307-14.

Pike, A. C. W., Brzozowski, A. M., Walton, J., Hubbard, R. E., Thorsell, A., Li, Y., Gustafsson, J., and Carlquist, M. (2001). Structural Insights into the Mode of Action of a Pure Antiestrogen. Structure *9*, 145-153.

Pil, P. M., and Lippard, S. J. (1992). Specific binding of chromosomal protein HMG1 to DNA damaged by the anticancer drug cisplatin. Science *256*, 234-7.

Platz, E. A., Leitzmann, M. F., Visvanathan, K., Rimm, E. B., Stampfer, M. J., Willett, W. C., and Giovannucci, E. (2006). Statin Drugs and Risk of Advanced Prostate Cancer. J. Natl. Cancer Inst. *98*, 1819-1825.

Pont, A., Williams, P. L., Loose, D. S., Feldman, D., Reitz, R. E., Bochra, C., and Stevens, D. A. (1982). Ketoconazole blocks adrenal steroid synthesis. Ann Intern Med *97*, 370-2.

Reed, E., Yuspa, S. H., Zwelling, L. A., Ozols, R. F., and Poirier, M. C. (1986). Quantitation of cis-diamminedichloroplatinum II (cisplatin)-DNA-intrastrand adducts in testicular and ovarian cancer patients receiving cisplatin chemotherapy. J Clin Invest *77*, 545-50.

Rink, S. M., Solomon, M. S., Taylor, M. J., Rajur, S. B., McLaughlin, L. W., and Hopkins, P. B. (1993). Covalent structure of a nitrogen mustard-induced DNA interstrand cross-link: an N7-to-N7 linkage of deoxyguanosine residues at the duplex sequence 5'-d(GNC). Journal of the American Chemical Society *115*, 2551-2557.

Rink, S., Yarema, K., Solomon, M., Paige, L., Tadayoni-Rebek, B., Essigmann, J., and Croy, R. (1996). Synthesis and biological activity of DNA damaging agents that form decoy binding sites for the estrogen receptor. Proc Natl Acad Sci U S A. *93*, 15063–15068.

Rocco, J. W., and Sidransky, D. (2001). p16(MTS-1/CDKN2/INK4a) in Cancer Progression. Experimental Cell Research *264*, 42-55.

Ross, J. S., Sheehan, C. E., Hayner-Buchan, A. M., Ambros, R. A., Kallakury, B. V., Jr, R. P. K., Fisher, H. A., Rifkin, M. D., and Muraca, P. J. (1997). Prognostic significance of HER-2/neu gene amplification status by fluorescence in Situ hybridization of prostate carcinoma. Cancer *79*, 2162-2170.

Roth, T., Tang, W., and Eisenbrand, G. (1995). Synthesis of novel androgen-linked phosphoramide mustard prodrugs and growth-inhibitory activity in human breast cancer cells. Anticancer Drug Des *10*, 655-66.

Roy, A. K., Tyagi, R. K., Song, C. S., Lavrovsky, Y., Ahn, S. C., Oh, T. S., and Chatterjee, B. (2001). Androgen receptor: structural domains and functional dynamics after ligand-receptor interaction. Ann N Y Acad Sci *949*, 44-57.

van Royen, M. E., Cunha, S. M., Brink, M. C., Mattern, K. A., Nigg, A. L., Dubbink, H. J., Verschure, P. J., Trapman, J., and Houtsmuller, A. B. (2007). Compartmentalization of androgen receptor protein–protein interactions in living cells. J Cell Biol. *177*, 63–72.

Sakr, W. A., Haas, G. P., Cassin, B. F., Pontes, J. E., and Crissman, J. D. (1993). The frequency of carcinoma and intraepithelial neoplasia of the prostate in young male patients. J Urol *150*, 379-85.

Saporita, A. J., Zhang, Q., Navai, N., Dincer, Z., Hahn, J., Cai, X., and Wang, Z. (2003). Identification and characterization of a ligand-regulated nuclear export signal in androgen receptor. J Biol Chem *278*, 41998-2005.

Schaufele, F., Carbonell, X., Guerbadot, M., Borngraeber, S., Chapman, M. S., Ma, A. A. K., Miner, J. N., and Diamond, M. I. (2005). The structural basis of androgen receptor activation: Intramolecular and intermolecular amino–carboxy interactions. Proceedings of the National Academy of Sciences of the United States of America *102*, 9802-9807.

Schmitz, M., Grignard, G., Margue, C., Dippel, W., Capesius, C., Mossong, J., Nathan, M., Giacchi, S., Scheiden, R., and Kieffer, N. (2007). Complete loss of PTEN expression as a possible early prognostic marker for prostate cancer metastasis. Int J Cancer *120*, 1284-92.

Schoenmakers, E., Alen, P., Verrijdt, G., Peeters, B., Verhoeven, G., Rombauts, W., and Claessens, F. (1999). Differential DNA binding by the androgen and glucocorticoid receptors involves the second Zn-finger and a C-terminal extension of the DNA-binding domains. Biochem J *341 (Pt 3)*, 515-21.

Schoenmakers, E., Verrijdt, G., Peeters, B., Verhoeven, G., Rombauts, W., and Claessens, F. (2000). Differences in DNA binding characteristics of the androgen and glucocorticoid receptors can determine hormone-specific responses. J Biol Chem *275*, 12290-7.

Schwabe, J. W., Chapman, L., Finch, J. T., and Rhodes, D. (1993). The crystal structure of the estrogen receptor DNA-binding domain bound to DNA: how receptors discriminate between their response elements. Cell *75*, 567-78.

Shaffer, P. L., Jivan, A., Dollins, D. E., Claessens, F., and Gewirth, D. T. (2004). Structural basis of androgen receptor binding to selective androgen response elements. Proc Natl Acad Sci U S A. *101*, 4758–4763.

Sharma, U., Marquis, J. C., Nicole Dinaut, A., Hillier, S. M., Fedeles, B., Rye, P. T., Essigmann, J. M., and Croy, R. G. (2004). Design, synthesis, and evaluation of estradiol-linked genotoxicants as anti-cancer agents. Bioorg Med Chem Lett *14*, 3829-33.

Sheflin, L., Keegan, B., Zhang, W., and Spaulding, S. W. (2000). Inhibiting proteasomes in human HepG2 and LNCaP cells increases endogenous androgen receptor levels. Biochem Biophys Res Commun *276*, 144-50.

Singer, B. (1975). The chemical effects of nucleic acid alkylation and their relation to mutagenesis and carcinogenesis. Prog Nucleic Acid Res Mol Biol *15*, 219-84.

Slotman, B. J., and Rao, B. R. (1988). Ovarian cancer (review). Etiology, diagnosis, prognosis, surgery, radiotherapy, chemotherapy and endocrine therapy. Anticancer Res *8*, 417-34.

Smith, D. C., Jodrell, D. I., Egorin, M. J., Ambinder, R. M., Zuhowski, E. G., Kreis, W., Ellis, P. G., and Trump, D. L. (1993). Phase II trial and pharmacokinetic assessment of intravenous melphalan in patients with advanced prostate cancer. Cancer Chemother Pharmacol *31*, 363-8.

Steinberg, G. D., Carter, B. S., Beaty, T. H., Childs, B., and Walsh, P. C. (1990). Family history and the risk of prostate cancer. Prostate *17*, 337-47.

Stiller, C. A. (2004). Epidemiology and genetics of childhood cancer. Oncogene *23*, 6429-6444.

Strähle, U., Boshart, M., Klock, G., Stewart, F., and Schütz, G. (1989). Glucocorticoid- and progesterone-specific effects are determined by differential expression of the respective hormone receptors. Nature *339*, 629-32.

Takahara, P. M., Rosenzweig, A. C., Frederick, C. A., and Lippard, S. J. (1995). Crystal structure of double-stranded DNA containing the major adduct of the anticancer drug cisplatin. Nature *377*, 649-52.

Takahara, P. M., Frederick, C. A., and Lippard, S. J. (1996). Crystal Structure of the Anticancer Drug Cisplatin Bound to Duplex DNA. Journal of the American Chemical Society *118*, 12309-12321.

Tanenbaum, D. M., Wang, Y., Williams, S. P., and Sigler, P. B. (1998). Crystallographic comparison of the estrogen and progesterone receptor's ligand binding domains. Proceedings of the National Academy of Sciences of the United States of America *95*, 5998-6003.

Tavtigian, S. V., Simard, J., Teng, D. H., Abtin, V., Baumgard, M., Beck, A., Camp, N. J., Carillo, A. R., Chen, Y., Dayananth, P., et al. (2001). A candidate prostate cancer susceptibility gene at chromosome 17p. Nat Genet *27*, 172-180.

Thompson, I. M., Pauler, D. K., Goodman, P. J., Tangen, C. M., Lucia, M. S., Parnes, H. L., Minasian, L. M., Ford, L. G., Lippman, S. M., Crawford, E. D., et al. (2004). Prevalence of prostate cancer among men with a prostate-specific antigen level < or =4.0 ng per milliliter. N Engl J Med *350*, 2239-46.

Tomlins, S. A., Laxman, B., Dhanasekaran, S. M., Helgeson, B. E., Cao, X., Morris, D. S., Menon, A., Jing, X., Cao, Q., Han, B., et al. (2007). Distinct classes of chromosomal rearrangements create oncogenic ETS gene fusions in prostate cancer. Nature *448*, 595-9.

Tomlins, S. A., Rhodes, D. R., Perner, S., Dhanasekaran, S. M., Mehra, R., Sun, X., Varambally, S., Cao, X., Tchinda, J., Kuefer, R., et al. (2005). Recurrent Fusion of TMPRSS2 and ETS Transcription Factor Genes in Prostate Cancer. Science *310*, 644-648.

Toney, J. H., Donahue, B. A., Kellett, P. J., Bruhn, S. L., Essigmann, J. M., and Lippard, S. J. (1989). Isolation of cDNAs encoding a human protein that binds selectively to DNA modified by the anticancer drug cis-diamminedichloroplatinum(II). Proc Natl Acad Sci U S A *86*, 8328-32.

Trapman, J., Klaassen, P., Kuiper, G. G., van der Korput, J. A., Faber, P. W., van Rooij, H. C., Geurts van Kessel, A., Voorhorst, M. M., Mulder, E., and Brinkmann, A. O. (1988). Cloning, structure and expression of a cDNA encoding the human androgen receptor. Biochem Biophys Res Commun *153*, 241-8.

Treiber, D. K., Zhai, X., Jantzen, H. M., and Essigmann, J. M. (1994). Cisplatin-DNA adducts are molecular decoys for the ribosomal RNA transcription factor hUBF (human upstream binding factor). Proceedings of the National Academy of Sciences of the United States of America *91*, 5672-5676.

Trimmer, E. E., Zamble, D. B., Lippard, S. J., and Essigmann, J. M. (1998). Human Testis-Determining Factor SRY Binds to the Major DNA Adduct of Cisplatin and a Putative Target Sequence with Comparable Affinities. Biochemistry *37*, 352-362.

Tsihlias, J., Zhang, W., N Bhattacharya, Flanagan, M., Klotz, L., and Slingerland, J. (2000). Involvement of p27Kip1 in G1 arrest by high dose 5|[alpha]|-dihydrotestosterone in LNCaP human prostate cancer cells.

Tyagi, R. K., Lavrovsky, Y., Ahn, S. C., Song, C. S., Chatterjee, B., and Roy, A. K. (2000). Dynamics of Intracellular Movement and Nucleocytoplasmic Recycling

of the Ligand-Activated Androgen Receptor in Living Cells. Mol Endocrinol *14*, 1162-1174.

U.S. Preventive Services Task Force (2002). Screening for Prostate Cancer: Recommendation and Rationale. Ann Intern Med *137*, 915-916.

Umesono, K., and Evans, R. M. (1989). Determinants of target gene specificity for steroid/thyroid hormone receptors. Cell *57*, 1139-1146.

Veldscholte, J., Berrevoets, C. A., Zegers, N. D., van der Kwast, T. H., Grootegoed, J. A., and Mulder, E. (1992). Hormone-induced dissociation of the androgen receptor-heat-shock protein complex: use of a new monoclonal antibody to distinguish transformed from nontransformed receptors. Biochemistry *31*, 7422-30.

Visakorpi, T., Hyytinen, E., Koivisto, P., Tanner, M., Keinänen, R., Palmberg, C., Palotie, A., Tammela, T., Isola, J., and Kallioniemi, O. P. (1995). In vivo amplification of the androgen receptor gene and progression of human prostate cancer. Nat Genet *9*, 401-6.

Voegel, J. J., Heine, M. J., Zechel, C., Chambon, P., and Gronemeyer, H. (1996). TIF2, a 160 kDa transcriptional mediator for the ligand-dependent activation function AF-2 of nuclear receptors. EMBO J *15*, 3667-75.

Wang, Z., Chen, Z., Xu, Z., Christodoulopoulos, G., Bello, V., Mohr, G., Aloyz, R., and Panasci, L. C. (2001). In Vitro Evidence for Homologous Recombinational Repair in Resistance to Melphalan. J. Natl. Cancer Inst. *93*, 1473-1478.

Warburg, O. (1930). On Metabolism of Tumors (London: Constable).

Whittemore, A. S., Wu, A. H., Kolonel, L. N., John, E. M., Gallagher, R. P., Howe, G. R., West, D. W., Teh, C. Z., and Stamey, T. (1995). Family history and prostate cancer risk in black, white, and Asian men in the United States and Canada. Am J Epidemiol *141*, 732-40.

Williams, S. A., Singh, P., Isaacs, J. T., and Denmeade, S. R. (2007). Does PSA play a role as a promoting agent during the initiation and/or progression of prostate cancer? Prostate *67*, 312-29.

Williamson, S. K., Wolf, M. K., Eisenberger, M. A., O'Rourke, M. A., Brannon, W., and Crawford, E. D. (1996). Phase II evaluation of ifosfamide/mesna in metastatic prostate cancer. A Southwest Oncology Group study. Am J Clin Oncol *19*, 368-70.

Wilman, D., and Conners, T. (1980). Molecular Aspects of Anti-Cancer Drug Action S. Neidle and M. Waring, eds. (London: Macmillan Press Limited).

Wilson, C. M., and McPhaul, M. J. (1996). A and B forms of the androgen receptor are expressed in a variety of human tissues. Molecular and Cellular Endocrinology *120*, 51-57.

Wong, H. Y., Burghoorn, J. A., Leeuwen, M. V., Ruiter, P. E. D., Schippers, E., Blok, L. J., Li, K. W., Dekker, H. L., Jong, L. D., Trapman, J., et al. (2004). Phosphorylation of androgen receptor isoforms. Biochem J. *383*, 267–276.

Wu, X., Dong, X., Liu, W., and Chen, J. (2006). Characterization of CHEK2 mutations in prostate cancer. Human Mutation *27*, 742-747.

Xu, J., Zheng, S. L., Komiya, A., Mychaleckyj, J. C., Isaacs, S. D., Hu, J. J., Sterling, D., Lange, E. M., Hawkins, G. A., Turner, A., et al. (2002). Germline mutations and sequence variants of the macrophage scavenger receptor 1 gene are associated with prostate cancer risk. Nat Genet *32*, 321-5.

Xu, Y., Chen, S., Ross, K. N., and Balk, S. P. (2006). Androgens Induce Prostate Cancer Cell Proliferation through Mammalian Target of Rapamycin Activation and Post-transcriptional Increases in Cyclin D Proteins. Cancer Res *66*, 7783-7792.

Zamble, D. B., Mu, D., Reardon, J. T., Sancar, A., and Lippard, S. J. (1996). Repair of Cisplatin−DNA Adducts by the Mammalian Excision Nuclease. Biochemistry *35*, 10004-10013.

Zhai, X., Beckmann, H., Jantzen, H., and Essigmann, J. M. (1998). Cisplatin−DNA Adducts Inhibit Ribosomal RNA Synthesis by Hijacking the Transcription Factor Human Upstream Binding Factor. Biochemistry *37*, 16307-16315.

Zhao, X. Y., Boyle, B., Krishnan, A. V., Navone, N. M., Peehl, D. M., and Feldman, D. (1999). Two mutations identified in the androgen receptor of the new human prostate cancer cell line MDA PCa 2a. J Urol *162*, 2192-9.

Zhou, Z., Lane, M., Kemppainen, J., French, F., and Wilson, E. (1995). Specificity of ligand-dependent androgen receptor stabilization: receptor domain interactions influence ligand dissociation and receptor stability. Mol Endocrinol *9*, 208-218.

Chapter 2: Effects of 11β Compounds on AR Regulation and Activity

Introduction

Prostate cancer, despite continuous advances in detection and treatment, remains a leading killer of males in developed countries (Jemal et al., 2008). New strategies are warranted to combat this disease, especially in later stages when chemotherapeutic regimens do little to prolong life. We have previously described a novel potential strategy for treatment of this disease, involving the creation of small molecules capable of forming sites of DNA damage that will attract the androgen receptor (AR) (Marquis et al. 2005). The rationale behind this strategy stems from studies of the molecular action of cisplatin, which is highly successful in combination therapy for the treatment of testicular cancer, affording 5-year survival rates greater than 95% (Horner et al., 2009). Our laboratory and others have shown that cisplatin is able to form sites of DNA damage that can go on to recruit binding of specific transcription factors (Toney et al., 1989; Donahue et al., 1990; Bruhn et al., 1992; Pil and Lippard, 1992; Treiber et al., 1994). Furthermore, we have proposed that toxicity is enhanced due to limited access of repair enzymes as well as by removal of these transcription factors from their normal transcriptional targets. As a further test of this hypothesis and to determine whether this strategy could be modified to expand the efficacy into other cancers, we initially designed molecules capable of forming sites of DNA damage that recruited the estrogen receptor (ER) (Rink et al., 1996; Mitra et al., 2002; Sharma et al., 2004), as it is highly expressed in breast and ovarian cancers. These molecules successfully formed DNA damage sites that maintained affinity for ER and displayed selective toxicity toward ER (+) cells, serving as proof of principle.

We then expanded our initial scope by creating a molecule, 11β[1], which would function identically as our ER-interacting compounds, but employ the AR as its target. As with cisplatin, 11β has the capacity to form sites of DNA damage, in this case by a bis-2-chloroethyl aniline functionality analogous with the clinically used anticancer agent chlorambucil. Chemically tethered to the DNA-damaging portion of 11β is a ligand for

[1] 2-(6-((8S,11S,13S,14S,17S)-17-hydroxy-13-methyl-3-oxo-2,3,6,7,8,11,12,13,14,15,16,17 dodecahydro-1H-cyclopenta[a]phenanthren-11-yl)hexylamino)ethyl 3-(4-(bis(2-chloroethyl)amino)phenyl)propylcarbamate

the androgen receptor, 17β-OH(estra-4,9(10)-dien-3-one), with attachment at carbon 11 of the steroid structure with β (*S*) stereochemistry (giving rise to our shorthand nomenclature of 11β), analogous to RU486. The linker between these functional groups has been optimized such that molecules have the greatest solubility and stability while maintaining the capacity to simultaneously damage DNA and bind to AR. We propose that by recruitment of AR to sites of DNA damage, access of repair enzymes will be hindered, in a mechanism we term repair shielding (Figure 2.1). In non-cancerous cells expressing less AR, the adducts would instead be easily repaired and removed, providing a therapeutic window. Additionally, as the AR is heavily involved in prostate cancer progression and survival due to its function as a transcription factor regulating expression of pro-survival genes (Lu et al. 1997; Xu et al. 2006), we propose that its titration away from normal targets to sites of DNA damage will increase toxicity—a mechanism we term transcription factor hijacking. Together, we believe the mechanisms of repair shielding and transcription factor hijacking can allow 11β to achieve similar efficacy in the treatment of prostate cancer as cisplatin has toward testicular cancer.

The previous work on 11β has demonstrated its efficacy in eliciting apoptosis in the AR (+) prostate cancer cell line LNCaP (Marquis et al. 2005). Furthermore, 11β has high affinity for AR (~20% of the affinity of dihydrotestosterone (DHT)), and adducted 16-mer oligonucleotides maintain significant affinity to the AR. Of utmost importance, it is effective in preventing the growth of LNCaP xenograft tumors in NIH Swiss (*nu/nu*) mice, while displaying low systemic toxicity (Marquis et al. 2005; Hillier et al. 2006). 11β forms similar levels of adducted DNA in LNCaP xenograft tumors as in the same cells grown in culture dishes at respective therapeutically relevant doses and concentrations (Hillier et al. 2006). As such, 11β has proven efficacy as a potential prostate cancer therapeutic agent, and further studies are warranted to understand the role of AR in this toxicity. Additionally, the non-DNA damaging version of this compound, 11β-dimethoxy, does not cause apoptosis in LNCaP cells at equivalent concentrations, but does display the interesting characteristic of arresting cells in G1 phase of the cell cycle. As such, it is likely that DNA damage is necessary for greatest toxicity, but potentially the AR-interacting and linker portions of the compounds have significant effects on their own.

The primary treatment for metastatic prostate cancer is anti-hormonal therapy, achieved by minimization of AR activity through removal of circulating androgens and use of AR antagonists. AR antagonists function by competing with natural androgens testosterone and DHT for binding in the ligand binding pocket of AR, while failing to induce the AR to undergo conformational changes necessary to appropriately drive transcription of target genes. On a detailed molecular level, these conformational changes are still not completely understood, because the structure of AR has not been solved in an antagonist conformation. Limited proteolysis studies provide some clues as to how AR agonists and antagonists affect the structural conformation of the AR and affect its ability to act as a transcription factor. These experiments show that the AR is sensitive to complete proteolysis by trypsin in the absence of any androgen. Addition of androgens, however, causes a conformational change to the receptor that immediately results in protection of a 35 kDa fragment. This 35 kDa receptor fragment is then converted to a trypsin-resistant 29 kDa fragment within one hour of androgen stimulation (Kuil et al., 1995). These fragments each correspond to the very C-terminus of AR, with the 35 kDa form containing further extension into the hinge region. Several AR antagonists also allowed for immediate protection of the 35 kDa fragment, but did not allow formation of the 29 kDa form. As such, it seems that these AR antagonists (cyproterone acetate, hydroxyflutamide, bicalutamide, nilutamide) function in part by not allowing the conformational changes that result in protection of a 29 kDa region of the ligand binding domain (LBD). Interestingly, RU486 initially protects the 35 kDa fragment before allowing conversion to the smaller 29 kDa form and a unique 25 kDa form (Kuil et al., 1995). This unique 25 kDa fragment corresponds to deletion of the most C-terminal amino acids, likely due to displacement of helix 12 as seen in the crystal structure of RU486 complexed with glucocorticoid receptor (GR) (Kauppi et al., 2003), toward which RU486 also acts antagonistically. Furthermore, the estrogen receptor (ER) LBD has been solved in both agonist and antagonist conformations. The most striking difference between these conformations is the inability for helix 12 to close over the ligand binding pocket in the antagonist conformation (Brzozowski et al., 1997). By limiting helix 12 closure in the AR, it is presumed that AF2 formation does not occur as

favorably, and coactivator binding gives way to corepressor binding, limiting AR transcriptional activity (Hodgson et al., 2008).

Several steps are involved in the progression of AR from a cytoplasmic unliganded receptor into its trans-active conformation, all caused by changes induced by initial ligand binding. The receptor must dissociate from a complex with heat shock proteins, relocalize to the nucleus, become phosphorylated, self-dimerize, bind at androgen response elements in gene promoters and enhancers, and recruit appropriate coactivator proteins, chromatin remodeling machinery and associated general transcriptional elements in order to successfully drive transcription (Brinkmann et al. 1999). Theoretically, an AR antagonist could function by limiting the ability of AR to carry out any of these steps.

Mutation of AR is a common occurrence during antiandrogen treatment of advanced prostate cancer, often allowing cells to resume growth in the presence of antiandrogens. The LNCaP AR serves as an example, as a threonine at position 877 within the ligand binding pocket is mutated to alanine. This mutation allows for a switch for the antiandrogen hydroxyflutamide from an antagonist to an agonist (Veldscholte et al., 1992). Bicalutamide still functions as an antagonist toward this mutated receptor, but other mutations within the ligand binding pocket can occur in order to allow it to also activate the AR (Culig et al., 1999).

Despite mutations allowing prostate cancers to progress with less androgens or with antiandrogens, the AR remains a viable target because of its continued expression in most hormone refractory prostate cancers (van der Kwast et al. 1991; Visakorpi et al. 1995; Gregory et al. 1998; Holzbeierlein et al. 2004; Mohler et al. 2004). Thus, our strategy represents a novel method which could prove successful in treatment of all stages of prostate cancer progression. The work here has addressed the effects of 11β treatment on AR expression, phosphorylation, nuclear localization, association with DNA androgen response elements (AREs), and ultimate transcriptional activity.

Materials and Methods

Chemicals: Flutamide, 5α-dihydrotestosterone (DHT), Z-Leu-Leu-Leu-al (MG-132), and cycloheximide were acquired from Sigma-Aldrich (St Louis, MO). Bicalutamide was from LKT Laboratories, Inc. (St. Paul, MN) and R1881 from Perkin-Elmer Life Science (Waltham, MA). Synthesis of 11β-dichloro (referred to herein as 11β) and 11β-dimethoxy were performed in our laboratory and have previously been described (Marquis et al. 2005).

Cell Culture: LNCaP cells (ATCC, Rockville, MD) were maintained in RPMI 1640 media supplemented with glucose (2.5 g/L), 1 mM sodium pyruvate, 10 mM HEPES, and 10% fetal bovine serum. Media and supplements were obtained from Invitrogen (Carlsbad, CA), except for fetal bovine serum (Hyclone, Salt Lake City, UT). COS7 cells (ATCC) were grown in DMEM (Invitrogen) supplemented with 10% fetal bovine serum. CWR22Rv1 and C4-2B cells (ATCC) were grown in RPMI 1640 with 10% fetal bovine serum. MDA-MB-453 cells (ATCC) were grown in MEM-α media supplemented with 1 ng/mL EGF, 2 μg/mL human recombinant insulin, 100 mM non-essential amino acids, 10 mM HEPES (all Invitrogen), and 10% fetal bovine serum (Hyclone). All cells were grown in a humidified 5% CO_2/air atmosphere at 37°C. For transcriptional reporter assays and where otherwise indicated, media formulations were the same except for use of phenol red free versions supplemented with 10% charcoal dextran treated FBS (CDTFBS) (Hyclone) in order to remove all androgens.

Western blots: Cells were harvested by scraping into media, washing with PBS, and subsequently lysing in RIPA buffer (Santa Cruz Biotechnology, Santa Cruz, CA) containing PMSF, sodium orthovanadate, and protease inhibitor cocktail at 0°C. Cellular debris was pelleted by centrifugation at 14,000 RPM in a bench top microcentrifuge, supernatants were collected, and protein quantified by Bradford dye binding assay (Bio-Rad Laboratories, Hercules, CA). For cellular fractionation, NE-PER nuclear and cytoplasmic extraction reagents kit (Pierce, Rockford, IL) was used according to instructions. Equal quantities of protein were electrophoretically separated on a bis-tris precast polyacrylamide gel (Invitrogen) and transferred to Immobilon-P PVDF

membrane (Millipore, Billerica, MA). Non-specific protein binding was blocked with 5% milk in Tris-buffered saline (0.1% Tween 20, 10 mM Tris [pH 7.4], 150 mM NaCl) and proteins were detected by primary antibodies followed by horseradish peroxidase (HRP) conjugated secondary antibodies and chemiluminescent HRP substrate (Supersignal West; Pierce, Rockford, IL). Antibodies used were as follows: AR (SC-7305, Santa Cruz), Phospho-AR (Ser81) (#07-1375; Millipore), β-actin (SC-1615R; Santa Cruz), PARP (06-557; Upstate Biotechnology, Lake Placid, NY; now Millipore), α-tubulin (CP06, Calbiochem, San Diego, CA), and HRP-conjugated secondary antibodies (#7076, anti-mouse IgG; #7074 anti-rabbit IgG; Cell Signaling Technology, Danvers, MA).

Expression Vectors: The vectors pGL4.10 (promoterless firefly luciferase) and pGL4.74 (*renilla* luciferase driven by thymidylate kinase promoter) were acquired from Promega (Madison, WI). We prepared pGL4PSA containing promoter and enhancer regions of the *KLK3* (PSA) gene. A 662 base pair segment of the PSA promoter (-631 to +31), containing AREI and AREII was obtained by PCR amplification from MDA-MB231 genomic DNA using forward primer (5'-GCG GAG CTC AAT TCC ACA TTG TTT GCT GCA C-3') and reverse primer (5'-ATA CTC GAG ACT CTC CGG GTG CAG GTG GTA A-3'), containing SacI and XhoI restriction sites, respectively. The reverse primer also contains an additional A between the XhoI restriction site and the PSA promoter sequence in order to prevent creation of a second SacI restriction site following ligation. An additional 1446 base pair segment of the PSA enhancer (-5321 to -3877, containing AREIII) was amplified from LNCaP genomic DNA using forward primer GCG TAT GGT ACC AGA GAT TTT TTG GGG G and reverse primer TAT GCG GAG CTC GTA TCT GTG TGT CTT CT, containing KpnI and SacI restriction sites, respectively. The amplified PSA promoter and enhancer regions were ligated in tandem upstream of the luciferase gene in pGL4.10. This completed vector was sequenced at the MIT CCR Biopolymers Laboratory and found to match published human genome sequence AC011523 except for two substitutions (-4363 G->T, -4264 C->A), both outside of known ARE's. Vectors pCINeo, pCINeoAR, VP16-AR, VP16-AR

NTD (1-538), pm-AR LBD (644-919), and pG5-Luc were all generous gifts from the laboratory of Steven Balk (Beth-Israel Deaconess Medical Center, Boston, MA).

Luciferase Transcriptional Reporter Assays: For testing of AR transcriptional activity in LNCaP or MDA-MB-453 cells, 24-well tissue culture plates were used and cells were cotransfected with pGL4PSA and pGL4.74 in a 24:1 ratio using lipofectamine and PLUS reagent in Opti-MEM media according to manufacturer's instructions (Invitrogen). After 3 hrs, media was supplemented to 10% FBS, and after 24 hrs replaced with fresh phenol red free media containing 10% CDTFBS. Following a further 24 hr incubation, test compounds were diluted 1,000-fold into CDTFBS containing media and cells incubated 24 hrs prior to cell lysis and luciferase detection using dual-luciferase reporter assay system (Promega) with TD 20/20 luminometer (Turner Biosystems, Sunnyvale, CA). All samples were performed in at least quadruplicate and firefly luciferase measurements were normalized to *renilla* luciferase readings. To test activity in COS7 cells, transfection was performed with lipofectamine 2000 reagent according to manufacturer instructions (Invitrogen) and included pCINeo (negative control), pCINeoAR (AR expression plasmid), or VP16-AR (VP16 activation domain fused to N-terminus of full length AR). The procedure was otherwise identical.

N/C Terminal AR Interaction Assay: In order to test interaction of N and C termini of AR, COS7 cells were co-tranfected with VP16-AR NTD (1-538) (herpes simplex virus VP16 activation domain fused to NTD of AR), pm-AR LBD (644-919) (*S. cerevisiae* Gal4 DNA binding domain fused to AR ligand binding domain), pG5-Luc (five Gal4 response elements upstream of firefly luciferase), and pGL4.74 using lipofectamine 2000. Assay was otherwise performed as with luciferase transcriptional reporter assays.

PSA Media Assay. PSA secretion into culture media was detected by ELISA (Bio-Quant, Inc., San Diego, CA). LNCaP cells were cultured for 48 hrs in CDTFBS media prior to addition of test compounds for 24 hrs. Aliquots of media were collected and used to detect PSA secretion, while cells were isolated and used for RT-PCR analysis of androgen-regulated genes.

RT-PCR: RNA was isolated from cells using RNEasy kit with optional on-column DNAse digestion (Qiagen, Valencia, CA) and quantified by UV absorbance. RT-PCR was performed with Quantitect SYBR Green RT-PCR kit (Qiagen) at MIT BioMicro Center on MJ Research Real-Time PCR Machine with *GAPDH* as control. Primers were designed using Primer3 software (Rozen and Skaletsky, 2000) and are as follows: *AR* (based on accession NM_00044) Forward: GCA GGA AGC AGT ATC CGA AG, Reverse: TGG CGT TGT CAG AAA TGG T; *GAPDH* (based on accession NM_002046) Forward: ACA GTC AGC CGC ATC TTC TT, Reverse: GCC CAA TAC GAC CAA ATC C; *KLK3* (PSA) (based on accession BC_005307) Forward: AAC GCA CCA GAC ACT CAC AG, Reverse: TCC TTA CTT CAT CCC CAT CC; *KLK2* (based on accession NM_001002231) Forward: AGG ATA AGC TGG AGC CAC AA, Reverse: GGA TCC TCC CCT TCT TTC TG. For analysis of *KLK2* and *KLK3* mRNA, cells were cultured for 48 hrs in CDTFBS media prior to addition of test compounds for 24 hrs and subsequent transcript detection.

Statistics: Significance tests were performed with unpaired 2-tailed student's t-test as implemented in Excel 2002 (Microsoft, Redmond, WA).

Results

AR Steady-State Levels are Reduced by 11β Treatment

11β was designed to kill cancer cells selectively by creating sites of damage that would recruit the AR and result in enhanced toxicity. As such, it is prudent to determine the effects of treatment on expression and turnover of this protein target. LNCaP cells are the AR positive cell line of choice used in most of the following studies. Thus, these cells were treated with 11β at different concentrations and durations to determine effects on AR protein expression, revealing a dose and time-dependent decrease in AR protein upon treatment. However, previous reports (Marquis et al. 2005; Hillier et al. 2006) have demonstrated that 11β is highly toxic to LNCaP cells at concentrations greater than 5 μM, confounding the interpretation and meaning of biochemical analysis at these higher doses.

As such, 5 μM 11β was chosen as an optimal concentration to test effects of treatment on AR protein expression and turnover. At this concentration, it is evident that 11β causes a significant decrease in the steady state level of AR protein, lowering it by as much as ~80% following 15 hrs of treatment (Figure 2.2). Furthermore, it was demonstrated that this same concentration of 11β could cause a reduction in AR protein levels in two other androgen-insensitive prostate cancer cell lines, C4-2B and CWR22Rv1 (Figure 2.3), demonstrating that this may be a general effect.

Protein Level Decrease is Due to Enhanced Proteasomal Degradation

The reduction in steady-state levels of AR protein could be the result of either decreased expression or increased turnover (degradation). One possibility is that 11β causes transcription of the *AR* gene to be reduced, resulting in less protein expression from a smaller pool of mRNA. However, Figure 2.4 demonstrates that 11β does not have a significant effect on AR mRNA expression at this concentration within 24 hrs. Alternatively, 11β, by interacting with the AR and inducing a receptor conformation distinct from a stabilizing conformation, may increase receptor turnover and result in lower steady-state levels. This possibility was first addressed by testing the effects of treatment with the non-DNA damaging compound 11β-dimethoxy on AR protein levels. 11β-dimethoxy also results in reduced steady-state AR protein, increasing the likelihood that direct interaction of these compounds with AR is responsible for its reduced levels (Figure 2.5).

The AR is known to be degraded through the ubiquitin-proteasome system (Sheflin et al. 2000; Lin, Wang et al. 2002). Thus, 11β may function in part by enhancing ubiquitylation of AR leading to subsequent proteasomal degradation. To address this possibility, cells were co-treated with 11β and the proteasome inhibitor MG-132, before monitoring AR expression over time and comparing to levels in untreated cells or individual 11β or MG-132 treatment (Figure 2.6). As can be seen, addition of MG-132 increases steady-state protein levels. Notably, MG-132 has an effect of also hindering AR transcription (Lin, Altuwaijri et al. 2002). Thus, after ~3 hrs of treatment, AR levels begin to fall, returning to previous untreated levels within 15 hrs. As already

demonstrated, 11β treatment alone results in immediate reduction of AR levels. However, in the presence of proteasomal inhibition, 11β is unable to cause this immediate reduction in AR levels, instead increasing in expression just like with MG-132 treatment alone. Furthermore, AR levels in co-treated cells continue to match the levels seen in MG-132 treated cells after longer treatment, increasing support for the view that the decrease in AR protein caused by 11β is due to proteasomal degradation.

Protein Turnover is not Significantly Increased in Absence of Protein Synthesis

To substantiate the finding that 11β increases receptor turnover, LNCaP cells were treated with the translational inhibitor cycloheximide in the presence or absence of 11β to determine whether AR half-life was decreased in the presence of 11β. Figure 2.7 demonstrates that cycloheximide treatment results in a time-dependent reduction in AR levels, as less protein is being synthesized, while receptor degradation continues. Comparing protein levels between 11β treated and cycloheximide treated cells shows a slightly faster rate of decrease in cells treated with 11β, supporting the hypothesis that 11β enhances receptor turnover (AR $t_{1/2}$ = 6.5 hrs in 11β treated cells, 9.6 hrs in cycloheximide treated cells). However, when 11β and cycloheximide are co-administered to LNCaP cells, 11β does not enhance the rate of receptor turnover above that seen with cycloheximide.

Reduction in AR Levels is Hindered by Competition with Ligand for AR

An additional experiment involved testing effects of 11β on AR levels in LNCaP cells grown in androgen-depleted CDTFBS media, with and without addition of 1 nM synthetic androgen R1881 as competitor. Under these conditions, AR protein levels are ~30% lower than in cells grown in full media, presumably due to increased receptor turnover in absence of stabilizing hormone. Addition of 11β causes reduction in AR protein levels, but to a lesser extent than in cells grown in normal growth media containing androgens (Figure 2.8, compare with Figure 2.2). Addition of 1 nM R1881 to these androgen-deprived cells allows AR to recover to levels seen in normal media. Concurrent addition of R1881 with 11β limits the ability of 11β to elicit decreased AR

levels. Based on this finding, it is likely that interaction of 11β with the AR is necessary to increase receptor turnover. The results are consistent with the view that 11β increases receptor turnover by interfering with natural androgen binding and promoting proteasomal degradation.

The Androgen Receptor Is Phosphorylated and Transported to the Nucleus Upon 11β and 11β-Dimethoxy Treatment

We next sought to determine whether 11β could affect the ability of AR to act as a transcription factor. As a first step toward understanding this possibility, phosphorylation of AR at Ser81 was measured. This site was previously demonstrated to display the highest stoichiometric increase in phosphorylation upon addition of androgen to androgen-deprived cells (Gioeli et al., 2002). First, it was demonstrated that 1 nM R1881 results in a robust increase in Ser81 phosphorylation (Figure 2.9). Somewhat surprisingly, 5 μM 11β was also able to elicit a similar increase in AR phosphorylation after 3 hrs treatment. At later time points, R1881 appears to maintain greater AR phosphorylation. However, it is important to recall that 11β at this concentration ultimately results in a decrease in total receptor levels. The ability of 11β to interfere with R1881-induced AR phosphorylation was also tested, but 11β appears to have little to no effect on the phosphorylation elicited by R1881.

Since 11β is designed to form a nuclear complex sandwiched in between DNA and AR, an additional important experiment involved monitoring AR subcellular location following 11β treatment. The AR is a cytoplasmic protein in absence of ligand, and as such, if free 11β compound interacts with unliganded AR in the cytoplasm, its capacity to damage DNA and form a complex would be minimized if the receptor remained cytoplasmic. LNCaP cells grown in CDTFBS media were treated as above with 1 nM R1881, 1 μM 11β, or the combination for 24 hrs prior to isolation and separation into cytoplasmic and nuclear extracts. These were individually probed for AR expression, as well as for markers of nuclear (PARP) and cytoplasmic (β-tubulin) compartments. While R1881 elicited relocalization of AR from cytoplasmic into a nuclear compartment as expected, it was quite interesting that 11β effectively recruited AR into the nuclear

compartment as well (Figure 2.10). Since 11β was activating toward the AR re-localization on its own, it did not hinder the ability of R1881 to effect AR re-localization to the nucleus.

11β and 11β-Dimethoxy Potently Inhibit Interaction of N and C termini of AR

An additional effect of androgen binding to AR is a conformational change that allows interaction between the N and C termini of the receptor. Generally speaking, this N/C interaction is prompted by low concentrations of potent androgens, whereas it is inhibited by AR antagonists (Langley et al. 1995; Kemppainen et al. 1999). A mammalian two-hybrid assay was used to monitor this interaction. The N-terminus of AR (1-538) was fused to the herpes simplex virus VP16 transactivation domain, while a separate vector contained a fusion between the AR LBD (644-919) and the *S. cerevisiae* Gal4 DBD. A Gal4 responsive reporter was co-transfected to measure interaction between the N and C terminal halves of AR, while a *renilla* luciferase plasmid was used to control for transfection efficiency. The AR LBD and Gal4 DBD are unable to drive transcription from this promoter effectively without also recruiting the strong activation domain present in VP16, which will only be recruited by interaction between the N and C termini of the AR. As anticipated, DHT is able to enhance the N/C interaction of the AR quite robustly (Figure 2.11B). 11β or 11β-dimethoxy are unable to cause this N/C interaction (no increase in reporter activity over vehicle treatment, data not shown), but are both quite effective at inhibiting the interaction. In fact, at concentrations of 11β-compounds as low as 10 nM, inhibition is evident and becomes quite potent at higher concentrations (Figure 2.11B).

11β and 11β-Dimethoxy are Weak AR Agonists, but 11β Efficiently Promotes AR Binding to Androgen Response Elements

The findings that 11β could induce AR phosphorylation and nuclear localization prompted us to study this interaction further and determine whether 11β could act as a normal androgen and enhance transcriptional activity of AR. To study this possibility, a luciferase reporter system was designed by cloning promoter and enhancer elements of the androgen-responsive *KLK3* (PSA) gene upstream of firefly luciferase, as has been

performed elsewhere (Latham et al., 2000; Jia et al., 2003). Figure 2.12A demonstrates that this system responds appropriately by increasing firefly luciferase expression in the presence of DHT (R1881 is also effective, Figure 2.14C). Figure 2.12B shows that the 11β-compounds are able to increase transcription of this reporter significantly, but to much less extent than that induced by DHT. 11β-Dimethoxy is slightly more effective as an androgen than 11β, but both compounds are relatively weak AR agonists. Concentrations greater than 1 μM were not tested in these reporter assays due to enhanced cellular toxicity related to transfection conditions. Additionally, competition for binding to AR with 10 μM of the AR antagonist flutamide is able to inhibit the activation caused by 1 μM 11β, demonstrating that the enhanced transcription is likely due to direct interaction between 11β and the AR (Figure 2.12C).

To test whether 11β could efficiently promote AR binding to response elements in the promoters of androgen-regulated genes, the same PSA promoter/enhancer driven reporter system was used, but now with a fusion of AR to the VP16 activation domain in otherwise AR negative COS7 cells. By creating a fusion of the strong activation domain of VP16 to AR, the AR gains the ability to increase transcription from a promoter as long as it is recruited effectively. While 11β may cause effective recruitment of the AR to androgen response elements within gene promoter elements, if the receptor does not undergo conformational changes allowing for additional recruitment of specific co-activator proteins, it will not effectively drive transcription. By using this VP16-AR fusion, however, it is easily demonstrated that 11β is quite effective at recruiting AR to the promoter/enhancer regions of PSA within a reporter plasmid (Figure 2.13). While DHT enhances transcriptional activity through VP16-AR at 1 nM, 100-fold more 11β is necessary in order to enhance this transcription. It is clear, however, that 100 nM 11β is similarly effective as an equivalent concentration of DHT at promoting this interaction. Thus, 11β efficiently promotes AR binding to androgen response elements (AREs) at concentrations typically used for treatment of LNCaP cells.

11β Compounds are Moderate AR Antagonists

Despite effectively relocalizing the AR into the nucleus and even to AREs in androgen-responsive gene promoters, 11β is not a very effective agonist to a normal AR, increasing luciferase reporter expression ~4-fold (Figure 2.12B). As such, and especially considering its robust ability to inhibit the N/C terminal interaction, it seemed likely that 11β could act as a potent antagonist of AR activation by DHT. To test this possibility, the same PSA promoter/enhancer reporter system was used in LNCaP cells, but increasing concentrations of 11β were co-administered with 1 nM DHT. Figure 2.14A shows that both 11β compounds are moderate antagonists of AR transcriptional activity, reducing DHT-induced activation by as much as ~60%. However, while the N/C terminal interaction was inhibited by concentrations of 11β compounds as low as 10 nM, antagonism of receptor activity requires concentrations $\geq$ 100 nM. Figure 2.14B demonstrates that the AR antagonist bicalutamide, at an equivalent 1 μM concentration, is more effective than 11β compounds at interfering with AR activity. Furthermore, Figure 2.14C shows that both 11β compounds are also able to antagonize AR activity driven by the more robust AR agonist, R1881. While both 11β and 11β-dimethoxy appear equivalent in their ability to antagonize transcription induced by DHT, 11β-dimethoxy is slightly more effective in competition with R1881.

As shown here, 11β is able to bring about a reduction in total steady-state AR protein levels. As such, it might be assumed that androgen regulated gene transcription would be decreased as a result of less available transcription factor. While this is likely to be true, 11β does not significantly decrease AR protein levels at concentrations $\leq$ 1 μM (the maximum concentration used in transcriptional reporter assays), making it very likely that 11β has a true antagonistic interaction with AR in addition to causing its eventual degradation (Figure 2.15).

11β is a Mild Agonist and Moderate Antagonist of AR Transcriptional Activity with Wild-Type AR

The AR expressed in LNCaP cells has a mutation from threonine to alanine at amino acid 877, which allows for more promiscuous binding of ligands and even for

certain molecules to switch from antagonists to agonists (Veldscholte et al., 1992). Additionally, performing reporter assays in LNCaP cells does not allow for assurance that observed effects depend on AR, because it is impossible to perform a control experiment in the absence of AR. To address these two concerns, COS7 cells were also used with transfected wild-type AR (pCINeoAR) or an empty vector (pCINeo) that lacks AR. These cells are unable to increase firefly luciferase transcription driven by DHT when transfected with empty vector (Figure 2.16A), demonstrating that the PSA promoter/enhancer driven reporter plasmid is not functional in these cells in absence of AR. After transfection of wild-type AR vector, however, the COS7 cells become very responsive to DHT stimulation (Figure 2.16B). Furthermore, 11β acts as a weak agonist and an effective antagonist just as seen in LNCaP cells with the mutant AR in that scenario. The assay was also performed in MDA-MB-453 cells (also WT-AR) (Hall et al. 1994) with the same general results (Figure 2.17). Interestingly, in these cells, 11β-dimethoxy is a more effective antagonist than 11β, as was seen in LNCaP cells when competition was against R1881.

Effects of 11β Treatment on AR Transcriptional Activity are Seen with Endogenous Androgen-Regulated Genes at mRNA and Protein Levels

Reporter assays are very useful for rapid identification of potential AR antagonists, but being synthetic, may not accurately reflect transcriptional events occurring on native chromatin. Another way to assess AR agonist/antagonist activity is to measure expression of endogenous androgen-regulated genes and protein products. Measurement of endogenous androgen-regulated genes was performed with LNCaP cells, analyzing expression of *KLK2* and *KLK3* (PSA) genes by RT-PCR. The assay format is slightly different than used for reporter assays—cells are cultured for 48 hrs in CDTFBS media prior to incubation with test compounds for 24 hrs, whereas reporter assays were conducted after only 24 hrs in CDTFBS media. This extended duration in androgen-deprived media made cells more responsive to addition of androgens, increasing the reliability of results. Analysis of *KLK2* and *KLK3* transcript levels confirmed 11β compounds as AR agonists (Figure 2.18). *KLK2* was found to be more responsive to addition of androgen than *KLK3*, increasing by ~100 fold with addition of 1 nM DHT,

and by ~50-fold by addition of 1 μM 11β. Both 11β compounds also remain weakly acting antagonists of AR activation by DHT. They appear to be less effective at antagonizing transcription of native genes than in the PSA promoter/enhancer reporter system, but this may reflect the heightened androgen-responsive nature of cells cultured for an extra day without androgen. Finally, PSA protein (*KLK3* gene product) secretion into culture media was measured in order to determine whether the effects of 11β on AR-mediated transcription are carried through the steps of protein translation. The 11β compounds act similarly in affecting secretion of PSA protein into cell culture media—driving its expression in absence of androgen, but interfering with the ability of DHT to drive its expression (Figure 2.19).

Discussion

We designed 11β so that it will form sites of DNA damage that specifically recruit the AR with the purpose of limiting both adduct repair as well as AR-mediated transcription. In order for AR to bind to sites of 11β-damaged DNA, it is necessary that its expression is maintained at a certain level and that it exists in a nuclear location. Alternatively, free 11β may interact with the AR first and subsequently form a site of DNA damage, but will likely be most effective if it is able to enhance AR nuclear import and DNA binding.

The results shown here demonstrate that 11β causes a decrease in AR steady-state protein levels, and are suggestive that this decrease is due to enhanced protein turnover, rather than decreased protein synthesis. It is well established that the AR is stabilized by the binding of androgens, but not by AR antagonists, even at much higher concentrations (Kemppainen et al. 1992). Furthermore, it has been shown that this stabilization requires interaction of the N and C termini, which also enhances ligand retention (Zhou et al. 1995). As such, the enhanced receptor turnover caused by 11β is potentially due to its ability to compete away androgen binding, inhibit N/C interaction, and thereby increase protein unfolding, leading to its ubiquitylation and proteasomal degradation. AR has been shown to interact with several E3 ubiquitin ligases, including Mdm2 (Lin, Wang et

al. 2002), CHIP (Cardozo et al., 2003), and SNURF (Poukka et al., 2000). Further studies will be necessary to identify whether 11β increases receptor turnover by increasing association with any of these ubiquitin ligases. Studies can also address whether AR ubiquitylation is enhanced by 11β treatment.

While the ability of 11β to increase receptor turnover may in turn limit the quantity of complexed DNA adducts, the existence of these complexes remains to be demonstrated, and it is unclear what quantity would be necessary in order to enhance toxicity. Potentially, even a small number of complexed adducts could create a significant burden if proven more difficult to repair. Additionally, most prostate cancers depend on the presence of AR to proliferate. Therefore, 11β-mediated AR degradation could enhance toxicity by physically removing the transcription factor crucial for survival.

Even in advanced disease, prostate cancers generally maintain AR expression, often continuing to rely on androgenic signaling while having evolved the means to proliferate with either much lower androgen concentrations or by feeding on antagonists. This perpetual presence of AR allows for continued strategies of targeting AR and its signaling mechanisms such as the one reported here. One strategy of killing these cancers that is increasingly attempted involves the physical removal of AR by various means, including siRNA or use of small molecules modulating receptor expression (Zhu et al., 1999; Xing et al., 2001; Cha et al., 2005; Liao et al., 2005; Burnstein, 2005; Bhattacharyya et al., 2006; Compagno et al., 2007; Eder et al., 2000). The advantage of removing AR from the picture is that such a mechanism could be effective against hormone refractory prostate cancers, and it is unlikely to lead to resistance mechanisms such as those that switch former AR antagonists into AR agonists. 11β may work, in part, by causing increased AR turnover in the same manner as some of these other strategies, thus increasing toxicity to cells that require AR for survival.

Likewise, the ability of 11β to interfere with AR transcriptional activity may enhance toxicity. One hypothesis is that sites of DNA damaged by 11β would recruit the AR away from its natural response elements in promoters of androgen-regulated genes and thereby antagonize transcription in a novel way. However, the data shown here do not provide support for this hypothesis, since the non-DNA damaging compound, 11β-dimethoxy, has an equal or greater capacity to disrupt signaling by the AR. The data do

not definitively rule out the possibility that adducts can recruit the AR, or even that these adduct complexes would be more effective in antagonizing AR signaling than free compound. However, a hypothesis that proposes that ligand localized to DNA is more accessible by AR than ligand that does not bind DNA is unsupported. Simply put, having the ability to damage DNA has not improved the antagonistic nature of these compounds.

11β was shown to induce phosphorylation of AR at Ser81 to a similar extent as the natural androgen DHT. A detailed understanding of AR phosphorylation and how it influences AR transcriptional activity is not completely known. Studies have shown that AR transcriptional activity is positively correlated with phosphorylation at this site (Mellinghoff et al., 2004), and also that a mutant AR defective in DNA binding arrests in subnuclear foci and is hypophosphorylated at Ser81 (Black et al., 2004). Finally, cyclin-dependent kinase 1 (Cdk1) was shown to have the ability to phosphorylate AR at this site in response to addition of androgens (Chen et al. 2006). However, this same study also showed that AR transcriptional activity does not depend on phosphorylation at this site. Based on these data, it seems that AR phosphorylation is more of an effect of AR transcriptional activation than a requisite cause. It was likely, based on AR phosphorylation at this site, that 11β could also induce nuclear localization and binding to AREs.

A very important finding is that 11β causes redistribution of AR from cytoplasm into the nucleus, and even enhances binding of the AR at the synthetic PSA promoter/enhancer. If 11β did not promote this nuclear localization, it is likely that DNA damage would be minimized because the compound would become trapped in the cytoplasm in a complex with cytoplasmic receptor and fail to access DNA. This is not to suggest that a hypothetical analogue of 11β that did not promote AR re-localization would not be able to form sites of DNA damage, but that it may have reduced ability to do so compared to the compound which does re-localize AR directly to DNA. The ability of 11β to cause AR redistribution into the nucleus is not altogether surprising, as several AR antagonists including hydroxyflutamide, bicalutamide, and RU486 also elicit the same nuclear transport (Kemppainen et al. 1992; Masiello et al. 2002). RU486 shares the same steroidal framework of 11β, and has similar effects on AR transcription, acting as a partial agonist. It is thought that the ability of RU486 to abrogate AR N/C

interaction and antagonize activity (Song et al., 2004) is due to the bulky dimethyl-amino-phenyl group appended at its position 11β preventing closure of helix 12, as demonstrated in the crystal structure of RU486 complexed to the highly structurally similar GR-LBD (Kauppi et al., 2003). As such, we deem it likely that 11β limits N/C interaction in AR by a similar displacement of helix 12. Inhibition of the N/C interaction does not always correlate with pure antagonism, and this is true in the case of both RU486 and 11β, as higher concentrations of each permit minimal AR transactivation. While this can be viewed as a limitation of standard AR antagonist therapies, we consider it advantageous that 11β successfully relocalizes the AR to AREs within androgen-responsive gene promoters, as this likely assists in formation of DNA adducts. Inhibiting the N/C interaction that occurs in the AR may also help explain increased receptor turnover.

While 11β is not an exceptional antagonist of AR activity, it remains effective in preventing growth of LNCaP xenograft tumors while sparing the mice bearing them. Further studies have been performed to determine more definitively whether the AR has a role in this mechanism of tumor-specific toxicity.

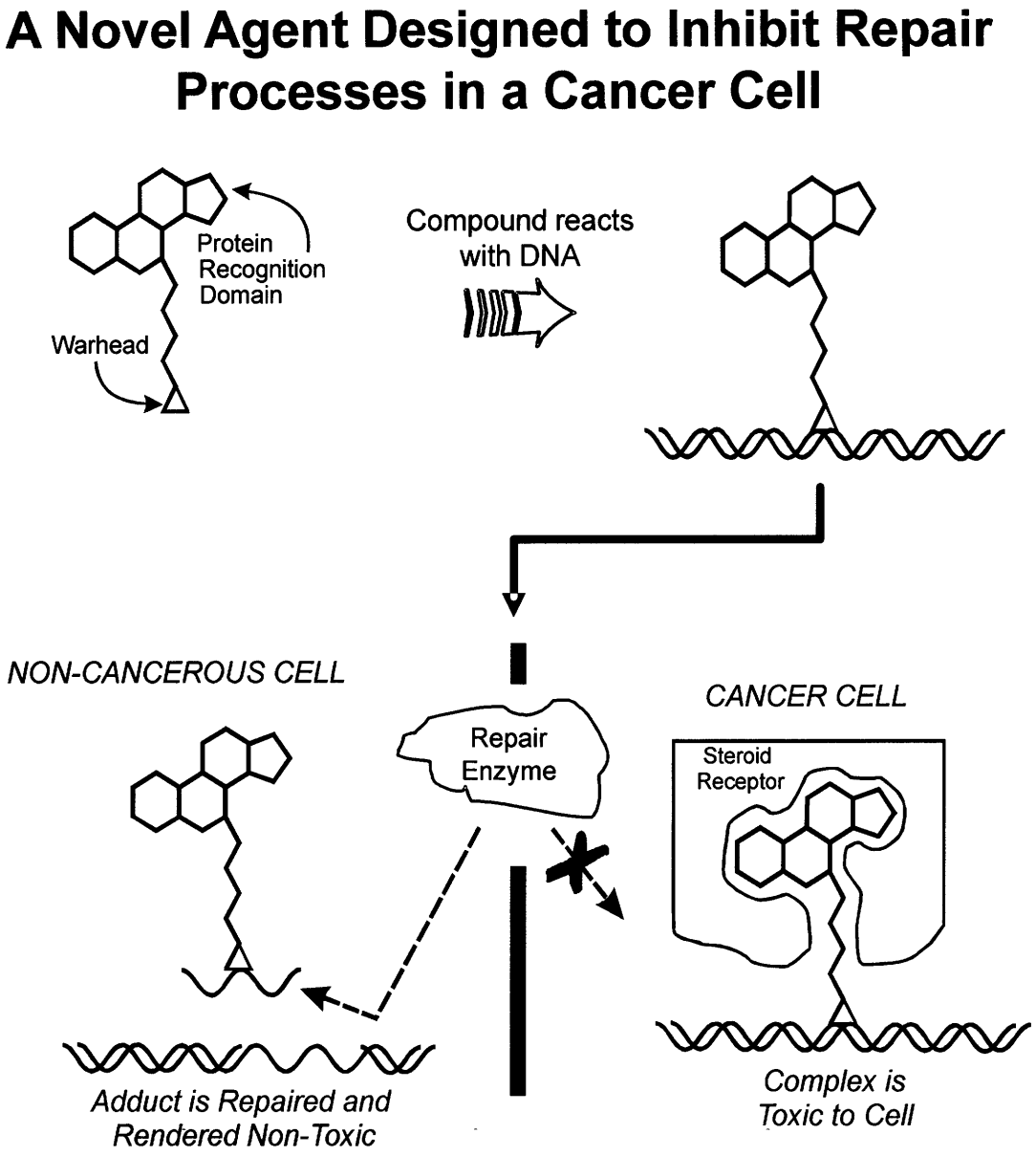

Fig 2.1 Rationale for drug design. Molecules are designed such that they have dual functionality– ability to damage DNA while maintaining affinity for a cancer-specific protein. As shown here, the molecule would enter cells and damage DNA. Then, in normal cells where this protein is expressed at lower levels, repair would occur, while in a cancer cell expressing the protein (steroid receptor in this example), the protein would bind to an adduct and physically shield it from repair enzymes. Additionally, where this cancer-specific protein is a transcription factor involved in survival, it is thought that titration away from response elements would enhance toxicity.

11β Causes Reduction in Steady-State Level of AR Protein in LNCaP Cells

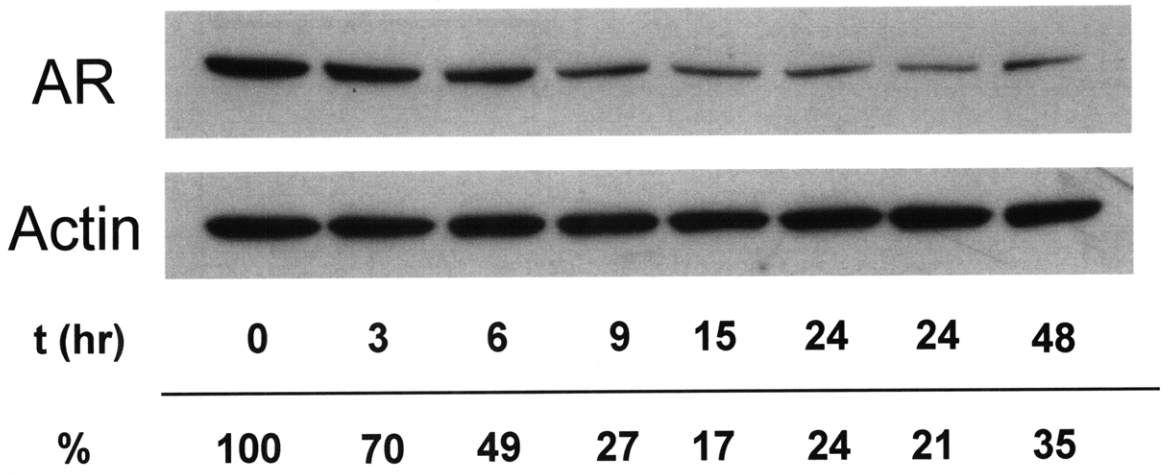

Fig 2.2 Measurement of AR protein levels in LNCaP cells. LNCaP cells were treated for times shown with 5 μM 11β, before isolation and measurement of protein levels by Western blot as discussed in Materials and Methods.

11β Causes Reduction in Steady-State Level of AR Protein in C4-2B and CWR22Rv1 Cells

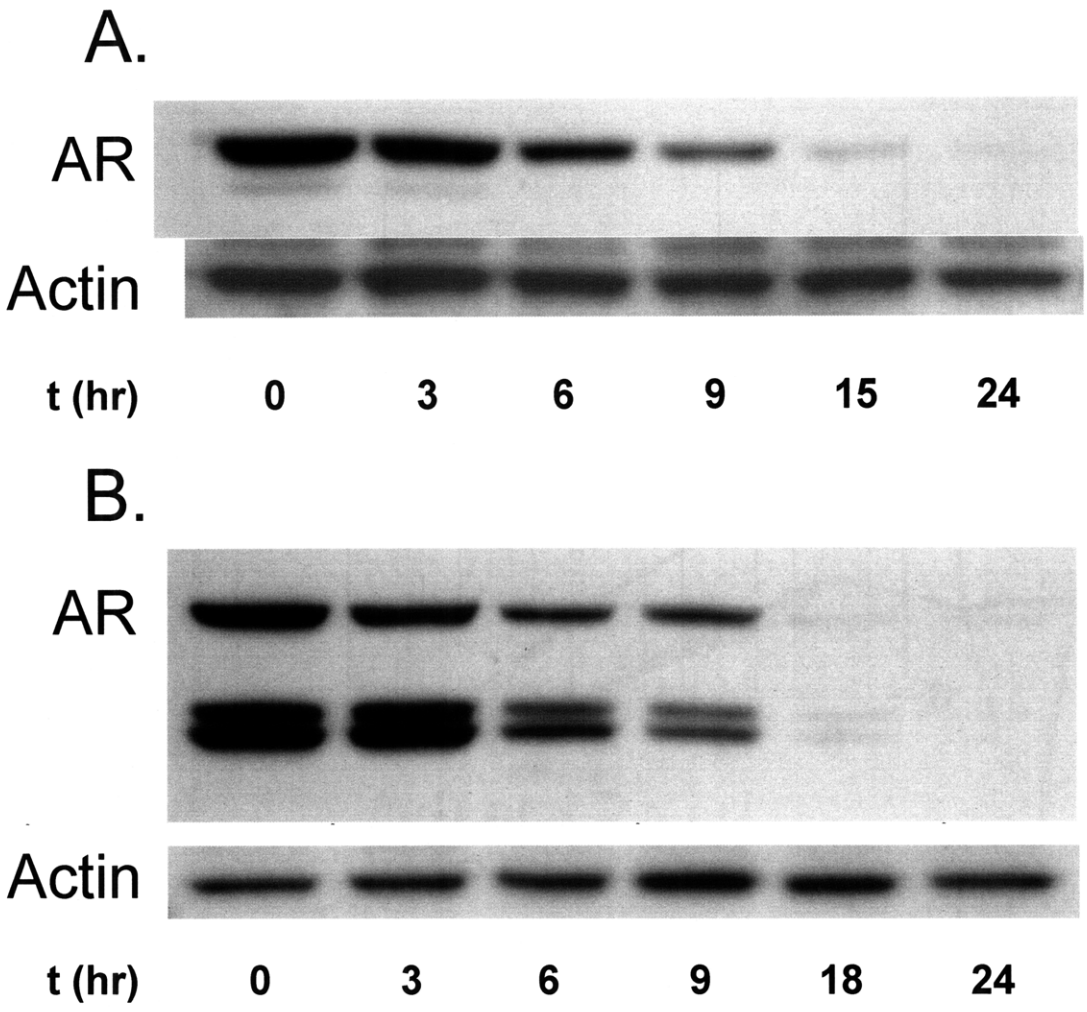

Fig 2.3 Measurement of AR protein levels in C4-2B (A) and CWR22Rv1 (B) cells. Cells were treated for times shown with 5 μM 11β, before isolation and measurement of protein levels by Western blot as discussed in Materials and Methods.

11β Does Not Significantly Affect AR mRNA Expression in LNCaP Cells

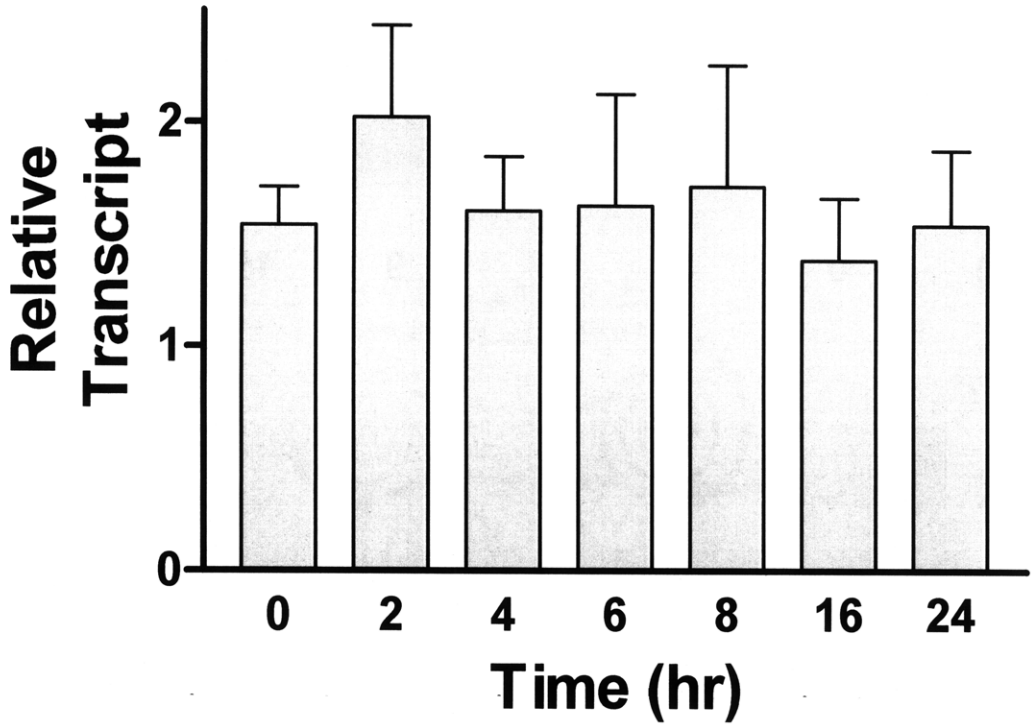

Fig 2.4 AR mRNA levels following 11β treatment. Cells were treated with 5 μM 11β for times shown prior to harvesting cells and isolating total mRNA. *AR* mRNA was measured by quantitative RT-PCR and normalized to *GAPDH* as discussed in Materials and Methods.

11β-Dimethoxy Also Causes Reduction in AR Protein Levels

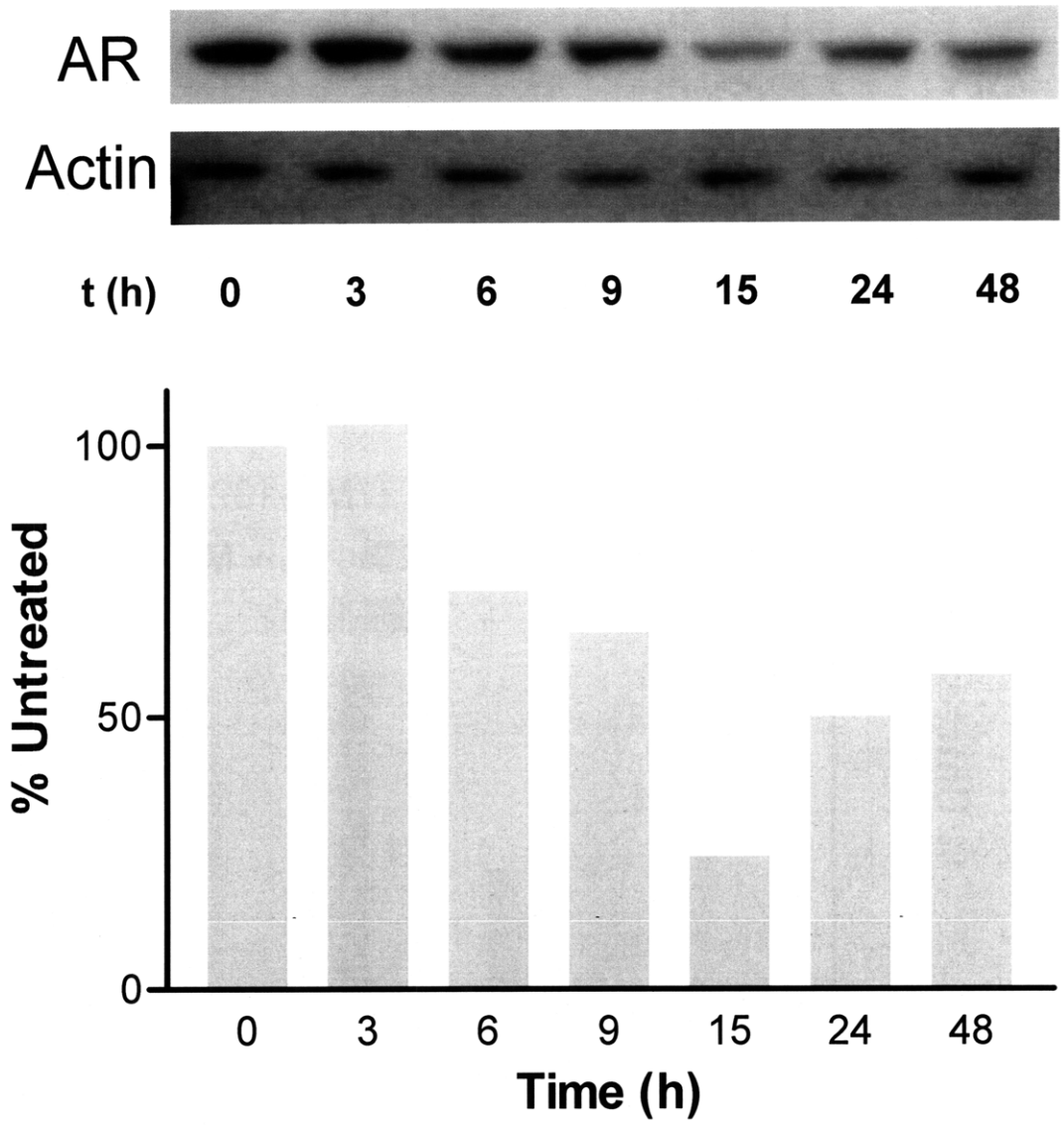

Fig 2.5 Analysis of AR protein levels after treatment with 5 μM 11β-dimethoxy for times shown, before isolation and measurement of protein levels by Western blot as discussed in Materials and Methods. Spot densitometry is shown below.

Proteasome Inhibition Hinders 11β-Mediated AR Down Regulation

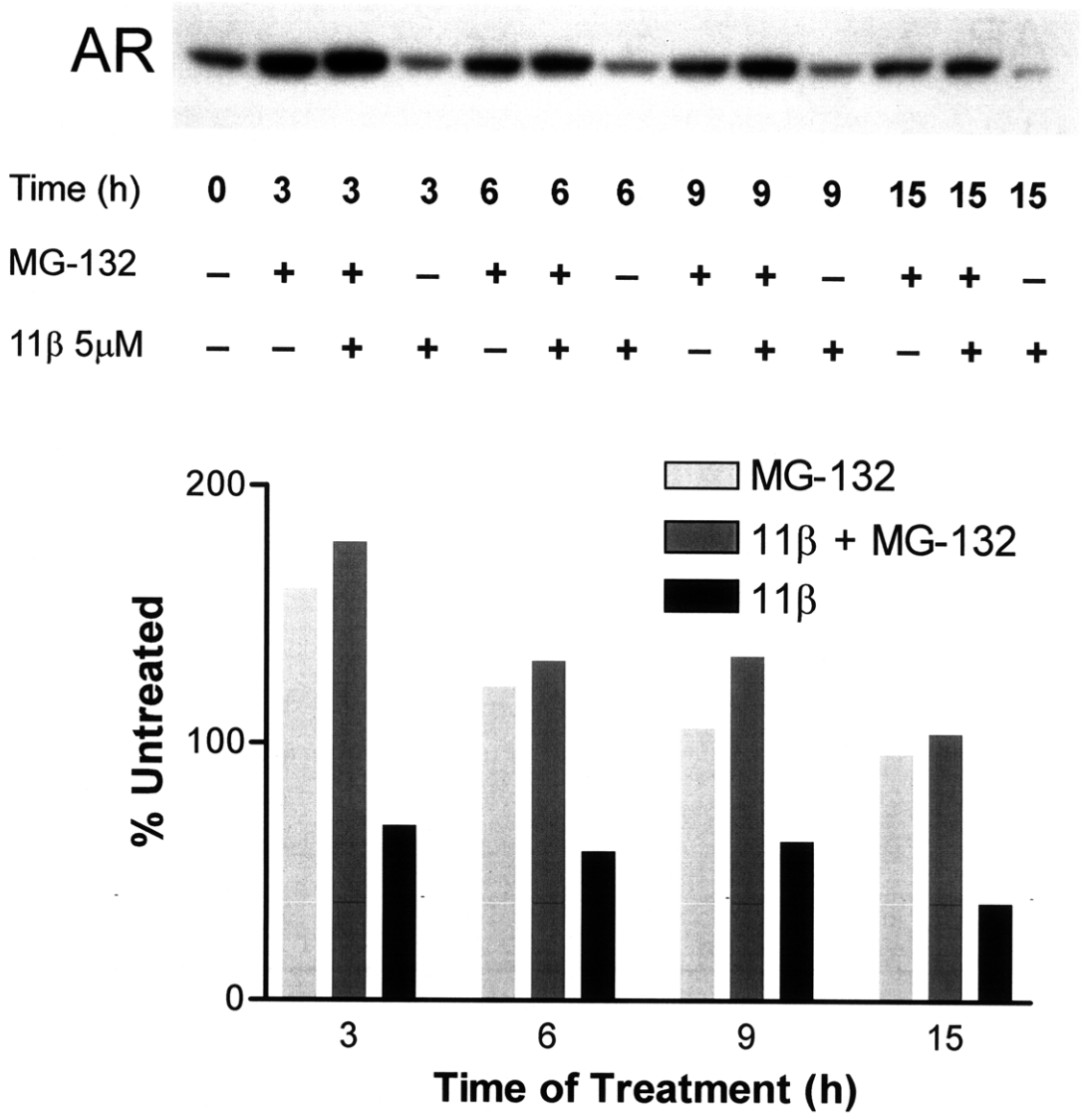

Fig 2.6 Analysis of AR protein levels after treatment with 11β in the presence of the proteasome inhibitor MG-132 (5 μM). Spot densitometry is shown below.

AR Degradation Is not Enhanced by 11β in Absence of New Protein Synthesis

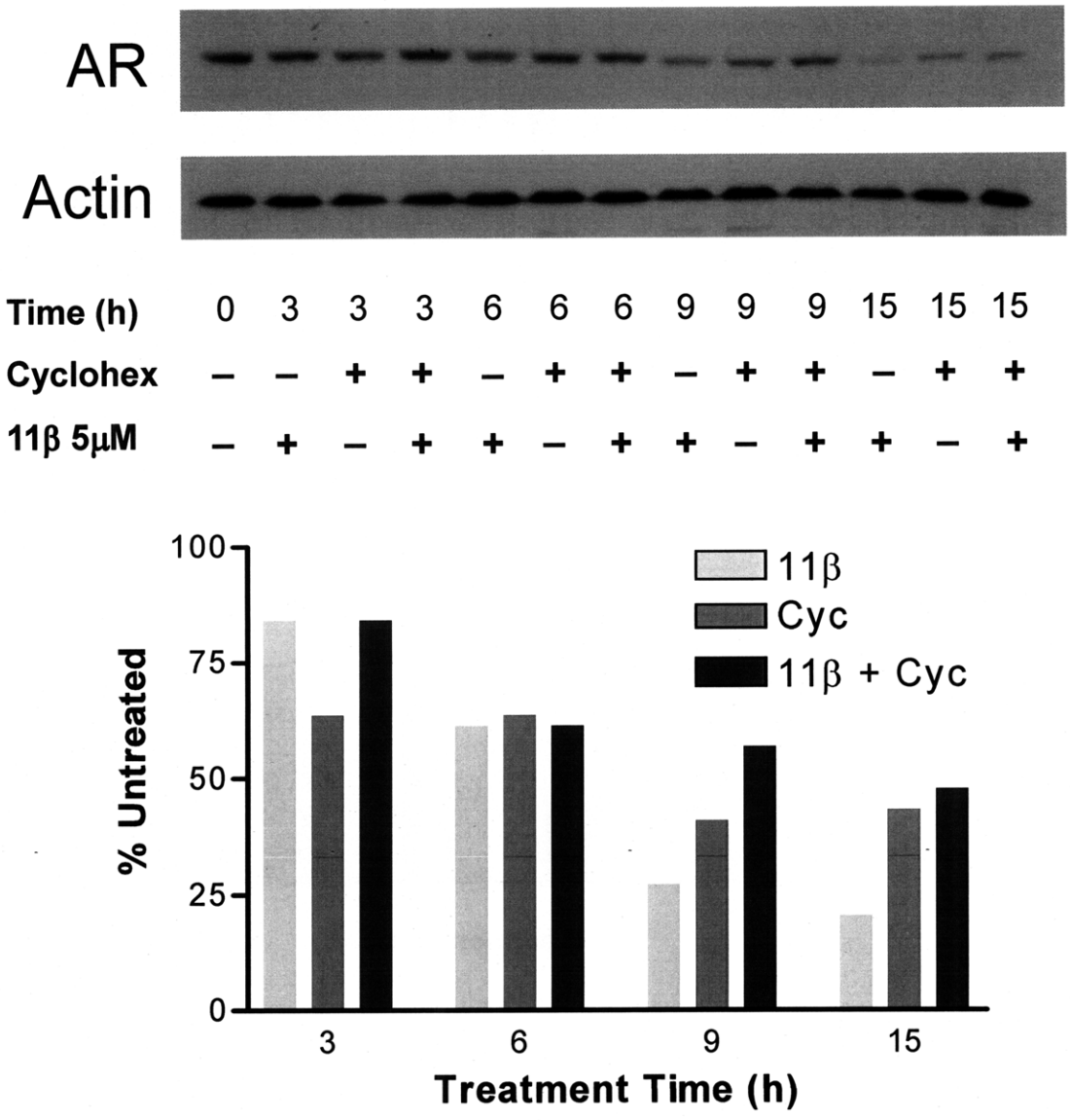

Fig 2.7 Analysis of AR protein levels after treatment with 11β in the presence of translational inhibitor cycloheximide (10 μM) for times shown. Spot densitometry is shown below.

Competition with Ligand for AR Limits 11β-Mediated AR Degradation

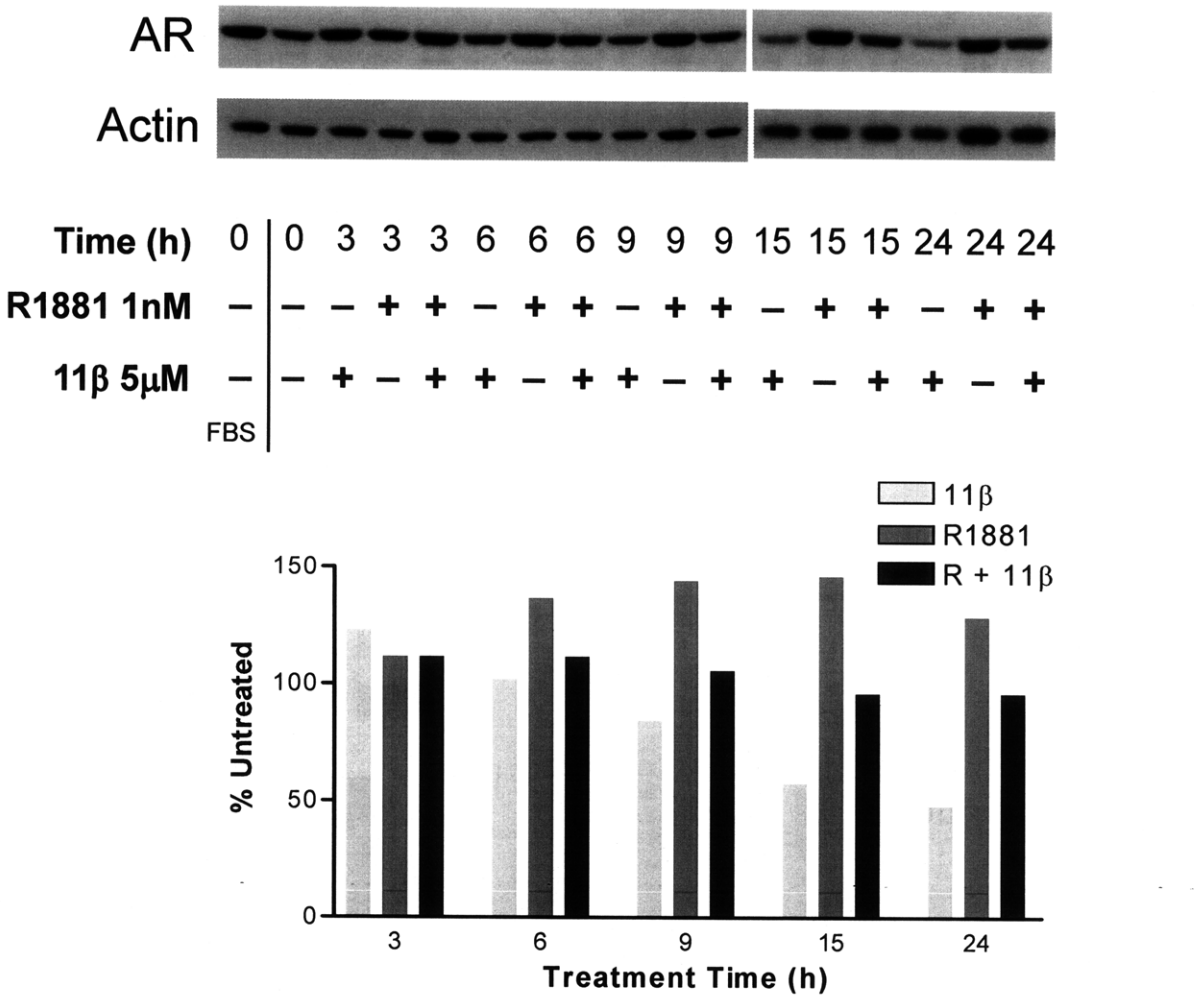

Fig 2.8 Analysis of AR protein levels after treatment with 11β in the presence of synthetic AR ligand R1881. First lane is from cells grown in media containing 10% FBS for comparison, while all other lanes are grown in media containing CDTFBS (androgen free). Spot densitometry is shown in graph below, relative to AR level in untreated cells (CDTFBS media).

AR Phosphorylation (Ser81) is Induced by 11β

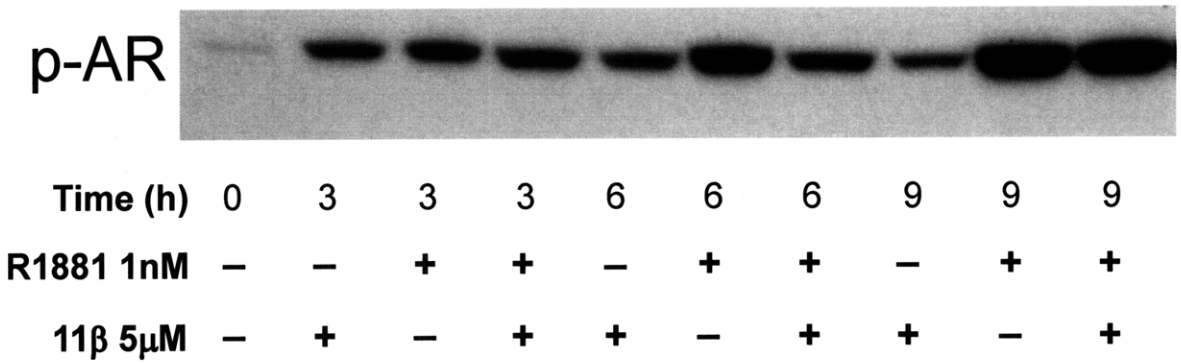

Fig 2.9 Analysis of AR protein phosphorylation by Western blot. LNCaP cells, growing in CDTFBS containing media, were treated as indicated before isolating proteins and immunoblotting for AR Ser81 phosphorylation.

11β Induces AR Nuclear Localization

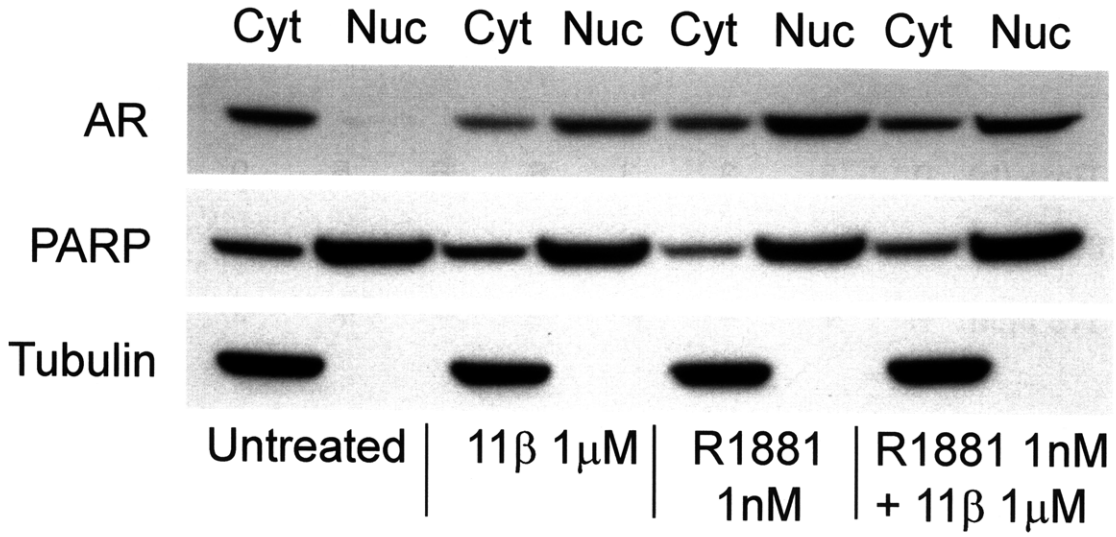

Fig 2.10 Analysis of AR location by Western blotting. LNCaP cells were treated for 24 hrs in CDTFBS containing media as indicated before separation of nuclear and cytoplasmic fractions. These extracts were then probed for expression of AR, PARP (nuclear protein), and β-tubulin (cytoplasmic protein). Cytoplasmic fractions = 20 μg total protein, nuclear fractions = 10 μg.

11β Compounds Inhibit N/C Terminal Interaction of the AR Induced by DHT

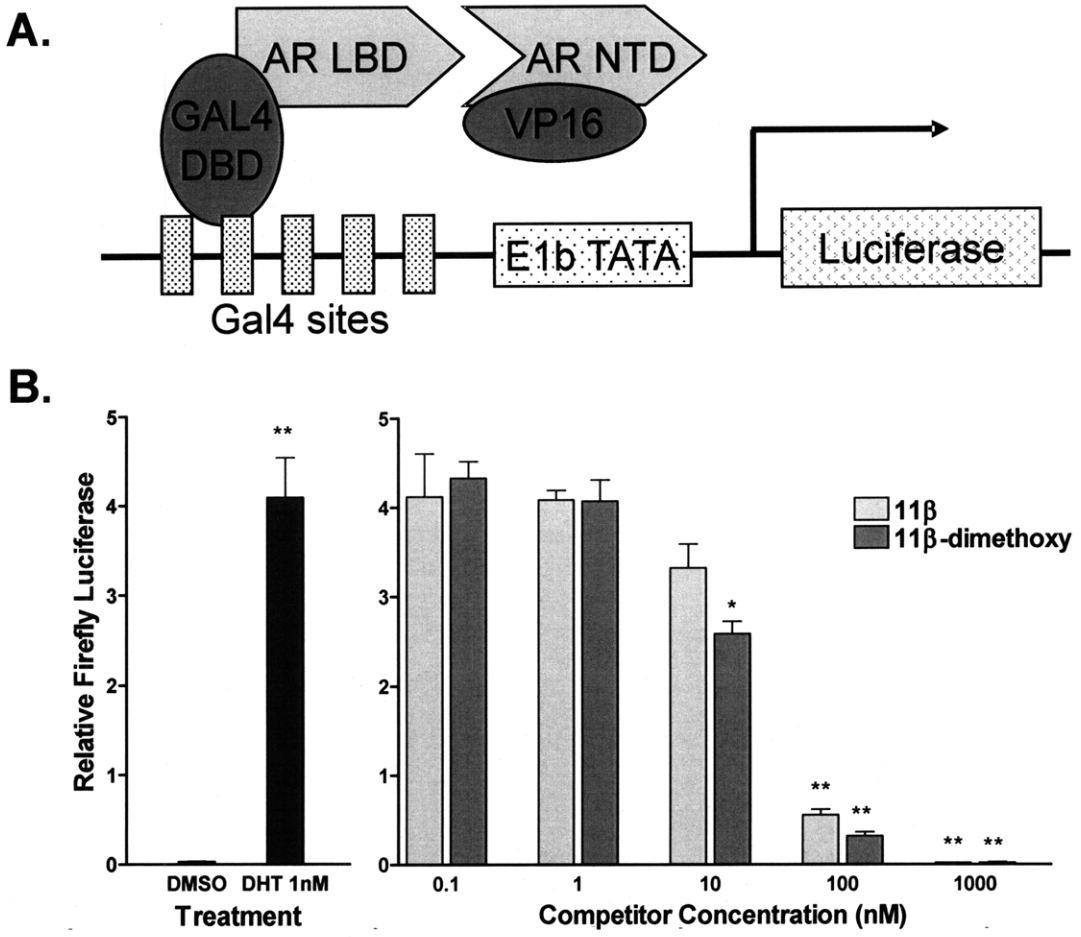

Fig 2.11 Measurement of N/C terminal interaction within the AR by mammalian two-hybrid assay. A. Schematic diagram of assay. B. COS7 cells were transfected with plasmids pmARLBD-649-919, VP16ARNTD1-538, pG5luc, and pgL4.74, then later treated with compounds shown in CDTFBS containing media for 24 hrs before isolation and measurement of firefly and *renilla* luciferase. Right graph contains 1 nM DHT in all samples. Error bars are +/- SEM. *p-val < 0.05, **p-val < 0.01 (significance of differential expression is in comparison to 1 nM DHT in graph on right).

11β Compounds Are Weak AR Agonists

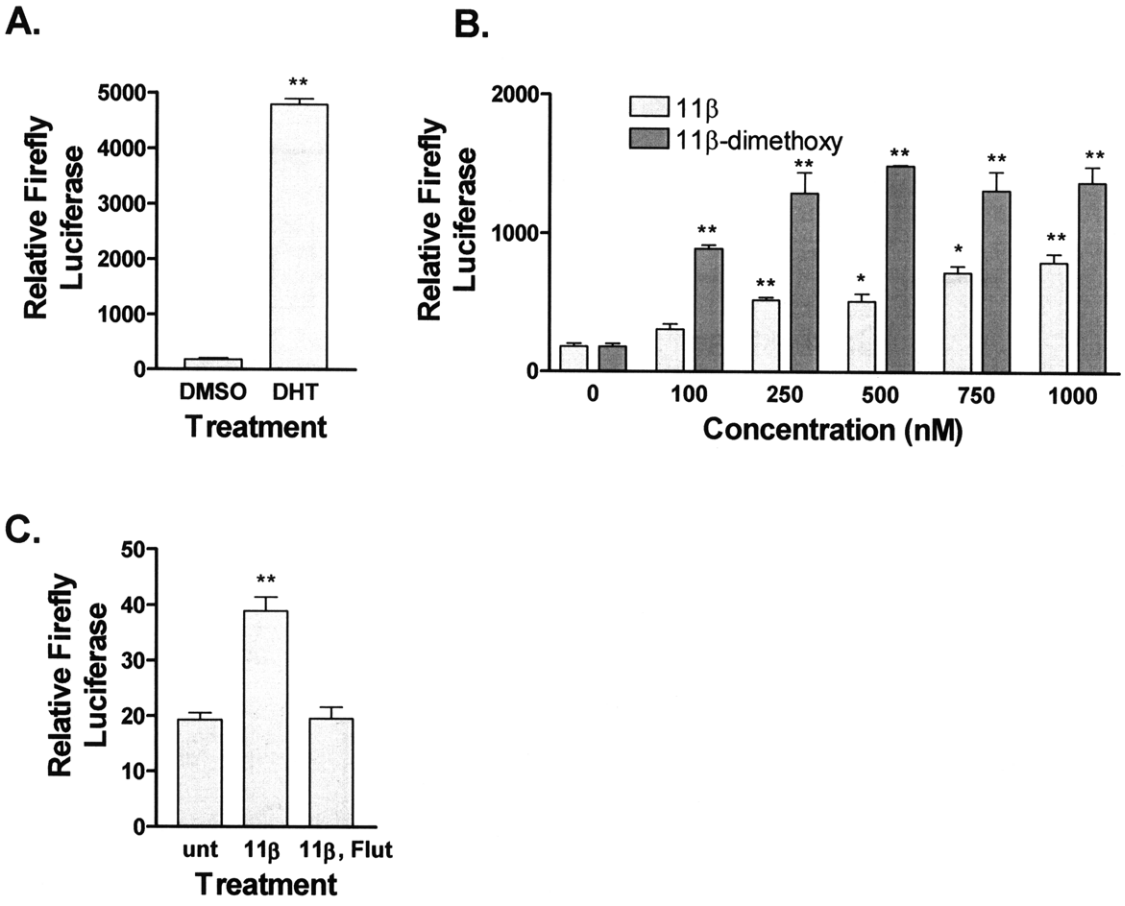

Fig 2.12 Measurement of AR Activation by luciferase reporter assay. LNCaP cells were transfected with plasmids pGL4PSA and pGL4.74 before treatment for 24 hrs in CDTFBS containing media with compounds indicated. A. 1 nM DHT induces ~27-fold activity over background, B. 1 μM 11β and 11β-dimethoxy induce ~4 and 7-fold enhanced transcription over background, respectively. C. Enhanced activation of AR is dependent on interaction between 11β and AR, as 10 μM flutamide (Flut) prevents 1 μM 11β activation. Error bars are +/- SEM. *p-val < 0.05, **p-val < 0.01.

11β Promotes Efficient Association of AR with the PSA Promoter

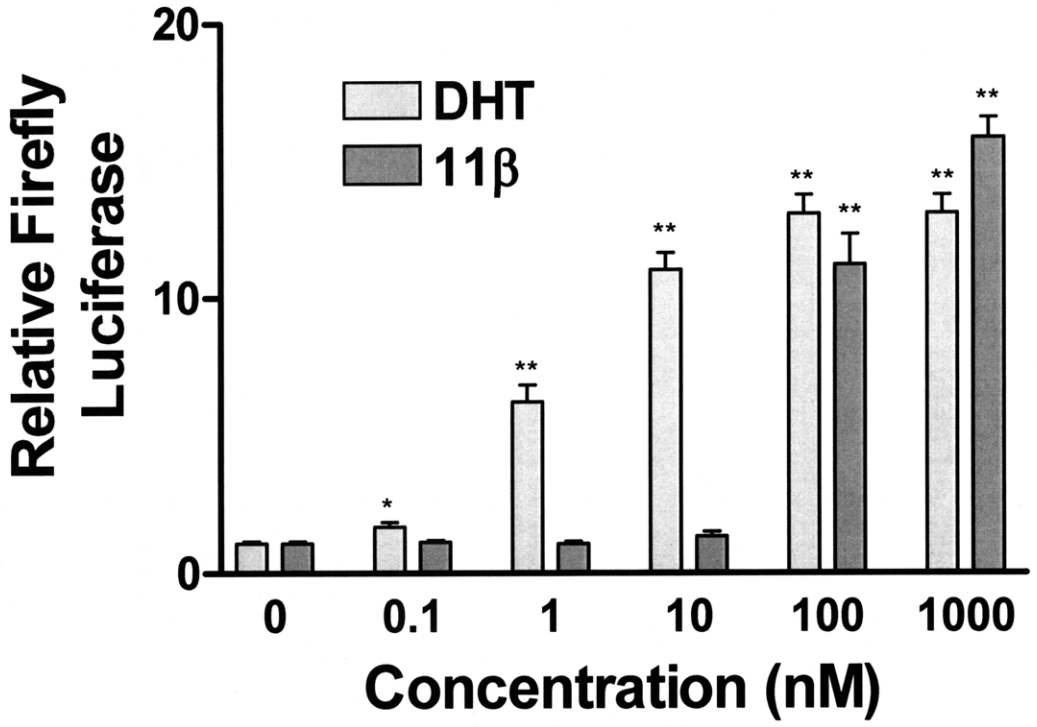

Fig 2.13 Measurement of AR activation by luciferase reporter assay. COS7 cells were transfected with plasmids VP16-AR, pGL4PSA, and pGL4.74 before treatment for 24 hrs in CDTFBS containing media with compounds indicated. Error bars are +/- SEM. *p-val < 0.05, **p-val < 0.01.

11β Compounds are Moderate AR Antagonists

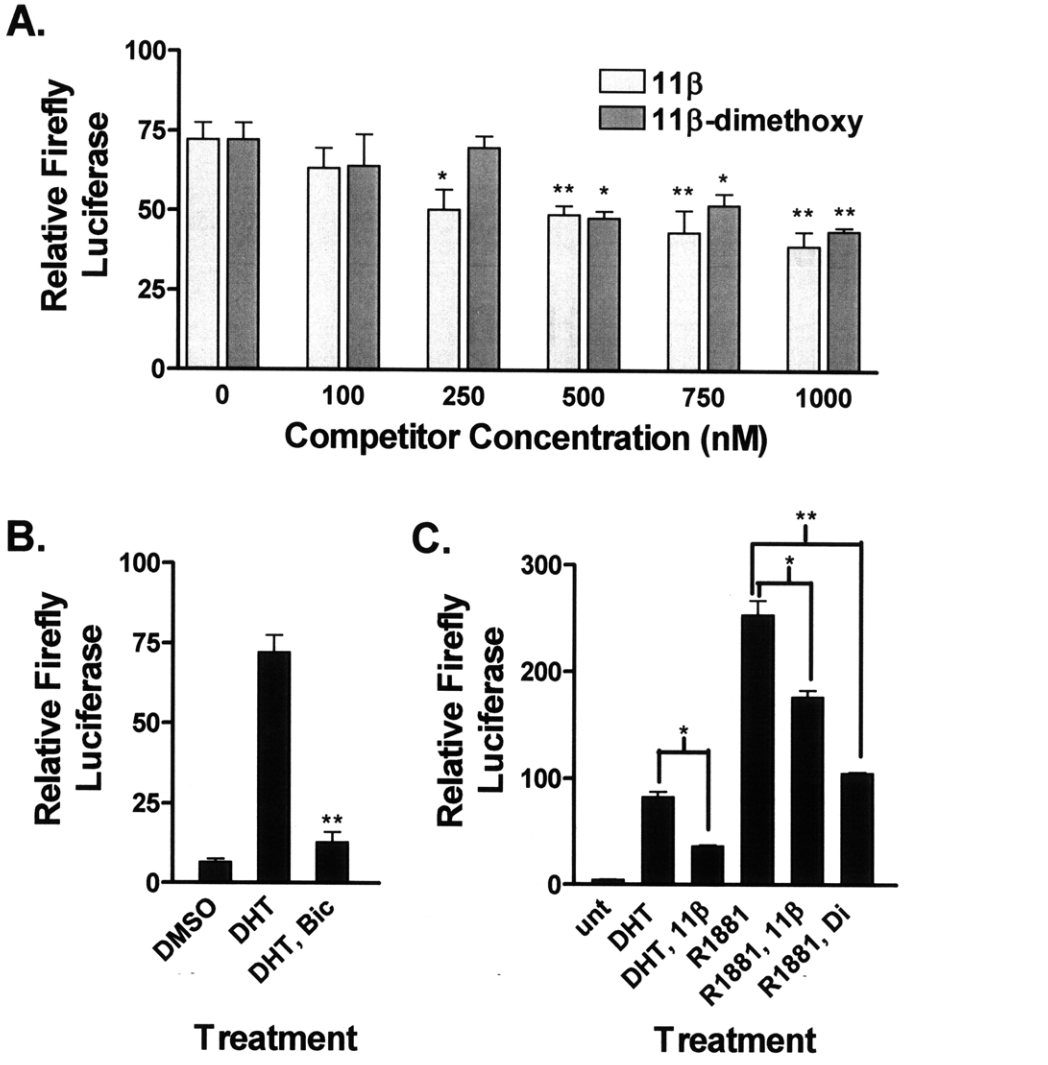

Fig 2.14 Measurement of AR activation by luciferase reporter assay. LNCaP cells were transfected with plasmids pGL4PSA and pGL4.74 before treatment for 24 hrs with compounds and concentrations indicated, in CDTFBS containing media. A. 11β compounds are able to antagonize DHT-enhanced AR activity by as much as ~60% B. DHT activation of AR transcription is ~27-fold greater than background, while 1 μM bicalutamide (bic) effectively antagonizes most of this activity. C. 11β (1 μM) is able to antagonize AR activity driven by DHT or R1881; 11β-dimethoxy (Di) is slightly more effective than 11β against R1881-driven AR transcriptional activity. Error bars are +/- SEM. *p-val < 0.05, **p-val < 0.01.

11β Does Not Significantly Reduce AR Levels at Concentrations ≤ 1μM

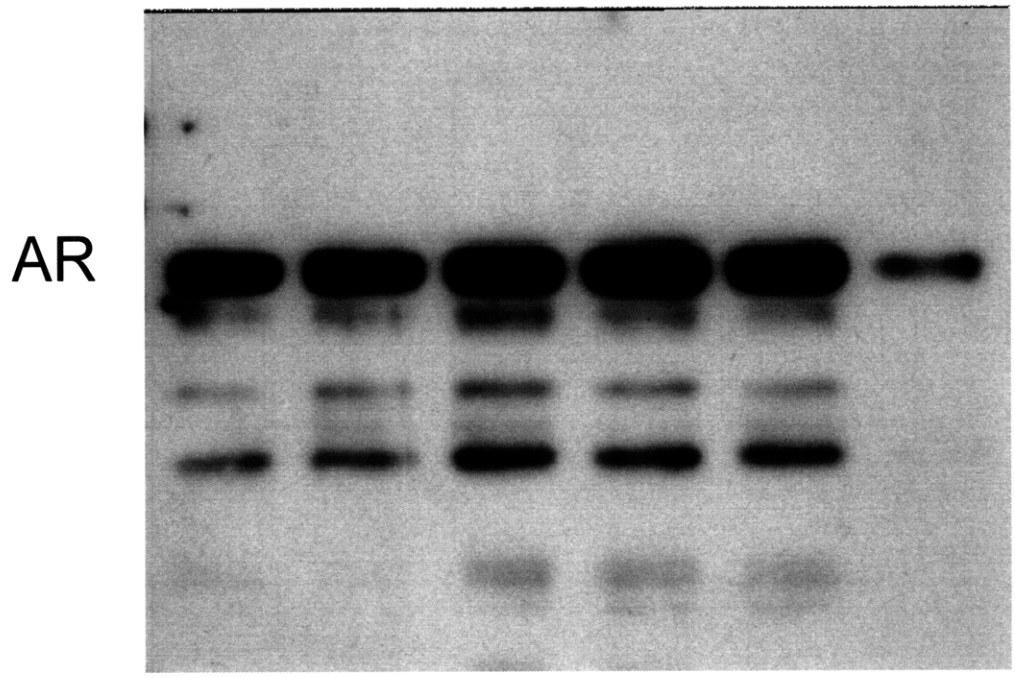

Fig 2.15 Western blot of AR level in LNCaP cells treated with 11β. Cells were treated as indicated prior to analysis of AR protein levels by immunoblot. Concentrations up to 1 μM do not significantly affect AR protein levels.

11β Acts as Mild Agonist and Moderate Antagonist Toward Wild-Type AR (COS7 cells)

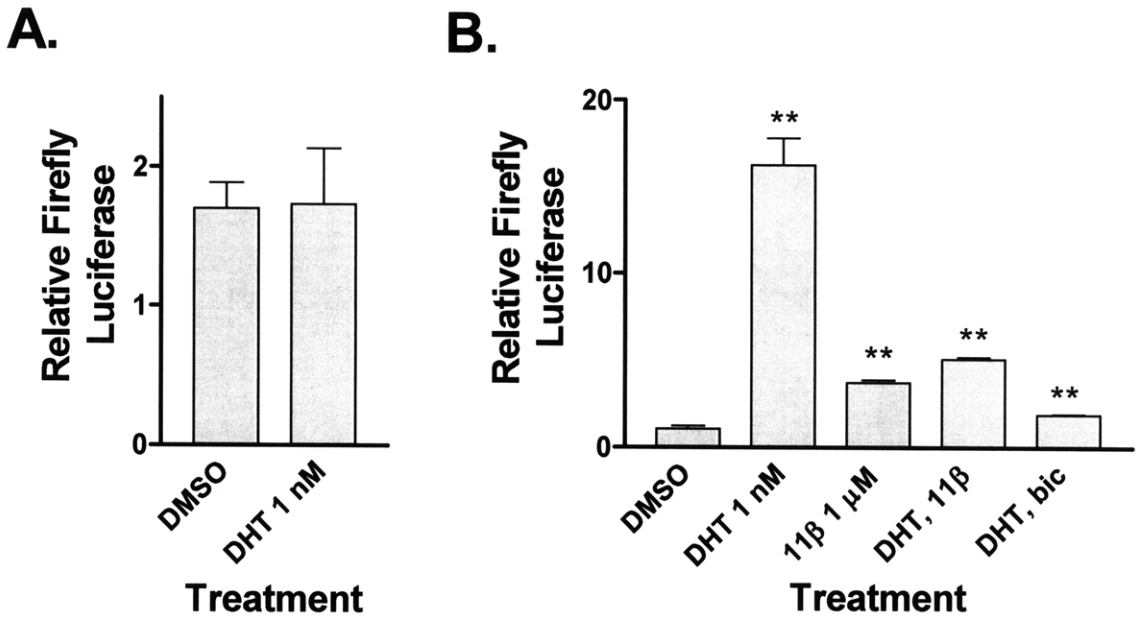

Fig 2.16 Measurement of AR activation by luciferase reporter assay. COS7 cells were transfected with plasmids pGL4PSA, pGL4.74, and pCINeo (A) or pCINeoAR (B) before treatment for 24 hrs with compounds indicated in CDTFBS containing media. A. There is no enhanced firefly luciferase expression in absence of AR. B. When wild-type AR is transfected, 11β is a weak agonist and a moderate antagonist of AR activity. Bic = bicalutamide, 1 μM. Error bars are +/- SEM. **p-val < 0.01; DHT, 11β are with reference to DMSO, DHT + 11β or bicalutamide are with reference to 1 nM DHT.

11β Acts as Mild Agonist and Moderate Antagonist Toward Wild-Type AR (MDA-MB-453 Cells)

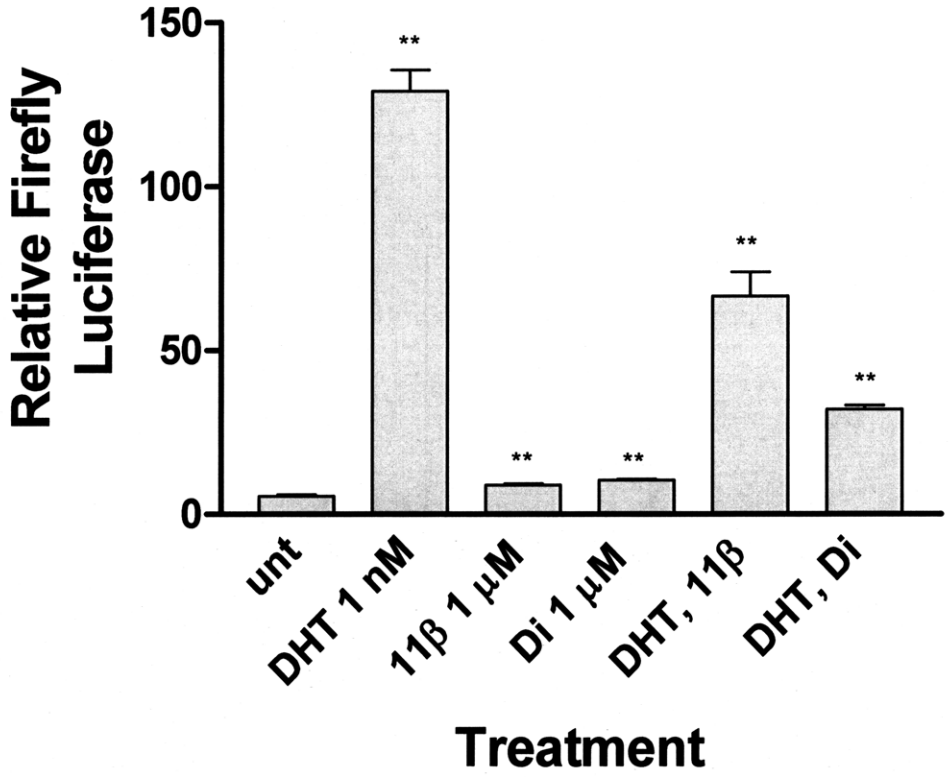

Fig 2.17 Measurement of AR transcriptional activity in MDA-MB-453 cells. Cells were transfected with pGL4PSA and pGL4.74 vectors prior to indicated treatments for 24 hrs in CDTFBS containing media. Extracts were then prepared and assayed for firefly and renilla luciferase. 11β acts as a weak agonist, and also as a moderate antagonist towards the wild-type AR expressed in these breast cancer cells. Error bars are +/- SEM. **p-val < 0.01; for DHT, 11β and 11β-dimethoxy (di), comparison is to untreated. For DHT + 11β or 11β-dimethoxy, comparison is to 1 nM DHT.

Identification of 11β Compounds as Partial AR Agonists is Supported by RT-PCR of Androgen-Regulated Genes

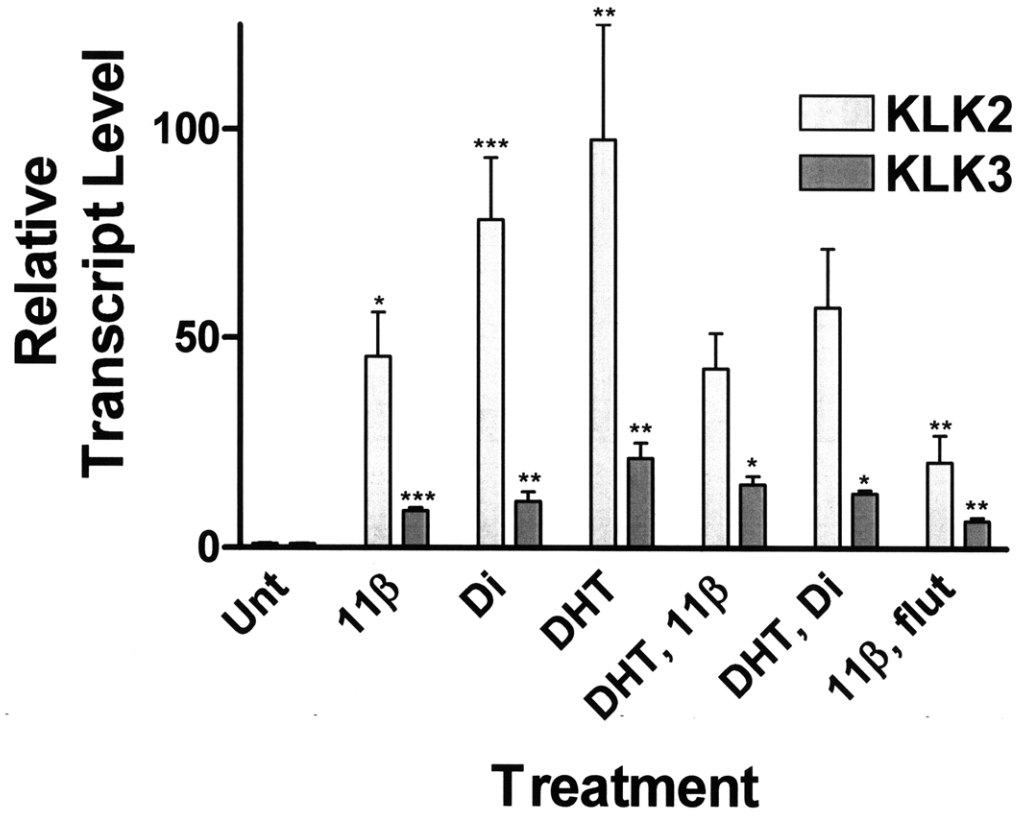

Fig 2.18 Measurement of *KLK2* and *KLK3* (PSA) mRNA levels by RT-PCR. LNCaP cells, previously grown in hormone-depleted media for 48 hrs, were treated with compounds shown (DHT, 1 nM; 11β, 1 μM; Di = 11β-dimethoxy, 1 μM; flut = flutamide, 10 μM) for 24 hrs prior to isolation of RNA and analysis as described in materials and methods. Error bars are +/- SEM. *p-val < 0.1, **p-val < 0.05, ***p-val < 0.01; For 11β, 11β-dimethoxy (di), and DHT, comparison is to untreated, for DHT + 11β or 11β-dimethoxy, comparison is to DHT, for 11β + flutamide, comparison is to 11β.

11β Increases Secretion of PSA into Culture Media and is Weakly Antagonistic toward DHT-induced PSA Secretion

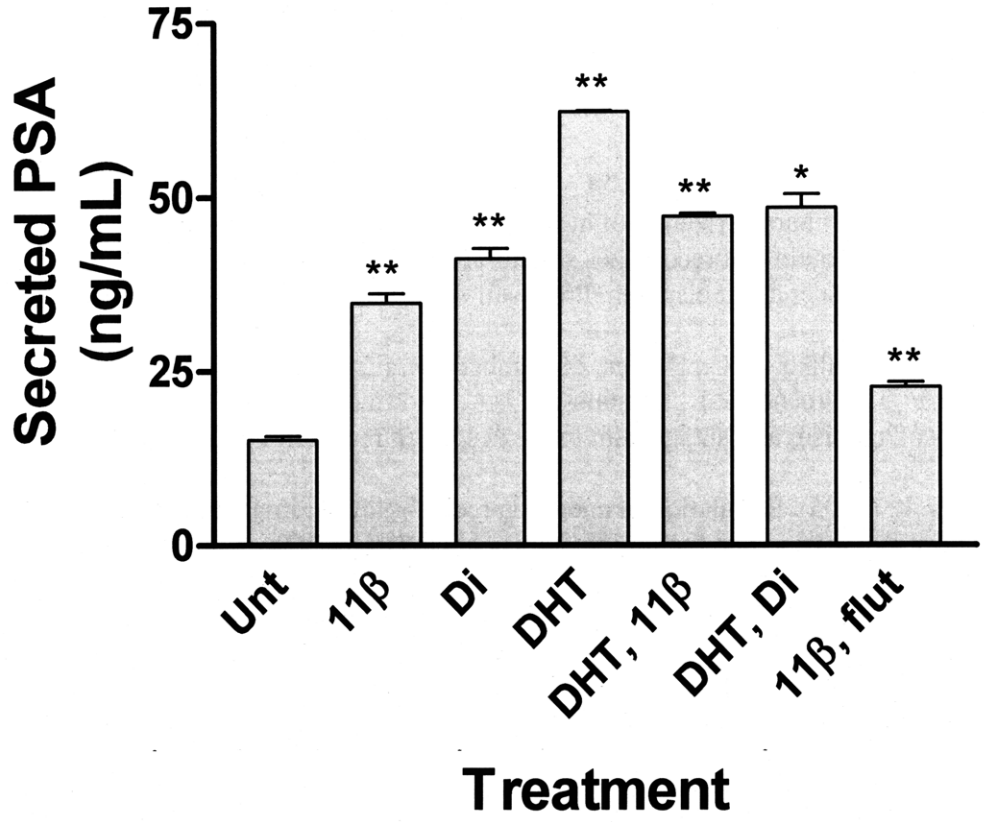

Fig 2.19 Measurement of PSA secretion into media of growing LNCaP cells, previously cultured in hormone-depleted media for 48 hrs before treatment with compounds shown (DHT, 1 nM; 11β, 1 μM; Di = 11β-dimethoxy, 1 μM; flut = flutamide, 10 μM) for 24 hrs prior to isolation of RNA and analysis as described in materials and methods. Error bars are +/- SEM. *p-val < 0.05, **p-val < 0.01; For 11β, 11β-dimethoxy, and DHT, comparison is to untreated, For DHT + 11β or 11β-dimethoxy, comparison is to DHT. For 11β + flutamide, comparison is to 11β.

References

Bhattacharyya, R. S., Krishnan, A. V., Swami, S., and Feldman, D. (2006). Fulvestrant (ICI 182,780) down-regulates androgen receptor expression and diminishes androgenic responses in LNCaP human prostate cancer cells. Mol Cancer Ther *5*, 1539-49.

Black, B. E., Vitto, M. J., Gioeli, D., Spencer, A., Afshar, N., Conaway, M. R., Weber, M. J., and Paschal, B. M. (2004). Transient, ligand-dependent arrest of the androgen receptor in subnuclear foci alters phosphorylation and coactivator interactions. Mol Endocrinol *18*, 834-50.

Brinkmann, A. O., Blok, L. J., de Ruiter, P. E., Doesburg, P., Steketee, K., Berrevoets, C. A., and Trapman, J. (1999). Mechanisms of androgen receptor activation and function. The Journal of Steroid Biochemistry and Molecular Biology *69*, 307-313.

Bruhn, S. L., Pil, P. M., Essigmann, J. M., Housman, D. E., and Lippard, S. J. (1992). Isolation and characterization of human cDNA clones encoding a high mobility group box protein that recognizes structural distortions to DNA caused by binding of the anticancer agent cisplatin. Proc Natl Acad Sci U S A *89*, 2307-11.

Brzozowski, A. M., Pike, A. C., Dauter, Z., Hubbard, R. E., Bonn, T., Engström, O., Ohman, L., Greene, G. L., Gustafsson, J. A., and Carlquist, M. (1997). Molecular basis of agonism and antagonism in the oestrogen receptor. Nature *389*, 753-8.

Burnstein, K. L. (2005). Regulation of androgen receptor levels: implications for prostate cancer progression and therapy. J Cell Biochem *95*, 657-69.

Cardozo, C. P., Michaud, C., Ost, M. C., Fliss, A. E., Yang, E., Patterson, C., Hall, S. J., and Caplan, A. J. (2003). C-terminal Hsp-interacting protein slows androgen receptor synthesis and reduces its rate of degradation. Arch Biochem Biophys *410*, 134-40.

Cha, T., Qiu, L., Chen, C., Wen, Y., and Hung, M. (2005). Emodin Down-Regulates Androgen Receptor and Inhibits Prostate Cancer Cell Growth. Cancer Res *65*, 2287-2295.

Chen, S., Xu, Y., Yuan, X., Bubley, G. J., and Balk, S. P. (2006). Androgen receptor phosphorylation and stabilization in prostate cancer by cyclin-dependent kinase 1. Proc Natl Acad Sci U S A. *103*, 15969–15974.

Compagno, D., Merle, C., Morin, A., Gilbert, C., Mathieu, J. R. R., Bozec, A., Mauduit, C., Benahmed, M., and Cabon, F. (2007). SIRNA-Directed In Vivo Silencing of Androgen Receptor Inhibits the Growth of Castration-Resistant Prostate Carcinomas. PLoS ONE *2*, e1006.

Culig, Z., Hoffmann, J., Erdel, M., Eder, I. E., Hobisch, A., Hittmair, A., Bartsch, G., Utermann, G., Schneider, M. R., Parczyk, K., et al. (1999). Switch from antagonist to agonist of the androgen receptor bicalutamide is associated with prostate tumour progression in a new model system. Br J Cancer *81*, 242-51.

Donahue, B. A., Augot, M., Bellon, S. F., Treiber, D. K., Toney, J. H., Lippard, S. J., and Essigmann, J. M. (1990). Characterization of a DNA damage-recognition protein from mammalian cells that binds specifically to intrastrand d(GpG) and d(ApG) DNA adducts of the anticancer drug cisplatin. Biochemistry *29*, 5872-80.

Eder, I. E., Culig, Z., Ramoner, R., Thurnher, M., Putz, T., Nessler-Menardi, C., Tiefenthaler, M., Bartsch, G., and Klocker, H. (2000). Inhibition of LncaP prostate cancer cells by means of androgen receptor antisense oligonucleotides. Cancer Gene Ther *7*, 997-1007.

Gioeli, D., Ficarro, S. B., Kwiek, J. J., Aaronson, D., Hancock, M., Catling, A. D., White, F. M., Christian, R. E., Settlage, R. E., Shabanowitz, J., et al. (2002). Androgen Receptor Phosphorylation. Regulation and Identification of the Phosphorylation Sites. J. Biol. Chem. *277*, 29304-29314.

Gregory, C. W., Hamil, K. G., Kim, D., Hall, S. H., Pretlow, T. G., Mohler, J. L., and French, F. S. (1998). Androgen receptor expression in androgen-independent prostate cancer is associated with increased expression of androgen-regulated genes. Cancer Res *58*, 5718-24.

Hall, R. E., Birrell, S. N., Tilley, W. D., and Sutherland, R. L. (1994). MDA-MB-453, an androgen-responsive human breast carcinoma cell line with high level androgen receptor expression. Eur J Cancer *30A*, 484-90.

Hillier, S. M., Marquis, J. C., Zayas, B., Wishnok, J. S., Liberman, R. G., Skipper, P. L., Tannenbaum, S. R., Essigmann, J. M., and Croy, R. G. (2006). DNA adducts formed by a novel antitumor agent 11{beta}-dichloro in vitro and in vivo. Mol Cancer Ther *5*, 977-984.

Hodgson, M. C., Shen, H. C., Hollenberg, A. N., and Balk, S. P. (2008). Structural basis for nuclear receptor corepressor recruitment by antagonist-liganded androgen receptor. Mol Cancer Ther *7*, 3187-3194.

Holzbeierlein, J., Lal, P., LaTulippe, E., Smith, A., Satagopan, J., Zhang, L., Ryan, C., Smith, S., Scher, H., Scardino, P., et al. (2004). Gene expression analysis of human prostate carcinoma during hormonal therapy identifies androgen-responsive genes and mechanisms of therapy resistance. Am J Pathol *164*, 217-27.

Horner, M., Ries, L., Krapcho, M., Neyman, N., Aminou, R., Howlader, N., Altekruse, S., Feuer, E., Huang, L., Mariotto, A., et al. eds. (2009). SEER Cancer Statistics Review, 1975-2006 (Bethesda, MD: National Cancer Institute).

Jemal, A., Siegel, R., Ward, E., Hao, Y., Xu, J., Murray, T., and Thun, M. J. (2008). Cancer statistics, 2008. CA Cancer J Clin *58*, 71-96.

Jia, L., Kim, J., Shen, H., Clark, P. E., Tilley, W. D., and Coetzee, G. A. (2003). Androgen receptor activity at the prostate specific antigen locus: steroidal and non-steroidal mechanisms. Mol Cancer Res *1*, 385-92.

Kauppi, B., Jakob, C., Farnegardh, M., Yang, J., Ahola, H., Alarcon, M., Calles, K., Engstrom, O., Harlan, J., Muchmore, S., et al. (2003). The Three-dimensional Structures of Antagonistic and Agonistic Forms of the Glucocorticoid Receptor Ligand-binding Domain: RU-486 Induces a Transconformation that Leads to Active Antagonism. J. Biol. Chem. *278*, 22748-22754.

Kemppainen, J. A., Lane, M. V., Sar, M., and Wilson, E. M. (1992). Androgen receptor phosphorylation, turnover, nuclear transport, and transcriptional activation. Specificity for steroids and antihormones. J Biol Chem *267*, 968-74.

Kemppainen, J. A., Langley, E., Wong, C., Bobseine, K., Kelce, W. R., and Wilson, E. M. (1999). Distinguishing Androgen Receptor Agonists and Antagonists: Distinct Mechanisms of Activation by Medroxyprogesterone Acetate and Dihydrotestosterone. Mol Endocrinol *13*, 440-454.

Kuil, C. W., Berrevoets, C. A., and Mulder, E. (1995). Ligand-induced Conformational Alterations of the Androgen Receptor Analyzed by Limited Trypsinization. J. Biol. Chem. *270*, 27569-27576.

van der Kwast, T. H., Schalken, J., Ruizeveld de Winter, J. A., van Vroonhoven, C. C., Mulder, E., Boersma, W., and Trapman, J. (1991). Androgen receptors in endocrine-therapy-resistant human prostate cancer. Int J Cancer *48*, 189-93.

Langley, E., Zhou, Z. X., and Wilson, E. M. (1995). Evidence for an anti-parallel orientation of the ligand-activated human androgen receptor dimer. J Biol Chem *270*, 29983-90.

Latham, J. P., Searle, P. F., Mautner, V., and James, N. D. (2000). Prostate-specific antigen promoter/enhancer driven gene therapy for prostate cancer: construction and testing of a tissue-specific adenovirus vector. Cancer Res *60*, 334-41.

Liao, X., Tang, S., Thrasher, J. B., Griebling, T. L., and Li, B. (2005). Small-interfering RNA-induced androgen receptor silencing leads to apoptotic cell death in prostate cancer. Mol Cancer Ther *4*, 505-515.

Lin, H., Altuwaijri, S., Lin, W., Kan, P., Collins, L. L., and Chang, C. (2002). Proteasome activity is required for androgen receptor transcriptional activity via regulation of androgen receptor nuclear translocation and interaction with coregulators in prostate cancer cells. J Biol Chem *277*, 36570-6.

Lin, H., Wang, L., Hu, Y., Altuwaijri, S., and Chang, C. (2002). Phosphorylation-dependent ubiquitylation and degradation of androgen receptor by Akt require Mdm2 E3 ligase. EMBO J *21*, 4037-48.

Lu, S., Tsai, S. Y., and Tsai, M. J. (1997). Regulation of androgen-dependent prostatic cancer cell growth: androgen regulation of CDK2, CDK4, and CKI p16 genes. Cancer Res *57*, 4511-6.

Marquis, J. C., Hillier, S. M., Dinaut, A. N., Rodrigues, D., Mitra, K., Essigmann, J. M., and Croy, R. G. (2005). Disruption of gene expression and induction of apoptosis in prostate cancer cells by a DNA-damaging agent tethered to an androgen receptor ligand. Chem Biol *12*, 779-87.

Masiello, D., Cheng, S., Bubley, G. J., Lu, M. L., and Balk, S. P. (2002). Bicalutamide functions as an androgen receptor antagonist by assembly of a transcriptionally inactive receptor. J Biol Chem *277*, 26321-6.

Mellinghoff, I. K., Vivanco, I., Kwon, A., Tran, C., Wongvipat, J., and Sawyers, C. L. (2004). HER2/neu kinase-dependent modulation of androgen receptor function through effects on DNA binding and stability. Cancer Cell *6*, 517-27.

Mitra, K., Marquis, J. C., Hillier, S. M., Rye, P. T., Zayas, B., Lee, A. S., Essigmann, J. M., and Croy, R. G. (2002). A rationally designed genotoxin that selectively destroys estrogen receptor-positive breast cancer cells. J Am Chem Soc *124*, 1862-3.

Mohler, J. L., Gregory, C. W., Ford, O. H., Kim, D., Weaver, C. M., Petrusz, P., Wilson, E. M., and French, F. S. (2004). The androgen axis in recurrent prostate cancer. Clin Cancer Res *10*, 440-8.

Pil, P. M., and Lippard, S. J. (1992). Specific binding of chromosomal protein HMG1 to DNA damaged by the anticancer drug cisplatin. Science *256*, 234-7.

Poukka, H., Karvonen, U., Yoshikawa, N., Tanaka, H., Palvimo, J. J., and Jänne, O. A. (2000). The RING finger protein SNURF modulates nuclear trafficking of the androgen receptor. J Cell Sci *113 (Pt 17)*, 2991-3001.

Rink, S., Yarema, K., Solomon, M., Paige, L., Tadayoni-Rebek, B., Essigmann, J., and Croy, R. (1996). Synthesis and biological activity of DNA damaging agents that form decoy binding sites for the estrogen receptor. Proc Natl Acad Sci U S A. *93*, 15063–15068.

Rozen, S., and Skaletsky, H. J. (2000). Bioinformatics Methods and Protocols: Methods in Molecular Biology S. Krawetz and S. Misener, eds. (Totowa, NJ: Humana Press).

Sharma, U., Marquis, J. C., Nicole Dinaut, A., Hillier, S. M., Fedeles, B., Rye, P. T., Essigmann, J. M., and Croy, R. G. (2004). Design, synthesis, and evaluation of estradiol-linked genotoxicants as anti-cancer agents. Bioorg Med Chem Lett *14*, 3829-33.

Sheflin, L., Keegan, B., Zhang, W., and Spaulding, S. W. (2000). Inhibiting proteasomes in human HepG2 and LNCaP cells increases endogenous androgen receptor levels. Biochem Biophys Res Commun *276*, 144-50.

Song, L., Coghlan, M., and Gelmann, E. P. (2004). Antiandrogen effects of mifepristone on coactivator and corepressor interactions with the androgen receptor. Mol Endocrinol *18*, 70-85.

Toney, J. H., Donahue, B. A., Kellett, P. J., Bruhn, S. L., Essigmann, J. M., and Lippard, S. J. (1989). Isolation of cDNAs encoding a human protein that binds selectively to DNA modified by the anticancer drug cis-diamminedichloroplatinum(II). Proc Natl Acad Sci U S A *86*, 8328-32.

Treiber, D. K., Zhai, X., Jantzen, H. M., and Essigmann, J. M. (1994). Cisplatin-DNA adducts are molecular decoys for the ribosomal RNA transcription factor hUBF (human upstream binding factor). Proceedings of the National Academy of Sciences of the United States of America *91*, 5672-5676.

Veldscholte, J., Berrevoets, C. A., Ris-Stalpers, C., Kuiper, G. G., Jenster, G., Trapman, J., Brinkmann, A. O., and Mulder, E. (1992). The androgen receptor in LNCaP cells contains a mutation in the ligand binding domain which affects steroid binding characteristics and response to antiandrogens. J Steroid Biochem Mol Biol *41*, 665-9.

Visakorpi, T., Hyytinen, E., Koivisto, P., Tanner, M., Keinänen, R., Palmberg, C., Palotie, A., Tammela, T., Isola, J., and Kallioniemi, O. P. (1995). In vivo amplification of the androgen receptor gene and progression of human prostate cancer. Nat Genet *9*, 401-6.

Xing, N., Chen, Y., Mitchell, S. H., and Young, C. Y. (2001). Quercetin inhibits the expression and function of the androgen receptor in LNCaP prostate cancer cells. Carcinogenesis *22*, 409-14.

Xu, Y., Chen, S., Ross, K. N., and Balk, S. P. (2006). Androgens Induce Prostate Cancer Cell Proliferation through Mammalian Target of Rapamycin Activation and Post-transcriptional Increases in Cyclin D Proteins. Cancer Res *66*, 7783-7792.

Zhou, Z., Lane, M., Kemppainen, J., French, F., and Wilson, E. (1995). Specificity of ligand-dependent androgen receptor stabilization: receptor domain interactions influence ligand dissociation and receptor stability. Mol Endocrinol *9*, 208-218.

Zhu, W., Smith, A., and Young, C. Y. (1999). A nonsteroidal anti-inflammatory drug, flufenamic acid, inhibits the expression of the androgen receptor in LNCaP cells. Endocrinology *140*, 5451-4.

Chapter 3: AR Involvement in Toxicity of 11β

Introduction

Prostate cancer remains a leading killer of males in developed countries, despite continuing medical advances in detection and treatment of this disease (Jemal et al., 2008). Especially in late-stage, hormone-refractory prostate cancer, there is little help offered by chemotherapeutic treatment, and new therapies that continue to treat the disease are much needed. Treatment of metastatic prostate cancer consists of minimizing AR activity through chemical castration methods and use of AR antagonists. However, antagonistic therapies eventually fail as the tumor develops mechanisms to grow with lower androgen levels or acquires mutations allowing former antagonists to function as AR agonists. Nevertheless, the AR remains a tractable target because it continues to be expressed in a majority of cases (van der Kwast et al. 1991; Visakorpi et al. 1995; Holzbeierlein et al. 2004; Mohler et al. 2004), and usually continues to function in promoting expression of pro-growth and pro-survival genes (Gregory et al. 1998; Zegarra-Moro et al. 2002). As an example of a way to continue employing AR as a target, therapies that can eradicate AR have been proposed and attempted with some success in pre-clinical scenarios (Zhu et al. 1999; Xing et al. 2001; Cha et al. 2005; Liao et al. 2005; Burnstein 2005; Bhattacharyya et al. 2006; Eder et al. 2000; Eder et al. 2002).

Our proposed strategy for achieving selective toxicity toward prostate cancer cells involves the chemical tethering of a DNA damaging agent to a ligand for the AR within a single compound, 11β[1]. Together, the ligand and damaging agent will form sites of DNA damage that go on to recruit AR association, resulting in two potential means for enhanced toxicity to cells expressing AR: 1) AR could physically block the access of DNA repair enzymes, leading to adduct persistence, and 2) the AR may be titrated away from its normal sites of transcriptional activity in the promoters of genes related to growth and survival, leading to reduced expression. Either separately or in combination, these two proposed mechanisms would increase the toxicity of compounds toward AR positive prostate cancer cells. Importantly, if these mechanisms of toxicity are achievable, the only crucial factor is AR expression. Advanced disease stage that may have acquired

[1] 2-(6-((8S,11S,13S,14S,17S)-17-hydroxy-13-methyl-3-oxo-2,3,6,7,8,11,12,13,14,15,16,17 dodecahydro-1H-cyclopenta[a]phenanthren-11-yl)hexylamino)ethyl 3-(4-(bis(2-chloroethyl)amino)phenyl)propylcarbamate

independence from androgen signaling either by mutation within the AR ligand binding pocket allowing promiscuity for different ligands, or activation independent of androgen binding would still be treatable by creating persistent sites of DNA damage and physically removing AR from sites of gene activation.

To address whether AR enhances the toxicity of 11β toward prostate cancer cells, we have employed three primary strategies: 1) interference with 11β binding to AR by free steroid ligand, 2) use of isogenic cell lines differing, presumably, only in AR expression status, and 3) synthesis of an 11β variant compound, 17α-OH-11β, with reduced affinity to AR. Since the mechanisms proposed depend on a persistent interaction of 11β with the AR, it is thought that addition of a large quantity of free AR ligand will disrupt their association and reduce toxicity. A previous report demonstrated that 11β has approximately 10% of the affinity to AR as the synthetic androgen R1881 (Marquis et al., 2005). Thus, addition of 1 μM R1881 to cells undergoing treatment with toxic micromolar concentrations of 11β should be able to disrupt association and inhibit toxic effects. Isogenic cell lines allow for testing the effects of changing a single variable, rather than testing cell lines that differ in AR expression but are of distinct lineage, which would confound interpretation of results. The only drawback to isogenic cells in this specific case is that the cell lines employed do not depend on AR for survival. As such, they are most useful for testing the hypothesis that AR can hinder repair of 11β-DNA adducts and increase toxicity. Finally, by synthesizing a control compound with similar physicochemical parameters but with less affinity for AR, we can address the importance of the interaction between 11β and the AR in the mechanism of compound toxicity.

In synthesizing a compound with reduced affinity to AR, we chose to follow a route that would result in the least modification of our compound. We hoped to avoid any misinterpretation of results that could occur from altered solubility, cellular uptake and distribution, metabolism, or loss or gain of interaction with factors other than AR. Previous studies have shown that the AR prefers an alcohol function at the 17 position of the steroid, in the β (*S*) stereoisomer. In fact, it has been shown that inversion of this alcohol from β to α in some steroids results in a 200 fold reduction in binding affinity to AR (Fang et al., 2003). Crystal structures of AR complexed with testosterone,

dihydrotestosterone, or R1881 demonstrate that the alcohol at C-17 forms hydrogen bonds with Thr-877 and Asn-705 (Matias et al., 2000; Sack et al., 2001; Pereira de Jésus-Tran et al., 2006), and presumably would be unable to maintain the hydrogen bonding upon alcohol inversion. As such, our strategy for reducing affinity of 11β for AR was inversion of the alcohol at C-17, creating 17α-OH-11β. We were then able to determine how reducing affinity affected toxicity toward cells expressing AR.

The results shown here demonstrate that AR is not, in fact, a requirement for toxicity of our compound. Competition with AR ligand was unable to interfere with toxicity toward LNCaP or PC3-AR cell lines. Moreover, an isogenic pair of cell lines differing only in AR status proved to be equally sensitive to 11β, and the 17α-OH-11β compound proved to have only slightly lower toxicity than 11β to several cell lines, which was most likely due to an unforeseen reduced ability to form DNA damage.

Materials and Methods

Chemicals: 5α-Dihydrotestosterone (DHT) was acquired from Sigma-Aldrich. Bicalutamide was from LKT Laboratories, Inc. (St. Paul, MN). [^{3}H]-R1881 and R1881 were from Perkin-Elmer Life Science (Waltham, MA). Synthesis of 11β-dichloro (referred to herein as 11β) and 11β-dimethoxy were performed in our laboratory and have previously been described (Marquis et al. 2005). Synthesis of [^{14}C]-11β (25mCi/mmol) was also conducted in house and described previously (Hillier et al., 2006).

Chemical Synthesis of 17α-OH-11β

17β-OH(estra-$\Delta^{4,9(10)}$-dien-3-one), otherwise known as 9(10)nandrolone, was acquired from Brighton Co., LTD (Changsha, Hunan, China). All other chemicals and reagents for synthesis were obtained from Sigma-Aldrich, EMD Biosciences, or Mallinckrodt. Please refer to Scheme 3.1 for synthetic route.

Mitsunobu Inversion of 17-OH of Starting Material 17β-OH(estra-$\Delta^{4,9(10)}$-dien-3-one) to Form (8S,13S,14S,17R)-17-hydroxy-13-methyl-6,7,8,11,12,13,14,15,16,17-decahydro-1H-cyclopenta[a]phenanthren-3(2H)-one

To 4.89 g (17.9 mmol) of the starting dienone was added 6.11 g (23.3 mmol, 1.3 eq) PPh_3 and 4.04 g (24.2 mmol, 1.35 eq) 4-nitrobenzoic acid in a flame-dried round bottom flask under argon. 40 mL anhydrous THF was added and reaction mixture was heated to 70°C to dissolve. 4.9 g (24.2 mmol, 1.35 eq) DIAD was added dropwise over 5 minutes with stirring. Reaction was maintained at 70°C for 2 hrs, then allowed to cool to RT. 100 mL sat. $NaHCO_3$ was added and product extracted with EtOAc, dried over $MgSO_4$, and concentrated under reduced pressure. Product was purified by flash chromatography on silica gel (15% → 25% EtOAc in hexanes) and used directly in the following reaction.

Ester hydrolysis to form 17α-hydroxy-4,9-estradien-3-one

The resulting 4-nitrobenzoate was dissolved in 40 mL anhydrous MeOH and 38 mg K_2CO_3 (0.36 mmol, 0.02 eq) was added. Reaction was heated to 60°C with vigorous stirring for 14 hrs, then concentrated. Product was partitioned between water and EtOAc and dried over $MgSO_4$. Product **(1)** was purified by flash chromatography on silica gel (15% → 25% → 50% EtOAc in hexanes) to produce a white powder (3.08 g, 63.2% yield over 2 steps).

Two-dimensional gradient-selected correlation spectroscopy (gCOSY), heteronuclear single quantum coherence (HSQC), and gradient-selected heteronuclear multiple bond correlation (gHMBC) NMR experiments were performed to completely assign all spectra and identify successful epimerization of the 2° alcohol at C-17.

^{1}H NMR ($CDCl_3$): δ 5.68 (s, 1H), δ 3.83 (dd, 1H), δ 2.86 (ddd, 1H), δ 2.91 (dψt, 1H), δ 2.55 (m, 1H), δ 2.48, δ 2.45 (m, 2H), δ 2.42 (ψt, 1H), δ 2.36 (ψt, 1H), δ 2.13- δ 2.28 (m, 3H), δ 1.95 (dψq, 1H), δ 1.83 (dddd, 1H), δ 1.72 (ψtd, 1H), δ 1.61 (m, 2H), δ 1.54 (dddd, 1H), δ 1.45 (d, 1H), δ 1.36 (ψtdd,1H), δ 1.30 (ψqdd, 2H), δ 0.83 (s, 3H)

^{13}C NMR ($CDCl_3$): δ 16.392, 24.683, 25.497, 25.909, 27.800, 30.858, 31.307, 32.620, 37.166, 39.492, 45.164, 49.078, 79.424, 122.052, 125.348, 146.424, 157.489, 199.925

Complete synthesis of 11β has been described previously (Marquis et al., 2005). We have slightly modified the literature procedure as described here for synthesis of 17α-OH-11β.

Synthesis of 3,3-Ethylenedioxy-17β-hydroxy-5(10)9(11)-estradiene

To 3.06 g (11.2 mmol) **(1)** dissolved in 100 mL anhydrous benzene was added 6.97 g (112 mmol, 10 eq) ethylene glycol, followed by 209 mg (1.1 mmol, 0.1 eq) p-toluenesulfonic acid. Flask was fitted with a Dean-Stark apparatus and condenser column, heated to reflux 1 hr. Reaction was cooled and poured into a separatory funnel. Flask was washed with hexanes. Benzene/hexane layer collected and concentrated. Product was purified by flash chromatography on silica gel (50% EtOAc/hexanes), concentrated and used immediately in following reaction.

Silylation of 2° Alcohol

Steroid was dissolved in 50 mL anhydrous CH_2Cl_2. 2.29 g (33.6 mmol, 3 eq) imidazole, 134 mg (1.1 mmol, 0.1 eq) 4-dimethylaminopyridine, and then 3.38 g (22.4 mmol, 2 eq) TBS-Cl was added. Reaction was stirred RT 1hr, concentrated, washed with brine and extracted with EtOAc. Product was purified by flash chromatography on silica gel (5% EtOAc/hexanes) and used immediately in the following reaction.

Epoxidation to form 3,3-Ethylenedioxy-17β-*tert*-butyldimethylsilyloxy-5α,10α-oxido-9(11)-estrene (2)

Steroid was dissolved in 50 mL anhydrous CH_2Cl_2 and cooled to 0°C. 0.74 mL (5.31 mmol, 0.5 eq) hexafluoroacetone trihydrate added, followed by 0.74 mL pyridine. 3.6 mL (31.83 mmol, 3 eq) 30% H_2O_2 added dropwise and reaction was allowed to warm to RT gradually with vigorous stirring over 13 hrs. 5% Sodium thiosulfate and CH_2Cl_2 were added and the organic phase was separated and dried over $MgSO_4$. Product **(2)** was purified by flash chromatography on silica gel (10% EtOAc/hexanes) (3.84 g, 76.8% yield from **(1)**).

Preparation of the Grignard and alkylation of (2) to form (5R,8S,11S,13S,14S,17R)-17-(tert-butyldimethylsilyloxy)-11-(6-(tert-butyldimethylsilyloxy)hexyl)-13-methyl-1,2,4,5,6,7,8,11,12,13,14,15,16,17-tetradecahydrospiro[cyclopenta[a]phenanthrene-3,2'-[1,3]dioxolan]-5-ol

Grignard reagent was prepared *in situ* from (6-bromohexyloxy)*tert*-butyl-dimethyl-silane. Briefly, 1.25 g (51.6 mmol, 6 eq) flaked magnesium was added to a flame dried 3-neck round bottom flask and dried with heat gun 15 minutes. 40 mL anhydrous THF was added, followed by 15.23 g (51.6 mmol, 6 eq) of (6-bromohexyloxy)*tert*-butyl-dimethyl-silane, and reaction was heated to reflux 2.5 hrs to form Grignard. At this time, the reaction was cooled to -20°C, and 1.06 g (5.16 mmol, 0.6 eq) copper(I)bromide-dimethylsulfide complex was added. 3.84 g (8.60 mmol) epoxide **(2)** was dissolved in 10 mL anhydrous THF and added. Reaction was maintained at -20°C for 1.5 hrs with stirring. 50 mL ice-cold sat. NH_4Cl was added and reaction was filtered through celite and concentrated. Product **(3)** was purified by flash chromatography on silica gel (10% EtOAc/hexanes) (4.57 g, 80.2%).

Deprotection of Primary Alcohol

4.57 g (6.89 mmol) **(3)** was dissolved in 20 mL anhydrous THF. 10.3 mL (10.3 mmol) tetrabutylammonium fluoride (1M in THF) was added and reaction was stirred RT 4 hrs. Product was purified by flash chromatography on silica gel (50% EtOAc/hexanes) (2.74 g, 72.5%).

Iodination to Synthesize (5R,8S,11S,13S,14S,17R)-17-(tert-butyldimethylsilyloxy)-11-(6-iodohexyl)-13-methyl-1,2,4,5,6,7,8,11,12,13,14,15,16,17-tetradecahydrospiro[cyclopenta[a]phenanthrene-3,2'-[1,3]dioxolan]-5-ol (4)

To a 3-necked flame-dried round bottom flask, 1.39 g (5.49 mmol, 1.1 eq) finely crushed I_2 was added. 40 mL anhydrous CH_2Cl_2 was added and mixture was stirred 15 minutes to dissolve. In separate flask, 2.74 g steroid (4.99 mmol) was dissolved in 10 mL anhydrous CH_2Cl_2 and cooled to 0°C. 1.44 g (5.49 mmol, 1.1 eq) triphenylphosphine and 679 mg (9.98 mmol, 2 eq) imidazole was added. I_2 solution was then added dropwise to the mixture over 20 minutes. Reaction turns from clear to yellow toward end of addition.

The reaction was allowed to proceed 4 hrs, gradually reaching RT. 25 mL 20% sodium bisulfite was added to quench reaction, causing clearing, followed by 50 mL CH_2Cl_2. The organic layer was collected, filtered over celite, concentrated, and purified by flash chromatography on silica gel (50% EtOAc/hexanes) to yield 2.85 g **(4)** (86.6%).

Reaction of (4) with N-(2-(*tert*-butyldimethylsilyl)oxyethyl)-2-nitrobenzene sulfonamide

To a flame-dried 3 neck round bottom flask, 1.63 g (4.51 mmol, 1.1 eq) N-(2-(*tert*-butyldimethylsilyl)oxyethyl)-2-nitrobenzene sulfonamide was dissolved in 20 mL anhydrous CH_3CN. 30.3 mg (82 μmol, 0.02 eq) tetrabutylammonium iodide was added, followed by 1.47 g (4.51 mmol, 1.1 eq) Cs_2CO_3, turning the reaction bright yellow. Steroid **(4)** was dissolved in 5 mL anhydrous THF and added. Vessel was fitted with an oven-dried condenser column and heated to reflux for 2 hrs. The reaction was then cooled, filtered twice through celite, concentrated, and purified by flash chromatography on silica gel (20% EtOAc/hexanes), yielding 3.23 g **(5)**, 88.5%.

Deprotection of 2° Amine

To a flame-dried round bottom flask, 2.73 g (3.06 mmol) of steroid **(5)** was added and dissolved in 30 mL anhydrous CH_3CN. 1.95 g (14.1 mmol, 4.6 eq) K_2CO_3 added, followed by 626 μL (6.13 mmol, 2 eq) thiophenol. Reaction was heated to 37°C, allowed to proceed 30 minutes, then filtered and concentrated. Product **(6)** was purified by flash chromatography on silica gel (50% EtOAc/hexanes → 5% MeOH/CH_2Cl_2), yielding 1.96 g (90.7%) (structure not shown in Scheme 3.1).

Reprotection of 2° Amine with diphenylphosphine

970 mg (1.37 mmol) steroid **(6)** was dissolved in 25 mL CH_2Cl_2 and cooled to 0°C. 382 μL (2.74 mmol, 2 eq) Et_3N added. 284 μL (1.51 mmol, 1.1 eq) diphenylphosphinic chloride was dissolved in 5 mL CH_2Cl_2 and added dropwise over 30 minutes. Reaction was allowed to proceed at RT for 3 hrs with vigorous stirring, then extracted with H_2O and CH_2Cl_2 and dried over $MgSO_4$. Product **(7)** was purified by flash chromatography on silica gel (100% EtOAc), giving 1.01 g (81.5%) (structure not shown in Scheme 3.1).

Deprotection of 1° Alcohol to Form N-(6-((5R,8S,11S,13S,14S,17R)-17-(tert-butyldimethylsilyloxy)-5-hydroxy-13-methyl-1,2,4,5,6,7,8,11,12,13,14,15,16,17-tetradecahydrospiro[cyclopenta[a]phenanthrene-3,2'-[1,3]dioxolane]-11-yl)hexyl)-N-(2-hydroxyethyl)-P,P-diphenylphosphinic amide (8)

1.51 g (1.67 mmol) steroid **(7)** was dissolved in 10 mL anhydrous THF. 1.83 mL (1.83 mmol, 1.1 eq) tetrabutylammonium fluoride was added and reaction was stirred vigorously for 30 minutes. Reaction was concentrated, and product **(8)** was purified by flash chromatography on silica gel (100% EtOAc → 5% MeOH/CH_2Cl_2), giving 1.24 g (93.9%).

Synthesis of 2-((6-((5R,8S,11S,13S,14S,17R)-17-(tert-butyldimethylsilyloxy)-5-hydroxy-13-methyl-1,2,4,5,6,7,8,11,12,13,14,15,16,17-tetradecahydrospiro[cyclopenta[a]phenanthrene-3,2'-[1,3]dioxolane]-11-yl)hexyl)(diphenylphosphoryl)amino)ethyl 4-nitrophenyl carbonate (9)

1.24 g (1.56 mmol) steroid **(8)** was dissolved in 10 mL anhydrous THF. 654 μL (4.70 mmol, 3 eq) Et_3N was added, followed by 947 mg (4.70 mmol, 3 eq) 4-nitrophenyl chloroformate. Some precipitation occurred and reaction became cloudy yellow. Reaction was allowed to proceed 3hrs at RT. 100 mL EtOAc and 50 mL sat. $NaHCO_3$ was added. The organic layer was collected, washed three times with sat. $NaHCO_3$ and once with H_2O, dried over $MgSO_4$, and concentrated. Product **(9)** was purified by flash chromatography on silica gel (50% EtOAc/hexanes → 100% EtOAc), giving 1.28 g (85.3%).

Reaction of 4-(3-aminopropyl)-*N,N*-bis(2-chloroethyl)aniline with p-nitrophenyl carbonate

640 mg (669 μmol) carbonate **(9)** was dissolved in 4 mL anhydrous THF. 4-(3-aminopropyl)-*N,N*-bis(2-chloroethyl)aniline was dissolved in 4 mL anhydrous THF and added dropwise to reaction, turning it bright yellow. Reaction was allowed to proceed with stirring 1 hr. 150 mL EtOAc and 50 mL sat. $NaHCO_3$ added, organic layer collected and washed twice with $NaHCO_3$ and once with H_2O, dried over $MgSO_4$, filtered, and

concentrated. Product **(10)** was purified by flash chromatography on silica gel (75% EtOAc/hexanes → 100% EtOAc), yielding 616 mg of a white foamy solid (84.3%).

Removal of tert-butyldimethylsilanoxy- and phosphinamido- groups from compound (10) to form 2-(6-((8S,11S,13S,14S,17R)-17-hydroxy-13-methyl-3-oxo-2,3,6,7,8,11,12,13,14,15,16,17-dodecahydro-1H-cyclopenta[a]phenanthren-11-yl)hexylamino)ethyl 3-(4-(bis(2-chloroethyl)amino)phenyl)propylcarbamate (11), 17α-OH-11β

616 mg (563 μmol) steroid **(10)** was dissolved in 1 mL dioxane. 1.13 mL (4.5 mmol, 8 eq) 4M HCl in dioxane was added dropwise and reaction was allowed to proceed 2 hrs, turning deep purple. 500 mg $NaHCO_3$ was added to quench HCl. Reaction was filtered through glass pipette stuffed with kimwipe, concentrated, and purified by flash chromatography on silica gel (5% → 10% MeOH/CH_2Cl_2), then re-purified by flash chromatography on alumina (2% MeOH/CH_2Cl_2), giving 308 mg final product **(11)** (76.3%).

^1H NMR ($CDCl_3$): δ 7.05 (d, 2H), δ 6.62 (d, 2H), δ 5.64 (s, 1H), δ 4.81, (s broad, 1H), δ 4.18, (t, 2H), δ 3.7 (m, 5H), δ 3.62 (m, 4H), δ 3.19-3.09 (m, 2H), δ 3.07 (m, 1H), 2.85 (m, 3H), δ 2.59 (dt, 5H), δ 2.44-2.20 (m, 6H), δ 1.96 (m, 1H), δ 1.88 (m, 1H), δ 1.78 (m, 3H) δ 1.64-1.22 (m, 17H), δ 0.83 (s, 3H).
HRMS (ESI): calculated for $C_{40}H_{59}O_4NCl_2$ [M + H]: 716.3955, found: 716.3922
Purity by HPLC > 94%.

Preparation of *N*-(2-(*tert*-butyldimethylsilyl)oxyethyl)-2-nitrobenzene sulfonamide

1.98 mL (32.7 mmol, 1.1 eq) ethanolamine and 4.56 mL (32.7 mmol, 1.1 eq) Et_3N were dissolved in 100 mL CH_2Cl_2 and cooled to 0°C. 6.6 g (29.8 mmol) 2-nitrobenzene sulfonyl chloride was added, causing some precipitation. Reaction proceeded for 20 minutes. Product was partitioned between CH_2Cl_2 and H_2O. Organic layer concentrated and used immediately in subsequent reaction.
Crude sulfonamide was dissolved in 60 mL CH_2Cl_2 and cooled to 0°C. 2.23 g (32.7 mmol, 1.1 eq) imidazole, 364 mg (2.9 mmol ,0.1 eq)) 4-dimethylaminopyridine, and

finally 4.94 g (32.7 mmol, 1.1 eq) TBS-Cl were added. Reaction was removed from ice, allowed to proceed 1 hour. Product was partitioned between CH_2Cl_2 and H_2O, concentrated, and purified by flash chromatography on silica gel (20% EtOAc/hexanes), giving 10.02 g (93.4% over 2 steps).

Preparation of 4-(3-aminopropyl)-*N,N*-bis(2-chloroethyl)aniline

To a flame-dried round bottom flask, 2.00 g (6.57 mmol) chlorambucil was added and dissolved in 20 mL anhydrous THF. This was cooled to -78°C, and 0.87 mL (7.89 mmol, 1.2 eq) *N*-methylmorpholine was added, followed by 0.75 mL (7.89 mmol, 1.2 eq) ethyl chloroformate. Allowed to proceed 5 minutes, checked by TLC, and then moved to -10°C bath before adding 854 mg (13.15 mmol, 2 eq) sodium azide dissolved in 3 mL H_2O. Reaction allowed to proceed 20 minutes, then partitioned between brine and EtOAc. Organic layer was collected and dried over $MgSO_4$. Product 4-(4-(bis(2-chloroethyl)amino)phenyl)butanoyl azide used immediately in subsequent reaction.

Crude acyl azide was dissolved in 13mL anhydrous $CHCl_3$. 1.36 mL (13.15 mmol, 2 eq) benzyl alcohol added and reaction was warmed to reflux overnight. Reaction concentrated and purified by flash chromatography on silica gel (15% → 25% EtOAc/hexanes), giving 2.51 g benzyl 4-(4-(bis(2-chloroethyl)amino)phenyl) butanoylcarbamate (93.3%).

Immediately prior to use, Cbz protecting group was removed from aniline mustard. To a flame-dried round bottom flask, 411 mg (1 mmol) Cbz-protected aniline mustard was added, along with 106 mg (100 μmol) Pd on carbon. 5 mL MeOH was added, the reaction was purged with argon, and an H_2-filled balloon was attached. Reaction was allowed to proceed 1 hr, filtered over celite, concentrated, and used immediately in subsequent reaction.

Analytical Techniques: NMR data was collected at MIT Department of Chemistry Instrumentation Facility under the expert guidance of Dr. Jeff Simpson, using a Varian Inova 500 Mhz NMR spectrometer, which was equipped with a 5 mm inverse broadband z-axis gradient probe for use in 2D experiments.

^{13}C NMR experiments were performed using a Varian Inova 500 Mhz NMR spectrometer fitted with a 5 mm broadband probe. Samples were dissolved in $CDCl_3$ and referenced to TMS. All data was acquired and processed using Varian's VNMR 6.1C software running on a Sun microcomputer. Methods used included ^{1}H, ^{13}C, dimensional gradient-selected correlation spectroscopy (gCOSY), heteronuclear single quantum coherence (HSQC), and gradient-selected heteronuclear multiple bond correlation (gHMBC) experiments.

Reversed-phase HPLC analysis was performed using a Varian C_{18} Ultrasorb 5 μm 4.6 x 250mm column with a UV diode array detector (Varian ProStar 330 PDA). Compounds were separated using a 50% to 100% MeOH gradient over 20 minutes with a flow rate of 1mL/min. The aqueous phase used was 0.05 M sodium acetate and 10% CH_3CN in H_2O.

High resolution mass spectrometry was performed on an Agilent ESI-TOF spectrometer.

Cell Culture: LNCaP cells (ATCC, Rockville, MD) were maintained in RPMI 1640 media supplemented with glucose (2.5 g/L), 1 mM sodium pyruvate, 10 mM HEPES (all Invitrogen, Carlsbad, CA), and 10% fetal bovine serum (Hyclone, Salt Lake City, UT). MDA-MB-453 cells (ATCC) were grown in MEM-α media supplemented with 1 ng/mL EGF, 2 μg/mL human recombinant insulin, 100 mM non-essential amino acids, 10 mM HEPES (all Invitrogen), and 10% fetal bovine serum (Hyclone). All cells were grown in a humidified 5% CO_2/air atmosphere at 37°C. For transcriptional reporter assays and where otherwise indicated, media formulations were the same except for use of phenol red free versions supplemented with 10% charcoal dextran treated FBS (CDTFBS) (Hyclone) in order to remove all androgens. PC3-AR cells are a clonal cell line derived from PC3 cells stably transfected with a plasmid containing the coding region for the human androgen receptor. PC3-Neo cells were transfected with this same vector lacking the AR sequence. Both were generous gifts from Mien-Chie Hung (University of Texas M.D. Anderson Cancer Center). PC3-AR and PC3-Neo cells were grown in the same media as LNCaP with the addition of 400 μg/mL geneticin. PC3-AR1 and PC3-AR9 are also isogenic clonal sublines of PC3 made by transfection of AR, though PC3-AR1 do not express detectable AR and are unresponsive in an AR reporter assay, while PC3-AR9 cells express a functional AR for reporter assays (Shaoyong Chen, personal

communication). These were a kind gift from the laboratory of Steven Balk (Beth-Israel Deaconess Medical Center, Boston, MA). An additional PC3 subline expressing AR protein, A103, was also acquired from the Balk lab. PC3-AR1, PC3-AR9, and A103 cells were grown in RPMI 1640 with 10% fetal bovine serum and 400 μg/mL geneticin.

Western Blots: Cells were harvested by scraping into media, washing with PBS, and subsequently lysing in RIPA buffer (Santa Cruz Biotechnology, Santa Cruz, CA) containing PMSF, sodium orthovanadate, and protease inhibitor cocktail at 0°C. Cellular debris was pelleted by centrifugation at 14,000 RPM in a bench top microcentrifuge, supernatants were collected, and protein quantified by Bradford dye binding assay (Bio-Rad Laboratories, Hercules, CA). Equal quantities of protein were electrophoretically separated on a bis-tris precast polyacrylamide gel (Invitrogen) and transferred to Immobilon-P PVDF membrane (Millipore, Billerica, MA). Non-specific protein binding was blocked with 5% milk in Tris-buffered saline (0.1% Tween 20, 10 mM Tris [pH 7.4], 150 mM NaCl) and proteins were detected by primary antibodies followed by horseradish peroxidase (HRP) conjugated secondary antibodies and chemiluminescent HRP substrate (Supersignal West; Pierce, Rockford, IL). Antibodies used were as follows: AR (SC-7305, SC-816, Santa Cruz), β-actin (SC-1615R; Santa Cruz), and HRP-conjugated secondary antibodies (#7076, anti-mouse IgG; #7074 anti-rabbit IgG; Cell Signaling Technology, Danvers, MA).

Luciferase Transcriptional Reporter Assays: For testing of AR transcriptional activity in LNCaP cells, 24-well tissue culture plates were used and cells were co-transfected with pGL4PSA and pGL4.74 in a 24:1 ratio using lipofectamine and PLUS reagent in Opti-MEM media according to manufacturer's instructions (Invitrogen). After 3 hrs, media was supplemented to 10% FBS, and after 24 hrs replaced with fresh phenol red free media containing 10% CDTFBS. Following a further 24 hrs incubation, test compounds were diluted 1,000-fold into CDTFBS containing media and cells incubated 24 hrs prior to cell lysis and luciferase detection using dual-luciferase reporter assay system (Promega, Madison, WI) with TD 20/20 luminometer (Turner Biosystems, Sunnyvale, CA). All

samples were performed in at least quadruplicate and firefly luciferase measurements were normalized to renilla luciferase readings.

Expression Vectors: The vectors pGL4.10 (promoterless firefly luciferase) and pGL4.74 (renilla luciferase driven by thymidylate kinase promoter) were acquired from Promega. We prepared pGL4PSA containing promoter and enhancer regions of the KLK3 (PSA) gene. A 662 base pair segment of the PSA promoter (-631 to +31), containing AREI and AREII was obtained by PCR amplification from MDA-MB231 genomic DNA using forward primer (5'-GCG GAG CTC AAT TCC ACA TTG TTT GCT GCA C-3') and reverse primer (5'-ATA CTC GAG ACT CTC CGG GTG CAG GTG GTA A-3'), containing SacI and XhoI restriction sites, respectively. The reverse primer also contains an additional A between the XhoI restriction site and the PSA promoter sequence in order to prevent creation of a second SacI restriction site following ligation. An additional 1446 base pair segment of the PSA enhancer (-5321 to -3877, containing AREIII) was amplified from LNCaP genomic DNA using forward primer GCG TAT GGT ACC AGA GAT TTT TTG GGG G and reverse primer TAT GCG GAG CTC GTA TCT GTG TGT CTT CT, containing KpnI and SacI restriction sites, respectively. The amplified PSA promoter and enhancer regions were ligated in tandem upstream of the luciferase gene in pGL4.10. This completed vector was sequenced at the MIT CCR Biopolymers Laboratory and found to match published human genome sequence AC011523 except for two substitutions (-4363 G->T, -4264 C->A), both outside of known ARE's.

AR siRNA: Stealth™ Select 3 RNAi against AR was acquired from Invitrogen. Transfection was performed in PC3-AR cells with Lipofectamine 2000 (Invitrogen) according to manufacturer protocols. Cells were allowed 24 hrs to efficiently reduce AR expression prior to adding test compounds, which were left on an additional 24 hrs prior to counting attached cells. Negative control siRNA used was Stealth™ RNAi negative control Med GC content duplex #2 (Invitrogen).

Relative Binding Affinity Experiments: Whole cell extracts for use in relative binding affinity studies were acquired from LNCaP and MDA-MB-453 cells (Veldscholte et al., 1990). Competitive binding reactions were performed similarly as previously described (Fang et al., 2003). Samples in duplicate contained 5 nM [^{3}H]-R1881, from 0.1 nM to 10 μM unlabeled competitor, 125 μg whole cell extract, and 5% DMF in binding assay buffer in a total reaction volume of 100 μL. Reactions were mixed and allowed to incubate at 4°C for 18 hours. At this time, 200 μL of hydroxyapatite (HAP) slurry (50% HAP in 50 mM Tris, 1 mM EDTA solution) was added, and each reaction was vortexed in 5 minute intervals for 20 minutes. Samples were then centrifuged at top speed in a Beckman-Coulter 18 Microfuge for 10 minutes. Supernatants were aspirated, 1 mL of TE buffer was added to each, and samples were re-homogenized. This cycle of centrifugation, aspiration, and washing was repeated once more. Finally, 1.3 mL ethanol was used (in two 650 μL steps) to transfer pellets into 10 mL Ecoscint H (National Diagnostics, Atlanta, GA) scintillation fluid and counting was performed. The concentration of unlabeled competitor that resulted in a 50% decrease in [^{3}H]-R1881 binding (EC_{50}) was estimated by non-linear regression analysis (Prism, GraphPad Software, La Jolla, CA). Relative Binding Affinity (RBA) of the competitor was calculated as [EC_{50} R1881 /EC_{50} Competitor] x 100.

In some experiments covalently modified DNA was used as the unlabeled competitor. This DNA was prepared by allowing 11β or 17α-OH-11β (50 μM) to react with calf thymus DNA (3 mg/ml) in a solution containing 25% DMSO at 37°C overnight. The DNA was then isolated by ethanol precipitation in the presence of 0.1 M NaOAc, washed three times with 70% EtOH to remove unreacted compound, redissolved in H_2O and sonicated to reduce viscosity. The concentrations of adducts in DNA modified by either isomeric compound were estimated by performing a parallel reaction in which [^{14}C]-11β was allowed to react with DNA under identical conditions. The amount of covalently bound radioactivity in the isolated DNA was determined by liquid scintillation counting and the number of adducts per μg DNA was calculated based on the specific activity of the radiolabeled compound.

Growth Inhibition Assay: Cells for growth inhibition assays were plated in 6-well dishes and allowed to adhere for 48 hrs prior to treatment for times indicated. Cells were washed with PBS, trypsinized, and counted with a Z1 Coulter Counter (Beckman Coulter, Fullerton, CA).

Clonogenic Survival Assay: Cells at clonal density were treated by addition of media containing test compound. Colonies that developed over the subsequent 7-10 day period were fixed (methanol:acetic acid; 9:1), stained with crystal violet, and washed with several changes of DI H_2O. Colonies were counted manually, and experiments were conducted in triplicate.

[^{14}C]-11β Uptake by Cells and Formation of DNA Adducts: Cells in exponential growth phase were treated for 2 hrs with [^{14}C]-11β in complete growth media. Drug containing media was aspirated and cells were washed once each with fresh media and PBS and then trypsinized and collected by centrifugation. After an additional suspension in PBS to remove loosely associated 11β, cells were collected by centrifugation and lysed by addition of RIPA detergent solution (Santa Cruz). An aliquot of the lysed cell solution was used for protein determination by the Bradford assay (Bio-Rad, Hercules, CA). The ^{14}C activity in the remaining cell lysate was assayed by liquid scintillation counting.

To determine the amount of [^{14}C]-11β covalently bound to cellular DNA, identically treated PC3-AR and PC3-Neo cells were resuspended in 0.5 mL of 50 mM HEPES, 100 mM NaCl, 10 mM EDTA containing 0.7% SDS. After incubation with RNase A (0.5 mg, 37°C for 30 min) and proteinase K (0.4 mg, 37°C for 2 hrs) the solution was extracted with phenol/chloroform/isoamyl alcohol (25:24:1) and then with chloroform/isoamyl alcohol (24:1). DNA was isolated by ethanol precipitation and dissolved in deionized water. For assay of adduct formation in PC3-AR1 and PC3-AR9 cells, RNase A was omitted from initial lysis buffer. In this case, following proteinase digestion, DNA was isolated by ethanol precipitation, redissolved in TE buffer, and treated with RNase A (0.5 mg, 37°C, 30 mins). DNA was isolated by ethanol precipitation, and redissolved in deionized water. DNA concentration was quantified by UV absorption at 260 nm using a Beckman-Coulter DU730 spectrophotometer. The

amount of ^{14}C in the DNA sample was then determined by accelerator mass spectrometry (AMS) analysis as described previously (Hillier et al 2006).

Tandem Mass Spectrometric Quantification of Specific DNA Adducts of 11β and 17α-OH-11β: To measure the relative amounts of guanine and adenine adducts and guanine:guanine cross-links of 11β and 17α-OH-11β, compounds were incubated with calf thymus DNA overnight under identical conditions as for creation of adducts for RBA assays. The DNA was re-purified by ethanol precipitation and subjected to 0.05 N HCl hydrolysis for 3 hrs to release adducted bases. Samples were separated on a C18 reversed-phase HPLC column, connected in-line with a tandem quadrupole (QQQ) mass spectrometer (Agilent, Santa Clara, CA). Fragmentor and collision energy settings for multiple reaction monitoring (MRM) mode were optimized for detection of 11β-guanine, 11β-adenine, and 11β-guanine-guanine crosslink adducts. Standards were obtained by reaction of calf thymus DNA with 11β as described above, where the appropriate fraction of acid-hydrolyzed 11β-nucleobase adduct was monitored by diode array detector and collected, followed by verification of exact mass on an Agilent ESI-TOF mass spectrometer.

17α-OH-11β had a slightly longer retention time on a reversed-phase HPLC column than 11β, which was demonstrated by reacting DNA with a 1:1 mixture of 11β and 17α-OH-11β, and seeing 2 chromatographic peaks for each G, A, or GG adduct. Verification that 17α-OH-11β was eluted later was obtained by chromatography of the DNA hydrolysate from incubations using exclusively 11β or 17α-OH-11β. This finding was unambiguously confirmed by reacting 11β with ^{15}N-labeled DNA from *E. coli* (grown on $^{15}NH_4Cl$ with 100% isotopic abundance at all nucleobase nitrogens), and mixing it with 17α-OH-11β reacted with normal (^{14}N) calf thymus DNA prior to LC/MS/MS analysis with the appropriate ^{14}N and ^{15}N detection parameters. As expected, co-injection of 11β reacted with ^{14}N and ^{15}N DNA gave identical retention times.

Our ability to resolve the G, A, and GG adducts by not only nucleobase, but also by the structure of the drug for a specific base (perturbations of which were remarkably minor in some cases, such as a carbonyl vs. hydroxyl within a relatively large steroidal

compound), allowed us to perform co-incubations of DNA with two compounds to guarantee identical reaction conditions for a comparative analysis. For detection of single guanine adducts in MRM mode, the first quadrupole was set up to discriminate for the +2 charge state at *m/z* of 407.3 (free guanine base attached to 11β or 17α-OH-11β with one hydrolyzed chloroethyl arm), the second quadrupole was used for collision-induced decay, and the third quadrupole selected for a product of the +1 charge state at *m/z* of 152.1 (free guanine base). When detecting adenine adducts, Q1 selected for the +2 charge state mass at *m/z* 399.3, while Q3 selected for the +1 charge state at *m/z* 136.1 (free adenine base). Finally, for detecting guanine-guanine crosslinks, Q1 selected for +2 charge state mass 474.1, while Q3 selected for +1 charge state 152.1.

Reversed-phase separation of adducts was performed on a C_{18} column, with a gradient from 10-100% CH_3CN with 0.25% acetic acid over 140 mins at a flow rate of 6 μl per minute. The aqueous phase used was 10% CH_3CN, 0.25% acetic acid in H_2O.

Statistics: Significance tests were performed with unpaired 2-tailed student's t-test as implemented in Excel 2002 (Microsoft, Redmond, WA).

Results

11β Toxicity to LNCaP Cells Cannot be Competed Away with Ligand for AR

Experiments were conducted to determine whether AR is involved in the mechanism of toxicity for 11β toward prostate cancer cells. As a first test of AR involvement, we attempted to compete for binding of 11β to AR with 1 μM R1881 in the sensitive LNCaP prostate cancer cells. 11β has ~10% relative binding affinity (RBA) for AR in comparison to R1881 (Marquis et al., 2005), so it is anticipated that over the range of 11β concentrations from 2.5 μM to 7.5 μM, 1 μM R1881 will be successful in competing a significant quantity of 11β out of the ligand binding pocket of AR. However, over the course of the 24 hr treatment, this concentration of R1881 is unable to reduce toxicity of 11β (Figure 3.1).

11β Has Selective Toxicity to PC3-AR Cells, but Apparently <u>not</u> Due to AR

As a more rigorous method to address AR involvement in 11β toxicity, isogenic cells (PC3-AR and PC3-Neo) that differ only in AR expression status were acquired. A clonogenic assay demonstrated that AR expression increased sensitivity of these cells to 11β (Figure 3.2), which would be consistent with our original model of 11β action. Efforts were then made in an attempt to test this conclusion further. These efforts resulted in data that, on balance, contradicted our original model. First, competition experiments were conducted with a 1 μM concentration of R1881, as was performed in LNCaP cells. In accord with results from LNCaP cells, 1 μM R1881 was unable to compete away any of the toxicity of 11β toward PC3-AR cells, in both a growth inhibition format (Figure 3.3) and in a clonogenic assay (Figure 3.4). In the clonogenic assay, significant toxicity was achieved with as little as 1 μM 11β, making it very likely that 1 μM R1881 successfully saturates AR binding sites and limits 11β-AR interaction. Finally, siRNA was used to knock down AR expression in PC3-AR cells in an attempt to revert them to the PC3-Neo phenotype. Despite achieving a successful reduction in steady-state AR protein levels (Figure 3.5), toxicity of 11β toward the siRNA treated cells remained unaffected (Figure 3.6).

The level of full length AR expression in the PC3-AR cells is low—several fold less than in LNCaP cells (Figure S3.1). It is known that over time, most PC3 cells forced to express AR will begin to lose AR expression. Furthermore, this cell pair as originally acquired was based on a pooled population. While full-length AR is clearly expressed to a greater extent in PC3-AR than PC3-Neo cells, the PC3-AR cells also express an ~42 kDa band that is detected by two separate antibodies to AR and is repressed by AR siRNA (Figure 3.5). As such, this band is likely an AR fragment. Both antibodies used to detect AR were directed toward the N-terminal domain, but more specific identity of this "truncated AR" is unknown. Since the population was originally heterogeneous, we selected several clones to identify those with greatest AR expression and then chose a single clone with which to work. In all cases, the 42 kDa band persisted. Heightened sensitivity to 11β remained, however.

Despite the low level of full length AR expression in PC3-AR cells, the AR that is expressed in these cells is functional, increasing transcription of a luciferase reporter downstream of PSA promoter/enhancer upon induction with androgen (Figure S3.2). However, unlike LNCaP cells, in which AR protein levels are decreased upon 11β treatment, PC3-AR cells respond to 11β treatment with dramatic increases in AR protein expression (Figure S3.3A). In sum, while 11β was clearly more toxic to PC3-AR cells than PC3-Neo cells, results of competitive binding and AR siRNA experiments demonstrate that differential sensitivity is apparently not related to AR expression.

We also measured DNA adduct formation by [^{14}C]-11β in PC3-AR and PC3-Neo cells as a first step to determine whether AR presence could influence adduct formation. First, the level of 11β that was able to get into each cell line was assessed, finding equivalent association of 11β with both PC3-AR and PC3-Neo cells (Figure 3.7A). However, assessment of adduct formation by accelerator mass spectrometry (AMS) clearly demonstrated an ~2-fold greater adduct burden in PC3-AR cells over that seen in PC3-Neo (Figure 3.7B).

11β Toxicity is not Affected by AR Expression in PC3-AR1/AR9 Cell Pair

Due to the unexpected effects that are unrelated to AR presence in PC3-AR and PC3-Neo cells, a separate isogenic pair, (PC3-AR1 (AR-) and PC3-AR9 (AR+)), was acquired. Each of these cell lines displayed equivalent sensitivity to treatment with 11β (Figure 3.8). Furthermore, the level of AR expression, while still less than in LNCaP cells, was significantly greater than seen in PC3-AR cells (Figure 3.9). Western blotting detected only full length AR protein in PC3-AR9 cells, making the AR9/AR1 pair a better model for study. Since the PC3-AR1 cells were equally as sensitive as PC3-AR9 cells to 11β, AR presence does not have an effect on toxicity in these PC3 cells.

DNA Adduct formation was also monitored in PC3-AR1 and PC3-AR9 cells. There was a greater association of 11β with the AR negative PC3-AR1 cells than with the AR9 cells (Figure 3.10A). In line with the greater accumulation of 11β in PC3-AR1 cells, these cells also acquired a greater quantity of 11β-DNA adducts (Figure 3.10B). The increase in DNA adducts formed in PC3-AR1 cells is directly proportional to the

increased association of 11β with these cells. Since the quantity of adducts formed in PC3-AR1 and PC3-AR9 cells matches closely with the quantity of compound that was able to get into cells, it does not appear that presence of AR has influenced adduct burden.

Synthesis of 17α-OH-11β, a New 11β Compound with Reduced AR Binding Affinity

As an additional chemical means to address AR involvement in 11β toxicity toward prostate cancer cells, a similar compound with reduced affinity for AR was synthesized. The 17-hydroxyl group on the steroid backbone was epimerized from β to α (*S* to *R*) stereochemistry by Mitsunobu inversion (Dodge and Lugar, 1996; Tapolcsányi et al., 2004) (Scheme 3.1). After inversion, rigorous 2D NMR analysis was used to ensure correct stereochemistry at this position. A combination of ^{1}H, ^{13}C, two-dimensional gradient-selected correlation spectroscopy (gCOSY), heteronuclear single quantum coherence (HSQC), and gradient-selected heteronuclear multiple bond correlation (gHMBC) NMR experiments were performed in order to make complete structural NMR assignments (Table 3.1). In the ^{1}H and ^{13}C NMR spectra, differences between the 17α-OH and 17β-OH compounds were consistent with those reported in the literature for 17-OH epimeric sterols (Eggert et al. 1976; Ciuffreda et al. 2004). The resonance of H-18 at δ 0.83 in the 17α molecule was shifted upfield in comparison to the 17β isomer (H-18, δ 0.91). In the ^{13}C NMR spectrum, the C-18 resonance at δ 10.69 for the β isomer was shifted downfield to δ 16.59 in the 17α-OH compound. In addition, we confirmed positional assignments using 2D gHMBC to identify long-range couplings between ^{1}H and ^{13}C atoms. Strong couplings were observed between H-17→C-12 and H-17→C-18 in the 17β-OH isomer (Figure 3.11). The heteronuclear coupling between H-17→C-12 was absent or much weaker in the 17α-OH molecule, while increased coupling was seen between H-17→C-14, and H-17→C-15, demonstrating successful steroid epimerization. (Figure 3.12). The gHMBC observations are consistent with molecular models in which the dihedral angle between H-17 and C-14 in the 17β isomer is approximately 80°, resulting in weak heteronuclear coupling, while in the 17α-OH configuration, the dihedral angle between these nuclei is 160° and allows strong coupling to occur. A similar situation occurs for the dihedral angle between C-12 and H-17, which is approximately 90° for 17α-OH and ~30° for 17β-OH compounds.

17α-OH-11β Displays Reduced Affinity to AR

In order to determine whether inversion of the 17-alcohol within the steroid nucleus of 11β successfully reduced affinity to AR, the ability of both isomers to compete with [^{3}H]-R1881 for binding to AR in cell extracts was measured. Extracts were prepared from LNCaP cells that express mutant AR (T877A) or MDA-MB-453 cells that express wild-type AR. Both compounds were able to compete away [^{3}H]-R1881 for binding to AR in either cell extract. With LNCaP extracts, 11β was shown to have an RBA compared to R1881 of 15.5, similar to the previously reported value (Marquis et al., 2005), while 17α-OH-11β had ~10-fold lower RBA of 1.91 (Figure 3.13). With the wild-type AR expressed in MDA-MB-453 extracts, 11β was determined to have an RBA of 5.31, which is slightly lower than in LNCaP, but still very significant. Once again, 17α-OH-11β displayed ~10-fold less affinity than 11β, with an RBA of 0.51 (Figure 3.14).

17α-OH-11β is a Weaker AR Antagonist than 11β

A luciferase transcriptional reporter assay driven by the PSA promoter/enhancer was used to determine whether epimerization of the steroid portion of 11β, which reduced affinity to AR, also resulted in a depressed ability to affect AR-mediated transcription. Neither 11β nor 17α-OH-11β demonstrated very substantial agonistic activity in the luciferase assay. However, both compounds were significantly antagonistic toward AR activity (Figure 3.15). Importantly, 11β was more active as an antagonist than 17α-OH-11β, demonstrating that the difference in affinity to AR between the two compounds is enough to result in a measurably different biological response.

DNA Adducts of 17α-OH-11β Have Lower Affinity to AR than DNA Adducts of 11β

As the designed mechanism of toxicity is the formation of DNA adducts which will then bind AR, we next measured the relative binding affinity of DNA adducts of 11β and 17α-OH-11β for AR. Compounds were incubated with calf thymus DNA overnight prior to re-purification of DNA and use as competitors in AR RBA assays. In parallel,

DNA was treated with [^{14}C]-11β isolated in the same manner, and adducts were quantified by AMS. Based on the very minor modification made to 11β in creating 17α-OH-11β, adduct formation was assumed to be the same. Adduct concentrations used in the RBA assay were estimated from formation of adducts by radiolabeled compound. While both compounds formed adducts that displayed significantly lower binding affinity than their respective free compounds, the approximately 10-fold difference in affinity between them was maintained (Figure 3.16).

17α-OH-11β is Less Toxic to Cells than 11β

Both 11β and 17α-OH-11β were tested for toxicity toward several cell lines. It was initially anticipated that by reducing affinity of the compounds for AR, toxicity toward cells expressing the protein would be reduced, and this was confirmed. 11β proved more toxic than 17α-OH-11β to PC3-AR and MDA-MB-453 cells, both expressing wild-type AR, in a clonogenic survival assay (Figure 3.17A,B). Additionally, 11β proved to be slightly more toxic than 17α-OH-11β to LNCaP cells grown for 5 days in the presence of each compound (Figure 3.17C). However, 11β was also more toxic than 17α-OH-11β toward AR negative PC3-Neo cells (Figure 3.17D), suggesting that factors other than diminished interaction with AR protein were responsible for the differential toxicity of the two compounds in cells that do express AR.

11β Forms More DNA Adducts than 17α-OH-11β *in vitro*

To ensure that compounds formed the same quantity of DNA adducts, each was reacted overnight with calf thymus DNA, which was then re-purified and acid hydrolyzed to release adducted bases. These bases were analyzed by tandem quadrupole mass spectrometry (QQQ), and adducts to guanine, adenine, or cross-links of guanine-guanine were detected. Surprisingly, it was shown that 11β forms almost twice as many guanine adducts as 17α-OH-11β (Figure 3.18). In agreement with this observation, the level of guanine:guanine cross-links was also significantly higher from 11β treatment than 17α-OH-11β treatment (Figure 3.18). However, formation of adenine adducts occurred to an equivalent extent with both compounds, suggesting that interaction of the compounds

with DNA affected the pattern of reactivity (Figure 3.19). Because adducts of 17α-OH-11β had slightly longer retention times during reversed-phase HPLC than adducts of 11β, we were able to perform analysis by co-administering each compound to calf thymus DNA, ensuring identical reaction conditions. Furthermore, we verified that the different formation of adducts was a real event, as HPLC separation of adducts using a UV detector results in a similar differential between compounds (Figure 3.20). The extinction coefficients for both compounds are equivalent. The relative quantity of guanine adducts to adenine adducts formed is approximately 3 for 11β and approximately 2 for 17α-OH-11β. As such, the total adduct burden will likely be greater to cells treated with 11β, and it seems that the differential toxicity of 11β and 17α-OH-11β displayed toward various cell lines can most easily be explained by this greater DNA adduct burden.

Discussion

The experiments reported here sought to address by multiple means whether the presence of AR in prostate cancer cell lines was responsible for selective toxicity toward xenografted tumors (Marquis et al., 2005). LNCaP has been a model cell line of choice in previous studies, and attempts were first made in these cells to determine if AR involvement enhanced toxicity of 11β. However, LNCaP cells depend on AR presence and activity for survival (Eder et al. 2000; Liao et al. 2005). Thus, it is difficult to perform AR siRNA experiments to determine what effect 11β would have on these cells in the absence of AR. The most reliable test that can be performed involves the competition for binding to AR with a large quantity of the synthetic AR ligand R1881. We were unable to relieve any of the toxicity of 11β toward LNCaP cells by competing for AR binding with 1 μM R1881. Based on R1881 having a 10-fold greater affinity for AR than 11β, a 1 μM concentration should minimize interaction of 11β and AR over a concentration range of 2.5 – 7.5 μM, where toxicity is evident. As such, it is unlikely that the direct interaction of 11β with the AR is responsible for its toxicity toward these cells.

An additional means of determining if AR involvement could be a factor in toxicity of 11β involved the use of isogenic cell lines that differ only in AR expression.

These cells are all based on the parental PC3 prostate cancer lines, which have lost expression of AR during disease progression (Tilley et al., 1990). They are thus AR-independent and do not require androgens for survival. This is an advantage because it allows for a greater level of manipulation such as use of AR siRNA, as well as the measurement of effects that are independent of AR antagonism. AR-independent cells are most useful as a test of our theorized "repair shielding" mechanism, which states that AR associated with damaged DNA would preclude access of repair enzymes, leading to adduct persistence and cell death.

Initial results were tantalizing; we saw greater toxicity of 11β toward PC3-AR cells than PC3-Neo cells. However, follow-up experiments involving competition with R1881 and the repression of AR expression by siRNA did not revert the sensitive phenotype. It must then be the case that the presence of AR is not the only difference between the cell lines, and that AR is not responsible for the differential sensitivity to 11β. Potentially, during cell line creation, the AR gene may have inserted randomly into the coding sequence of another gene, such as one involved in DNA repair, and it might have been the lack of DNA repair capacity, for example, that heightened the sensitivity of PC3-AR cells to 11β. Further studies would be necessary to fully address the source of differential sensitivity between these cell lines.

A previous study with this cell pair determined that PC3-AR cells were more sensitive than PC3-Neo cells to the agent emodin, which correlated with decreased association of AR with Hsp90 and increased association with the ubiquitin ligase Mdm2, which promoted proteasomal degradation (Cha et al. 2005). However, the mechanism ultimately leading to these effects is unknown. Emodin is a known tyrosine kinase inhibitor (Zhang et al. 1995) and can increase reactive oxygen species (ROS) levels and inhibit NFkB and AP-1 activity (Yi et al., 2004), but is not known to interact directly with the AR. With regard to selective toxicity of emodin toward AR positive cells, this explanation is appropriate for cells which depend on AR expression for growth and survival. In the case of the PC3-AR cells, however, AR is not required for growth, and a different explanation for their heightened sensitivity is required, but is not provided.

The low level of AR expression and presence of a protein that is likely a truncated AR ultimately made these cells a non-ideal model of study. However, it was still

pertinent to identify whether the impressive differential sensitivity between PC3-AR and PC3-Neo cells was related to AR. It was clearly demonstrated that AR was not the governing factor driving this differential sensitivity.

We also addressed whether differential uptake or DNA adduct formation could explain the toxicity differences seen in PC3-AR and PC3-Neo cells. While 11β was associated to an equivalent extent in each cell line, the adduct level was found to be higher in PC3-AR cells. During the course of treatment (2 hrs), there was no discernible difference in growth of either cell line, and the 11β concentration that was used resulted in greater than 80% viability (data not shown). It is not clear whether the greater level of DNA damage seen in PC3-AR cells is due to increased formation of adducts, decreased repair, or both. Whatever the cause, the increased DNA adduct burden seen in PC3-AR cells provides a reasonable explanation for their heightened sensitivity. However, considering the finding that AR repression with siRNA did not relieve toxicity to PC3-AR cells, we find it unlikely that the adduct level is directly related to AR expression, although this possibility was not rigorously addressed in siRNA treated cells.

A separate pair of AR +/- isogenic cell lines, PC3-AR9 and PC3-AR1, displayed equal sensitivity to 11β, making it clear that in these cells, which also do not require the AR for their survival, 11β toxicity is not affected by presence or absence of AR. Furthermore, this isogenic pair was a better model of study due to greater expression of AR protein and existence of a single, full-length immunoreactive band. Equal sensitivity suggests once again that it is unlikely for repair shielding with the AR to be a viable mechanism of 11β toxicity.

DNA adduct formation in PC3-AR9 and PC3-AR1 cells was tested, and an opposite scenario from that seen in the PC3-AR/Neo pair was discovered. Slightly more compound was able to enter the AR null PC3-AR1 cells, which led to a proportionally greater level of DNA adducts. Since the increased uptake of 11β into PC3-AR1 cells led to a proportional increase in DNA adducts, it is suggested that AR presence is not responsible for greater formation or hindered repair of adducts. If anything, the presence of AR has limited the formation of 11β-DNA adducts. Interestingly, as the DNA adduct formation in PC3-AR9/AR1 cells did not correlate with sensitivity to 11β, other unknown factors are implicated.

In all AR expressing PC3 sublines tested (PC3-AR, PC3-AR9, and A103), 11β causes an increase in the level of immunoreactive AR protein. This is in direct contrast to the situation occurring in LNCaP cells discussed in Chapter 2. Those experiments demonstrated that 11β caused a decrease in AR protein consistent with enhanced proteasomal degradation. The AR expressed in PC3 sublines is under the control of a cytomegalovirus (CMV) promoter, which was previously shown to respond to various stress factors by increasing transcription of the downstream gene (Bruening et al., 1998). Thus, it may be that cell stress caused by 11β, mediated through pathways such as JNK, p38, or NFkB, leads to increased transcription of AR in PC3-AR sublines. In further support of this hypothesis, we have shown that in A103 cells, 11β up-regulates AR expression at both the protein and mRNA levels (Figure S3.3B,C).

The chemical synthesis of 17α-OH-11β represented a different angle of attack for determining relative involvement of AR in toxicity of 11β. Consistent with the literature (Fang et al., 2003), inversion of the 17-OH stereocenter led to reduced affinity for AR. However, the loss of affinity was less than anticipated—approximately 10-fold where epimerization of testosterone or estradiol resulted in 200-fold affinity loss. The explanation for less impact on binding affinity resulting from alcohol inversion in 11β is not entirely clear. In the LNCaP AR, T877A mutation leads to loss of one of two hydrogen bond partners to the 17β-OH group of androgens, and it might be anticipated that the binding of 17α-OH steroids to this receptor would not be as significantly reduced as a result. However, the differential affinity between 11β and 17α-OH-11β is similar, whether LNCaP (T877A AR) or MDA-MB-453 (WT AR) extract is used as the source of AR.

Interestingly, the story is slightly different for the dienone steroids lacking any attachment at the 11-position. The 17β-OH dienone has only a 5-fold greater binding affinity than the 17α-OH dienone to LNCaP AR, but a 25-fold greater binding affinity to WT AR (data not shown). Based on this information, the most logical explanation is that the bulky linker that extends from the steroid nucleus of 11β limits the conformational flexibility available to the steroid portion of the molecule. Based on the x-ray structures of the AR LBD and comparison to the highly homologous ER LBD in complex with

ICI 164384, which has similar alkyl extension from the steroid nucleus (Chapter 1, Figure 1.6), it is likely that the linker of 11β must extend through a pore where helix 12 would normally close in an agonist conformation. As such, the steroid portion of 11β may be "locked" into a conformation that does not maximize use of hydrogen bond partners T877 and N705 at the 17 position. If this is true, inversion of the 17-OH stereocenter would not reduce affinity as greatly as when the steroid is allowed more conformational flexibility and the 17β-OH can optimally hydrogen-bond. Nonetheless, the affinity difference between 11β and 17α-OH-11β was great enough to result in a measurably different ability to interfere with AR transcriptional activity (1 μM of 11β and 17α-OH-11β antagonize ~47% and ~19%, respectively, of the transcriptional activity induced by 1 nM DHT).

11β proved to have greater toxicity than 17α-OH-11β toward several cell lines. However, these included the PC3-Neo cells which do not express AR, raising suspicion that there was another variable at play. In light of this finding, we formally tested the ability of each compound to form DNA adducts. Compounds and associated adducts have slightly different retention times on HPLC, and with a slow gradient, individual adducts can be separated enough for quantification. With this attribute, we were able to co-incubate the compounds with calf thymus DNA and quantify guanine, adenine, and guanine:guanine adducts of both compounds by QQQ. As it turned out, 11β formed almost twice as many guanine and guanine:guanine adducts as 17α-OH-11β, while both compounds formed an equivalent amount of adenine adducts. The co-incubation of compounds ensured identical reaction conditions. The fact that the guanine/adenine adduct ratio is different for the two compounds (3.5:1 for 11β, 1.8:1 for 17α-OH-11β) suggests that there is a non-covalent interaction of the compounds with DNA that is able to affect their ability to form covalent DNA adducts. Furthermore, the greater level of guanine adducts in each species ultimately means that total adduct formation will be greater from 11β than from 17α-OH-11β.

Successful testing of relative adduct levels in living cells requires refinement to address issues of sensitivity, and attempts are ongoing to acquire these data. If we assume that adduct formation in cells follows the same trends seen *in vitro*, 11β will

result in approximately 60% greater total adducts than 17α-OH-11β. Furthermore, the greater level of guanine:guanine cross-links, which are believed to be much more lethal than mono-adducts, may create a greater disparity than the total adduct burden would belie. As such, it seems likely that the relatively small differences in sensitivity between cells treated with 11β or 17α-OH-11β can most easily be attributed to the relative reactivity of each compound toward DNA, rather than their relative interaction with AR.

The bulk of data collected do not support the hypothesis that AR is a factor in the mechanism of 11β toxicity. The experiments conducted in PC3 sublines especially demonstrate that in cell lines that do not depend on AR signaling for survival, toxicity of 11β is unaffected by AR. This strongly argues against the repair shielding mechanism of 11β toxicity. Between the inability to rescue toxicity of 11β with R1881 and the relatively small differential toxicity of 11β and 17α-OH-11β toward LNCaP cell lines, which can probably be explained most easily by less adduct formation, there is little support for involvement of AR in toxicity toward LNCaP cells either. However, to achieve toxicity to LNCaP cells, it is necessary to use micromolar concentrations of 11β. Given that 11β has roughly 10% the RBA of R1881 for AR, 1 μM R1881 cannot be guaranteed to out-compete 11β for binding to AR. Thus, interaction of 11β with AR may still occur under these conditions and influence toxicity.

Furthermore, the difference in RBA between 11β and 17α-OH-11β is not outstanding. While a reduced ability to antagonize AR-driven transcription is demonstrable, 17α-OH-11β still retains modest antagonistic activity. It is not therefore a binary system in which one compound interacts with and influences AR and the other does not. Unfortunately, a greater reduction in the affinity of 11β for AR is not possible without significant modification to the steroid moiety. The finding that modification within the steroid nucleus can affect the compound's ability to damage DNA introduces another possible confounding factor. With this molecule, it seems that the reduced ability to damage DNA and the property that it forms a qualitatively different adduct population (favoring damage of adenines) provide simple explanations for the generally reduced toxicity. However, since at least two variables were changed in creation of 17α-OH-11β (affinity to AR and DNA damage capacity), we can not rule out the influence of AR

expression on toxicity of 11β, so long as the cells being tested depend on this protein for growth and survival.

In Chapter 2, results showed that 11β could antagonize AR transcriptional activity in LNCaP cells and even reduce total cellular levels of AR protein in LNCaP, CWR22Rv1, and C4-2B cells. While it is difficult to address whether these observations play causal roles in cell death, it seems that they can only add to overall toxicity when AR activity is so tightly linked with growth and survival.

The AR is involved in progression through the prostate cancer cell cycle, acting as a master regulator of the G1/S transition (Knudsen et al. 1998). This is accomplished through mTOR-dependent increased translation of cyclin D (Xu et al. 2006), through induction of p21 (Lu et al. 1999) , and by degradation of p27 (Lu et al. 2002), which is related to persistence of its E3 ubiquitin ligase Skp2 (Wang et al. 2008). As a result of AR involvement in progression through the cell cycle, its involvement in toxicity can be complicated. For instance, it has been shown that androgen ablative therapies can hinder success of taxane-based therapy (Hess-Wilson et al., 2006), despite taxane therapy not formally utilizing the AR in its mechanism of action. Alternatively, it was shown that genotoxic agents can limit AR transcriptional activity and could thus increase effectiveness against prostate cancers via this unexpected mechanism (Mantoni et al. 2006). Based on these findings, and given that 11β has a demonstrable effect of antagonizing AR transcriptional activity, the possibility remains that interaction of 11β with the AR can increase overall toxicity. Furthermore, it is increasingly apparent that even in hormone-refractory prostate cancers that no longer require androgens for growth and survival, the AR protein remains extremely important (Liao et al. 2005; Burnstein 2005; Compagno et al. 2007; Yuan et al. 2006). Since 11β is able to decrease the steady-state levels of AR protein in LNCaP, CWR22Rv1, and C4-2B cells, cell cycle progression is likely to be limited as a result.

It is apparent, however, that 11β also causes toxicity that is independent of AR, as it can kill prostate cancer cells that lack AR without need of significantly increased drug concentrations. Furthermore, the compound is very toxic to HeLa cells, which do not express AR (Bogdan Fedeles, unpublished results), and is able to inhibit the growth of HeLa xenograft tumors (Dr. Shawn Hillier, unpublished results) similarly as the

inhibition of LNCaP xenogafts. Therefore, other mechanisms responsible for toxicity will be explored in the subsequent chapter.

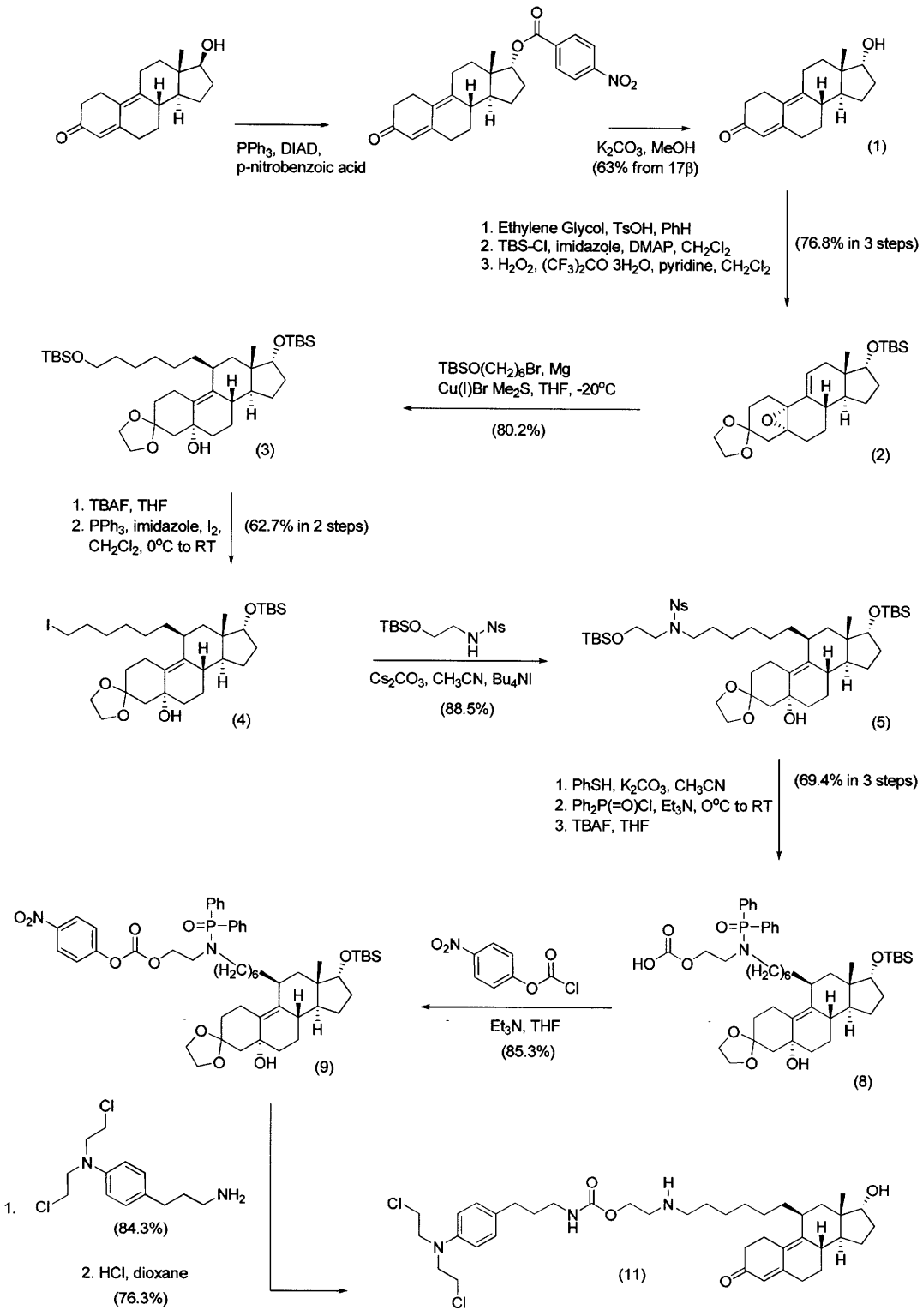

Scheme 3.1 Chemical synthesis of 17α-OH-11β (11)

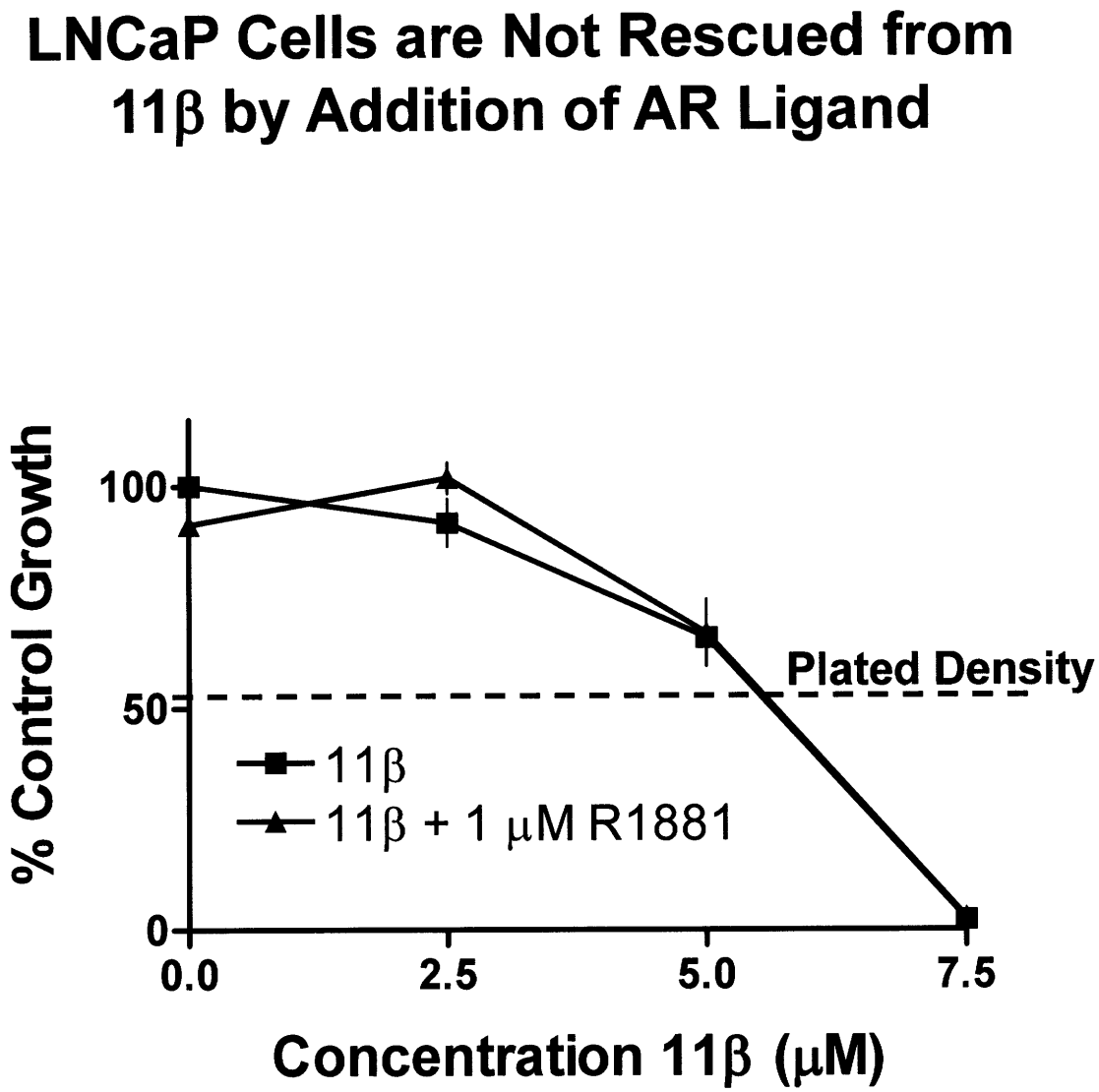

Fig 3.1 Growth inhibition assay comparing toxicity of 11β toward LNCaP cells, performed with and without addition of R1881. Cells were treated for 24 hrs and then counted.

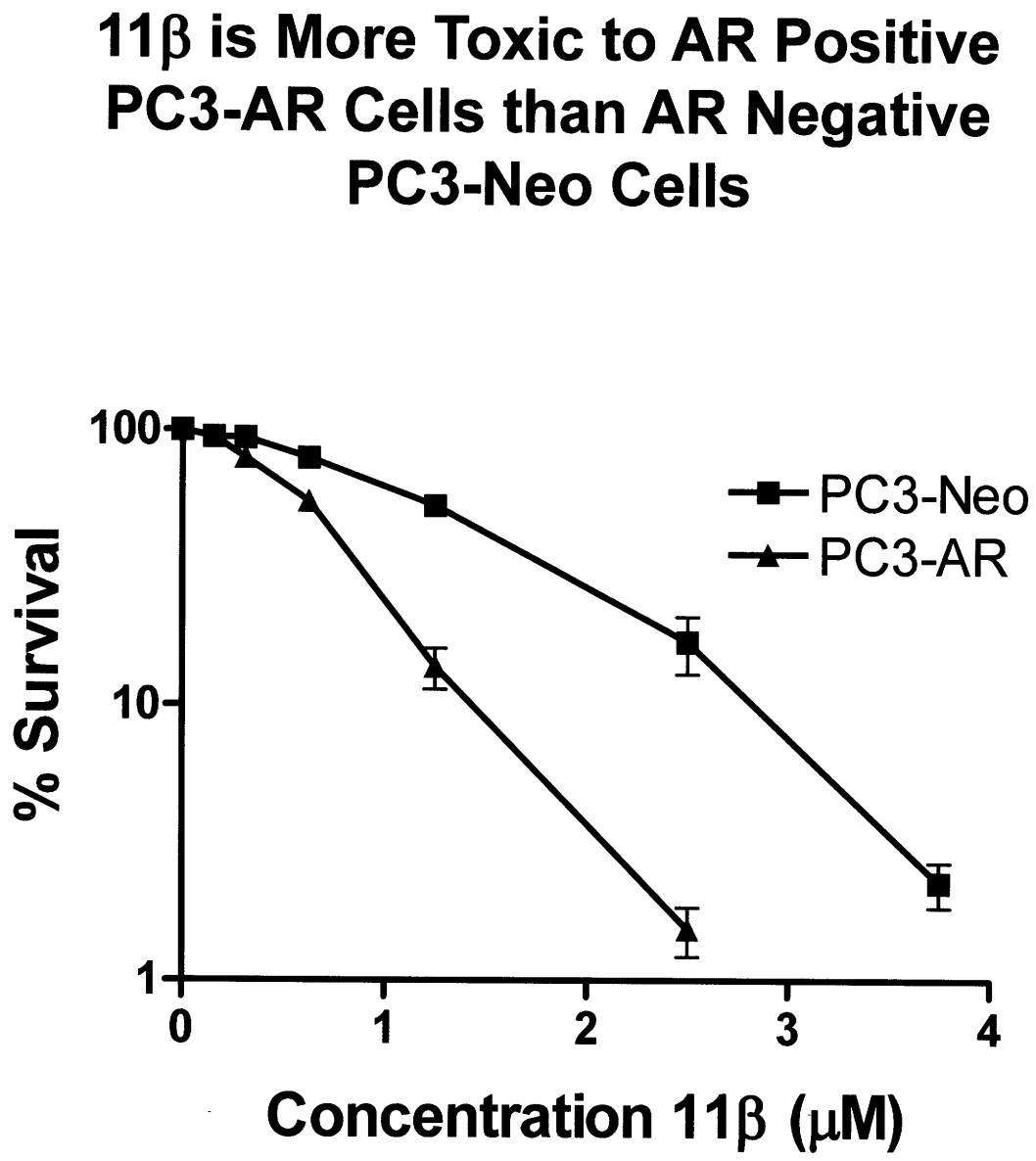

Fig 3.2 Clonogenic survival assay. PC3-Neo (AR -) and PC3-AR (AR +) cells were plated at clonal density, treated as shown, and colonies were manually counted after 7-10 days growth.

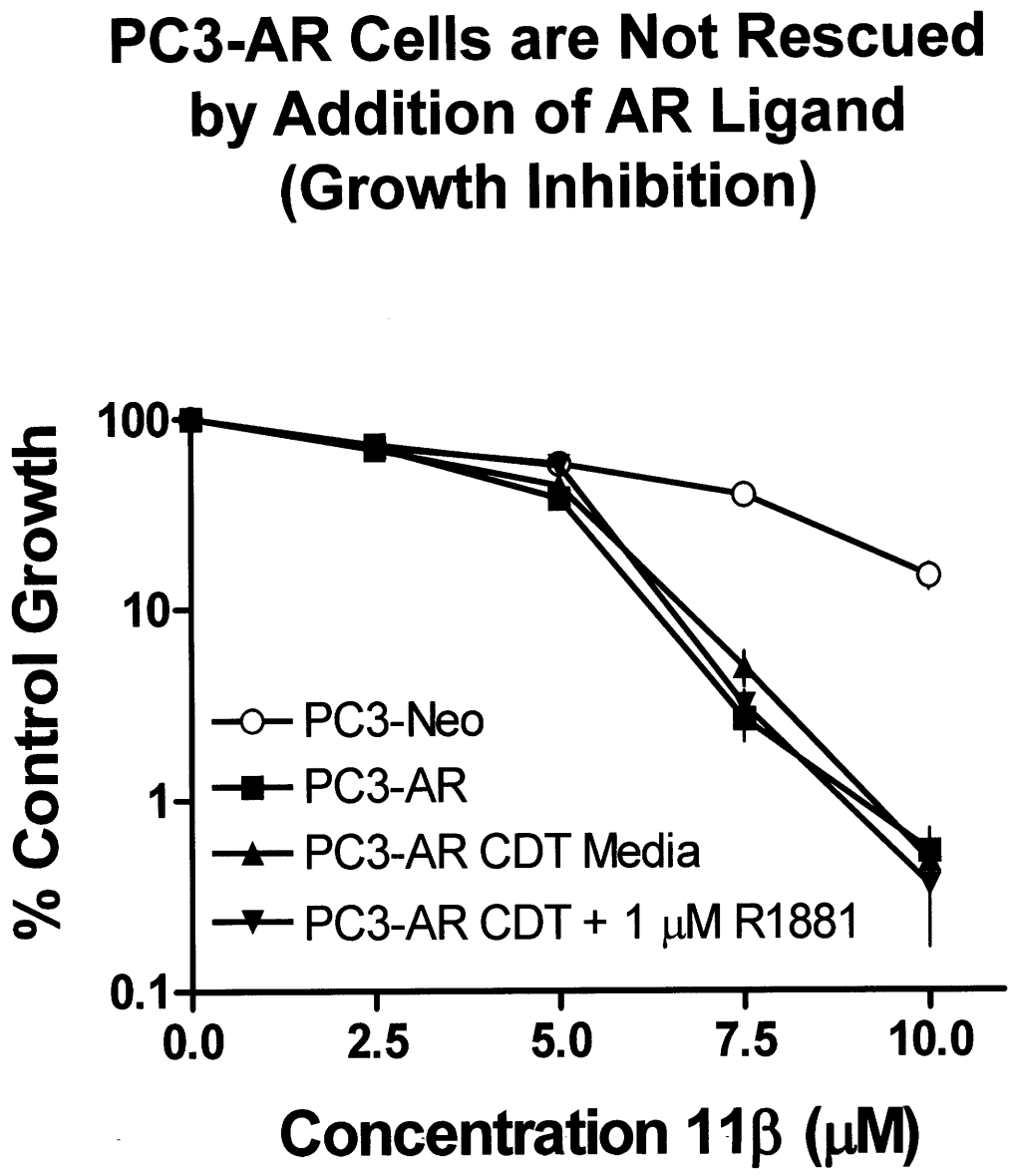

Fig 3.3 Growth inhibition assay comparing toxicity of 11β toward PC3-AR (AR -) cells with and without addition of AR ligand. Cells were treated for 24 hrs and then counted. Treatment was performed in normal media supplemented with 10% FBS, or in media supplemented with 10% charcoal-dextran treated FBS, either with or without addition of 1 μM R1881. PC3-Neo cells are shown for comparison.

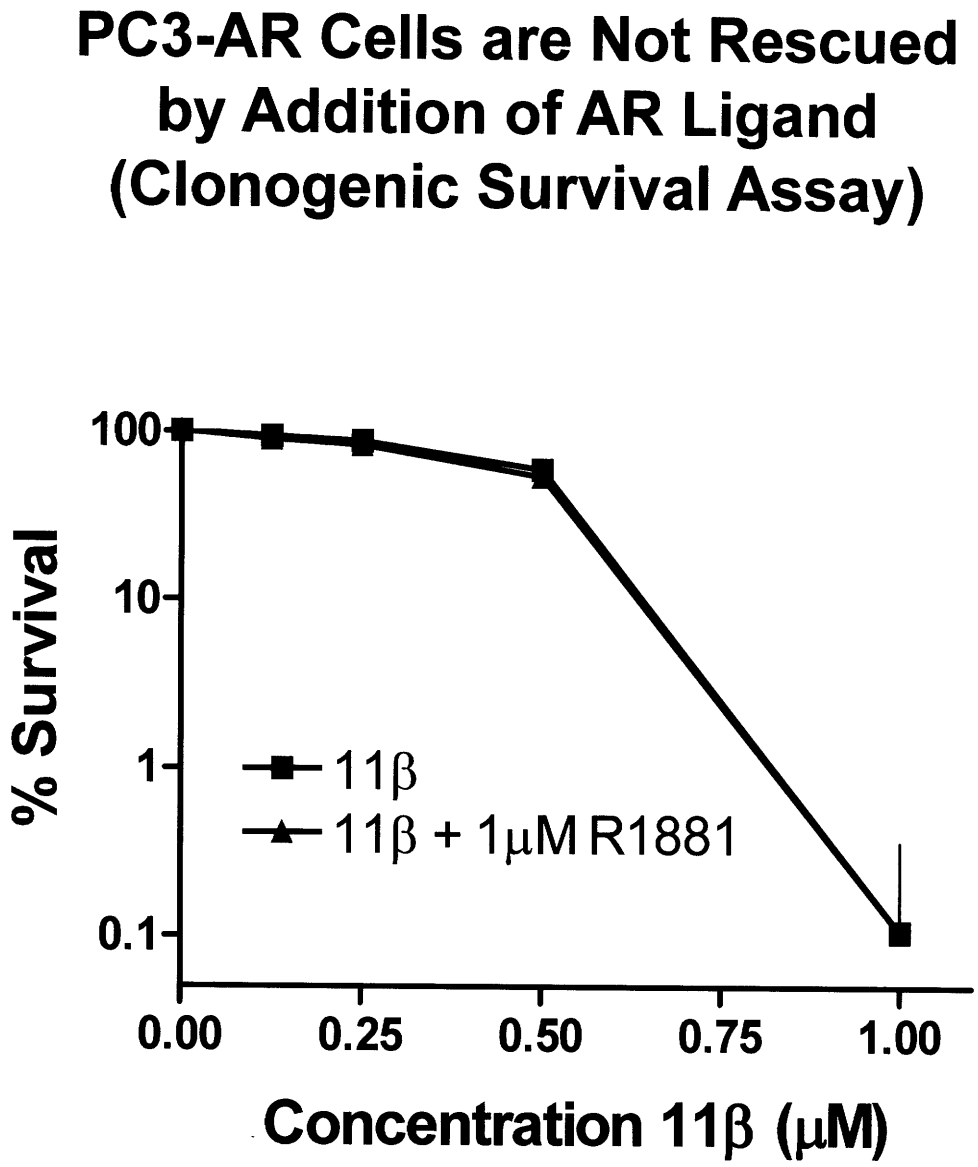

Fig 3.4 Clonogenic survival assay. PC3-AR cells were plated at clonal density and treated 48 hrs later with 11β at concentrations shown, with or without addition of 1 μM R1881, in CDTFBS media. After 7-10 days of continuous exposure to compounds, colonies were manually counted.

AR siRNA Effectively Knocks Down AR Level in PC3-AR cells

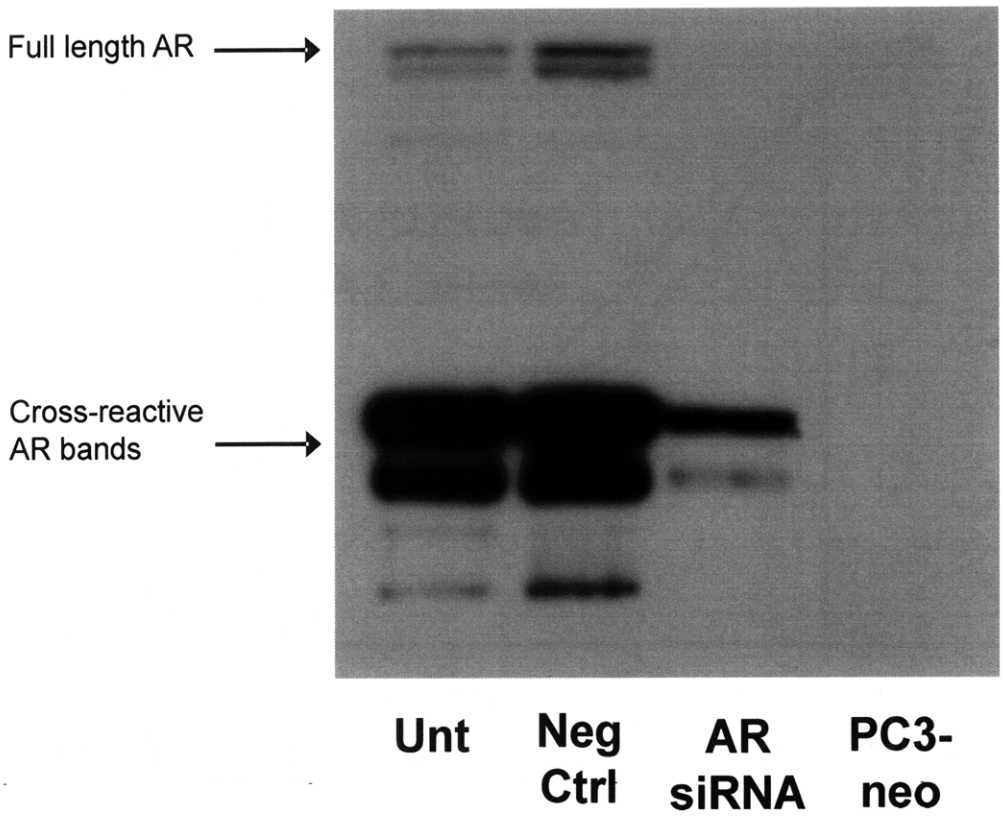

Fig 3.5 Western blot showing immunoreactive AR bands in PC3-AR cells, untreated or treated with negative control or AR siRNA. Sample from PC3-Neo cells is shown for comparison.

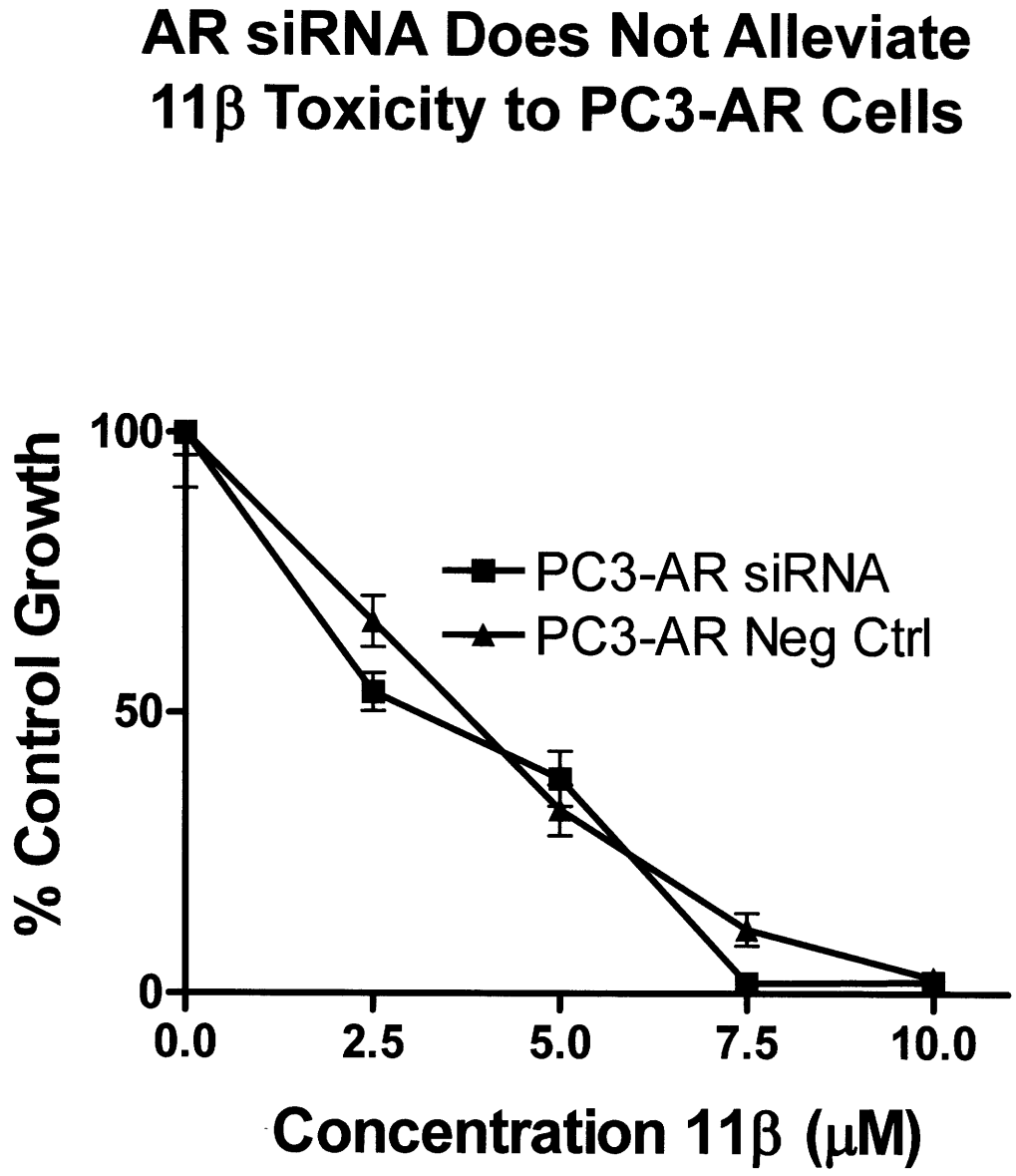

Fig 3.6 Growth inhibition assay. PC3-AR cells were treated with AR or negative control siRNA for 24 hrs prior to treatment with 11β. After 24 hrs of treatment, cells were counted.

11β Forms More DNA Adducts in PC3-AR Cells than PC3-Neo Cells

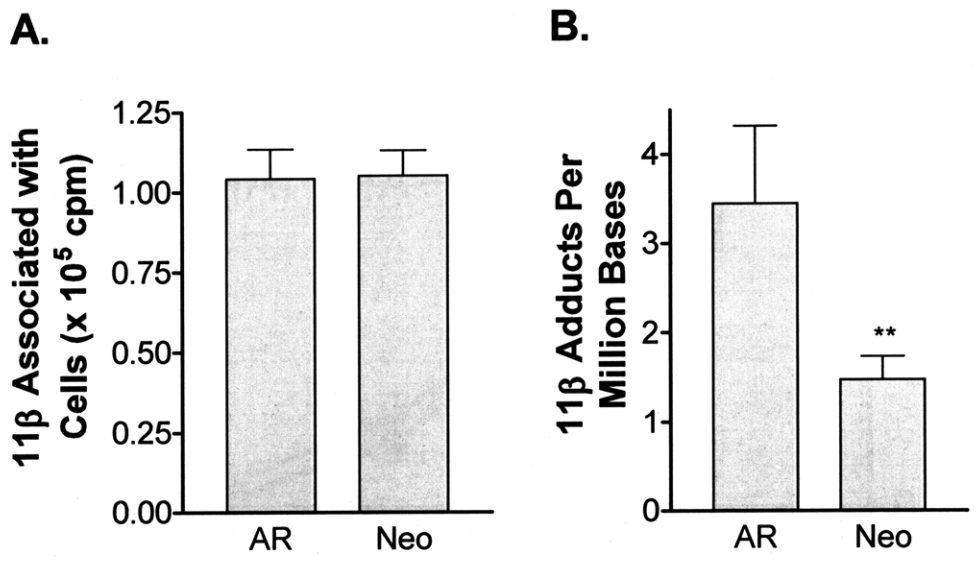

Fig 3.7 Analysis of 11β uptake and DNA adduct formation. A and B: PC3-AR and PC3-Neo cells were treated with 1.5 μM [^{14}C]11β for 2 hrs before lysis and scintillation counting (A), or DNA isolation and AMS analysis (B). Error bars are +/- SEM. **p-val < 0.01.

11β is Equally Toxic to the Isogenic AR+/- Cell Pair AR9/AR1

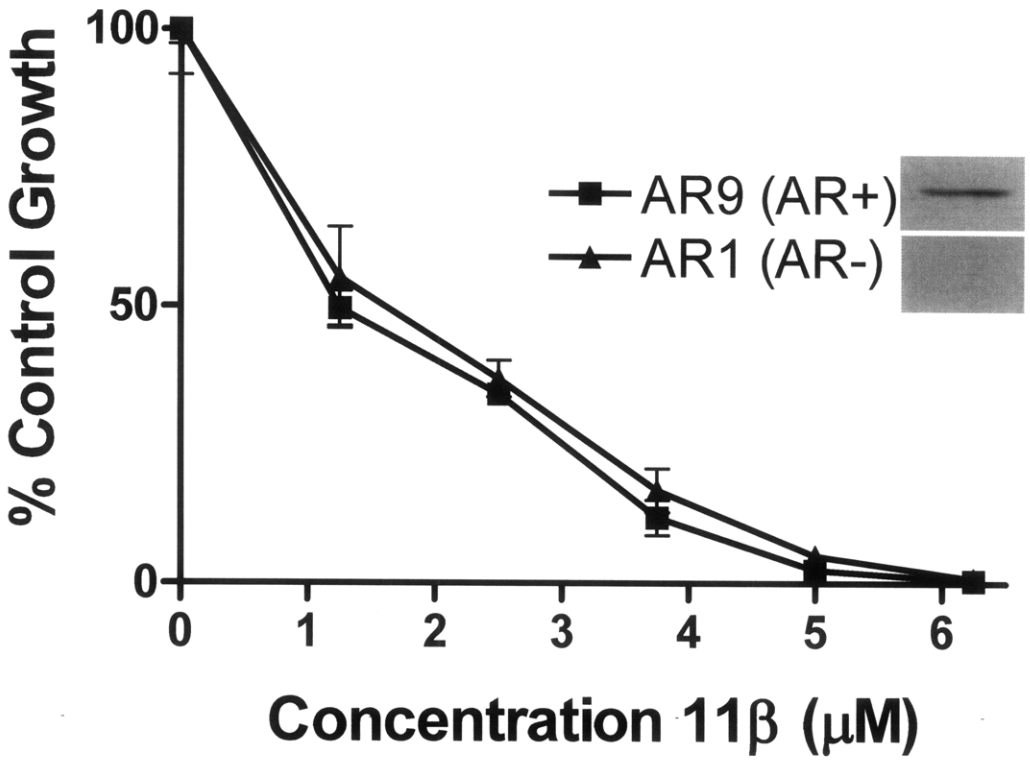

Fig 3.8 Growth inhibition assay. PC3-AR1 (AR -) and PC3-AR9 (AR +) cells were treated with 11β at concentrations shown for 72 hrs before counting. Western blot of immunoreactive AR (from 20 μg total protein extract) in each cell line is shown.

PC3-AR9 Cells Express Significant AR; AR1 Cells Express None

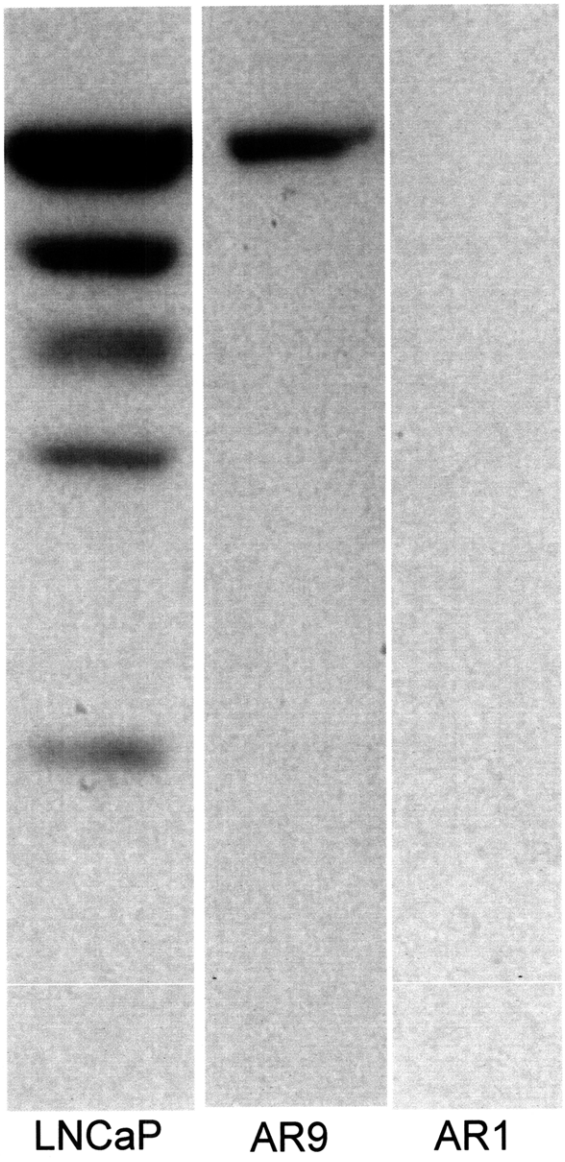

Fig 3.9 Western blot for AR in LNCaP, PC3-AR9, and PC3-AR1 cells. Equal quantities of total protein extract (20 μg) were loaded in each lane.

11β Forms More DNA Adducts in PC3-AR1 (AR-) Cells than PC3-AR9 (AR+) Cells

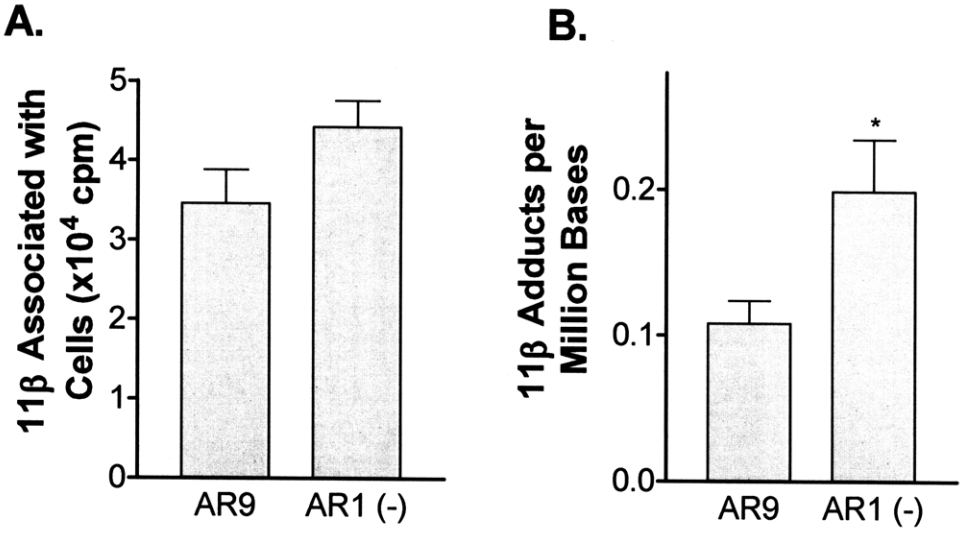

Fig 3.10 Analysis of 11β uptake and DNA adduct formation. A and B: PC3-AR9 (AR+) and PC3-AR1 (AR-) cells were treated with 0.4 μM [^{14}C]-11β for 2 hrs before lysis and scintillation counting (A), or DNA isolation and AMS analysis (B). Error bars are +/- SEM. *p-val < 0.1.

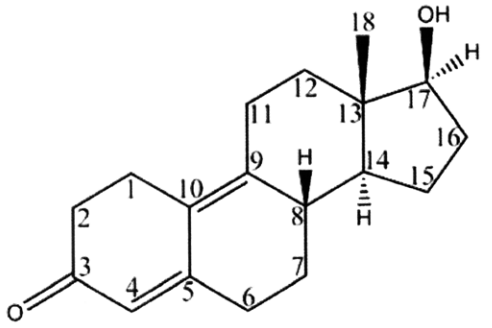

	17β dienone		17α dienone	
Atom	^{1}H shift(s)	^{13}C shift	^{1}H shift(s)	^{13}C shift
1	2.90, 2.54	26.04	2.91, 2.55	26.11
2	2.47, 2.44	37.32	2.48, 2.45	37.37
3	-	200.04	-	200.13
4	5.68	122.35	5.68	122.25
5	-	157.52	-	157.69
6	2.41, 2.36	30.83	2.42, 2.36	31.06
7	1.90, 1.26	27.31	1.95, 1.36	28.00
8	2.24	39.57	2.22	39.69
9	-	146.52	-	146.63
10	-	125.68	-	125.55
11	2.82, 2.15	25.84	2.86, 2.18	25.70
12	1.93, 1.23	36.70	1.72, 1.61	31.51
13	-	43.06	-	45.36
14	1.15	51.29	1.61	49.28
15	1.66, 1.38	23.63	1.83, 1.30	24.88
16	2.12, 1.53	31.01	2.24, 1.54	32.82
17	3.69, 1.54(OH)	81.56	3.83, 1.45(OH)	79.62
18	0.91	10.69	0.83	16.59

Table 3.1 Complete NMR assignment of 17β-OH and 17α-OH dienones. The most significant differences between the stereo-isomers are highlighted in gray. Steroid numbering scheme is shown above table for reference (17β-OH isomer).

gHMBC Plot for 17β Dienone

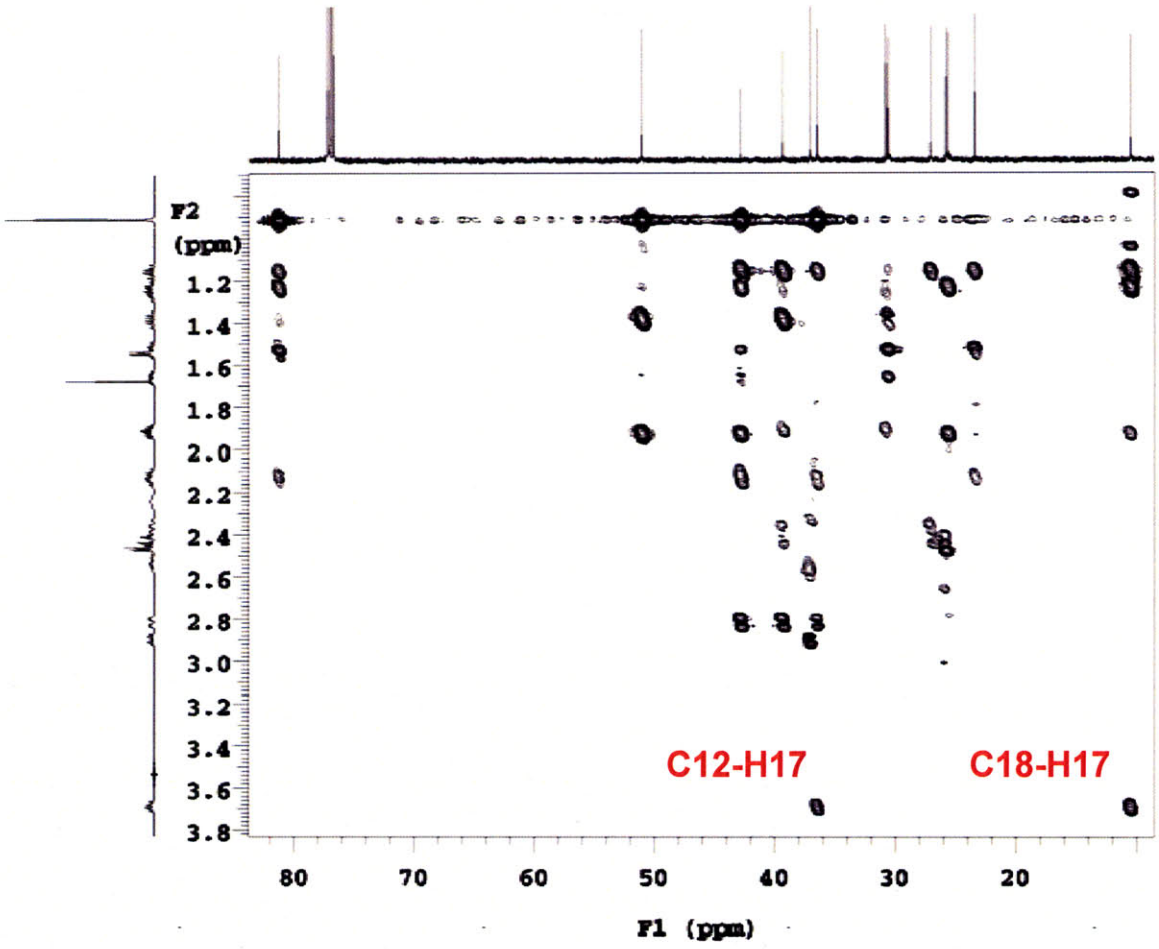

Fig 3.11 2D gHMBC NMR plot for 17β dienone shows cross coupling between H17 and C12 and C18.

gHMBC Plot for 17α Dienone; Alcohol Inversion is Successful

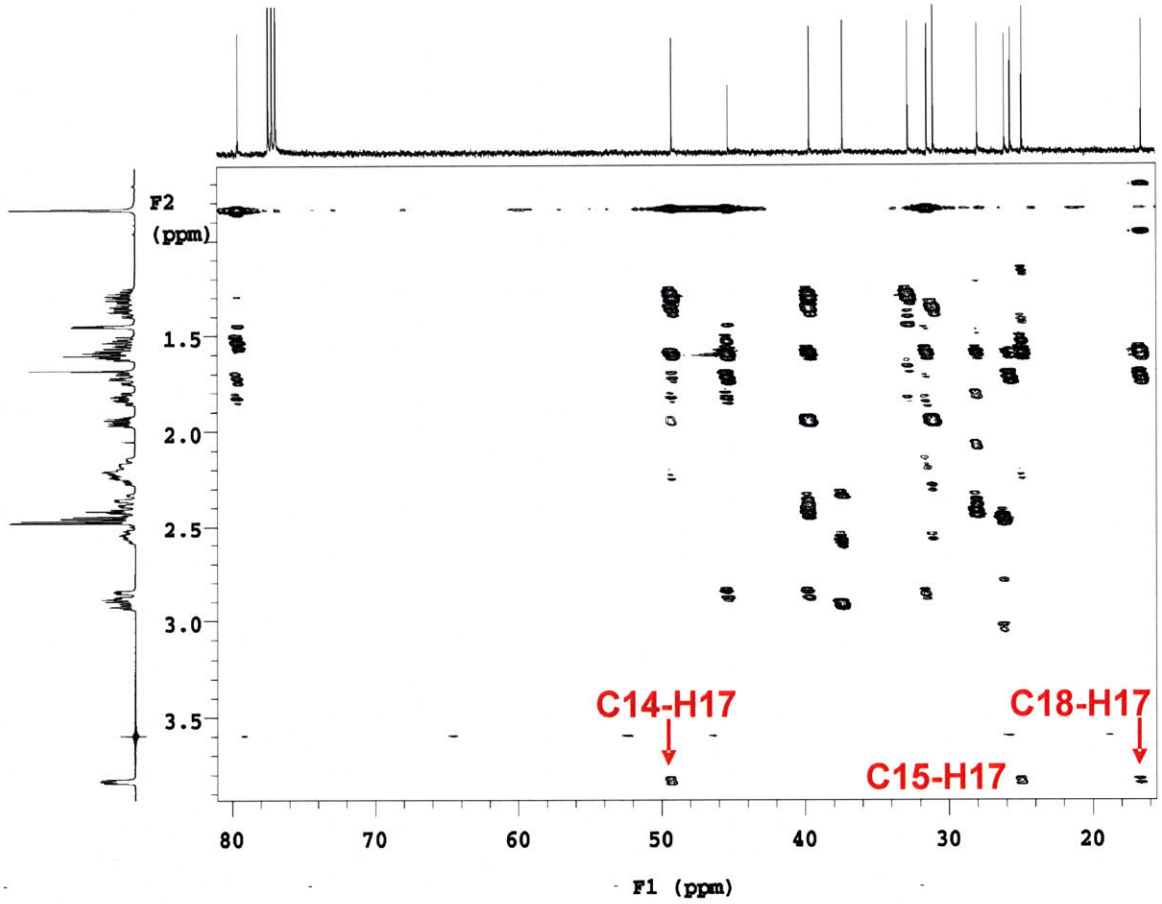

Fig 3.12 2D gHMBC NMR for 17α dienone shows significant cross-coupling between H17 and C14, C15, and C18, having lost coupling to C12 upon alcohol inversion.

17α-OH-11β Has Less Affinity than 11β for AR of LNCaP Cells

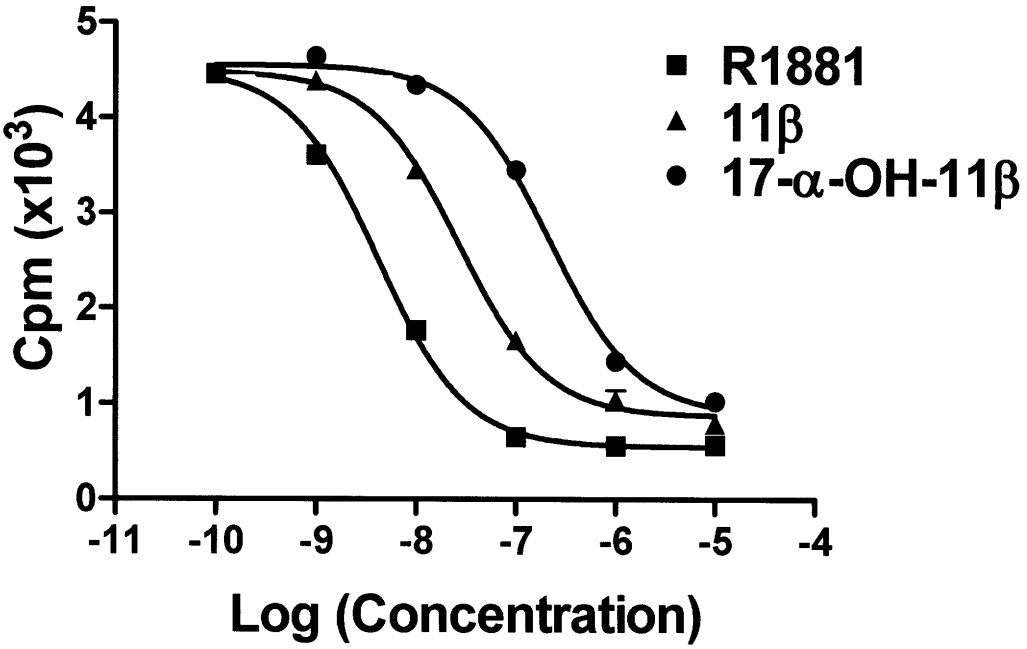

Fig 3.13 Competitive binding assay using LNCaP extracts (AR T877A Mutant). Extracts were incubated with 5 nM [^{3}H]-R1881 in the presence of competitors at concentrations shown, at 4°C for 18 hrs prior to isolation of total protein and liquid scintillation counting. Relative binding affinity: R1881=100, 11β=15.5, 17α-OH-11β=1.91; 17α-OH-11β has 12.3% RBA of 11β for LNCaP AR.

17α-OH-11β Has Less Affinity than 11β for AR of MDA-MB-453 Cells

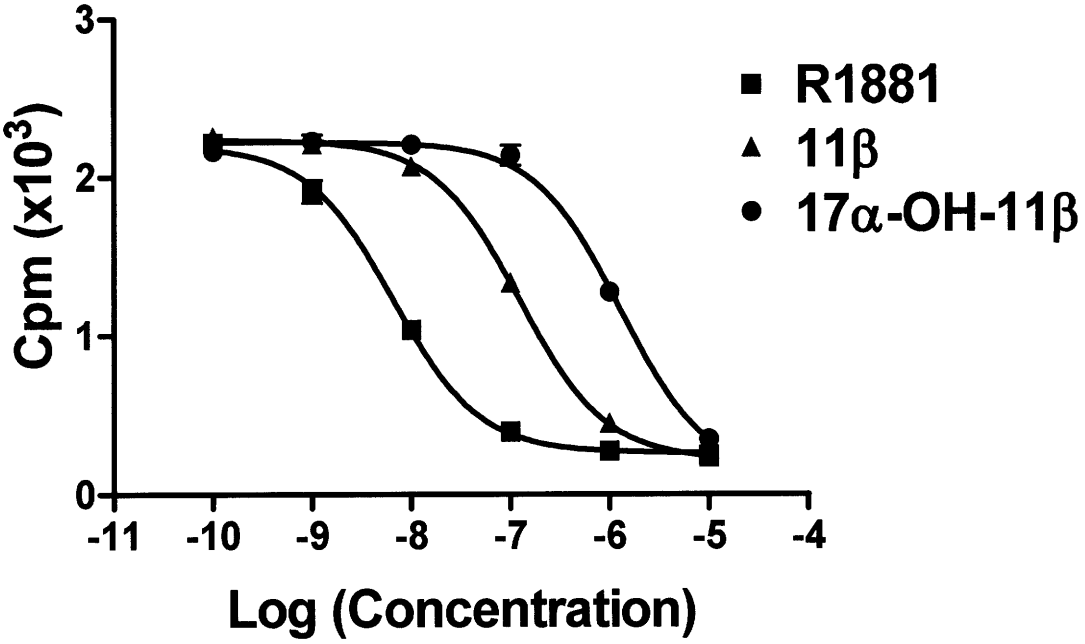

Fig 3.14 Competitive binding assay using MDA-MB-453 extracts (WT AR). Extracts were incubated with 5 nM [^{3}H]-R1881 in the presence of competitors at concentrations shown, at 4°C for 18 hrs prior to isolation of total protein and liquid scintillation counting. Relative binding affinity: R1881=100, 11β=5.31, 17α-OH-11β=0.51; 17α-OH-11β has 9.59% RBA of 11β for WT AR.

AR Transcriptional Reporter Assay Shows that 17α-OH-11β is a Weaker AR Antagonist than 11β

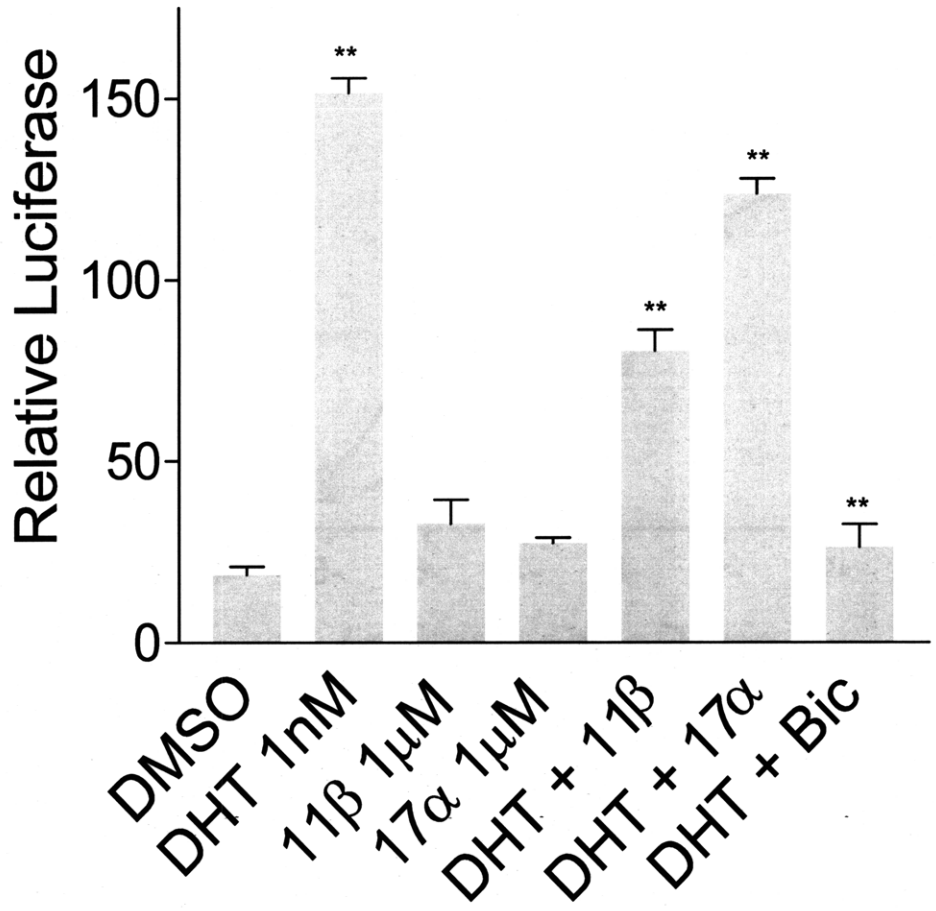

Fig 3.15 Luciferase reporter assay. LNCaP cells were transfected with plasmids pGL4PSA and pGL4.74 before treatment for 24 hrs with compounds shown in androgen-depleted media. Bic = bicalutamide, 10 μM; 17α=17α-OH-11β. In antagonist testing, DHT = 1 nM, 11β and 17α-OH-11β are 1 μM. Error bars are +/- SEM. **p-val < 0.01 (DHT is compared to DMSO, DHT + 11β, 17α, or bic is with reference to DHT).

DNA Adducts of 17α-OH-11β Have Lower Affinity to AR than 11β Adducts

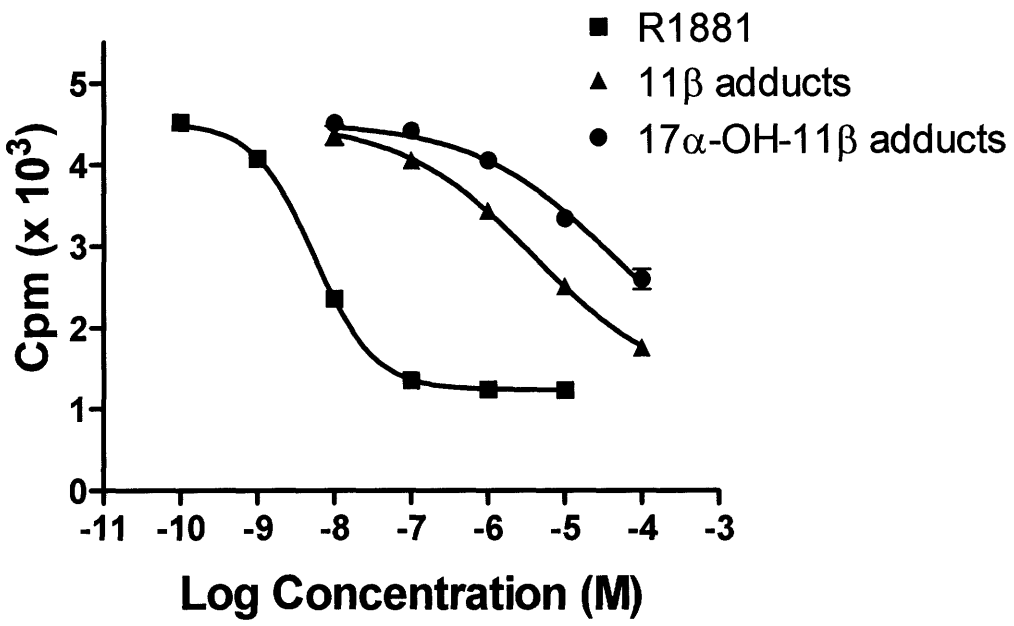

Fig 3.16 Competitive binding assay was used to determine affinity of 11β and 17α-OH-11β DNA adducts for AR of LNCaP extracts. Extracts were incubated with 5 nM [^{3}H]-R1881 in the presence of competitors at concentrations shown, at 4°C for 18hrs prior to isolation of total protein and liquid scintillation counting. RBA's: R1881=100, Adducts of 11β=0.11, Adducts of 17α-OH-11β=0.008; 17α-OH-11β adducts have 6.7% affinity of 11β adducts for AR of LNCaP cells. See materials and methods for information regarding adduct formation and quantitation.

11β is More Toxic than 17α-OH-11β

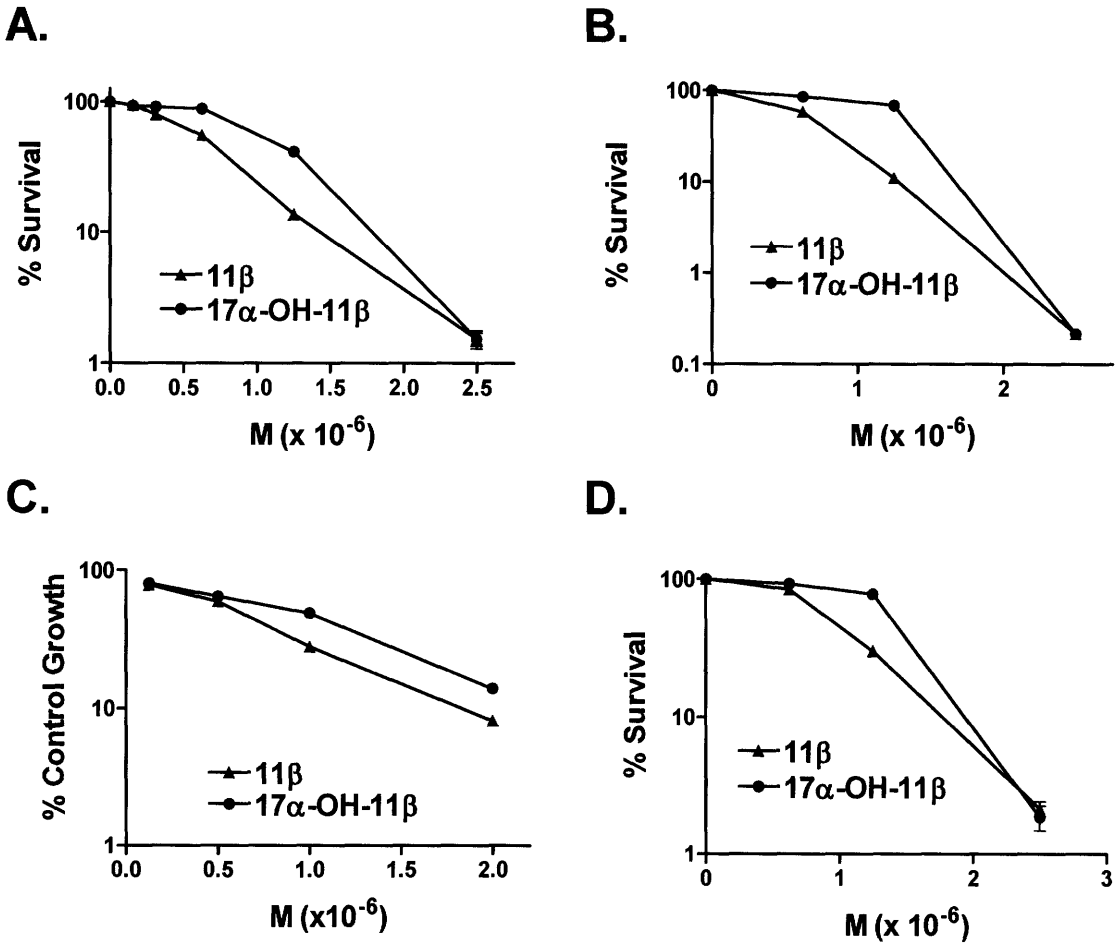

Fig 3.17 Toxicity of 11β and 17α-OH-11β measured in PC3-AR (A), MDA-MB-453 (B), LNCaP (C), and PC3-Neo cells (D). For A, B, and D, cells were treated at clonal density with concentrations of compound shown and then allowed to form colonies over 7-10 days before fixing, staining, and counting. For C, LNCaP cells were treated as shown for 5 days prior to counting attached cells.

11β Forms More Guanine Adducts and Guanine:Guanine Cross-links than 17α-OH-11β *in vitro*

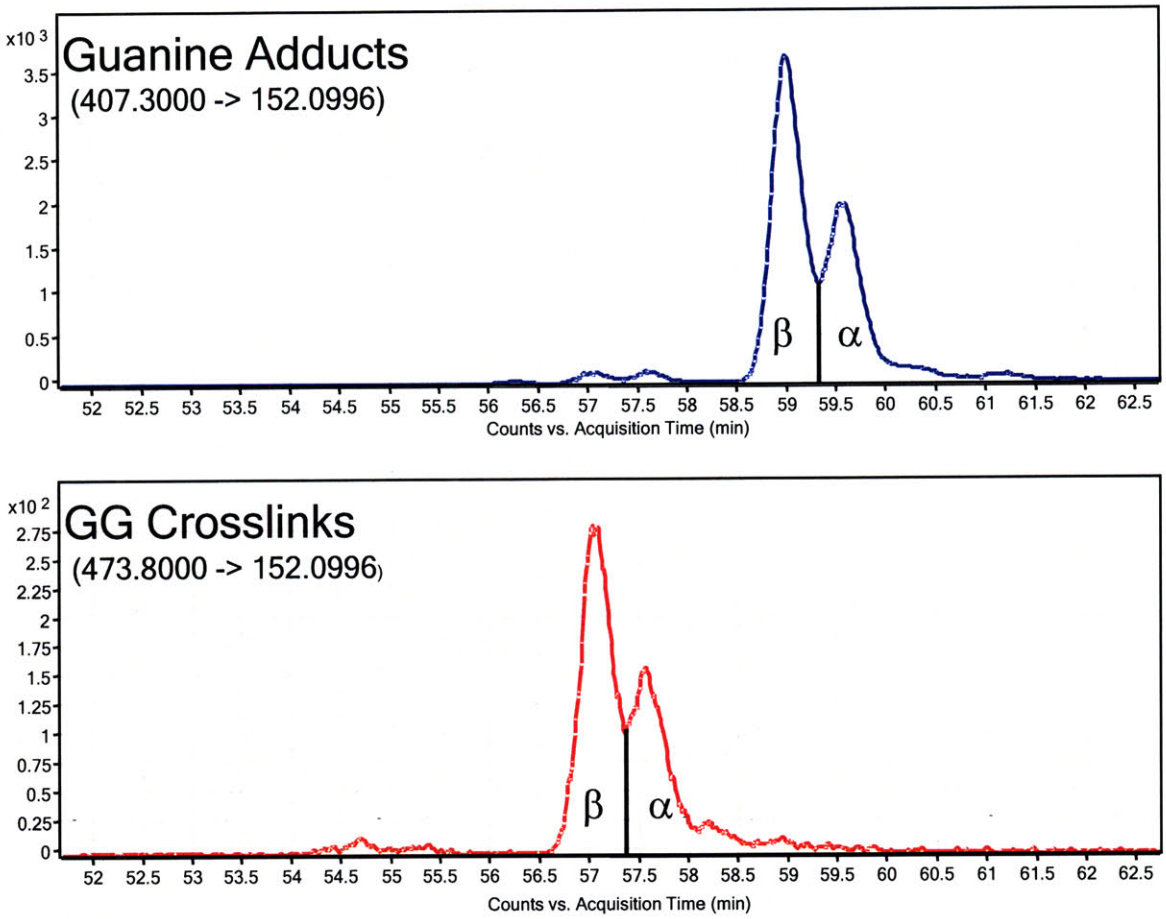

Fig 3.18 Adduction of calf thymus DNA by 11β and 17α-OH-11β. DNA was co-incubated with both compounds overnight, re-purified, and acid hydrolyzed to release adducted bases. Bases were analyzed by LC/tandem mass spectrometry to quantify compounds adducted to a single guanine base or guanine:guanine cross-links.

11β Forms an Equal Quantity of Adenine Adducts as 17α-OH-11β *in vitro*

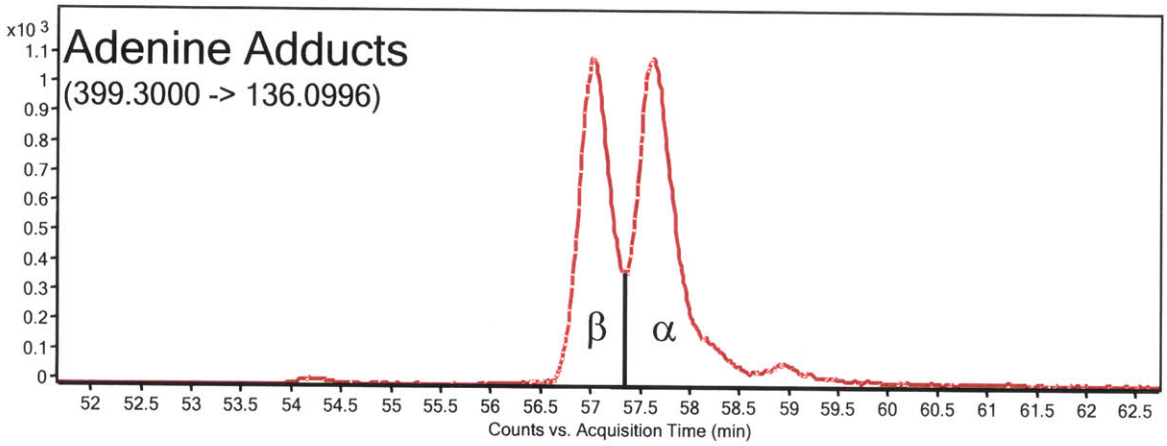

Fig 3.19 Adduction of calf thymus DNA by 11β and 17α-OH-11β. DNA was co-incubated with both compounds overnight, re-purified, and acid hydrolyzed to release adducted bases. Bases were analyzed by LC/tandem mass spectrometry to identify compounds adducted to a single adenine base. Relative abundance of adenine adducts compared to guanine adducts (Figure 3.17) was independently verified by UV absorbance.

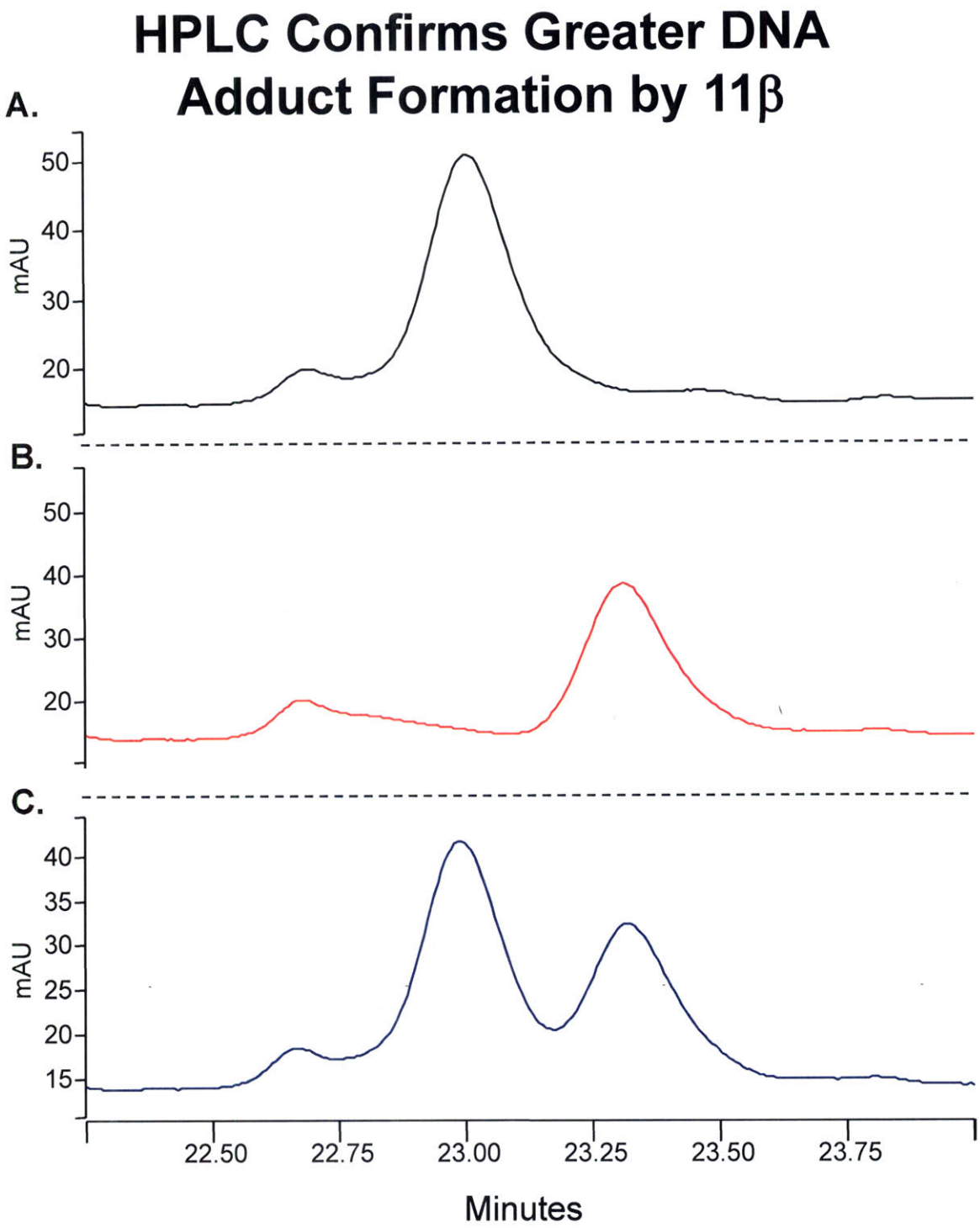

Fig 3.20 HPLC traces of hydrolyzed DNA bases adducted with 11β or 17α-OH-11β. Calf thymus DNA was reacted with 11β (A), 17α-OH-11β (B), or a combination of the two (C), prior to purification of DNA, acid hydrolysis to remove bases, and analysis on reversed-phase HPLC with monitoring at 254nm. Area under the curve (AUC) for major adduct, 22.99 minutes, is 2,350,997; AUC for 17α-OH-11β-guanine, 23.32 minutes, is 1,969,266.

AR Protein Expression is Increased by 11β Treatment in PC3-AR Cells

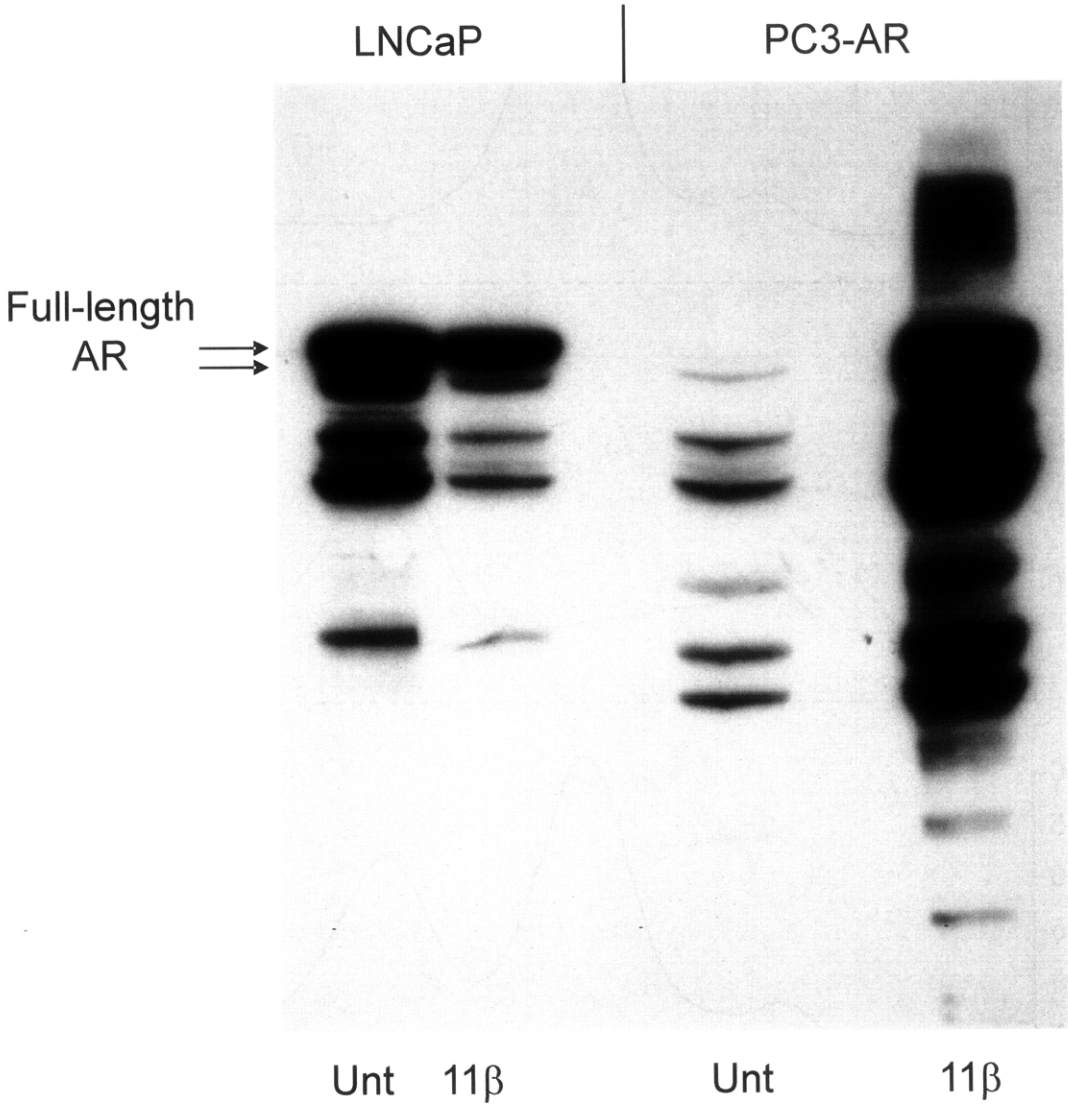

Fig S3.1 Western blot for AR in LNCaP and PC3-AR cells. Cells were either untreated or treated with 5 μM 11β for 24 hrs. 20 μg LNCaP whole cell extract or 66.6 μg PC3-AR whole cell extract were loaded per lane. Membrane was overexposed to bring out full-length AR expression in untreated PC3-AR cells.

AR Protein Expressed in PC3-AR Cells is a Functional Transcription Factor

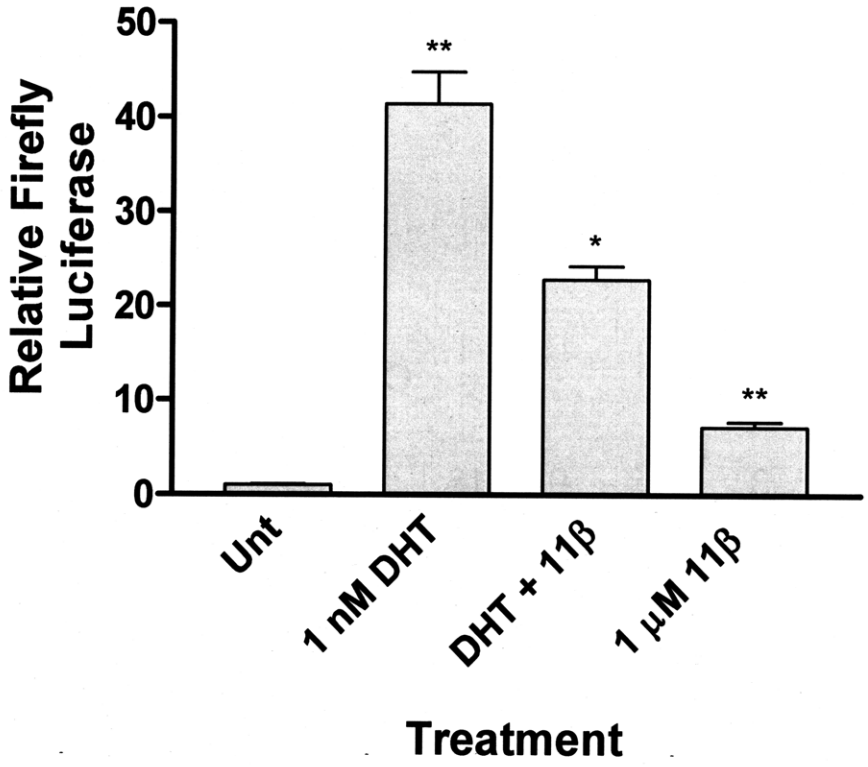

Fig S3.2 Luciferase assay performed in PC3-AR cells. Cells were transfected with pGL4PSA and PGL4.74. After 24 hrs, cells were changed to CDTFBS media, and after an additional 24 hrs, treated with compounds indicated for 24 hrs before assaying firefly and renilla luciferase. Error bars are +/- SEM. *p-val < 0.05, **p-val < 0.01.

AR Protein Expression is Increased by 11β Treatment in PC3-AR9 and A103 Cells

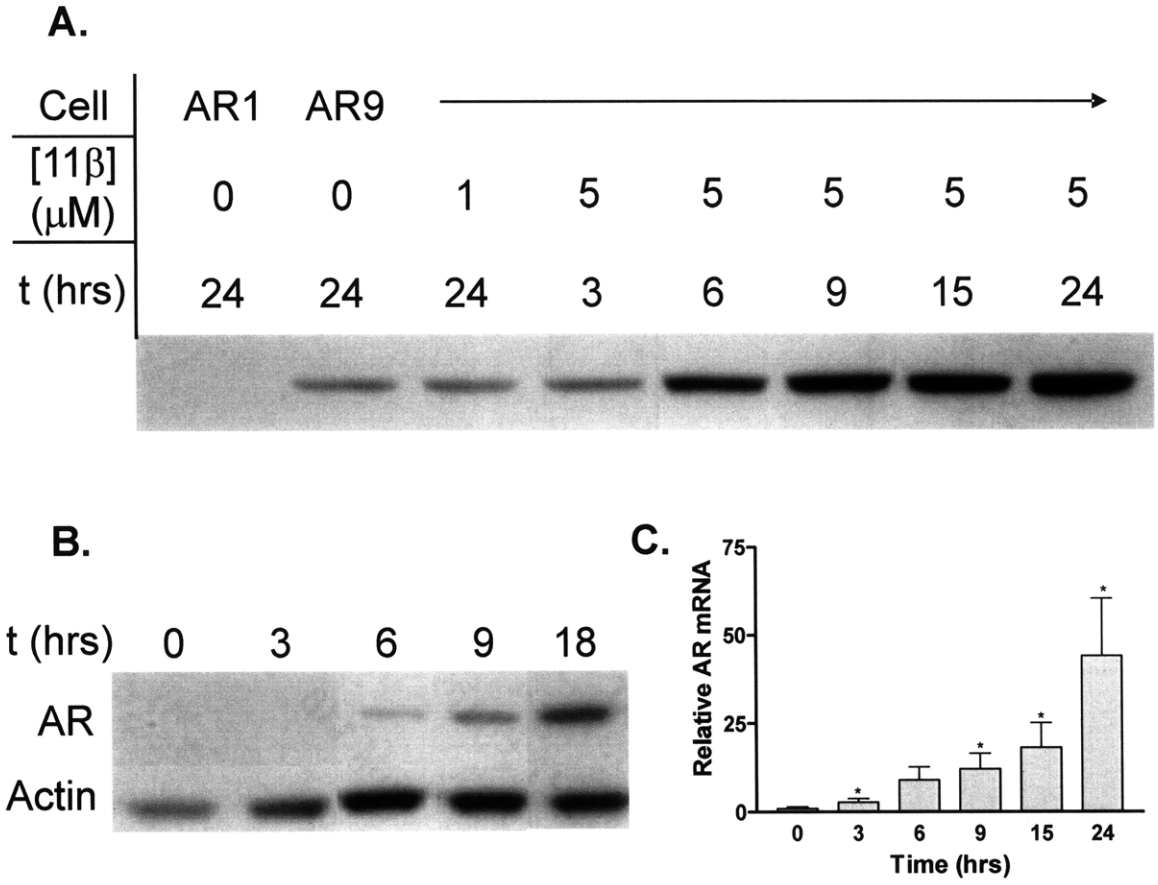

Fig S3.3 Analysis of AR protein and mRNA expression in PC3 cells expressing AR protein. A. Western blot for AR in PC3-AR9 (AR+) cells treated with 11β, at concentrations and times indicated. PC3-AR1 (AR-) cells are shown for comparison. B. Western blot for AR protein in A103 cells treated with 5 μM 11β for times indicated. C. RT-PCR for AR mRNA in A103 cells treated with 5 μM 11β. Error bars are +/- SEM. *p-val < 0.05.

References

Bhattacharyya, R. S., Krishnan, A. V., Swami, S., and Feldman, D. (2006). Fulvestrant (ICI 182,780) down-regulates androgen receptor expression and diminishes androgenic responses in LNCaP human prostate cancer cells. Mol Cancer Ther *5*, 1539-49.

Bruening, W., Giasson, B., Mushynski, W., and Durham, H. D. (1998). Activation of stress-activated MAP protein kinases up-regulates expression of transgenes driven by the cytomegalovirus immediate/early promoter. Nucleic Acids Res *26*, 486-9.

Burnstein, K. L. (2005). Regulation of androgen receptor levels: implications for prostate cancer progression and therapy. J Cell Biochem *95*, 657-69.

Cha, T., Qiu, L., Chen, C., Wen, Y., and Hung, M. (2005). Emodin Down-Regulates Androgen Receptor and Inhibits Prostate Cancer Cell Growth. Cancer Res *65*, 2287-2295.

Ciuffreda, P., Casati, S., and Manzocchi, A. (2004). Complete 1H and 13C NMR spectral assignment of 17-hydroxy epimeric sterols with planar A or A and B rings. Magn Reson Chem *42*, 360-3.

Compagno, D., Merle, C., Morin, A., Gilbert, C., Mathieu, J. R. R., Bozec, A., Mauduit, C., Benahmed, M., and Cabon, F. (2007). SIRNA-Directed In Vivo Silencing of Androgen Receptor Inhibits the Growth of Castration-Resistant Prostate Carcinomas. PLoS ONE *2*, e1006.

Dodge, J. A., and Lugar, C. W. (1996). Alcohol inversion of 17[beta]-steroids. Bioorganic & Medicinal Chemistry Letters *6*, 1-2.

Eder, I. E., Culig, Z., Ramoner, R., Thurnher, M., Putz, T., Nessler-Menardi, C., Tiefenthaler, M., Bartsch, G., and Klocker, H. (2000). Inhibition of LncaP prostate cancer cells by means of androgen receptor antisense oligonucleotides. Cancer Gene Ther *7*, 997-1007.

Eder, I. E., Hoffmann, J., Rogatsch, H., Schäfer, G., Zopf, D., Bartsch, G., and Klocker, H. (2002). Inhibition of LNCaP prostate tumor growth in vivo by an antisense oligonucleotide directed against the human androgen receptor. Cancer Gene Ther *9*, 117-25.

Eggert, H., VanAntwerp, C. L., Bhacca, N. S., and Djerassi, C. (1976). Carbon-13 nuclear magnetic resonance spectra of hydroxy steroids. J Org Chem *41*, 71-8.

Fang, H., Tong, W., Branham, W. S., Moland, C. L., Dial, S. L., Hong, H., Xie, Q., Perkins, R., Owens, W., and Sheehan, D. M. (2003). Study of 202 natural,

synthetic, and environmental chemicals for binding to the androgen receptor. Chem. Res. Toxicol *16*, 1338-1358.

Gregory, C. W., Hamil, K. G., Kim, D., Hall, S. H., Pretlow, T. G., Mohler, J. L., and French, F. S. (1998). Androgen receptor expression in androgen-independent prostate cancer is associated with increased expression of androgen-regulated genes. Cancer Res *58*, 5718-24.

Hess-Wilson, J. K., Daly, H. K., Zagorski, W. A., Montville, C. P., and Knudsen, K. E. (2006). Mitogenic Action of the Androgen Receptor Sensitizes Prostate Cancer Cells to Taxane-Based Cytotoxic Insult. Cancer Res *66*, 11998-12008.

Hillier, S. M., Marquis, J. C., Zayas, B., Wishnok, J. S., Liberman, R. G., Skipper, P. L., Tannenbaum, S. R., Essigmann, J. M., and Croy, R. G. (2006). DNA adducts formed by a novel antitumor agent 11{beta}-dichloro in vitro and in vivo. Mol Cancer Ther *5*, 977-984.

Holzbeierlein, J., Lal, P., LaTulippe, E., Smith, A., Satagopan, J., Zhang, L., Ryan, C., Smith, S., Scher, H., Scardino, P., et al. (2004). Gene expression analysis of human prostate carcinoma during hormonal therapy identifies androgen-responsive genes and mechanisms of therapy resistance. Am J Pathol *164*, 217-27.

Jemal, A., Siegel, R., Ward, E., Hao, Y., Xu, J., Murray, T., and Thun, M. J. (2008). Cancer statistics, 2008. CA Cancer J Clin *58*, 71-96.

Knudsen, K. E., Arden, K. C., and Cavenee, W. K. (1998). Multiple G1 Regulatory Elements Control the Androgen-dependent Proliferation of Prostatic Carcinoma Cells. J. Biol. Chem. *273*, 20213-20222.

van der Kwast, T. H., Schalken, J., Ruizeveld de Winter, J. A., van Vroonhoven, C. C., Mulder, E., Boersma, W., and Trapman, J. (1991). Androgen receptors in endocrine-therapy-resistant human prostate cancer. Int J Cancer *48*, 189-93.

Liao, X., Tang, S., Thrasher, J. B., Griebling, T. L., and Li, B. (2005). Small-interfering RNA-induced androgen receptor silencing leads to apoptotic cell death in prostate cancer. Mol Cancer Ther *4*, 505-515.

Lu, L., Schulz, H., and Wolf, D. (2002). The F-box protein SKP2 mediates androgen control of p27 stability in LNCaP human prostate cancer cells. BMC Cell Biology *3*, 22.

Lu, S., Liu, M., Epner, D. E., Tsai, S. Y., and Tsai, M. (1999). Androgen Regulation of the Cyclin-Dependent Kinase Inhibitor p21 Gene through an Androgen Response Element in the Proximal Promoter. Mol Endocrinol *13*, 376-384.

Mantoni, T. S., Reid, G., and Garrett, M. D. (2006). Androgen receptor activity is inhibited in response to genotoxic agents in a p53-independent manner. Oncogene *25*, 3139-3149.

Marquis, J. C., Hillier, S. M., Dinaut, A. N., Rodrigues, D., Mitra, K., Essigmann, J. M., and Croy, R. G. (2005). Disruption of gene expression and induction of apoptosis in prostate cancer cells by a DNA-damaging agent tethered to an androgen receptor ligand. Chem Biol *12*, 779-87.

Matias, P. M., Donner, P., Coelho, R., Thomaz, M., Peixoto, C., Macedo, S., Otto, N., Joschko, S., Scholz, P., Wegg, A., et al. (2000). Structural evidence for ligand specificity in the binding domain of the human androgen receptor. Implications for pathogenic gene mutations. J Biol Chem *275*, 26164-71.

Mohler, J. L., Gregory, C. W., Ford, O. H., Kim, D., Weaver, C. M., Petrusz, P., Wilson, E. M., and French, F. S. (2004). The androgen axis in recurrent prostate cancer. Clin Cancer Res *10*, 440-8.

Pereira de Jésus-Tran, K., Côté, P., Cantin, L., Blanchet, J., Labrie, F., and Breton, R. (2006). Comparison of crystal structures of human androgen receptor ligand-binding domain complexed with various agonists reveals molecular determinants responsible for binding affinity. Protein Sci *15*, 987-99.

Sack, J. S., Kish, K. F., Wang, C., Attar, R. M., Kiefer, S. E., An, Y., Wu, G. Y., Scheffler, J. E., Salvati, M. E., Krystek, S. R., et al. (2001). Crystallographic structures of the ligand-binding domains of the androgen receptor and its T877A mutant complexed with the natural agonist dihydrotestosterone. Proc Natl Acad Sci U S A *98*, 4904-9.

Tapolcsányi, P., Wélfling, J., Mernyák, E., and Schneider, G. (2004). The Mitsunobu Inversion Reaction of Sterically Hindered 17-Hydroxy Steroids. Monatshefte für Chemie / Chemical Monthly *135*, 1129-1136.

Tilley, W. D., Wilson, C. M., Marcelli, M., and McPhaul, M. J. (1990). Androgen Receptor Gene Expression in Human Prostate Carcinoma Cell Lines. Cancer Res *50*, 5382-5386.

Veldscholte, J., Voorhorst-Ogink, M. M., Bolt-de Vries, J., van Rooij, H. C., Trapman, J., and Mulder, E. (1990). Unusual specificity of the androgen receptor in the human prostate tumor cell line LNCaP: high affinity for progestagenic and estrogenic steroids. Biochim Biophys Acta *1052*, 187-94.

Visakorpi, T., Hyytinen, E., Koivisto, P., Tanner, M., Keinänen, R., Palmberg, C., Palotie, A., Tammela, T., Isola, J., and Kallioniemi, O. P. (1995). In vivo amplification of the androgen receptor gene and progression of human prostate cancer. Nat Genet *9*, 401-6.

Wang, H., Sun, D., Ji, P., Mohler, J., and Zhu, L. (2008). An AR-Skp2 pathway for proliferation of androgen-dependent prostate-cancer cells. J Cell Sci *121*, 2578-2587.

Xing, N., Chen, Y., Mitchell, S. H., and Young, C. Y. (2001). Quercetin inhibits the expression and function of the androgen receptor in LNCaP prostate cancer cells. Carcinogenesis *22*, 409-14.

Xu, Y., Chen, S., Ross, K. N., and Balk, S. P. (2006). Androgens Induce Prostate Cancer Cell Proliferation through Mammalian Target of Rapamycin Activation and Post-transcriptional Increases in Cyclin D Proteins. Cancer Res *66*, 7783-7792.

Yi, J., Yang, J., He, R., Gao, F., Sang, H., Tang, X., and Ye, R. D. (2004). Emodin Enhances Arsenic Trioxide-Induced Apoptosis via Generation of Reactive Oxygen Species and Inhibition of Survival Signaling. Cancer Res *64*, 108-116.

Yuan, X., Li, T., Wang, H., Zhang, T., Barua, M., Borgesi, R. A., Bubley, G. J., Lu, M. L., and Balk, S. P. (2006). Androgen Receptor Remains Critical for Cell-Cycle Progression in Androgen-Independent CWR22 Prostate Cancer Cells. Am J Pathol *169*, 682-696.

Zegarra-Moro, O. L., Schmidt, L. J., Huang, H., and Tindall, D. J. (2002). Disruption of androgen receptor function inhibits proliferation of androgen-refractory prostate cancer cells. Cancer Res *62*, 1008-13.

Zhang, L., Chang, C., Bacus, S. S., and Hung, M. (1995). Suppressed Transformation and Induced Differentiation of HER-2/neu-overexpressing Breast Cancer Cells by Emodin. Cancer Res *55*, 3890-3896.

Zhu, W., Smith, A., and Young, C. Y. (1999). A nonsteroidal anti-inflammatory drug, flufenamic acid, inhibits the expression of the androgen receptor in LNCaP cells. Endocrinology *140*, 5451-4.

Chapter 4: Global Transcriptional Response of LNCaP Cells to 11β Treatment

Introduction

The work discussed here pertains to 11β[1], which can form sites of DNA damage that attract the androgen receptor (AR) (Marquis et al. 2005; Hillier et al. 2006). The ability of 11β to repress strongly the growth of LNCaP xenograft tumors in NIH Swiss *nu/nu* mice with low collateral toxicity has demonstrated the potential use of 11β as a prostate cancer therapeutic agent (Marquis et al. 2005; Hillier et al. 2006). Furthermore, 11β is capable of eliciting apoptosis in LNCaP cells within ~15 hrs of treatment, while a control compound, 11β-dimethoxy, which lacks the ability to damage DNA, is incapable of apoptotic induction at similar concentrations (Marquis et al. 2005). Initially it was thought that 11β would induce toxicity in a manner that is strongly if not entirely dependent on the AR. It came as a surprise, therefore, that 11β is very effective at preventing growth of HeLa xenograft tumors, which lack AR (Hillier 2005). Furthermore, toxicity of 11β is unaffected by AR expression in PC3 cells (Chapter 3). As such, it is apparent that there are mechanistic explanations for the toxicity of 11β that do not depend on involvement of the AR. Additionally, there are likely to be mechanisms that are not related to formation of DNA damage, since 11β-dimethoxy has significant effects on some facets of cellular processes—cell rounding, induction of G1 arrest, Skp2 down-regulation, and p27 up-regulation (Marquis et al. 2005).

Gene microarray experiments provide a relatively rapid and simple method for acquiring a global perspective of the cellular processes perturbed by a small molecule. Given the need to find better explanations for the observed success of 11β in preventing growth of xenograft tumors, we have employed a microarray based structure-activity analysis, making comparisons between the effects of treating LNCaP cells with 11β, 11β-dimethoxy, chlorambucil (a nitrogen mustard DNA damaging agent), R1881 (androgen), or bicalutamide (anti-androgen). The different treatments were compared to probe how different portions of the complete 11β molecule may impinge on specific cellular processes and coordinate to produce the net effect of cell death. From this analysis, new

[1] 2-(6-((8S,11S,13S,14S,17S)-17-hydroxy-13-methyl-3-oxo-2,3,6,7,8,11,12,13,14,15,16,17 dodecahydro-1H-cyclopenta[a]phenanthren-11-yl)hexylamino)ethyl 3-(4-(bis(2-chloroethyl)amino)phenyl)propylcarbamate

discoveries have been made related to induction of cholesterol biosynthesis, activation of the unfolded protein response, and the similar transcriptional modulation triggered by 11β and 11β-dimethoxy, which together provide potential mechanistic explanations for observed efficacy.

Materials and Methods

Chemicals: Methyltrienolone (R1881) was acquired from Perkin-Elmer Life Sciences (Waltham, MA). Bicalutamide was from LKT Laboratories, Inc. (St. Paul, MN). Chlorambucil was acquired from Sigma-Aldrich (St. Louis, MO). Synthesis of 11β-dichloro (referred to here as 11β) and 11β-dimethoxy were performed in our laboratory and have previously been described (Marquis et al. 2005).

Cell Culture: LNCaP cells (ATCC, Rockville, MD) were maintained in RPMI 1640 media supplemented with glucose (2.5 g/L), 1 mM sodium pyruvate, 10 mM HEPES, and 10% fetal bovine serum. Media and supplements were obtained from Invitrogen (Carlsbad, CA), except for fetal bovine serum (Hyclone, Salt Lake City, UT). All cells were grown in a humidified 5% CO_2/air atmosphere at 37°C.

Cell Treatment for Microarray Preparation: LNCaP cells were plated at a density of 800,000 cells in 10 cm diameter tissue culture dishes and allowed to grow for 48 hrs prior to treatment. At this time, cells were treated with compounds indicated, diluted 1000x into fresh media. Three control treatments were performed: 1) no treatment, cells harvested at treatment time (unt 0 hrs), 2) fresh, untreated media, and 3) DMSO vehicle. Other treatments were: 4) 11β 1 μM, 5) 11β 5 μM, 6) 11β-dimethoxy 5 μM, 7) chlorambucil 5 μM, 8) bicalutamide 1 μM, and 9) R1881 1 nM. Samples 2-9 were harvested after 6 hrs of treatment. Please refer to Figure 4.1 and Table 4.1 for structures of compounds used and treatment details. Cells were scraped into media, centrifuged to pellet, washed once with PBS, re-pelleted, and stored at -70°C until RNA isolation. Individual treatments were repeated twice more, each three days (and one passage)

following the prior treatment, in order to obtain more meaningful biological replicates, producing each sample in triplicate.

RNA Isolation: RNA was isolated from frozen cell pellets with RNeasy® Mini kit, employing QIAshredder columns for sample homogenization (Qiagen, Valencia, CA). RNA concentration was assessed by UV absorbance, and quality was assessed with Agilent Technologies 2100 Bioanalyzer.

Microarray: Microarray analysis was performed at Paradigm Genetics, Inc. (Research Triangle Park, NC). Samples were processed by a standard Affymetrix protocol, and amplified complementary DNA was hybridized to Affymetrix HGU133Plus2.0 GeneChips®.

Data Analysis: Analysis of microarray data was performed in the statistical environment R (http://www.r-project.org) with the Bioconductor package (Gentleman et al. 2004). All samples were normalized using the GCRMA method (Li & Wong 2001; Irizarry et al. 2003; Wu et al. 2008). As a first step toward data reduction, the Affymetrix Microarray Suite 5.0 (MAS5) algorithm (as implemented in Bioconductor) was used to identify present transcripts. Transcripts were required to have a present call with p-value < 0.01 in at least 50% of the samples for any single treatment group (unt 0 hrs, unt 6 hrs, DMSO 6 hrs, 11β 1 μM 6 hrs, 11β 5 μM 6 hrs, 11β-dimethoxy 5 μM 6 hrs, chlorambucil 5 μM 6 hrs, R1881 1 nM 6 hrs, or bicalutamide 1 μM 6 hrs), leaving 20909 probe sets for further analysis. Next, to determine significance of differential expression, a linear modeling approach was used according to the limma package within Bioconductor (Smyth 2005). Standard linear modeling data analysis (MANOVA) was applied to identify probe sets with significantly different expression in pair-wise comparisons (unt 6hrs vs unt 0hrs; DMSO 6 hrs vs unt 6 hrs; 11β 1 μM 6 hrs vs DMSO 6 hrs; 11β 5 μM 6 hrs vs DMSO 6 hrs; 11β-dimethoxy 5 μM 6 hrs vs DMSO 6 hrs; chlorambucil 5 μM 6 hrs vs DMSO 6 hrs; R1881 1 nM 6 hrs vs DMSO 6 hrs; Bicalutamde 1 μM 6 hrs vs DMSO 6 hrs) (Table 4.1). The significance of each comparison was evaluated using t-statistics. Genes with associated p-values for differential expression of < 0.05, corrected by the method of

Benjamini & Hochberg to minimize false discovery (Benjamini & Hochberg 1995), and having a fold-change of at least two were selected for further analysis. Fold-change values for each pair-wise comparison are reported as Log_2 fold change (LFC); an LFC of 1 (or -1) is equivalent to a 2-fold difference in expression. A total of 615 probe sets was identified from the above requirements. All scripts for use in Bioconductor were provided by Dr. Jadwiga Bienkowska (Biogen-Idec, Cambridge, MA). Microsoft Excel (Redmond, WA) and Spotfire DecisionSite (TIBCO, Palo Alto, CA) were used for subsequent sorting and visualization of data.

Gene Classification: In order to classify genes into categories according to biological functions, genetools (http://genetools.microarray.ntnu.no) was used to annotate genes. Genes were sorted according to GO3 level biological process and manually refined to classify each gene into a single category for analysis.

Gene Ontology: WebGestalt (http://bioinfo.vanderbilt.edu/webgestalt/) was used to identify over-represented categories of genes differentially expressed by individual treatments. Differentially expressed probe sets were compared against the reference list of all probe sets included on the HGU133Plus2.0 array, using a hypergeometric test to identify over-represented categories with a significance level of 0.01 or less. Categories were chosen from the GOTree Directed Acyclic Graph by identifying the enriched groupings on the lowest "branches", providing the most detailed categorical descriptions.

Connectivity Map: The connectivity map (CMAP) is a tool developed through the Broad Institute in order to compare gene expression data between treatments of cultured human cells with various compounds having disparate biological mechanisms (Lamb et al. 2006; Lamb 2007). The software allows a researcher to compare the expression profile of a single compound against this reference library in order to identify other compounds that produce similar effects on global transcription. As such, new mechanisms can be discovered when it is learned that an expression profile is similar to agents or classes of agents with better-understood activities. We used this tool for further analysis of the expression profiles of agents tested, working with build 02 of the

connectivity map, which contains over 7,000 expression profiles representing 1,309 different compounds. All but four of the profiles contained in the CMAP library were generated by treatment with compounds for 6 hrs.

RT-PCR: RNA from isolation for microarray analysis was used for RT-PCR verification of a subset of genes. RT-PCR was performed with Quantitect SYBR Green RT-PCR kit (Qiagen) at MIT BioMicro Center on MJ Research Real-Time PCR Machine with *GAPDH* as control. Primers were designed using Primer3 software (Rozen & Skaletsky 2000) and are as follows: *GAPDH* (based on accession NM_002046) Forward: ACA GTC AGC CGC ATC TTC TT, Reverse: GCC CAA TAC GAC CAA ATC C; *GDF15* Forward: GAG GTG CAA GTG ACC ATG TG, Reverse: GTG CAG GCT CGT CTT GAT CT; *DDIT3* Forward: GAG GTG CAA GTG ACC ATG TG, Reverse: GTG CAG GCT CGT CTT GAT CT; *HMGCS1* Forward: GCT CAG AGA GGA CAC CCA TC, Reverse: GCC GAG CGT AAG TTC TTC TG; *ATF3* Forward: CTA ACC TGA CGC CCT TTG TC, Reverse: TTG TTC TGG ATG GCA AAC CT; *TRIB3* Forward: TTA GGC AGG GTC TGT CCT GT, Reverse: GTA TGG ACC TGG GAT TGT GG; *GADD45A* Forward: AAC GGT GAT GGC ATC TGA AT, Reverse: CCC TTG GCA TCA GTT TCT GT. A method was also developed to identify *XBP1*, both in its unspliced (*XBP1u*) and spliced (*XBP1s*) forms. To identify only the unspliced form, the forward primer was designed to anneal within the intronic region, while the forward primer used for identification of the spliced form was designed to span the intron. Primers for this were *XBP1u* Forward: CAG ACT ACG TGC ACC TCT GC, Reverse: ACT GGG TCC AAG TTG TCC AG; *XBP1s* Forward: CTG AGT CCG CAG CAG GTG, Reverse: ACT GGG TCC AAG TTG TCC AG.

Statistics: Significance tests were performed with unpaired 2-tailed student's t-test as implemented in Excel 2002 (Microsoft).

Results

Experimental Design

In order to explore potential mechanistic explanations for the anticancer activity of 11β, we chose to monitor the global gene transcriptional profiles of LNCaP cells treated with this agent. Concentrations of 1 μM and 5 μM were used in hopes of capturing the immediate effects of 11β treatment on cellular biochemical processes without unwanted side effects of general toxicity. A 5 μM concentration is a threshold for 11β toxicity to LNCaP cells in a 24 hr treatment; concentrations 5 μM and below result in growth inhibition (as discussed in Chapter 3, Figure 3.1), while higher concentrations result in apoptosis (Marquis et al. 2005). The 1 μM concentration was included to explore the relationship between drug concentration and transcriptional response. Treatments were performed for 6 hrs in order to identify the most immediate responses while minimizing secondary, downstream, or general toxicity effects. We also included the non-DNA damaging 11β analogue, 11β-dimethoxy, at 5 μM. In so doing, we were able to identify which effects on transcription could be attributed to covalent interactions. Furthermore, we included the nitrogen mustard chlorambucil at 5 μM in order to identify any transcriptional responses that a similar DNA damaging agent would have, irrespective of the steroid and linker regions of 11β. Finally, we included an androgen receptor agonist (R1881, 1 nM) and an AR antagonist (bicalutamide, 1 μM) to shed further light on how the interaction of 11β with the AR may influence cellular processes. Figure 4.1 provides the structures of all compounds tested. We hoped that by analyzing changes in gene expression induced in LNCaP cells exposed to this set of compounds, we could identify structure-activity relationships for the steroid and alkylating activities of the 11β molecule. Controls included: 1) isolation of cells at time of treatment (unt 0 hrs), 2) replacement with fresh media for the 6 hr duration (unt 6 hrs), or 3) treatment with DMSO vehicle. Control treatments were examined in comparison to the 0 hrs unt control sample and reveal very little significant transcriptional change elicited by either the 6 hrs fresh media treatment (2) or vehicle treatment (3) (Tables S4.13-S4.16, Figures S4.7, S4.8). As such, all comparisons discussed hereafter are with respect to DMSO vehicle.

Affymetrix Human Genome U133 Plus 2.0 microarrays, each containing 54,613 probe sets representing over 38,500 well-characterized human genes and Unigenes, were used to identify global mRNA transcript levels in each of these treatment groups. Pair-wise comparisons were made between each treatment and DMSO (Table 4.1). A cutoff of two-fold differential expression was used for most analyses, while this requirement was relaxed in a few indicated circumstances to acquire a more complete understanding. In all data discussed, p-values are < 0.05 unless otherwise specified. Fold-changes are often referred to by their $\log_2$ fold change (LFC); an LFC of 1 (or -1) is equivalent to a 2-fold difference in expression between treatment groups.

11β Significantly Alters Expression of Many Genes from Diverse Pathways

Figure 4.2 shows the numbers of unique genes significantly up- or down-regulated in each of the treatment groups, demonstrating that 5 μM 11β produced the most significant transcriptional response, increasing expression of 119 genes and decreasing expression of another 42 genes. 11β-Dimethoxy followed somewhat closely behind, increasing expression of 78 genes and decreasing expression of 13. As expected, 1 μM 11β had less effect than the higher concentration on overall transcription. R1881 treatment resulted in almost exclusive up-regulation of a set of genes, while bicalutamide only caused the decreased expression of 2 genes. Finally, using a 2-fold differential expression cutoff, no significantly differentially expressed genes were generated by treatment with chlorambucil or DMSO relative to the 6 hr untreated sample, or the 6 hr untreated sample relative to untreated cells isolated at time of treatment.

The key, primary question we sought to address by monitoring the expression profile of treatment with 11β was "Which biological pathways are activated or repressed?" The answer to this question can offer insight into the mechanisms responsible for 11β toxicity. After filtering data as discussed, different tools were used to increase our biochemical understanding of what these differentially expressed genes represent. First, known genes were classified into functional categories based on their associated biological processes as discussed in Materials and Methods. From this analysis, some striking effects of 5 μM 11β treatment were immediately noticed. As anticipated, 11β affects the expression of several genes related to progression through the

cell cycle—generally up-regulating cell cycle inhibitory genes and down-regulating cell cycle promotional genes, various aspects of transcription, and apoptosis (Figure 4.3, Table 4.2). More surprisingly, 11β treatment resulted in significant up-regulation of genes associated with cholesterol or lipid biosynthesis, and also those associated with a response to unfolded protein. There is a robust increase in expression of genes associated with various aspects of transport as well. While most of these processes are overwhelmingly up-regulated, protein synthesis and DNA repair are heavily down-regulated (Figure 4.3, Table 4.3).

It is even more meaningful to ask which gene categories are over-represented in each dataset. Over-representation refers to the statistical enrichment of genes belonging to a specific functional category, above what would be expected if genes were chosen randomly, and suggests that any changes seen in that class of genes can be interpreted to not have arisen by chance. A hypergeometric test addresses the likelihood that a certain subset would be selected at random, taking into account the total number of genes represented on a microarray, the number of genes included in a functional category, and the number of "hits" identified. This hypergeometric analysis demonstrates that 11β up-regulates an over-represented set of genes related to cell cycle arrest and sterol biosynthesis, among others (Table 4.4). While a response to unfolded protein is not over-represented by this test, genes related to endoplasmic reticulum (ER) membrane, which are often the same as those involved in response to unfolded protein, are over-represented. 11β is also shown by this analysis to have decreased expression of genes over-represented in categories of G1/S cell cycle transition, mitosis, rRNA processing, and mismatch and base-excision DNA repair (Table 4.5).

Performing the same analysis with genes affected by treatment with 1 μM 11β produces no significant category over-representation if a 2-fold differential cutoff is used. If this is relaxed to a 1.4-fold cutoff, however, cholesterol biosynthesis remains significantly over-represented as induced, while protein transport is the most striking category of genes whose expression is reduced by treatment (Table 4.6). Comparing 1 μM 11β with 5 μM 11β demonstrates that activation of several pathways depends on reaching a higher concentration. Cholesterol biosynthetic genes, being most sensitive to

1 μM 11β treatment, may provide a clue to the more specific effects of 11β treatment that can lead to growth inhibition and apoptosis.

11β and 11β-Dimethoxy Modulate a Strikingly Similar Set of Genes And Processes

Comparison between 11β and 11β-dimethoxy is valuable in determining which effects of 11β depend on DNA damage or other covalent interactions of the compound. While 11β-dimethoxy is less toxic than 11β to LNCaP cells, it is not without effects: it produces a G1 cell cycle arrest, reduces expression of Skp2, and increases expression of p27 (Marquis et al. 2005). Somewhat surprisingly, however, 11β-dimethoxy produced a very similar transcriptional response to that achieved with 11β. Of the 477 probe sets significantly altered in expression by 5 μM 11β, 200 are also significantly affected by 11β-dimethoxy (Figure 4.4). Generally, for most of these probe sets, the magnitude of change is greater with 11β treatment than with 11β-dimethoxy. Further, of the remaining 277 probe sets differentially expressed 2-fold by 11β, but less than 2-fold by 11β-dimethoxy, 209 of these are significantly differentially expressed (in the same direction) by 11β-dimethoxy by at least 1.4-fold (Figure 4.4, Table S4.1, S4.2). Thus, by drawing an arbitrary line at a 2-fold expression difference, some genes falling on either side of this line will be bracketed and considered unique, while in reality the story is more complex, with both compounds having similar effects on transcription of those genes.

Analysis of gene categories over-represented by 11β-dimethoxy produces many of the same associations seen with 11β, such as increased expression of genes related to cholesterol biosynthesis (Table 4.7, Table 4.8). Additionally, 11β-dimethoxy increases expression of genes over-represented in the category of response to unfolded protein. These same genes (*EIF2AK3*, *HERPUD1*, *EDEM1*) are also significantly up-regulated by 11β, and for the category of response to unfolded protein, 11β has a p-value of 0.012 (because a greater number of probe sets are perturbed by 11β treatment, thereby decreasing significance). As such, this pathway can be considered significantly over-represented by treatment with either compound.

A category that is uniquely over-represented by 11β, but not by 11β-dimethoxy, is cell-cycle arrest, which includes genes *CDKN1A*, *GADD45A*, *SESN2*, *HBP1*, and *DDIT3*.

However, the only gene in this group that is not also affected by 11β-dimethoxy treatment is *CDKN1A*; each of the other genes is induced at least 2-fold by 11β-dimethoxy, albeit more so by 11β treatment. *CDKN1A* codes for the protein p21, a downstream effector of p53 activation regulating the G1/S cell cycle progression (Harper et al. 1993). Its expression is initially decreased by 11β and 11β-dimethoxy, but it then recovers to untreated levels in 11β-dimethoxy treated cells, while amplifying several fold in cells treated with 11β (Marquis et al. 2005). The detailed biochemical understanding of how and why p21 levels initially decrease before being amplified by 11β treatment is still lacking. However, the microarray data support a hypothesis that the eventual amplification, which occurs with 11β but not with 11β-dimethoxy treatment, results from increased *CDKN1A* transcription.

Expression changes unique to 11β treatment were also identified by direct comparison of the gene expression levels in LNCaP cells following 11β or 11β-dimethoxy treatment. To do this, we calculated the ΔLFC, the difference between the LFC of treatment with 11β and the LFC of treatment with 11β-dimethoxy. We identified 57 probe sets that are more significantly perturbed by 11β treatment than by 11β-dimethoxy treatment ($\Delta LFC \geq 0.8$, or 1.74-fold difference between treatments; complete list available in Table S4.17 and Table S4.18). Each of these probe sets also has a significance of differential expression p-value for 11β < 0.05, and the absolute value of LFC for 11β is at least 0.5 (~1.4-fold). This group of 57 probe sets was analyzed for enrichment of categories, identifying cell cycle related processes and response to DNA damage stimulus (Table 4.9). The response to DNA damage stimulus is likely very important, as this is presumably the functional difference between 11β and 11β-dimethoxy.

BTG2 and *DDIT3* were identified among the 57 probe sets as members of the category that are responsive to DNA damage stimulus. *BTG2* is truly unique to 11β treatment (LFC = 1.29 for 11β, LFC = 0.30 for 11β-dimethoxy). BTG2 (also known as PC3 or TIS21) is a DNA-damage responsive, p53-regulated protein involved in G1/S cell cycle transition (Rouault et al. 1996; Guardavaccaro et al. 2000). Additionally *DDIT3* (DNA-Damage Induced Transcript 3), which encodes the protein CHOP (or GADD153),

was also identified in the category of response to DNA damage stimulus. While *DDIT3* was initially identified as DNA-damage responsive (Fornace, Alamo & Hollander 1988), it has since been observed to also respond to oxidative stress (Halleck et al. 1997) or other insults that result in endoplasmic reticulum stress (Wang et al. 1996). The ER stress pathway that is activated is also known as the unfolded protein response (UPR), and in this framework, CHOP plays a role in promoting apoptosis in cells that can not overcome the assault (Zinszner et al. 1998; McCullough et al. 2001; Marciniak et al. 2004). Unlike *BTG2*, The *DDIT3* gene is induced by both 11β (LFC = 3.46) and 11β-dimethoxy (LFC = 1.70). This suggests that the DNA-damage inflicted by 11β may enhance induction of *DDIT3*, but it is not absolutely required for this response.

We also identified a group of genes for which 11β-dimethoxy effects a significantly greater magnitude change than 11β. Interestingly, these genes can be roughly sorted into two categories. The first contains genes that respond similarly to treatment with 11β-dimethoxy or the AR agonist R1881 (Table 4.10), which suggests that these genes are likely androgen-regulated. This class includes *PMEPA1*, *FAM110B*, *ROR1*, *IGF1R*, *HPGD*, *FKBP5*, *PHLDB2*, *CSGALNACT1*, *MAF*, and *SNAI2*. Several of these, including *PMEPA1*, *HPGD*, *FKBP5*, *PHLDB2*, *MAF*, and *SNAI2* have previously been identified as androgen-regulated genes (Xu et al. 2000; Tong & Tai 2000; Nelson et al. 2002; Chen et al. 2006; Ngan et al. 2009). *IGF1R* has also been identified as a protein that is up-regulated by androgens and estrogens in prostate cancer cells via a pathway that does not depend on AR or ER binding to DNA (nongenotropic) (Pandini et al. 2009). *SNAI2*, *MAF*, *PMEPA1*, and *FAM110B* are significantly decreased in expression by the AR antagonist bicalutamide, increasing confidence that expression of these genes is related to interaction of 11β-dimethoxy with the AR (Table 4.10). *FAM110B*, *ROR1*, and *CSGALNACT1* have not previously been identified as androgen-regulated genes and may represent new AR transcriptional targets. However, most studies aiming to identify androgen-regulated genes compare mRNA levels after androgen treatment to those present in cells grown in androgen-depleted media. In contrast, all treatments for microarray analysis discussed here were performed in normal media supplemented with 10% FBS. It is not entirely surprising that 11β-dimethoxy affected the expression of androgen-regulated genes to a greater extent than 11β in this analysis. It was

demonstrated in Chapter 2 that 11β-dimethoxy is a slightly more potent AR agonist. However, in the results discussed in Chapter 2, 11β also acted as an AR agonist, whereas the subset of apparently androgen-regulated genes discovered in this expression analysis (Table S4.7) demonstrates no response to 11β treatment. This also likely reflects the different assay conditions: media containing serum with testosterone (here) or charcoal/dextran treated serum lacking it (Chapter 2).

The other category of genes that is more responsive to 11β-dimethoxy than 11β treatment is related to cholesterol and lipid biosynthesis (Table 4.10). This group includes the genes *HMGCS1*, *SQLE*, *LDLR*, *FDFT1*, and *THRSP*. *HMGCS1* (3-hydroxyl-3-methylglutaryl coenzyme A synthase 1) encodes the protein that catalyzes condensation of acetoacetyl-CoA with acetyl-CoA to form HMG-CoA, initiating the cholesterol biosynthetic pathway. *SQLE* encodes squalene epoxidase, which acts at a later stage in cholesterol synthesis, catalyzing the first oxygenation step, and is considered to be one of the rate-limiting enzymes in the pathway. *LDLR* encodes a low-density lipoprotein receptor, a cell-surface receptor that binds low-density lipoprotein, which is the major carrier of cholesterol in blood plasma. *FDFT1* (farnesyl-diphosphate farnesyltransferase) is the first cholesterol-specific enzyme in the biosynthetic pathway, catalyzing dimerization of two farnesyl diphosphate molecules to form squalene. Finally, *THRSP* (thyroid-hormone responsive) does not have a specific known function, but is associated with enhanced lipogenesis in tumors (Moncur et al. 1998), and as its name suggests, is responsive to thyroid hormone. *LDLR* induction appeared to be unique to 11β-dimethoxy treatment (LFC = 1.66 for 11β-dimethoxy, 0.42 for 11β). There is also one probe set for *SQLE* which is uniquely affected by 11β-dimethoxy, but two other probe sets are induced by both compounds (to a greater extent with 11β-dimethoxy). The generalization that 11β-dimethoxy is more inducive to the processes of cholesterol biosynthesis and lipogenesis holds true for other genes of this type as well, including *HMGCR* (HMGCoA reductase), *INSIG1* (insulin-induced gene 1), *STARD4*, *SC4MOL*, *DHCR7*, *FASN* (Fatty Acid Synthase), *FADS1* (Fatty Acid Desaturase 1), and *IDI1*. It is known that androgens can increase lipogenic gene expression in AR positive cell lines (Heemers et al. 2001). This provides a simple explanation for the greater induction of lipogenesis-related genes by 11β-dimethoxy, since it behaves more as an androgen.

However, it is clear that interaction with the AR is not required for induction of cholesterol biosynthetic pathways, as *HMGCS1* was also shown to be significantly up-regulated by 11β in HeLa cells that lack AR expression (Bogdan Fedeles, unpublished results). Potentially, however, the interaction of 11β-dimethoxy with the AR enhances induction of cholesterol biosynthetic genes.

Chlorambucil has Minor Effects on Transcription

Treatment of LNCaP cells with 5μM chlorambucil, a DNA damaging mustard analogous to the DNA damaging portion of 11β (Figure 4.1), did not result in very strong repression or induction of gene expression. Chlorambucil is significantly less toxic toward LNCaP cells compared to 11β and is unable to induce apoptosis as 11β does (Marquis et al. 2005). Chlorambucil was unable to perturb expression of any genes beyond a 2-fold difference. However, relaxation of this filter to ~1.4-fold (absolute value of LFC $\geq$ 0.5) allows for identification of eight unique up-regulated genes and five unique down-regulated genes. Only one of the genes down-regulated by chlorambucil (*ESCO2*) is significantly down-regulated by 11β treatment greater than 2-fold (LFC = -1.1). However, this same gene is also significantly down-regulated by 11β-dimethoxy (LFC = -0.84), making it unlikely that the capacity of 11β to damage DNA is responsible for down-regulation of this gene. There are also a handful of genes which are up-regulated greater than LFC = 0.5 with chlorambucil and greater than LFC = 1 with 11β. *KLHL24* and *ELF3* are two of these for which the induction by 11β is significantly greater than that by 11β-dimethoxy, increasing likelihood that the DNA damage component is responsible for the greater induction of these genes. However, to our knowledge these genes have not previously been associated with a response to DNA damage.

Transcriptional Effects Identified by Microarray are Confirmed with RT-PCR

We used RT-PCR to verify that a subset of the genes identified from gene microarrays are affected by 11β or 11β-dimethoxy treatment. The genes *GDF15*, *DDIT3*, *ATF3*, *GADD45A*, *TRIB3*, and *HMGCS1* were chosen as a subset representing some of

the interesting classes of perturbed genes. Figure 4.5 demonstrates that each of these genes was significantly increased in expression by either 11β or 11β-dimethoxy. Furthermore, analysis accurately identified *HMGCS1* as more greatly up-regulated by 11β-dimethoxy than by 11β, while transcription of each of the remaining genes is amplified more greatly by 11β. The expression of *GDF15* and *DDIT3* was also monitored as a function of treatment duration. Their analysis showed a transient increase in expression, which lasted for ~6 hrs before leveling off or regressing (Figure 4.6).

Having identified the UPR as a pathway potentially activated by 11β, further testing was performed to confirm this finding. The UPR consists of three primary enzymes located in the membrane bilayer of endoplasmic reticulum: IRE1α, PERK, and ATF6. These enzymes respond to the stimulus of an unfolded protein burden in the endoplasmic reticulum in multiple ways. One hallmark of this pathway's activation is unconventional splicing of X-box binding protein 1 (*XBP1*) mRNA by IRE1α to remove a 26-base intron, which shifts the reading frame and results in expression of active transcription factor (Yoshida et al. 2001; Calfon et al. 2002). This spliced form (*XBP1s*) drives expression of various genes related to protection from the unfolded protein assault (Lee et al. 2003). Levels of both the unspliced form (*XBP1u*) and *XBP1s* were tested after treatment with 5 μM 11β. While *XBP1u* is not significantly affected by treatment, *XBP1s* is increased ~10-fold, indicating an activated IRE1 arm of the UPR (Figure 4.7).

Several genes were also analyzed for expression changes in HeLa cells to determine effects that are general for 11β treatment or that potentially depend on factors unique to LNCaP cells. *GDF15*, *DDIT3*, *TRIB3*, *CCNG2*, and *HMGCS1* were all demonstrated to be increased in expression to a similar extent as in LNCaP cells, while *CCNE2* was demonstrated as down-regulated, also consistent with its repression in LNCaP cells (Bogdan Fedeles, personal communication). Furthermore, splicing of *XBP1* was shown to occur, increasing *XBP1s* levels several fold (Bogdan Fedeles, personal communication).

The Connectivity Map Identifies Various Agents with Similar Effects as 11β on Global Transcriptional Profiles

The connectivity map (CMAP) was used to identify other compounds that induce a similar transcriptional profile as 11β. CMAP allows a researcher to compare an interesting set of genes (often from microarray experiments using small molecules) against a large library of microarray data produced by individually treating cultured human cells with many different pharmacologically active small molecules (Lamb et al. 2006; Lamb 2007). CMAP calculates similarity between the input list of genes and each of the profiles within its library, ultimately providing a list of compounds with similar activity. From this list, one can infer logical hypotheses about the activity of a tested compound, taking into account the known mechanisms of other compounds.

To determine similarity, CMAP analysis calculates "up" and "down" scores, which are absolute measures (Lamb et al. 2003) of overlap between the up- and down-regulated genes within a query list and those of the reference gene list (produced from individual treatments within the CMAP library). Essentially, the up values are largest in magnitude when the genes up-regulated in the query list are among the most up-regulated genes for any particular treatment from the reference library (and vice-versa). A perfect up score would mean that the submitted list was identical to the most up-regulated genes from one treatment. The up and down scores are combined to produce an overall "connectivity score" for each individual treatment. The connectivity scores are arbitrarily scaled from +1 for the most positively correlated treatment to -1 for the most negatively correlated treatment, and data is sorted accordingly. Connectivity scores are also sometimes averaged over multiple individual treatments (for one compound or class of compounds), further indicating that a certain correlation is generally applicable.

Query of the CMAP database with the set of genes perturbed by 5 μM 11β treatment produces quite interesting results. The best overall match for a single treatment is the antihelminthic agent pyrvinium, at a concentration of 3 μM in MCF7 breast cancer cells (Table 4.10A). Other compounds in this table include the antihistamine astemizole and another antihelminthic, niclosamide. Interestingly, niclosamide, which has been reported to decouple oxidative phosphorylation (Weinbach & Garbus 1969; MacDonald et al. 2006), exhibits the highest mean connectivity score for correlation with 11β when averaged over treatments, whether this average is independent of (mean score 0.801,

n = 5, p-val = 4e-5), or with respect to, cell line (MCF7, mean score = 0.933, n = 2, p-val < 2e-5).

In addition to antihelminthics and antihistamines, two quaternary ammonium detergents, benzethonium chloride and methylbenzethonium chloride, are identified in the top 20 compounds most correlated with 11β. Additional agents with high correlation to 11β include those with general effects on ion transport, for example monensin (#24 overall), ionomycin (#57 overall), and the calcium channel blockers bepridil and fendiline (represented in Table 4.11B by ATC category C08EA, best match is fendiline, #39).

Other agents of interest include the classic UPR inducer thapsigargin, which, while only the 68th best match of individual treatments, is the 15th best match when considering only up-regulated genes. Thus, 11β and thapsigargin induce a common set of genes related to UPR. Interestingly, compounds that are inhibitory toward the proteasome correlate well with 11β, including MG-132, MG-262, celastrol (Yang et al. 2006), and withaferin A (Yang et al. 2007) (mean score = 0.634, n = 9), perhaps due to their ability to induce the UPR by preventing protein degradation (Bush et al. 1997; Fribley et al. 2004; Obeng et al. 2006).

Another useful means of averaging connectivity scores is based on the Anatomical Therapeutic Chemical (ATC) classification of compounds, which only considers therapeutically relevant molecules. Averaging connectivity scores with respect to ATC classification shows that 11β correlates well with several agents that belong to the class of phenothiazines, including thioridazine, chlorpromazine, trifluoperazine, fluphenazine, and prochlorperazine (Table 4.11). Additionally, this comparison identifies phenylalkamine derivatives and non-selective monoamine reuptake inhibitors such as trimipramine.

Figure 4.8 provides a graphical view of the correlation between 11β and some of the phenothiazines. A bar view demonstrates that most of the treatments with agents from the ATC class N05AB (phenothiazines with piperazine structure, including trifluoperazine, prochlorperazine, fluphenazine, and thioproperazine) have strong correlation (green) with the transcriptional profile generated with 11β (Figure 4.8A). The antipsychotic agent trifluoperazine from this class has even better correlation with 11β

(Figure 4.8B). Chlorambucil, on the other hand, does not produce a transcriptional profile with significant correlation to 11β treatment, in line with the findings reported here (Figure 4.8C).

Discussion

Analyzing the effects of treating LNCaP cells with 11β, 11β-dimethoxy, and control compounds on global transcription has provided new avenues worthy of exploration. From this examination, it was discovered that 11β significantly increases expression of genes related to cholesterol biosynthesis, UPR, cell cycle arrest, and apoptosis, while decreasing expression of those related to protein synthesis, DNA damage repair, and cell cycle progression. Quite interestingly, 11β-dimethoxy, despite being significantly less toxic to LNCaP cells than 11β, modulates a very similar set of genes as 11β. Importantly, there are some genes affected by 11β expression that are unaffected with 11β-dimethoxy, such as the DNA-damage responsive *CDKN1A* and *BTG2* genes. However, the magnitude change for a majority of genes affected by 11β is simply larger than the change induced by 11β-dimethoxy. This observation suggests that covalency of interaction, a subtle difference of intracellular trafficking, or association with specific proteins may be involved in the relative differences in toxicity between the two compounds. In other words, 11β does not seem to affect transcription of a significant set of genes that are unaffected by 11β-dimethoxy, as one might expect if the activities of these compounds were strikingly different. Instead, the transcriptional profiles suggest that both compounds have very similar activities, while 11β is more effective at eliciting them. However, it is important not to overanalyze these data, which at this stage have only captured the effects of treatment at the transcriptional level. Potentially, many of the effects of 11β treatment occur at translational and post-translational stages and could provide better explanation as to the mechanistic differences between 11β and 11β-dimethoxy.

Cholesterol biosynthesis and lipogenesis are two pathways that are significantly up-regulated by both 11β and 11β-dimethoxy. Furthermore, these pathways are the ones most significantly up-regulated by the low dose of 1 μM 11β, making it likely that their

activation is more immediate or specific. These genes are regulated by the sterol regulatory element-binding protein (SREBP) family of transcription factors, which are located in the ER membrane and are responsible for adapting to changes in cholesterol availability (Horton et al. 2002). During conditions of low cholesterol, SREBPs associate with SREBP cleavage-activating protein (SCAP). SCAP then transports SREBP to the golgi apparatus, where it is cleaved by site 1 and site 2 proteases, producing an active transcription factor that drives synthesis of cholesterol and lipids (Goldstein et al. 2002; Horton et al. 2002). However, when cholesterol is present, it is directly sensed by SCAP, causing SCAP to bind to insulin-induced genes 1 and 2 (INSIG-1 and INSIG-2) (Yang et al. 2002; Yabe et al. 2002). These proteins thereby inhibit SCAP transport of SREBP to the golgi, and cholesterol biosynthesis is not activated. INSIG-1 is also up-regulated by active cleaved SREBP, providing a feedback mechanism of regulation. INSIGs have their own ability to directly bind oxysterols, cholesterol derivatives with additional hydroxyl or keto groups. Binding of oxysterols to INSIGs produces the same net effect as binding of sterols to SCAP—increased association of SCAP and INSIG, which retains SREBP in the ER membrane and disallows cholesterol biosynthetic gene expression (Radhakrishnan et al. 2007).

Beyond this canonical cholesterol homeostatic paradigm lie other agents of diverse structure that are also able to modulate cholesterol and lipid biosynthesis. In direct contrast to sterols and oxysterols, a class of cationic amphiphiles, including trifluoperazine and imipramine, increases expression of genes related to cholesterol and lipid biosynthesis (Lange & Steck 1994), generating transcriptional profiles identified through CMAP as similar to 11β. A prevailing model for the effect of cationic amphiphiles on cholesterol homeostasis is that they partition into lipid bilayers and "confuse" the machinery that normally senses sterols.

Yet other compounds that elicit transcriptional effects similar to 11β, including phenothiazines (Prozialeck & Weiss 1982), antihistamines, tricyclic antidepressants, and antimalarials (Weiss et al. 1980; Prozialeck & Weiss 1982) are capable of inhibiting calmodulin. This protein binds calcium and regulates various cellular processes, and its functional disruption can lead to toxicity. The ionophoric polyether antibiotic monensin,

identified by CMAP analysis as a modulator of the same pathways as 11β, can similarly dysregulate calcium localization and gradients and cause the same toxic effects.

One of the primary functions of the ER is sequestration of calcium. Agents such as thapsigargin, which interfere with the maintenance of this gradient, will lead to an integrated ER stress response—the UPR (Ghosh et al. 1991; Berridge 1993; Kaufman 1999). Calcium is involved in folding of a subset of proteins within the ER, presumably due to interaction with certain folding chaperones (Lodish & Kong 1990; Lodish et al. 1992; Corbett et al. 1999). Thus, interference with calcium homeostasis can lead directly to the effects consistent with UPR.

The UPR in mammalian cells consists of three main paths of activation from ER-resident proteins IRE1α, PERK (EIF2AK3), and ATF6. Each of these proteins has a translumenal domain extending into the ER where it can sense the protein folding environment. It is believed that BiP (HSPA5, GRP78) is a negative regulator of these pathways that functions by binding to the lumenal regions of these proteins and preventing their dimerization or activation. However, when unfolded proteins are present in excess, BiP is attracted to their unfolded regions, freeing IRE1, PERK, and ATF6 for activation. When IRE1 is freed from BiP, it dimerizes and activates a ribonuclease activity which will act on *XBP1* mRNA, cleaving it in a non-conventional manner into an active transcription factor coding sequence. This transcription factor then drives expression of various genes related to protein folding. PERK also dimerizes, after which it phosphorylates eukaryotic translation initiation factor 2 (eIF2) on the alpha subunit at Ser51, thereby limiting its ability to recognize AUG start codons and minimizing general protein translation. However, a subset of transcripts is preferentially translated when eIF2α is phosphorylated, possibly by cap-independent translational initiation. This class includes the protein ATF4, which is involved in the transcriptional up-regulation of *DDIT3* (CHOP) (Fawcett et al. 1999; Harding et al. 2000). Finally, ATF6 is translocated to the golgi apparatus as a result of unfolded protein excess in a manner reminiscent of the SREBP activation. In fact, ATF6 is processed in the golgi by the exact same site 1 and site 2 proteases, producing another activated transcription factor (Ye et al. 2000; Lee et al. 2002).

It has recently been appreciated that ER stress can lead directly to activation of SREBP2, manifesting in enhanced lipogenesis (Colgan et al. 2007). Enhanced lipogenesis during ER stress is logical, since the increased need for protein folding may require synthesis of new ER, composed of lipids and cholesterol. Finally, a connection between calcium, UPR, and cholesterol biosynthesis may provide an explanation for why ionophores like monensin can increase cholesterol biosynthesis (Lange & Steck 1994), as well as provide an additional explanation for how phenothiazines modulate this pathway.

UPR activation may be an important factor in the mechanism of 11β toxicity toward LNCaP and other cancer cells. It was demonstrated that *XBP1* splicing occurs in both LNCaP and HeLa cells upon 11β treatment, providing evidence that the IRE1 arm of the UPR is activated. Several other genes belonging to this class are up-regulated greater than 2-fold by treatment, including *HSPA5*, *EIF2AK3*, *DDIT3*, *DNAJB9*, *EDEM1*, and *HERPUD1*, among others (Table 4.2). Furthermore, *ATF6* is up-regulated 1.7-fold, and *ATF4* is up-regulated just under 2-fold (LFC = 0.99). The UPR functions much like p53 in the sensing of DNA damage—initially protecting a cell in this case by generally halting protein synthesis, assessing the situation, and recovering if possible. However, just as p53 will signal apoptotic processes in the face of unbearable genome damage, the UPR will activate apoptotic processes when the unfolded protein burden is too great. The UPR can effect apoptosis with or without mitochondrial involvement (Rao et al. 2002; Breckenridge et al. 2003). For example, CHOP is able to down-regulate BCL2 expression, increasing reactive oxygen species and cytochrome c release (McCullough et al. 2001). The de-activation of BCL2 could provide enhanced understanding for our ability to use alkylation therapy for prostate cancer treatment, a situation that is usually not amenable to this strategy (McDonnell et al. 1992; DiPaola & Aisner 1999).

Cancer cells often display increased expression of genes related to the UPR, likely as a result of the general dysregulation of many systems in these tumors and of limiting nutrients (Gazit et al. 1999; Fernandez et al. 2000; Song et al. 2001; Chen et al. 2002; Shuda et al. 2003). Furthermore, hypoxia, a common condition in solid tumor formation, can lead to up-regulation of the PERK arm of the UPR (Koumenis et al. 2002). With the UPR pathway already activated, it is possible that further assault in the form of ER stress will overwhelm this system and create cell death, while normal cells have an ability to

up-regulate protective mechanisms and overcome the insult. In support of targeting UPR as an anticancer therapy, it has been demonstrated in some cases that induction of UPR in cancer cells sensitizes them to treatment with DNA damaging agents or other chemotherapeutics (Chatterjee et al. 1997; Belfi et al. 1999; Wu et al. 2009). In this manner, selective toxicity may be achieved.

It is not entirely clear which aspects of 11β treatment are initiators and which are effectors of cholesterol biosynthesis and UPR. Perhaps the simplest explanation is that 11β acts like some cationic amphiphiles that modulate cholesterol biosynthesis by diffusing into lipid bilayers. 11β could be described as a cationic amphiphile, as it is a very lipophilic molecule and will bear a positive charge on the secondary amine within the linker at physiological pH (pKa ~ 9-10). Furthermore, the chlorine groups will have partial negative charges associated with them, increasing the amphiphilicity of the overall compound. This may create a type of membrane damage that displays its effects through disruption of cholesterol homeostasis, leakage of calcium gradients, and down-stream activation of UPR. Of course it is also possible that like the phenothiazines, 11β first specifically inhibits calmodulin, disrupting calcium levels and leading to the other processes.

While 11β was originally designed to create selective toxicity toward cells expressing the androgen receptor, increasing evidence argues against the direct involvement of AR in the mechanisms related to toxicity (Chapter 3). Paradoxically, 11β is effective at preventing growth of both LNCaP and HeLa xenograft tumors, while displaying relatively little toxicity to the mice in which they grow. Therefore, it is important to address other potential mechanisms that may influence and explain selective toxicity. Here we have identified the UPR as a pathway that is activated by 11β, and this may provide the sought-after explanation as to why cancer cells have heightened 11β sensitivity. 11β-Dimethoxy treatment also causes increased expression of UPR-related genes, but in almost all cases, the magnitude is greater with 11β. Therefore, it is possible that 11β generally acts upon the same cellular targets as 11β-dimethoxy, but has a greater activity due to unknown reasons. The ability of 11β to damage DNA or to form other covalent attachments with macromolecules probably aids in its toxicity. Further

experiments are necessary to address the intricate details that explain the different activities of 11β and 11β-dimethoxy.

It is not entirely clear what the initial activator of the UPR is, but a few potential explanations have been offered, including membrane damage, calmodulin inhibition, calcium dysregulation, or general disruption of cholesterol homeostasis. Cholesterol biosynthetic dysregulation may be the most specific of these mechanisms, since it is the most significantly affected process at 1 μM 11β. However, the heightened ability of 11β-dimethoxy to modulate this pathway argues that there is another factor necessary for creating maximum toxicity.

We could also add another pathway to this list of potential effectors of 11β toxicity: the increase of intracellular reactive oxygen species. It was demonstrated that in HeLa cells, 11β, at concentrations as low as 2.5 μM, is able to elicit a rapid increase (within 2-3 hrs) in ROS levels (Bogdan Fedeles, personal communication). ROS levels have not as yet been monitored in LNCaP cells, but if the subset of gene transcription analyzed by RT-PCR is any indication, the mechanisms responsible for toxicity in these cells could be quite similar. Furthermore, it was shown that intracellular calcium levels increase quite significantly within 30 minutes following addition of 8 μM 11β to HeLa cells (Bogdan Fedeles, personal communication). Lower concentrations more comparable to the experiments reported here have not been tested as yet. The oxidative stress represented by increased ROS could also be the initial event that leads to UPR and other aforementioned processes. The CMAP finding that niclosamide produces a similar transcriptional profile as 11β provides a potential mechanistic explanation for the induction of ROS by 11β, since niclosamide is an agent known to decouple oxidative phosphorylation. Lipophilic cations have a tendency to accumulate in mitochondria and can act as protonophores, releasing the H^+ gradient, without concurrent generation of ATP. This could result in accelerated electron transport, causing an increased release of ROS, in addition to loss of energy as heat. In line with this possibility, the second best correlated compound identified from CMAP, chlorpromazine, also has reported oxidative phosphorylation decoupling ability (Berger et al. 1956).

Clearly, further experiments are necessary to elucidate the order of events that occur upon exposure of cells to 11β. Some of these include a more thorough comparison

of dose-response relationships of both 11β and 11β-dimethoxy, in order to determine whether concentrations of 11β-dimethoxy exist that yield equivalent responses as lower concentrations of 11β. Alternatively, certain genes such as *CDKN1A* and *BTG2* may not respond to any concentration of 11β-dimethoxy, or the magnitude change of genes such as *DDIT3*, *GDF15*, and *ATF3* may never be as great from any concentration of 11β-dimethoxy. In those instances, it would be valuable to attempt modulation of such genes through gain or loss of function experiments to determine if susceptibility of a cell to treatment with 11β or 11β-dimethoxy could be equalized.

Activation of the UPR provides a reasonable explanation for enhanced sensitivity of cancer cells to 11β. A crucial experiment will involve detection of UPR activation in xenograft tumors at therapeutically relevant concentrations of 11β. In cells, there are several experiments that can be conducted to identify some of the initial effectors that are likely to lead to UPR induction and apoptosis. Some of these are already underway; for example, it has been found that addition of radical scavengers such as N-acetylcysteine and vitamin E to HeLa cells that are treated with 11β decreases cell death (Bogdan Fedeles, personal communication). Along these lines, it should be determined whether the reduction in toxicity achieved with N-acetylcyesteine also correlates with decreased activation of UPR. Other experiments will address whether interference with 11β-induced calcium redistribution by small-molecules (i.e. BAPTA, A23187) can modulate toxicity. The genes identified through this transcriptional analysis can be used as biomarkers of specific pathways in all cases.

Please refer to supplemental Tables S4.1-S4.16 for top 50 (or fewer in some cases, absolute value of LFC must be $\geq$ 0.5 for inclusion) lists of genes significantly differentially expressed in each pair-wise comparison, and also Figures S4.1-S4.8 for volcano plots of these comparisons. Finally, Figure S4.9 includes structures of compounds identified from CMAP analysis as inducing similar transcriptional profiles as 5 μM 11β for reference.

Compounds Tested

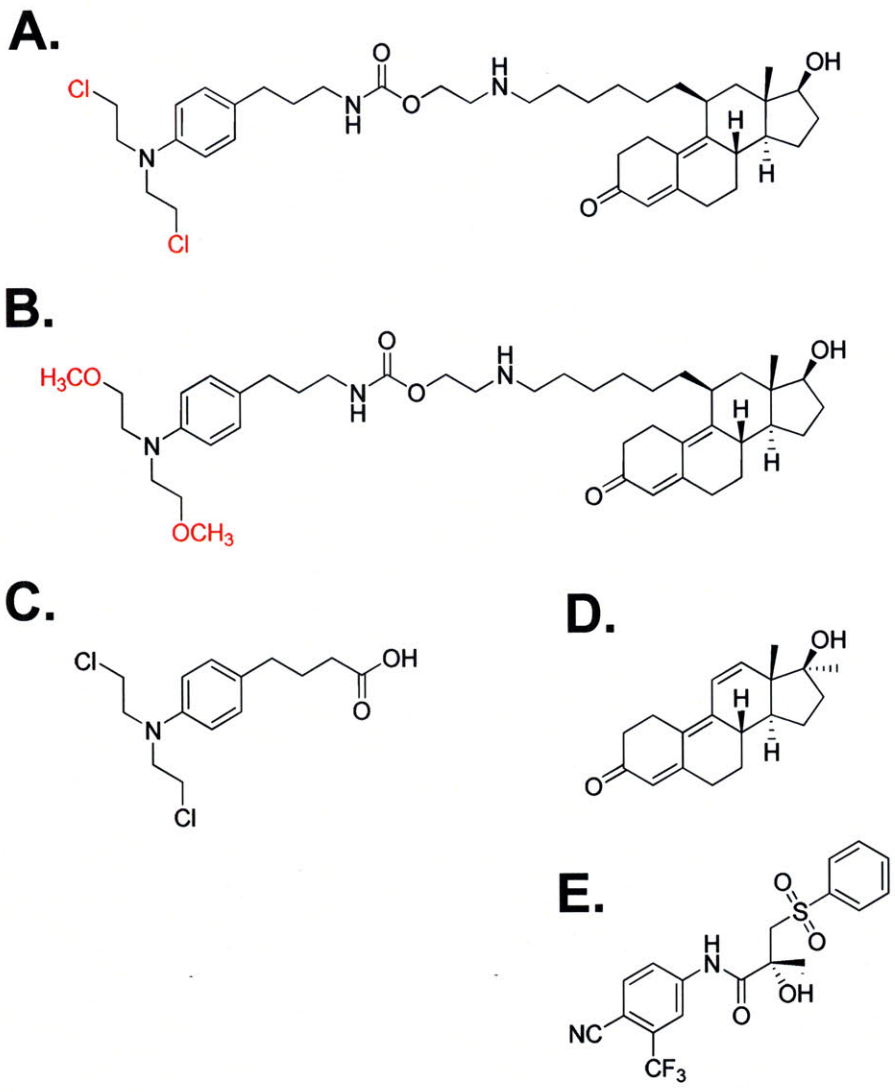

Fig 4.1 Structures of compounds tested for transcriptional response in LNCaP cells. **A.** 11β **B.** 11β-Dimethoxy **C.** Chlorambucil **D.** R1881 (AR Agonist) **E.** Bicalutamide (AR Antagonist)

Table 4.1. Treatments and pair-wise comparisons for gene microarray analysis.

Treatment	Duration	Sample Name	Pair-wise comparison with reference to:
None; harvested at treatment time	0 hrs	Unt 0 hrs	N/A
Fresh media	6 hrs	Unt 6 hrs	Unt 0 hrs
DMSO	6 hrs	DMSO	Unt 6 hrs
11β 1 μM	6 hrs	11β 1 μM	DMSO
11β 5 μM	6 hrs	11β 5 μM	DMSO
11β-Dimethoxy 5 μM	6 hrs	11β-dimethoxy	DMSO
Chlorambucil 5 μM	6 hrs	Cbl	DMSO
R1881 1 nM	6 hrs	R1881	DMSO
Bicalutamide 1 μM	6 hrs	Bicalutamide	DMSO

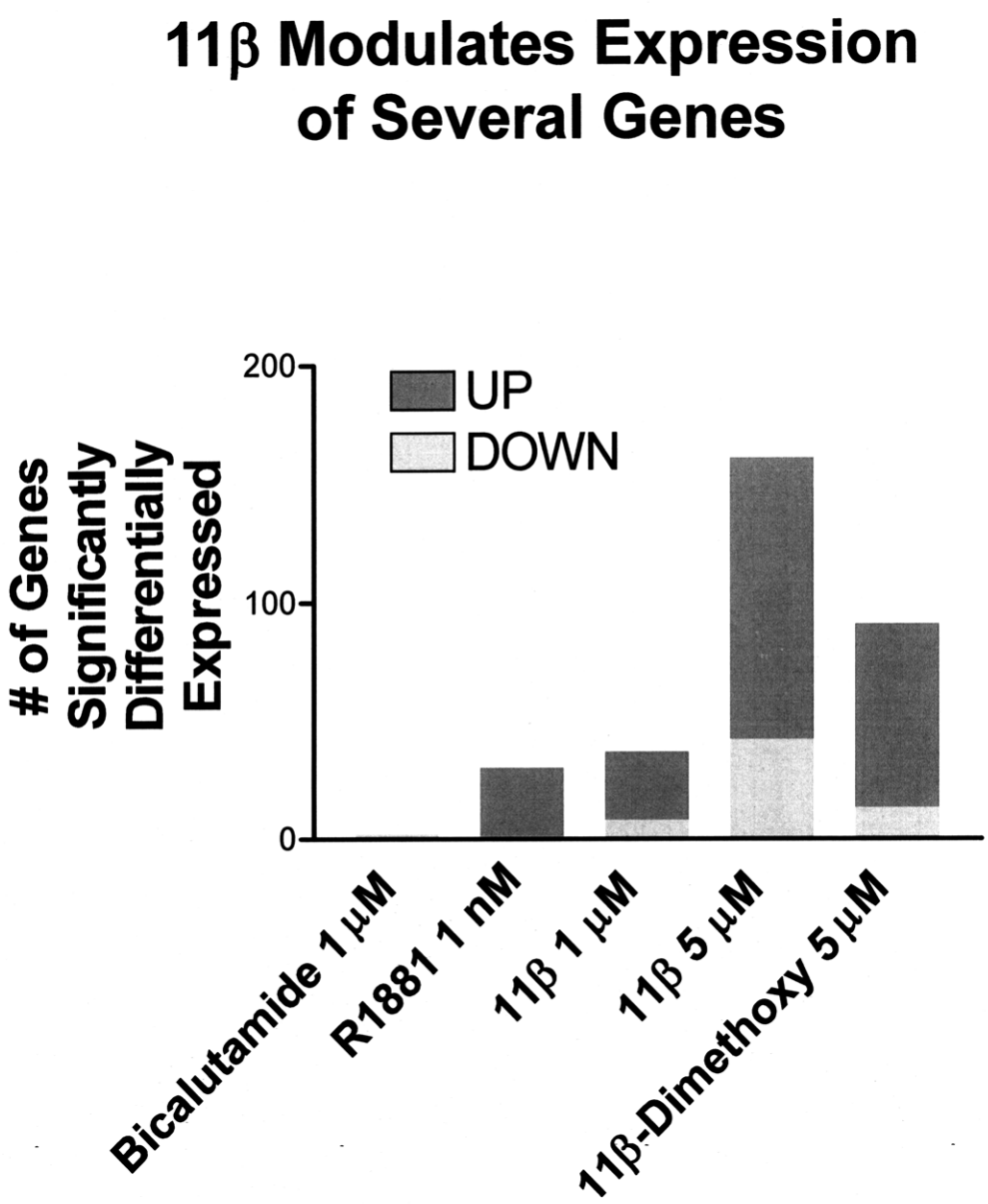

Figure 4.2 Numbers of unique genes significantly differentially expressed by various treatments. Growth in fresh media for 6 hrs as compared to cells at treatment time, DMSO compared to 6 hrs untreated sample, and 5 μM chlorambucil did not significantly affect expression of any genes (p-value < 0.05, 2-fold change, present in at least one treatment group)

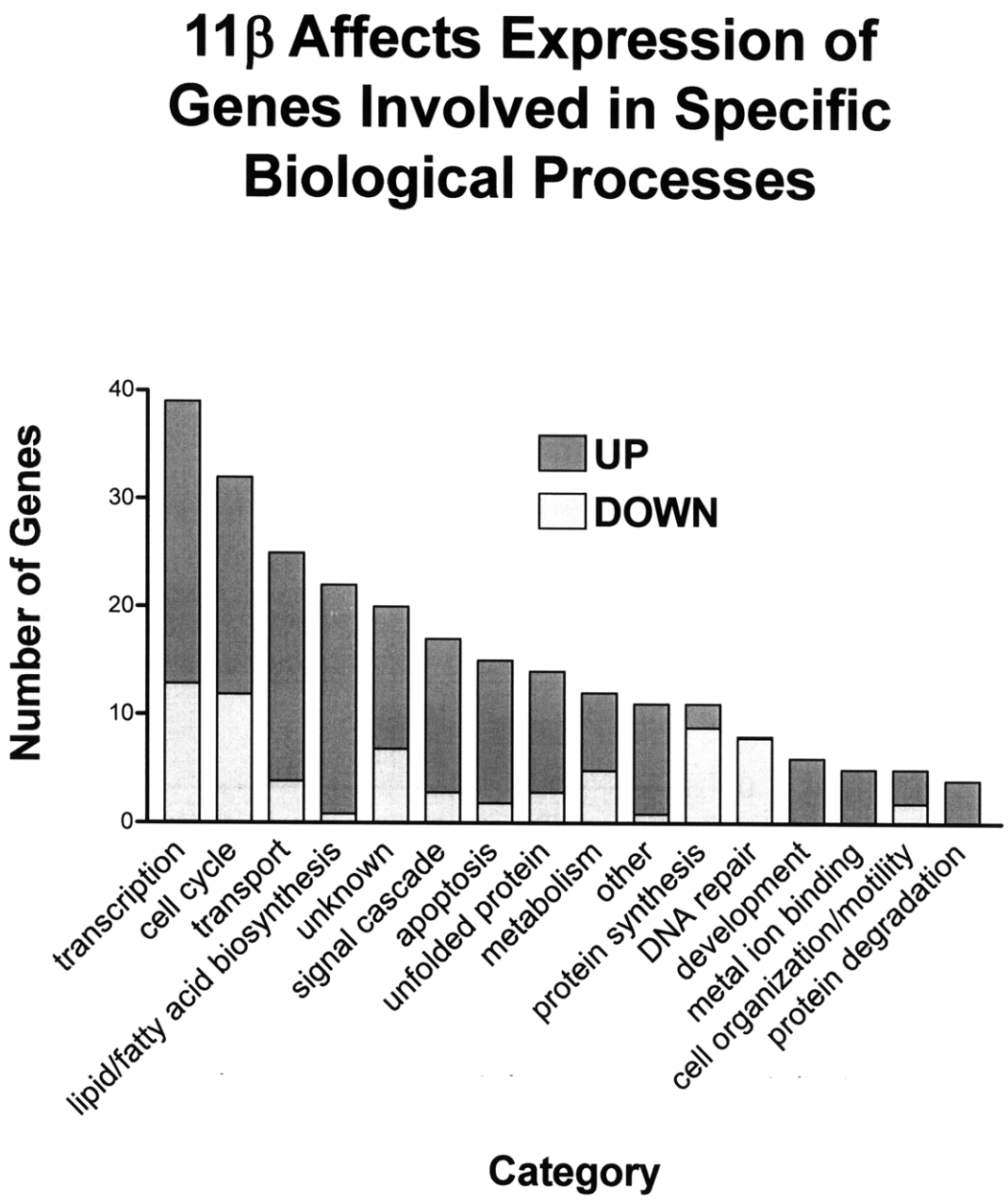

Figure 4.3 Numbers of genes in functional categories affected by treatment with 5 μM 11β.

Table 4.2 Genes significantly up-regulated by treatment with 5 μM 11β. Genes are categorized with respect to biological process.

Category	Gene Symbols
Apoptosis	ATXN1, DDIT4, DRAM ,GADD45A, GDF15, JMY, NUPR1, RRAGC, SQSTM1, TNFSF15, TP53INP1, TRIB3, WIPI1
Cell Cycle	BTG2, CCNG2, DCTN2, FICD, FLCN, FNIP1, GPNMB, JUB, LIFR, PTCH1, RB1CC1, SIRT2, TNFSF4, TSPYL2, VEGFA, NA (226725_a), CDKN1A, HBP1, SESN2
Cell Organization/Motility	GABARAPL1, PKD1, TUBE1
Development	AHNAK, FBN1, HECA, IFRD1, PTPRR, RNF103
Lipid/Fatty Acid Biosynthesis	ACSL1, ACSS2, ALDH1A3, ANKRA2, CHKA, CHPT1, FADS1, FASN, FDFT1, HMGCR, HMGCS1, HSD17B7, INSIG1, LPIN1, LSS, PNLIPRP3, SC4MOL, SQLE, STARD4, THRSP, VLDLR
Metabolism	DIO1, ENPP5, FUT1, GDPD1, GFPT1, NEU1, RDH10
Metal Ion Binding	CHAC1, MT1F, SLC30A1, SLC3A2, STC2
Other	CD55, DSE, GOLGA2, INHBE, KDSR, KIAA0247, LGALS8, LYSMD3, N4BP2L2, TRIM2
Protein Degradation	PRSS8, SYVN1, TAGLN, USP54
Protein Synthesis	MARS, MTHFR
Signal Cascade	AKAP5, BLNK, C20orf74, CBLB, DUSP16, EFNA1, FZD7, FZD8, GUCY1A3, NEK8, PIK3C2A, RPS6KA2, SAV1, TBC1D8B
Transcription	ANG, RNASE4, ATF3, BHLHB2, CEBPB, CEBPG, CHD2, CREB3L2, ELF3, JMJD1A, JMJD1C, JUND, KLF4, LARP6, MEF2A, MLXIP, NFAT5, NR1D2, OVOL1, RBM35A, RFX6, SFRS1, TSC22D1, TSC22D3, TULP3, ZNF165
Transport	ATP8B2, CDRT4, COG3, LYST, MCFD2, RAB39B, SEC24D, SLC17A5, SLC1A4, SLC25A36, SLC33A1, SLC7A1, SLC7A11, SNX9, SPIRE1, STX3, STX5, TMCO3, TMED10, TMED5, CNNM2
Unfolded Protein	DDIT3, DNAJB9, EDEM1, EDEM3, EIF2AK3, FAM129A, FKBP11, FKBP14, HERPUD1, HSPA13, HSPA5
Unknown	ARMCX3, BTN3A3, C4orf34, C5orf41, TTC39B, CTAGE5, KLHL24, LOC729873, PPAPDC2, TMEM170, TMEM39A, TMEM56, TOR1AIP2, TTC39B

Table 4.3 Genes significantly down-regulated by treatment with 5 μM 11β. Genes are categorized according to biological process.

Category	Gene Symbols
Apoptosis	CARD10, NEK6
Cell Cycle	AGGF1, CCNA2, CCNE1, CCNE2, CCNF, CDC25A, CDCA2, FBXO5, PLK1, SKP2, SUV39H2, E2F8
Cell Organization/Motility	MYLIP, TUBA4A
DNA Repair	ESCO2, EXO1, MCM10, MCM4, MSH6, NEIL3, RIF1, RRM2
Lipid/Fatty Acid Biosynthesis	DGAT2
Metabolism	ALDH1B1, DHODH, NFS1, PFKFBP3, PPCDC
Other	MAT2A
Protein Synthesis	EXOSC2, EXOSC3, EXOSC4, EXOSC6, GEMIN5, MRPS12, NOL5A, POP1, PUS1
Signal Cascade	DDIT4L, EFNB2, PRAGMIN
Transcription	CDCA7, CHD9, ID1, MAFB, MYB, NARG1, PINX1, PITX1, PSPC1, SFRS7, SP110, ZBTB24, ZNF239
Transport	SLC16A14, SLC16A6, SLC29A1, TIMM8A
Unfolded Protein	DNAJB1, HSPA1A, PPIF
Unknown	CMTM7, DCTN5, DSEL, KLHL29, LRFN1, TMEM177, TRIM59

Table 4.4 Gene ontological class enrichment of genes significantly up-regulated by 5 μM 11β treatment.

BIOLOGICAL PROCESS	**GENE SYMBOLS**	**P-VALUE**
cell fate determination	IFRD1, KLF4	9.59E-03
cell cycle arrest	CDKN1A, HBP1, GADD45A, SESN2, DDIT3	1.33E-03
sterol biosynthesis	SQLE, SC4MOL, HMGCR, HMGCS1	4.49E-04
amino acid transport	SLC1A4, SLC7A11, SLC3A2, SLC7A1	1.16E-03
germ cell migration	HMGCR, PPAP2B	4.70E-04
MOLECULAR FUNCTION	**GENE SYMBOLS**	**P-VALUE**
low-density lipoprotein binding	ANKRA2, VLDLR	5.02E-03
protein kinase binding	SQSTM1, TRIB3, FASN, PTPRR	5.38E-03
protein dimerization activity	RRAGC, CEBPG, VEGFA, CREB3L2, ATF3, JUND, CEBPB, DDIT3, MAFF	6.74E-04
transcription factor activity	OVOL1, MEF2A, CEBPG, NR1D2, ELF3, CREB3L2, BTG2, NFAT5, NR1D2, BHLHB2, TSC22D1, ATF3, KLF4, CEBPB, TSC22D3, DDIT3, AFF4, MAFF, ZNF165	1.70E-03
mannosyl-oligosaccharide 1\2-alpha-mannosidase activity	EDEM1, EDEM3	3.93E-03
non-G-protein coupled 7TM receptor activity	FZD7, FZD8	7.55E-03
Wnt receptor activity	FZD7, FZD8	2.97E-03
amino acid permease activity	SLC7A11, SLC7A1	2.97E-03
CELLULAR COMPONENT	**GENE SYMBOLS**	**P-VALUE**
endoplasmic reticulum membrane	HMGCR, SLC33A1, HERPUD1, HSPA5, EDEM1	5.12E-03

Table 4.5 Ontological class enrichment of genes significantly down-regulated by 5 μM 11β treatment.

BIOLOGICAL PROCESS	GENE SYMBOLS	P-VALUE
regulation of cyclin-dependent protein kinase activity	CCNE2, CDC25A, CCNA2	9.52E-04
G1/S transition of mitotic cell cycle	SKP2, CCNE1	4.89E-03
mitosis	NEK6, CCNF, PLK1, CDC25A, CCNA2	8.53E-04
rRNA processing	EXOSC2, EXOSC4, GEMIN4, NOL5A	5.48E-04
nuclear mRNA splicing via spliceosome	GEMIN4, MYB, SFRS7, GEMIN5	3.96E-03
mismatch repair	EXO1, MSH6	4.42E-03
base-excision repair	EXO1, MSH6, NEIL3	2.00E-04
MOLECULAR FUNCTION	**GENE SYMBOLS**	**P-VALUE**
3'-5'-exoribonuclease activity	EXOSC2, EXOSC4	1.81E-03
DNA N-glycosylase activity	NEIL3, MSH6	2.13E-03
endodeoxyribonuclease activity	EXO1, NEIL3	2.85E-03
CELLULAR COMPONENT	**GENE SYMBOLS**	**P-VALUE**
exosome (RNAse complex)	EXOSC2, EXOSC4	1.10E-03
chromosome, telomeric region	RIF1, PINX1	3.64E-03
nucleolus	POP1, GEMIN4, EXOSC4, ZNF239, NOL5A	1.29E-04
spliceosome complex	GEMIN4, MYB, GEMIN5	3.73E-03

Table 4.6 Ontological class enrichment of genes significantly up-regulated (A) or down-regulated (B) by 1 μM 11β treatment.

A.

BIOLOGICAL PROCESS	GENE SYMBOLS	P-VALUE
cholesterol biosynthesis	IDI1, FDFT1, HMGCS1, DHCR7	1.52E-06
MOLECULAR FUNCTION	**GENE SYMBOLS**	**P-VALUE**
magnesium ion binding	NEK8, FDFT1, IDI1, ATP8B2, MAP3K2, ACSL1	3.64E-04
ligase activity\forming carbon-sulfur bonds	ACSL1, ACSL2	9.49E-04
oxidoreductase activity\acting on the CH-CH group of donors\ NAD or NADP as acceptor	FASN, DHCR7	8.15E-04
CELLULAR COMPONENT	**GENE SYMBOLS**	**P-VALUE**
perinuclear region	MAP1S, HSPA5	3.06E-03
peroxisome	IDI1, ACSL1, PEX10	1.30E-03

B.

BIOLOGICAL PROCESS	GENE SYMBOLS	P-VALUE
protein amino acid acetylation	PCAF, NARG1L	8.74E-04
protein transport	RIMS1, KIF18A, LRSAM1, RAB23, NUP43	9.74E-03
MOLECULAR FUNCTION	**GENE SYMBOLS**	**P-VALUE**
acetyltransferase activity	PCAF, NARG1L	4.15E-03

11β and 11β-Dimethoxy Affect Expression of Many of the Same Genes

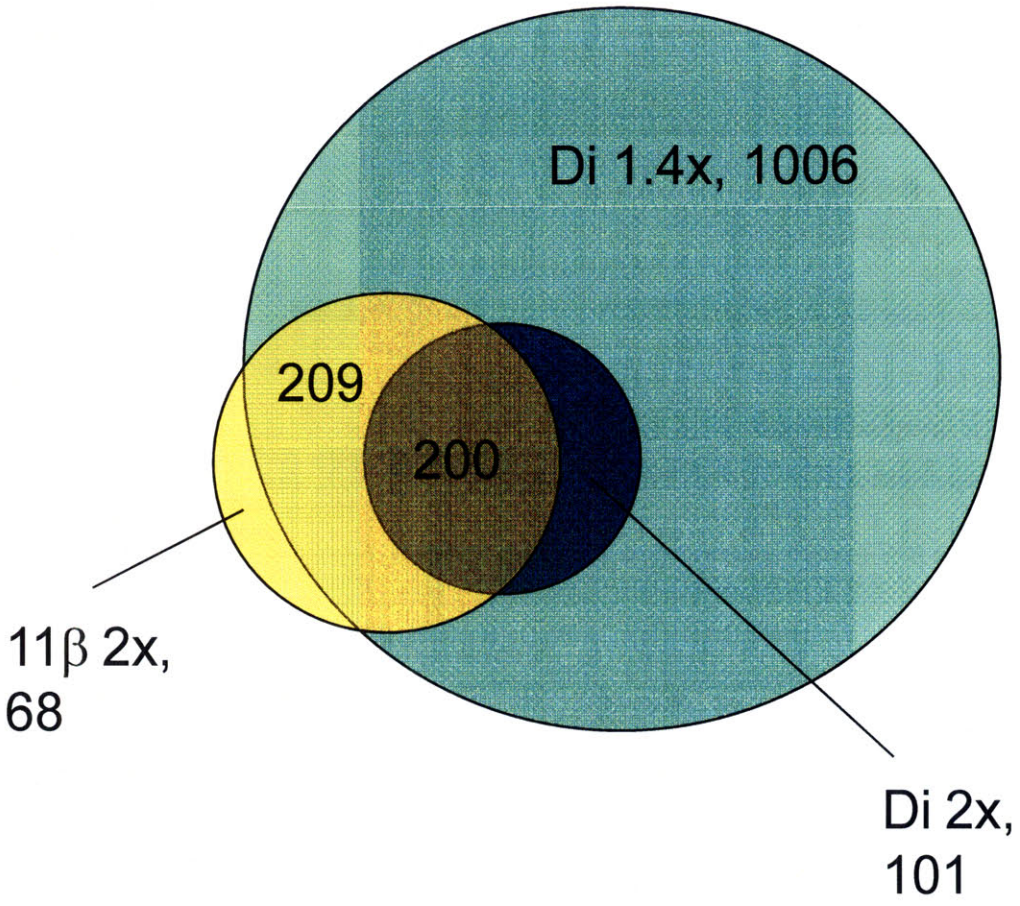

Figure 4.4 Venn diagram showing common genes between 11β and 11β-dimethoxy treatment. Yellow circle represents all probe sets significantly differentially expressed by 5 μM 11β treatment ≥ 2-fold (477). Blue circle represents all probe sets significantly differentially expressed by 11β-dimethoxy (Di) treatment ≥ 2-fold (301). 200 of these probe sets are common to both 11β and 11β-dimethoxy. The green circle represents all probe sets differentially expressed greater than 1.4-fold by 11β-dimethoxy in order to emphasize the minor subset of probe sets which are most unique to 11β treatment (68). Drawing is to scale.

Table 4.7 Gene ontological class enrichment of genes significantly up-regulated by 5 μM 11β-dimethoxy treatment

BIOLOGICAL PROCESS	GENE SYMBOLS	P-VALUE
parturition	HPGD, MAFF	2.31E-03
allene biosynthesis	IDI1, HPGD	7.23E-03
fatty acid biosynthesis	SCD, FASN, HPGD	8.83E-03
isoprenoid biosynthesis	IDI1, FDFT1	6.23E-03
cholesterol biosynthesis	HMGCS1, DHCR7, IDI1, FDFT1, HMGCR	1.83E-06
germ cell migration	PPAP2B, HMGCR	2.55E-04
lipid transport	LDLR, VLDLR, CHKA, STARD4	2.43E-03
response to unfolded protein	EIF2AK3, HERPUD1, EDEM1	5.18E-03
MOLECULAR FUNCTION	**GENE SYMBOLS**	**P-VALUE**
protein kinase binding	PTPRR, TRIB3, FASN, AKAP5	1.47E-03
protein dimerization activity	ATF3, VEGFA, MAF, CREB3L2, FOSL2, HPGD, DDIT3, MAFF	2.68E-04
low-density lipoprotein receptor activity	LDLR, VLDLR	1.05E-03
non-G-protein coupled 7TM receptor activity	FZD7, FZD8	3.75E-03
Wnt receptor activity	FZD7, FZD8	1.46E-03
transmembrane receptor protein tyrosine phosphatase activity	PTPRR, PTPRK	8.98E-03
mannosyl-oligosaccharide 1\2-alpha-mannosidase activity	EDEM1, EDEM3	1.94E-03
oxidoreductase activity\ acting on the CH-CH group of donors\ NAD or NADP as acceptor	DHCR7, FASN	5.26E-03
ligase activity\ forming carbon-sulfur bonds	ACSL1, ACSS2	6.11E-03
lipid transporter activity	LDLR, ATP8B2, VLDLR, STARD4	2.00E-03
neutral amino acid transporter activity	SLC7A11, SLC1A4	5.26E-03
CELLULAR COMPONENT	**GENE SYMBOLS**	**P-VALUE**
peroxisome	IDI1, PEX10, ACSL1, HMGCR	3.95E-03
integral to endoplasmic reticulum membrane	RRBP1, EDEM1, HSPA5	3.28E-03

Table 4.8 Gene ontological class enrichment of genes significantly down-regulated by 5 μM 11β-dimethoxy treatment.

BIOLOGICAL PROCESS	GENE SYMBOLS	P-VALUE
steroid hormone receptor signaling pathway	CCNE1, RBM14	2.57E-03
regulation of progression through cell cycle	RBL1, CCNE1, PIK3CB, CCNE2	6.38E-03
nucleobase\nucleoside\nucleotide and nucleic acid transport	NUP160, SLC29A1	5.08E-03
regulation of kinase activity	RBL1, PIK3CB, CCNE2	2.42E-03
MOLECULAR FUNCTION	**GENE SYMBOLS**	**P-VALUE**
DNA-dependent ATPase activity	MCM4, DHX9	1.89E-03

Table 4.9 Ontological class enrichment of genes more greatly altered in expression by 5 μM 11β treatment than 11β-dimethoxy treatment (ΔLFC ≥ 0.8).

BIOLOGICAL PROCESS	GENE SYMBOLS	P-VALUE
cell fate determination	IFRD1, KLF4	5.76E-04
transcription from RNA polymerase II promoter	MEF2A, ID1 (down), SQSTM1, MDM2, DDIT3	9.26E-03
cell cycle arrest	CDKN1A, GADD45A, DDIT3, SESN2	4.11E-05
regulation of cyclin-dependent protein kinase activity	CDKN1A, GADD45A	5.54E-03
response to DNA damage stimulus	BTG2, DDB2, GADD45A, DDIT3	4.65E-03
MOLECULAR FUNCTION	**GENE SYMBOLS**	**P-VALUE**
transcriptional repressor activity	ID1 (down), ATF3, KLF4, DDIT3	1.29E-03
CELLULAR COMPONENT	**GENE SYMBOLS**	**P-VALUE**
basement membrane	FBN1, LAMA1 (down)	9.58E-03

Table 4.10 Genes which are more greatly altered in expression by 11β-dimethoxy (Di) treatment than 5 μM 11β treatment (ΔLFC ≥ 0.8). For these genes, LFC for R1881 and Bicalutamide (Bic) are shown for comparison. Gray cells indicate p-value > 0.05; *p-value is < 0.05 for another probe set for this gene.

Probe ID	Gene Symbol	Gene Name	11β	Di	R1881	Bic
236207_at	SSFA2	sperm specific antigen 2	-0.37	-1.36	-0.54	-0.12
204567_s_at	ABCG1	ATP-binding cassette, sub-family G (WHITE), member 1	0.41	-0.91	-0.81	0.47
204781_s_at	FAS	Fas (TNF receptor superfamily, member 6)	0.62	-0.73	-0.27	0.13
217373_x_at	MDM2	Mdm2 p53 binding protein homolog (mouse)	0.37	-0.51	-0.35	-0.22
224856_at	FKBP5	FK506 binding protein 5	-0.38	0.79	1.69	-0.49
228790_at	FAM110B	family with sequence similarity 110, member B	-0.27	0.90	0.95	-0.86
225330_at	IGF1R	insulin-like growth factor 1 receptor	0.08	0.91	1.30	-0.34
213158_at	NA	NA	0.05	0.97	0.29	0.00
205805_s_at	ROR1	receptor tyrosine kinase-like orphan receptor 1	-0.17	1.04	1.08	0.24
219049_at	CSGALNACT1	chondroitin sulfate N-acetylgalactosaminyltransferase 1	0.22	1.06	2.13	0.00
211548_s_at	HPGD	hydroxyprostaglandin dehydrogenase 15-(NAD)	0.15	1.07	1.37	-0.22
225688_s_at	PHLDB2	pleckstrin homology-like domain, family B, member 2	-0.07	1.16	1.97	-0.36
206363_at	MAF	v-maf musculoaponeurotic fibrosarcoma oncogene homolog (avian)	0.20	1.31	2.38	-0.52
213139_at	SNAI2	snail homolog 2 (Drosophila)	-0.11	1.34	2.64	-1.57
1557352_at	SQLE	squalene epoxidase	0.24	1.48	0.14	0.20
222450_at	PMEPA1	prostate transmembrane protein, androgen induced 1	0.58	1.51	0.64*	-0.57
202068_s_at	LDLR	low density lipoprotein receptor	0.42	1.66	0.09	-0.01
230256_at	C1orf104	chromosome 1 open reading frame 104	0.89	1.89	0.31	0.04
238666_at	NA	NA	0.97	2.02	0.47	-0.03
241954_at	FDFT1	farnesyl-diphosphate farnesyltransferase 1	1.08	2.20	0.35	0.17
205822_s_at	HMGCS1	3-hydroxy-3-methylglutaryl-Coenzyme A synthase 1 (soluble)	1.89	2.81	0.18	-0.10
229476_s_at	THRSP	thyroid hormone responsive (SPOT14 homolog, rat)	1.48	2.98	0.00	0.01

Microarray Findings are Verified by RT-PCR of a Subset of Genes

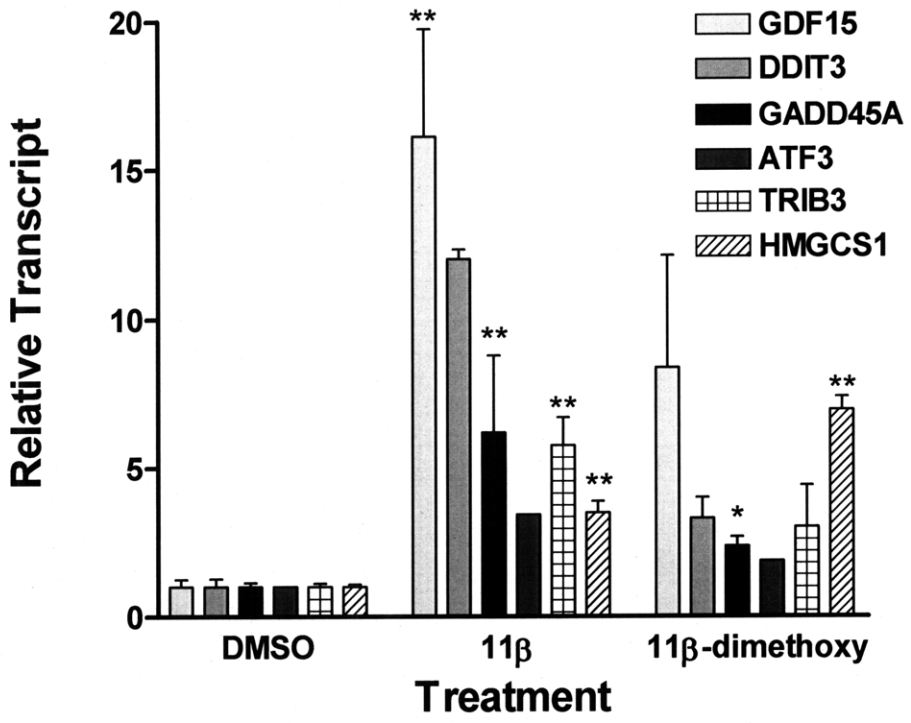

Figure 4.5 RT-PCR analysis of interesting genes identified with microarrays as up-regulated by 5μM 11β and 11β-dimethoxy treatment. LNCaP cells were treated for 6 hrs. *p-val < 0.1, **p-val < 0.05

The Two Genes Most Up-Regulated by 11β Treatment are Maximized in Expression after 6 hrs

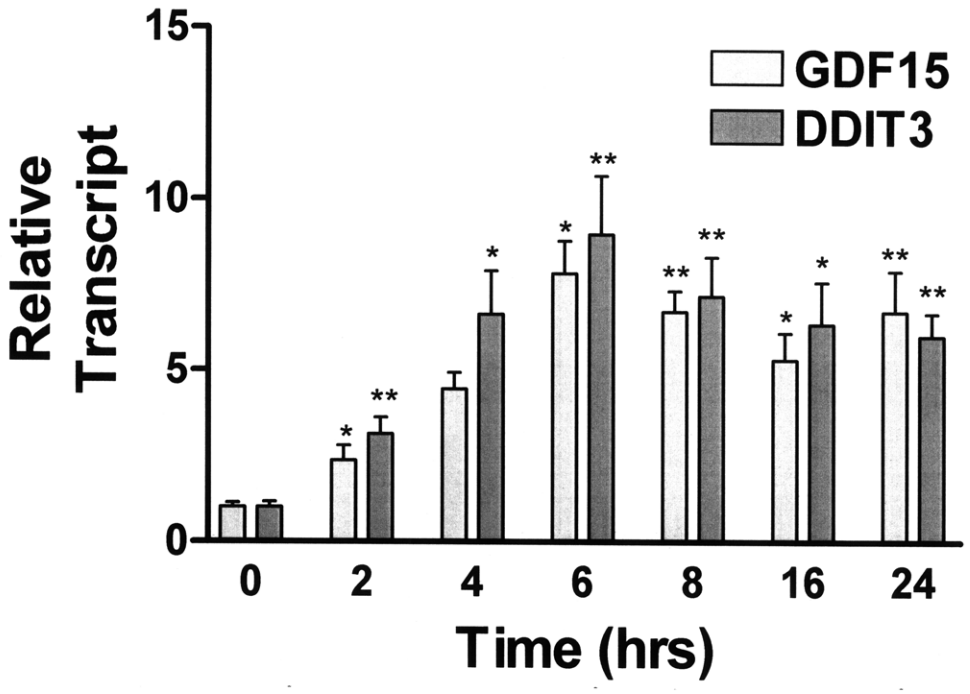

Figure 4.6 RT-PCR analysis of *GDF15* and *DDIT3*. These two genes, which were determined to have the greatest response to 5 μM 11β treatment, were monitored for expression over a 24 hr period in LNCaP cells. Each increases to a similar extent but is maximized after 6 hrs. *p-val < 0.1, **p-val < 0.05

11β Induces Cleavage of XBP1 into an Active Transcription Factor, Consistent with Activation of Unfolded Protein Response

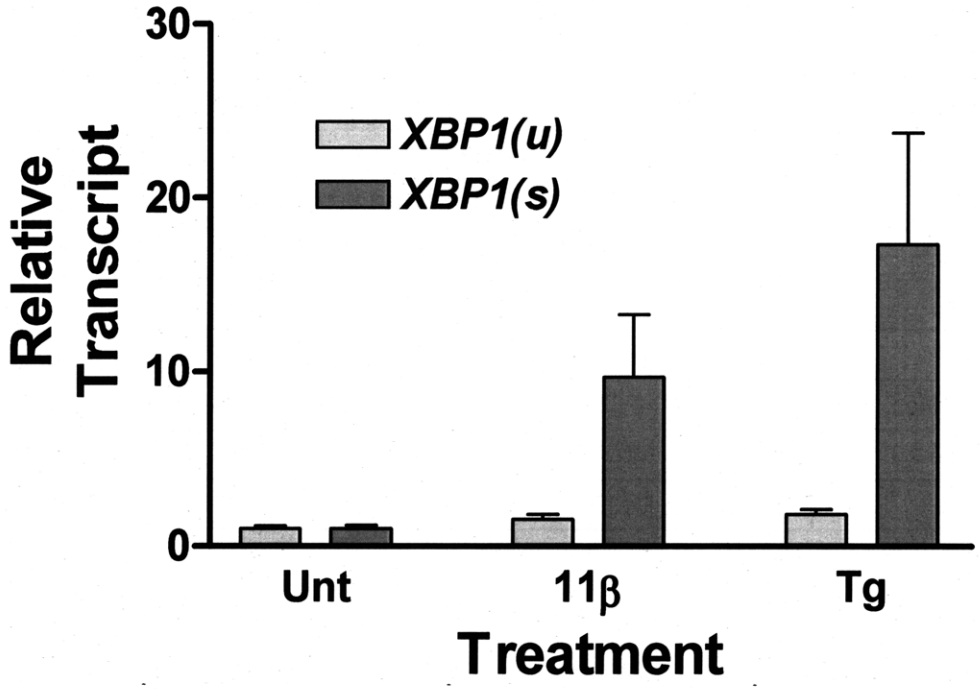

Figure 4.7 RT-PCR analysis of *XBP1* cleavage in LNCaP cells treated with 5μM 11β. *XBP1(u)* is the unspliced form while *XBP1(s)* is the spliced, active transcription factor. Thapsigargin (Tg), 200 nM, is included as a positive control. Cells were treated for 6 hrs with 11β, 5 hrs with Tg.

Table 4.11 Top Matches from Connectivity Map for 5 μM 11β. A. Top 10 matches for correlation with 5μM 11β treatment. Score is arbitrarily set as 1 for best match, -1 for worst match, and scaled accordingly, while Up and Down Scores represent absolute measures of similarity (1 means up-regulated genes in query list are the most up-regulated genes in treatment instance within CMAP library, -1 means down-regulated genes in query list are identical to most down-regulated genes in treatment instance within CMAP library). B. Top five results averaged by Anatomical Therapeutic Chemical (ATC) classification, sorted by p-value. Mean is the average score for all instances, N is number of instances in category, Enrich is a measure of over-representation of an ATC class, while P-val is a permutation p-value reflecting the likelihood that this level of enrichment is by chance. Specificity is a measure of the uniqueness of a score by comparing against public expression data available from MSigDB: http://www.broad.mit.edu/gsea/msigdb/ (higher value indicates greater number of gene lists from this database which score at least as well as the queried gene list; lower value means greater specificity). % non-null represents the percentage of instances in each category which have a score in the same direction as the gene list queried

A.

Compound	Dose	Cell	Score	Up	Down	Instance ID
pyrvinium	3 μM	MCF7	1	0.407	-0.524	3518
chlorpromazine	11 μM	PC3	0.988	0.487	-0.432	5074
thioridazine	10 μM	MCF7	0.982	0.518	-0.397	1010
pyrvinium	3 μM	MCF7	0.965	0.434	-0.465	5439
astemizole	9 μM	MCF7	0.965	0.541	-0.357	6807
niclosamide	12 μM	MCF7	0.964	0.463	-0.434	1498
perhexiline	10 μM	MCF7	0.912	0.443	-0.406	7441
trifluoperazine	10 μM	PC3	0.91	0.453	-0.394	4448
niclosamide	12 μM	MCF7	0.903	0.425	-0.416	4136
thioridazine	10 μM	MCF7	0.901	0.467	-0.372	5227

B.

ATC Category	Mean	N	Enrich	P-Val	Specificity	% Non-null
N05AC; phenothiazines with piperidine structure	0.601	24	0.727	< 2e-5	0	87
N05AB; phenothiazines with piperazine structure	0.615	60	0.709	< 2e-5	0	95
N06AA; non-selective monoamine reuptake inhibitors	0.501	46	0.616	< 2e-5	0	86
D01AC; imidazole and triazole derivatives	0.388	35	0.414	< 2e-5	0.0118	74
C08EA; phenylalkamine derivatives (non-selective calcium channel blockers)	0.621	7	0.782	2e-5	0.0104	100

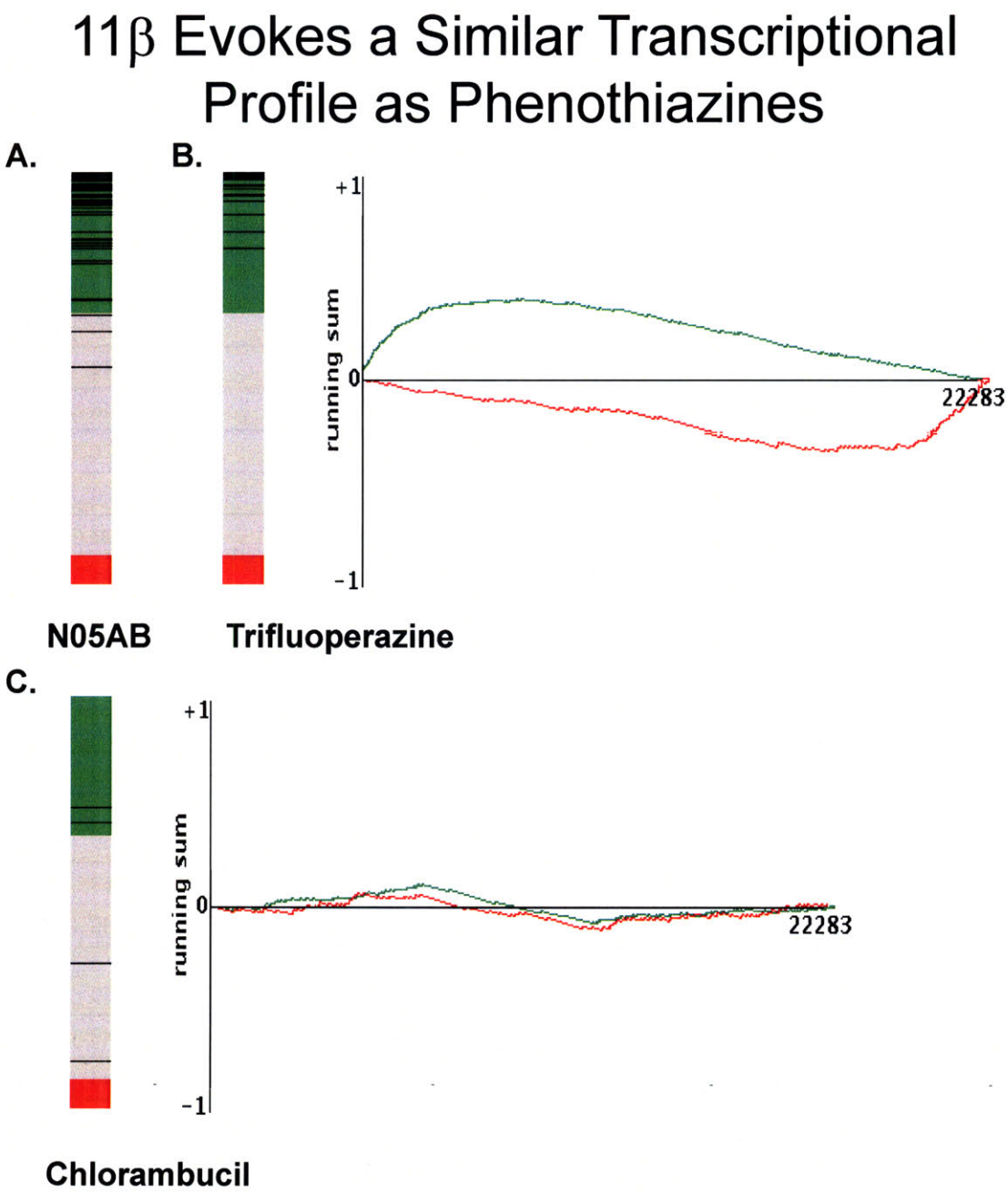

Figure 4.8 Connectivity Map visual display of 5 μM 11β transcriptional similarity with phenothiazines. A. bar view display of instances in the ATC class N05AB (phenothiazines with piperazine structure). Green area represents positive correlation, red denotes inverse correlation, gray indicates overall score of zero. Black horizontal lines are individual treatment instances. B. Bar view and plot of trifluoperazine. Plot shown is for one instance of trifluoperazine treatment. Green line represents probe sets up-regulated by 11β, while red line denotes probe sets down-regulated. Probes for each instance are ordered with most upregulated at the left and most down regulated at the right. Thus, good correlation can be visualized by the green line being more positive in the left portion of the graph and the red line being more negative toward the right portion of the graph, as seen. C. Bar view and plot for chlorambucil is shown for comparison to an agent with poor correlation (plot is of treatment with the highest correlation to 11β).

Table S4.1 Top 50 probe sets up-regulated by treatment with 5 μM 11β. Probe ID is identifier for probe set from Affymetrix HGU133 Plus 2.0 GeneChip®. Values shown are Log_2 fold-changes (LFC of 1 = 2-fold change). LFC of treatment with 11β-dimethoxy (Di) is shown for comparison. Gray cells indicate p-value > 0.05.

Probe ID	Gene Symbol	Gene Name	LFC	
			11β 5μM	Di 5μM
221577_x_at	GDF15	growth differentiation factor 15	3.48	2.08
209383_at	DDIT3	DNA-damage-inducible transcript 3	3.46	1.71
225239_at	NA	NA	3.25	2.45
1554018_at	GPNMB	glycoprotein (transmembrane) nmb	3.00	2.34
234989_at	TncRNA	trophoblast-derived noncoding RNA	2.93	2.30
238695_s_at	RAB39B	RAB39B, member RAS oncogene family	2.93	2.25
227062_at	TncRNA	trophoblast-derived noncoding RNA	2.77	2.09
215209_at	SEC24D	SEC24 related gene family, member D (S. cerevisiae)	2.75	1.36
1554462_a_at	DNAJB9	DnaJ (Hsp40) homolog, subfamily B, member 9	2.70	1.92
219910_at	FICD	FIC domain containing	2.69	2.32
36711_at	MAFF	v-maf musculoaponeurotic fibrosarcoma oncogene homolog F (avian)	2.68	2.03
226158_at	KLHL24	kelch-like 24 (Drosophila)	2.63	1.88
202843_at	DNAJB9	DnaJ (Hsp40) homolog, subfamily B, member 9	2.59	1.84
202375_at	SEC24D	SEC24 related gene family, member D (S. cerevisiae)	2.50	2.22
202887_s_at	DDIT4	DNA-damage-inducible transcript 4	2.48	2.13
201627_s_at	INSIG1	insulin induced gene 1	2.46	3.10
230075_at	RAB39B	RAB39B, member RAS oncogene family	2.42	1.82
225957_at	C5orf41	chromosome 5 open reading frame 41	2.40	1.52
202842_s_at	DNAJB9	DnaJ (Hsp40) homolog, subfamily B, member 9	2.38	1.84
225956_at	C5orf41	chromosome 5 open reading frame 41	2.35	1.42
242088_at	KLHL24	kelch-like 24 (Drosophila)	2.34	1.26
221750_at	HMGCS1	3-hydroxy-3-methylglutaryl-Coenzyme A synthase 1 (soluble)	2.24	2.61
221986_s_at	KLHL24	kelch-like 24 (Drosophila)	2.21	1.58
208763_s_at	TSC22D3	TSC22 domain family, member 3	2.20	1.38
203725_at	GADD45A	growth arrest and DNA-damage-inducible, alpha	2.19	1.22

Probe ID	Gene Symbol	Gene Name	LFC	
			11β 5μM	Di 5μM
201625_s_at	INSIG1	insulin induced gene 1	2.18	2.96
221985_at	KLHL24	kelch-like 24 (Drosophila)	2.17	1.49
210587_at	INHBE	inhibin, beta E	2.16	0.53
201626_at	INSIG1	insulin induced gene 1	2.12	2.32
238476_at	C5orf41	chromosome 5 open reading frame 41	2.12	1.26
212274_at	LPIN1	lipin 1	2.11	2.25
202557_at	HSPA13	heat shock protein 70kDa family, member 13	2.11	1.62
212810_s_at	SLC1A4	solute carrier family 1 (glutamate/neutral amino acid transporter), member 4	2.11	2.02
212276_at	LPIN1	lipin 1	2.10	2.22
214696_at	C17orf91	chromosome 17 open reading frame 91	2.09	1.53
226771_at	ATP8B2	ATPase, class I, type 8B, member 2	2.09	2.15
212272_at	LPIN1	lipin 1	2.07	2.06
218696_at	EIF2AK3	eukaryotic translation initiation factor 2-alpha kinase 3	2.05	1.63
219270_at	CHAC1	ChaC, cation transport regulator homolog 1 (E. coli)	2.02	0.90
202766_s_at	FBN1	fibrillin 1	2.02	0.98
238320_at	TncRNA	trophoblast-derived noncoding RNA	2.01	0.87
227020_at	YPEL2	yippee-like 2 (Drosophila)	2.01	1.32
223195_s_at	SESN2	sestrin 2	1.97	0.95
228234_at	TICAM2	toll-like receptor adaptor molecule 2	1.95	1.16
210675_s_at	PTPRR	protein tyrosine phosphatase, receptor type, R	1.95	1.50
201170_s_at	BHLHB2	basic helix-loop-helix domain containing, class B, 2	1.95	2.19
218145_at	TRIB3	tribbles homolog 3 (Drosophila)	1.93	1.44
202672_s_at	ATF3	activating transcription factor 3	1.92	1.11
235369_at	C14orf28	chromosome 14 open reading frame 28	1.91	1.12
229242_at	NA	NA	1.91	0.36

Table S4.2 Top 50 probe sets down-regulated by treatment with 5 μM 11β. Probe ID is identifier for probe set from Affymetrix HGU133 Plus 2.0 GeneChip®. Values shown are Log_2 fold-changes (LFC of 1 = 2-fold change). LFC of treatment with 11β-dimethoxy (Di) is shown for comparison. Gray cells indicate p-value > 0.05.

Probe ID	Gene Symbol	Gene Name	LFC	
			11β 5μM	Di 5μM
226064_s_at	DGAT2	diacylglycerol O-acyltransferase homolog 2 (mouse)	-2.14	-1.32
200769_s_at	MAT2A	methionine adenosyltransferase II, alpha	-2.10	-1.63
209645_s_at	ALDH1B1	aldehyde dehydrogenase 1 family, member B1	-1.78	-1.36
204798_at	MYB	v-myb myeloblastosis viral oncogene homolog (avian)	-1.76	-1.67
227048_at	LAMA1	laminin, alpha 1	-1.70	-0.48
207038_at	SLC16A6	solute carrier family 16, member 6 (monocarboxylic acid transporter 7)	-1.60	-0.52
201008_s_at	TXNIP	thioredoxin interacting protein	-1.54	-1.40
212525_s_at	H2AFX	H2A histone family, member X	-1.51	-0.78
213523_at	CCNE1	cyclin E1	-1.49	-1.00
1554036_at	ZBTB24	zinc finger and BTB domain containing 24	-1.47	-0.50
205217_at	TIMM8A	translocase of inner mitochondrial membrane 8 homolog A (yeast)	-1.46	-0.95
210387_at	HIST1H2BG	histone cluster 1, H2bg	-1.46	-0.72
238953_at	NA	NA	-1.44	-0.78
228990_at	C1orf79	chromosome 1 open reading frame 79	-1.39	-1.44
204695_at	CDC25A	cell division cycle 25 homolog A (S. pombe)	-1.38	-0.82
212170_at	RBM12	RNA binding motif protein 12	-1.38	-0.68
223159_s_at	NEK6	NIMA (never in mitosis gene a)-related kinase 6	-1.38	-0.83
202668_at	EFNB2	ephrin-B2	-1.37	-0.73
230748_at	SLC16A6	solute carrier family 16, member 6 (monocarboxylic acid transporter 7)	-1.34	-0.25
235476_at	TRIM59	tripartite motif-containing 59	-1.34	-0.61
244852_at	DSEL	dermatan sulfate epimerase-like	-1.33	-1.46
224428_s_at	CDCA7	cell division cycle associated 7	-1.33	-1.24
218559_s_at	MAFB	v-maf musculoaponeurotic fibrosarcoma oncogene homolog B (avian)	-1.33	-1.21
220651_s_at	MCM10	minichromosome maintenance complex component 10	-1.30	-1.11
201490_s_at	PPIF	peptidylprolyl isomerase F (cyclophilin F)	-1.29	-1.24

Probe ID	Gene Symbol	Gene Name	LFC	
			11β 5μM	Di 5μM
218974_at	SOBP	sine oculis binding protein homolog (Drosophila)	-1.28	-0.93
219262_at	SUV39H2	suppressor of variegation 3-9 homolog 2 (Drosophila)	-1.28	-0.86
214963_at	NUP160	nucleoporin 160kDa	-1.27	-0.91
219990_at	E2F8	E2F transcription factor 8	-1.26	-0.85
212168_at	RBM12	RNA binding motif protein 12	-1.25	-0.73
224321_at	TMEFF2	transmembrane protein with EGF-like and two follistatin-like domains 2	-1.23	-1.09
223773_s_at	C1orf79	chromosome 1 open reading frame 79	-1.23	-1.24
1553947_at	EXOSC6	exosome component 6	-1.23	-0.79
226998_at	NARG1	NMDA receptor regulated 1	-1.23	-0.62
200874_s_at	NOL5A	nucleolar protein 5A (56kDa with KKE/D repeat)	-1.22	-0.96
229310_at	KLHL29	kelch-like 29 (Drosophila)	-1.22	-0.33
1554101_a_at	TMTC4	transmembrane and tetratricopeptide repeat containing 4	-1.22	-0.16
203418_at	CCNA2	cyclin A2	-1.22	-0.45
205241_at	SCO2	SCO cytochrome oxidase deficient homolog 2 (yeast)	-1.21	-0.86
213449_at	POP1	processing of precursor 1, ribonuclease P/MRP subunit (S. cerevisiae)	-1.21	-0.54
225687_at	FAM83D	family with sequence similarity 83, member D	-1.20	-0.60
226017_at	CMTM7	CKLF-like MARVEL transmembrane domain containing 7	-1.19	-0.88
219502_at	NEIL3	nei endonuclease VIII-like 3 (E. coli)	-1.19	-0.67
218726_at	HJURP	Holliday junction recognition protein	-1.19	-0.44
218897_at	TMEM177	transmembrane protein 177	-1.19	-0.94
202464_s_at	PFKFB3	6-phosphofructo-2-kinase/fructose-2,6-biphosphatase 3	-1.18	-0.86
200768_s_at	MAT2A	methionine adenosyltransferase II, alpha	-1.17	-0.85
1555639_a_at	RBM14	RNA binding motif protein 14	-1.17	-1.22
232825_s_at	DSEL	dermatan sulfate epimerase-like	-1.17	-0.82
206261_at	ZNF239	zinc finger protein 239	-1.17	-0.68

Table S4.3 Top 50 probe sets up-regulated by treatment with 5 μM 11β-dimethoxy. Probe ID is identifier for probe set from Affymetrix HGU133 Plus 2.0 GeneChip®. Values shown are Log_2 fold-changes (LFC of 1 = 2-fold change). LFC of treatment with 11β is shown for comparison.

Probe ID	Gene Symbol	Gene Name	LFC	
			11β 5μM	Di 5μM
201627_s_at	INSIG1	insulin induced gene 1	2.46	3.10
229476_s_at	THRSP	thyroid hormone responsive (SPOT14 homolog, rat)	1.48	2.98
201625_s_at	INSIG1	insulin induced gene 1	2.18	2.96
205822_s_at	HMGCS1	3-hydroxy-3-methylglutaryl-Coenzyme A synthase 1 (soluble)	1.89	2.81
221750_at	HMGCS1	3-hydroxy-3-methylglutaryl-Coenzyme A synthase 1 (soluble)	2.24	2.61
229477_at	THRSP	thyroid hormone responsive (SPOT14 homolog, rat)	1.09	2.56
225239_at	NA	NA	3.25	2.45
1554018_at	GPNMB	glycoprotein (transmembrane) nmb	3.00	2.34
234312_s_at	ACSS2	acyl-CoA synthetase short-chain family member 2	1.64	2.32
219910_at	FICD	FIC domain containing	2.69	2.32
201626_at	INSIG1	insulin induced gene 1	2.12	2.32
234989_at	TncRNA	trophoblast-derived noncoding RNA	2.93	2.30
212274_at	LPIN1	lipin 1	2.11	2.25
238695_s_at	RAB39B	RAB39B, member RAS oncogene family	2.93	2.25
202375_at	SEC24D	SEC24 related gene family, member D (S. cerevisiae)	2.50	2.22
212276_at	LPIN1	lipin 1	2.10	2.22
241954_at	FDFT1	farnesyl-diphosphate farnesyltransferase 1	1.08	2.20
201170_s_at	BHLHB2	basic helix-loop-helix domain containing, class B, 2	1.95	2.19
226771_at	ATP8B2	ATPase, class I, type 8B, member 2	2.09	2.15
202887_s_at	DDIT4	DNA-damage-inducible transcript 4	2.48	2.13
227062_at	TncRNA	trophoblast-derived noncoding RNA	2.77	2.09
221577_x_at	GDF15	growth differentiation factor 15	3.48	2.08
212272_at	LPIN1	lipin 1	2.07	2.06
209218_at	SQLE	squalene epoxidase	1.36	2.04
36711_at	MAFF	v-maf musculoaponeurotic fibrosarcoma oncogene homolog F (avian)	2.68	2.03

Probe ID	Gene Symbol	Gene Name	LFC	
			11β 5μM	Di 5μM
212810_s_at	SLC1A4	solute carrier family 1 (glutamate/neutral amino acid transporter), member 4	2.11	2.02
238666_at	NA	NA	0.97	2.02
226390_at	STARD4	StAR-related lipid transfer (START) domain containing 4	1.49	1.98
1554462_a_at	DNAJB9	DnaJ (Hsp40) homolog, subfamily B, member 9	2.70	1.92
230256_at	C1orf104	chromosome 1 open reading frame 104	0.89	1.89
213577_at	SQLE	squalene epoxidase	1.21	1.89
226158_at	KLHL24	kelch-like 24 (Drosophila)	2.63	1.88
209146_at	SC4MOL	sterol-C4-methyl oxidase-like	1.38	1.86
202842_s_at	DNAJB9	DnaJ (Hsp40) homolog, subfamily B, member 9	2.38	1.84
202843_at	DNAJB9	DnaJ (Hsp40) homolog, subfamily B, member 9	2.59	1.84
230075_at	RAB39B	RAB39B, member RAS oncogene family	2.42	1.82
206457_s_at	DIO1	deiodinase, iodothyronine, type I	1.82	1.77
213562_s_at	SQLE	squalene epoxidase	1.12	1.74
211986_at	AHNAK	AHNAK nucleoprotein	1.04	1.74
205945_at	IL6R	interleukin 6 receptor	1.47	1.73
209383_at	DDIT3	DNA-damage-inducible transcript 3	3.46	1.71
218764_at	PRKCH	protein kinase C, eta	1.55	1.70
1563571_at	LOC285463	hypothetical protein LOC285463	1.22	1.68
226929_at	MTHFR	5,10-methylenetetrahydrofolate reductase (NADPH)	1.57	1.68
213836_s_at	WIPI1	WD repeat domain, phosphoinositide interacting 1	1.89	1.67
217678_at	SLC7A11	solute carrier family 7, (cationic amino acid transporter, y+ system) member 11	1.90	1.66
202068_s_at	LDLR	low density lipoprotein receptor	0.42	1.66
202245_at	LSS	lanosterol synthase (2,3-oxidosqualene-lanosterol cyclase)	1.09	1.65
202540_s_at	HMGCR	3-hydroxy-3-methylglutaryl-Coenzyme A reductase	1.18	1.65
209610_s_at	SLC1A4	solute carrier family 1 (glutamate/neutral amino acid transporter), member 4	1.67	1.64

Table S4.4 Top 50 probe sets down-regulated by treatment with 5 μM 11β-dimethoxy. Probe ID is identifier for probe set from Affymetrix HGU133 Plus 2.0 GeneChip®. Values shown are Log_2 fold-changes (LFC of 1 = 2-fold change). LFC of treatment with 11β is shown for comparison. Gray cells indicate p-value > 0.05.

Probe ID	Gene Symbol	Gene Name	LFC	
			11β 5μM	Di 5μM
204798_at	MYB	v-myb myeloblastosis viral oncogene homolog (avian)	-1.76	-1.67
200769_s_at	MAT2A	methionine adenosyltransferase II, alpha	-2.10	-1.63
211814_s_at	CCNE2	cyclin E2	-1.14	-1.51
244852_at	DSEL	dermatan sulfate epimerase-like	-1.33	-1.46
228990_at	C1orf79	chromosome 1 open reading frame 79	-1.39	-1.44
201008_s_at	TXNIP	thioredoxin interacting protein	-1.54	-1.40
1560224_at	AHCTF1	AT hook containing transcription factor 1	-0.66	-1.37
209645_s_at	ALDH1B1	aldehyde dehydrogenase 1 family, member B1	-1.78	-1.36
236207_at	SSFA2	sperm specific antigen 2	-0.37	-1.36
226064_s_at	DGAT2	diacylglycerol O-acyltransferase homolog 2 (mouse)	-2.14	-1.32
223774_at	C1orf79	chromosome 1 open reading frame 79	-1.16	-1.25
201490_s_at	PPIF	peptidylprolyl isomerase F (cyclophilin F)	-1.29	-1.24
223773_s_at	C1orf79	chromosome 1 open reading frame 79	-1.23	-1.24
237215_s_at	TFRC	transferrin receptor (p90, CD71)	-0.65	-1.24
224428_s_at	CDCA7	cell division cycle associated 7	-1.33	-1.24
230543_at	USP9X	ubiquitin specific peptidase 9, X-linked	-0.68	-1.22
1555639_a_at	RBM14	RNA binding motif protein 14	-1.17	-1.22
201801_s_at	SLC29A1	solute carrier family 29 (nucleoside transporters), member 1	-1.11	-1.21
218559_s_at	MAFB	v-maf musculoaponeurotic fibrosarcoma oncogene homolog B (avian)	-1.33	-1.21
214962_s_at	NUP160	nucleoporin 160kDa	-0.88	-1.21
1555465_at	MCOLN2	mucolipin 2	-0.85	-1.19
212105_s_at	DHX9	DEAH (Asp-Glu-Ala-His) box polypeptide 9	-0.79	-1.18
1557217_a_at	FANCB	Fanconi anemia, complementation group B	-0.94	-1.15
222108_at	AMIGO2	adhesion molecule with Ig-like domain 2	-0.52	-1.15
206902_s_at	ENDOGL1	endonuclease G-like 1	-1.08	-1.14

Probe ID	Gene Symbol	Gene Name	LFC	
			11β 5μM	Di 5μM
220007_at	METTL8	methyltransferase like 8	-0.87	-1.13
222670_s_at	MAFB	v-maf musculoaponeurotic fibrosarcoma oncogene homolog B (avian)	-1.13	-1.13
212142_at	MCM4	minichromosome maintenance complex component 4	-1.04	-1.13
207199_at	TERT	telomerase reverse transcriptase	-0.85	-1.11
221440_s_at	RBBP9	retinoblastoma binding protein 9	-0.80	-1.11
220651_s_at	MCM10	minichromosome maintenance complex component 10	-1.30	-1.11
224321_at	TMEFF2	transmembrane protein with EGF-like and two follistatin-like domains 2	-1.23	-1.09
222611_s_at	PSPC1	paraspeckle component 1	-1.11	-1.09
217620_s_at	PIK3CB	phosphoinositide-3-kinase, catalytic, beta polypeptide	-0.54	-1.09
228098_s_at	MYLIP	myosin regulatory light chain interacting protein	-1.07	-1.08
228057_at	DDIT4L	DNA-damage-inducible transcript 4-like	-1.06	-1.07
239316_at	LOC751071	hypothetical protein LOC751071	-0.56	-1.07
223130_s_at	MYLIP	myosin regulatory light chain interacting protein	-0.89	-1.07
225449_at	RDH13	retinol dehydrogenase 13 (all-trans/9-cis)	-0.81	-1.07
223785_at	FANCI	Fanconi anemia, complementation group I	-0.69	-1.07
232309_at	LOC202181	hypothetical protein LOC202181	-1.02	-1.05
201009_s_at	TXNIP	thioredoxin interacting protein	-1.15	-1.05
1559307_s_at	RBL1	retinoblastoma-like 1 (p107)	-0.86	-1.04
234728_s_at	DHX35	DEAH (Asp-Glu-Ala-His) box polypeptide 35	-0.54	-1.03
213606_s_at	ARHGDIA	Rho GDP dissociation inhibitor (GDI) alpha	-0.89	-1.03
228281_at	C11orf82	chromosome 11 open reading frame 82	-0.90	-1.02
222527_s_at	RBM22	RNA binding motif protein 22	-0.63	-1.01
209646_x_at	ALDH1B1	aldehyde dehydrogenase 1 family, member B1	-1.12	-1.01
213523_at	CCNE1	cyclin E1	-1.49	-1.00
205461_at	RAB35	RAB35, member RAS oncogene family	-0.94	-1.00

Table S4.5 Top 50 probe sets up-regulated by treatment with 1 μM 11β. Probe ID is identifier for probe set from Affymetrix HGU133 Plus 2.0 GeneChip®. Values shown are Log_2 fold-changes (LFC of 1 = 2-fold change).

Probe ID	Gene Symbol	Gene Name	LFC
225239_at	NA	NA	1.57
234989_at	TncRNA	trophoblast-derived noncoding RNA	1.40
201627_s_at	INSIG1	insulin induced gene 1	1.35
201625_s_at	INSIG1	insulin induced gene 1	1.28
1559360_at	NA	NA	1.22
232528_at	NA	NA	1.21
205822_s_at	HMGCS1	3-hydroxy-3-methylglutaryl-Coenzyme A synthase 1 (soluble)	1.21
212274_at	LPIN1	lipin 1	1.13
221750_at	HMGCS1	3-hydroxy-3-methylglutaryl-Coenzyme A synthase 1 (soluble)	1.11
212276_at	LPIN1	lipin 1	1.05
215385_at	NA	NA	1.03
232668_at	NA	NA	1.01
234314_at	C20orf74	chromosome 20 open reading frame 74	1.00
201626_at	INSIG1	insulin induced gene 1	0.99
235028_at	NA	NA	0.97
235879_at	MBNL1	muscleblind-like (Drosophila)	0.94
1563649_at	NA	NA	0.93
237839_at	NA	NA	0.92
213577_at	SQLE	squalene epoxidase	0.90
242476_at	NA	NA	0.90
210230_at	NA	NA	0.89
241893_at	NA	NA	0.88
233303_at	NA	NA	0.87
209218_at	SQLE	squalene epoxidase	0.87
225157_at	MLXIP	MLX interacting protein	0.85

Probe ID	Gene Symbol	Gene Name	LFC
212218_s_at	FASN	fatty acid synthase	0.83
239264_at	NA	NA	0.82
1556543_at	NA	NA	0.81
201791_s_at	DHCR7	7-dehydrocholesterol reductase	0.80
1559739_at	CHPT1	choline phosphotransferase 1	0.79
226390_at	STARD4	StAR-related lipid transfer (START) domain containing 4	0.79
229842_at	ELF3	E74-like factor 3 (ets domain transcription factor, epithelial-specific)	0.78
208962_s_at	FADS1	fatty acid desaturase 1	0.77
228674_s_at	EML4	echinoderm microtubule associated protein like 4	0.76
217042_at	RDH11	retinol dehydrogenase 11 (all-trans/9-cis/11-cis)	0.76
229470_at	NA	NA	0.74
218764_at	PRKCH	protein kinase C, eta	0.74
232344_at	NA	NA	0.73
202245_at	LSS	lanosterol synthase (2,3-oxidosqualene-lanosterol cyclase)	0.73
234312_s_at	ACSS2	acyl-CoA synthetase short-chain family member 2	0.73
232034_at	LOC203274	hypothetical protein LOC203274	0.73
1558695_at	NA	NA	0.73
220091_at	SLC2A6	solute carrier family 2 (facilitated glucose transporter), member 6	0.72
229685_at	LOC100134937	hypothetical LOC100134937	0.70
242439_s_at	ASXL1	additional sex combs like 1 (Drosophila)	0.70
244826_at	NA	NA	0.69
208806_at	CHD3	chromodomain helicase DNA binding protein 3	0.69
208881_x_at	IDI1	isopentenyl-diphosphate delta isomerase 1	0.69
210950_s_at	FDFT1	farnesyl-diphosphate farnesyltransferase 1	0.68

Table S4.6 Top 50 probe sets down-regulated by treatment with 1 μM 11β. Probe ID is identifier for probe set from Affymetrix HGU133 Plus 2.0 GeneChip®. Values shown are Log_2 fold-changes (LFC of 1 = 2-fold change).

Probe ID	Gene Symbol	Gene Name	LFC
206953_s_at	LPHN2	latrophilin 2	-0.93
207324_s_at	DSC1	desmocollin 1	-0.77
214598_at	CLDN8	claudin 8	-0.76
1553645_at	CCDC141	coiled-coil domain containing 141	-0.76
207103_at	KCND2	potassium voltage-gated channel, Shal-related subfamily, member 2	-0.74
1561969_at	ZPLD1	zona pellucida-like domain containing 1	-0.74
1554036_at	ZBTB24	zinc finger and BTB domain containing 24	-0.72
204897_at	PTGER4	prostaglandin E receptor 4 (subtype EP4)	-0.72
218559_s_at	MAFB	v-maf musculoaponeurotic fibrosarcoma oncogene homolog B (avian)	-0.71
210233_at	IL1RAP	interleukin 1 receptor accessory protein	-0.69
1564381_s_at	NA	NA	-0.69
212420_at	ELF1	E74-like factor 1 (ets domain transcription factor)	-0.68
238336_s_at	DNAJC21	DnaJ (Hsp40) homolog, subfamily C, member 21	-0.68
230060_at	CDCA7	cell division cycle associated 7	-0.65
1554099_a_at	SPIN3	spindlin family, member 3	-0.64
1553768_a_at	DCBLD1	discoidin, CUB and LCCL domain containing 1	-0.63
209535_s_at	NA	NA	-0.63
203845_at	KAT2B	K(lysine) acetyltransferase 2B	-0.62
203890_s_at	DAPK3	death-associated protein kinase 3	-0.61
1556283_s_at	FGFR1OP 2	FGFR1 oncogene partner 2	-0.60
236219_at	NA	NA	-0.59
228937_at	C13orf31	chromosome 13 open reading frame 31	-0.58
220549_at	LOC1001 28414	similar to fibrinogen silencer binding protein	-0.58
220295_x_at	DEPDC1	DEP domain containing 1	-0.57
241820_at	RIF1	RAP1 interacting factor homolog (yeast)	-0.57

Probe ID	Gene Symbol	Gene Name	LFC
231343_at	LOC647131	hypothetical LOC647131	-0.57
208167_s_at	MMP16	matrix metallopeptidase 16 (membrane-inserted)	-0.57
216944_s_at	ITPR1	inositol 1,4,5-triphosphate receptor, type 1	-0.56
214600_at	TEAD1	TEA domain family member 1 (SV40 transcriptional enhancer factor)	-0.56
228395_at	GNL3	guanine nucleotide binding protein-like 3 (nucleolar)	-0.56
238474_at	NUP43	nucleoporin 43kDa	-0.56
213618_at	CENTD1	centaurin, delta 1	-0.55
219473_at	GDAP2	ganglioside induced differentiation associated protein 2	-0.54
200769_s_at	MAT2A	methionine adenosyltransferase II, alpha	-0.54
1568817_at	NA	NA	-0.54
1553244_at	FANCB	Fanconi anemia, complementation group B	-0.54
219502_at	NEIL3	nei endonuclease VIII-like 3 (E. coli)	-0.54
209681_at	SLC19A2	solute carrier family 19 (thiamine transporter), member 2	-0.53
221258_s_at	KIF18A	kinesin family member 18A	-0.53
242349_at	HECTD1	HECT domain containing 1	-0.53
221686_s_at	RECQL5	RecQ protein-like 5	-0.53
216184_s_at	RIMS1	regulating synaptic membrane exocytosis 1	-0.52
239598_s_at	LPCAT2	lysophosphatidylcholine acyltransferase 2	-0.52
240690_at	NA	NA	-0.52
220955_x_at	RAB23	RAB23, member RAS oncogene family	-0.52
235449_at	LRSAM1	leucine rich repeat and sterile alpha motif containing 1	-0.51
1555450_a_at	NARG1L	NMDA receptor regulated 1-like	-0.51
204085_s_at	CLN5	ceroid-lipofuscinosis, neuronal 5	-0.50
228735_s_at	PANK2	pantothenate kinase 2	-0.50
204781_s_at	FAS	Fas (TNF receptor superfamily, member 6)	-0.50

Table S4.7 Top 50 probe sets up-regulated by treatment with 1 nM R1881. Probe ID is identifier for probe set from Affymetrix HGU133 Plus 2.0 GeneChip®. Values shown are Log_2 fold-changes (LFC of 1 = 2-fold change).

Probe ID	Gene Symbol	Gene Name	LFC
201739_at	SGK1	serum/glucocorticoid regulated kinase 1	3.37
1553645_at	CCDC141	coiled-coil domain containing 141	3.17
225987_at	STEAP4	STEAP family member 4	3.09
235146_at	TMCC3	transmembrane and coiled-coil domain family 3	2.64
213139_at	SNAI2	snail homolog 2 (Drosophila)	2.64
220786_s_at	SLC38A4	solute carrier family 38, member 4	2.43
1555345_at	SLC38A4	solute carrier family 38, member 4	2.42
206363_at	MAF	v-maf musculoaponeurotic fibrosarcoma oncogene homolog (avian)	2.38
229327_s_at	MAF	v-maf musculoaponeurotic fibrosarcoma oncogene homolog (avian)	2.36
209348_s_at	MAF	v-maf musculoaponeurotic fibrosarcoma oncogene homolog (avian)	2.19
224657_at	ERRFI1	ERBB receptor feedback inhibitor 1	2.16
235419_at	NA	NA	2.15
219049_at	CSGALNACT1	chondroitin sulfate N-acetylgalactosaminyltransferase 1	2.13
1563571_at	LOC285463	hypothetical protein LOC285463	2.03
225688_s_at	PHLDB2	pleckstrin homology-like domain, family B, member 2	1.97
223169_s_at	RHOU	ras homolog gene family, member U	1.79
224856_at	FKBP5	FK506 binding protein 5	1.69
203627_at	IGF1R	insulin-like growth factor 1 receptor	1.67
205876_at	LIFR	leukemia inhibitory factor receptor alpha	1.65
202499_s_at	SLC2A3	solute carrier family 2 (facilitated glucose transporter), member 3	1.65
223168_at	RHOU	ras homolog gene family, member U	1.61
227771_at	LIFR	leukemia inhibitory factor receptor alpha	1.60
219694_at	FAM105A	family with sequence similarity 105, member A	1.59
217028_at	CXCR4	chemokine (C-X-C motif) receptor 4	1.59
214446_at	ELL2	elongation factor, RNA polymerase II, 2	1.58

Probe ID	Gene Symbol	Gene Name	LFC
203372_s_at	SOCS2	suppressor of cytokine signaling 2	1.58
204560_at	FKBP5	FK506 binding protein 5	1.57
225571_at	LIFR	leukemia inhibitory factor receptor alpha	1.57
202644_s_at	TNFAIP3	tumor necrosis factor, alpha-induced protein 3	1.53
235445_at	NA	NA	1.51
230082_at	LOC100133660	hypothetical LOC100133660	1.51
200632_s_at	NDRG1	N-myc downstream regulated gene 1	1.50
209286_at	CDC42EP3	CDC42 effector protein (Rho GTPase binding) 3	1.49
224840_at	FKBP5	FK506 binding protein 5	1.47
219551_at	EAF2	ELL associated factor 2	1.43
213906_at	MYBL1	v-myb myeloblastosis viral oncogene homolog (avian)-like 1	1.42
210095_s_at	IGFBP3	insulin-like growth factor binding protein 3	1.41
235606_at	LOC344595	hypothetical LOC344595	1.41
204121_at	GADD45G	growth arrest and DNA-damage-inducible, gamma	1.40
204897_at	PTGER4	prostaglandin E receptor 4 (subtype EP4)	1.39
232397_at	NA	NA	1.39
226393_at	CYP2U1	cytochrome P450, family 2, subfamily U, polypeptide 1	1.37
211548_s_at	HPGD	hydroxyprostaglandin dehydrogenase 15-(NAD)	1.37
209822_s_at	VLDLR	very low density lipoprotein receptor	1.36
211596_s_at	LRIG1	leucine-rich repeats and immunoglobulin-like domains 1	1.36
205214_at	STK17B	serine/threonine kinase 17b	1.35
209212_s_at	KLF5	Kruppel-like factor 5 (intestinal)	1.35
1559360_at	NA	NA	1.34
1552673_at	RFX6	regulatory factor X, 6	1.34
225330_at	IGF1R	insulin-like growth factor 1 receptor	1.30

Table S4.8 Top 50 probe sets down-regulated by treatment with 1 nM R1881. Probe ID is identifier for probe set from Affymetrix HGU133 Plus 2.0 GeneChip®. Values shown are Log_2 fold-changes (LFC of 1 = 2-fold change).

Probe ID	Gene Symbol	Gene Name	LFC
205027_s_at	MAP3K8	mitogen-activated protein kinase kinase kinase 8	-1.40
222108_at	AMIGO2	adhesion molecule with Ig-like domain 2	-1.22
229242_at	NA	NA	-1.14
212558_at	SPRY1	sprouty homolog 1, antagonist of FGF signaling (Drosophila)	-1.00
238622_at	RAP2B	RAP2B, member of RAS oncogene family	-0.96
203304_at	BAMBI	BMP and activin membrane-bound inhibitor homolog (Xenopus laevis)	-0.93
230300_at	NA	NA	-0.92
210929_s_at	LOC100131613	PRO1454	-0.90
228708_at	RAB27B	RAB27B, member RAS oncogene family	-0.89
226884_at	LRRN1	leucine rich repeat neuronal 1	-0.89
201340_s_at	ENC1	ectodermal-neural cortex (with BTB-like domain)	-0.87
232914_s_at	SYTL2	synaptotagmin-like 2	-0.87
238479_at	NA	NA	-0.85
1554757_a_at	INPP5A	inositol polyphosphate-5-phosphatase, 40kDa	-0.84
244852_at	DSEL	dermatan sulfate epimerase-like	-0.84
237054_at	ENPP5	ectonucleotide pyrophosphatase/phosphodiesterase 5 (putative function)	-0.83
1558819_at	LOC100131819	similar to hCG1778814	-0.82
209890_at	TSPAN5	tetraspanin 5	-0.81
230179_at	LOC285812	hypothetical protein LOC285812	-0.81
204567_s_at	ABCG1	ATP-binding cassette, sub-family G (WHITE), member 1	-0.81
204021_s_at	PURA	purine-rich element binding protein A	-0.80
235783_at	MRTO4	mRNA turnover 4 homolog (S. cerevisiae)	-0.80
232740_at	MCM3APAS	minichromosome maintenance complex component 3 associated protein antisense	-0.79
229058_at	ANKRD16	ankyrin repeat domain 16	-0.78
1568817_at	NA	NA	-0.78

Probe ID	Gene Symbol	Gene Name	LFC
232395_x_at	AGBL3	ATP/GTP binding protein-like 3	-0.78
213803_at	KPNB1	karyopherin (importin) beta 1	-0.77
227481_at	CNKSR3	CNKSR family member 3	-0.77
222541_at	RSF1	remodeling and spacing factor 1	-0.77
204180_s_at	ZBTB43	zinc finger and BTB domain containing 43	-0.77
229944_at	OPRK1	opioid receptor, kappa 1	-0.76
232055_at	SFXN1	sideroflexin 1	-0.76
221823_at	C5orf30	chromosome 5 open reading frame 30	-0.76
207078_at	MED6	mediator complex subunit 6	-0.75
1554544_a_at	MBP	myelin basic protein	-0.75
207655_s_at	BLNK	B-cell linker	-0.75
223642_at	ZIC2	Zic family member 2 (odd-paired homolog, Drosophila)	-0.74
213568_at	OSR2	odd-skipped related 2 (Drosophila)	-0.73
242273_at	NA	NA	-0.73
223322_at	RASSF5	Ras association (RalGDS/AF-6) domain family member 5	-0.73
228338_at	LOC120376	hypothetical protein LOC120376	-0.72
220353_at	FAM86C	family with sequence similarity 86, member C	-0.72
1554029_a_at	TTC37	tetratricopeptide repeat domain 37	-0.72
217997_at	PHLDA1	pleckstrin homology-like domain, family A, member 1	-0.72
226272_at	RCAN3	RCAN family member 3	-0.71
233341_s_at	POLR1B	polymerase (RNA) I polypeptide B, 128kDa	-0.71
223204_at	C4orf18	chromosome 4 open reading frame 18	-0.71
1559190_s_at	RDH13	retinol dehydrogenase 13 (all-trans/9-cis)	-0.71
212977_at	CXCR7	chemokine (C-X-C motif) receptor 7	-0.70
231943_at	ZFP28	zinc finger protein 28 homolog (mouse)	-0.70

Table S4.9 Top 50 probe sets up-regulated by treatment with 1 μM bicalutamide. Probe ID is identifier for probe set from Affymetrix HGU133 Plus 2.0 GeneChip®. Values shown are Log_2 fold-changes (LFC of 1 = 2-fold change).

Probe ID	Gene Symbol	Gene Name	LFC
210756_s_at	NOTCH2	Notch homolog 2 (Drosophila)	0.91
242691_at	NA	NA	0.85
244790_at	MTCP1	mature T-cell proliferation 1	0.84
1552735_at	PCDHGC3	protocadherin gamma subfamily C, 3	0.84
208633_s_at	MACF1	microtubule-actin crosslinking factor 1	0.83
235801_at	NA	NA	0.81
223581_at	ZNF577	zinc finger protein 577	0.76
224218_s_at	TRPS1	trichorhinophalangeal syndrome I	0.76
232272_at	ZNF624	zinc finger protein 624	0.75
232231_at	RUNX2	runt-related transcription factor 2	0.74
214908_s_at	TRRAP	transformation/transcription domain-associated protein	0.74
225999_at	FAM80B	family with sequence similarity 80, member B	0.72
226811_at	FAM46C	family with sequence similarity 46, member C	0.72
235924_at	NA	NA	0.71
229842_at	ELF3	E74-like factor 3 (ets domain transcription factor, epithelial-specific)	0.71
216944_s_at	ITPR1	inositol 1,4,5-triphosphate receptor, type 1	0.71
210057_at	SMG1	PI-3-kinase-related kinase SMG-1	0.69
232034_at	LOC203274	hypothetical protein LOC203274	0.69
205842_s_at	JAK2	Janus kinase 2 (a protein tyrosine kinase)	0.69
212249_at	PIK3R1	phosphoinositide-3-kinase, regulatory subunit 1 (alpha)	0.68
229944_at	OPRK1	opioid receptor, kappa 1	0.68
212796_s_at	TBC1D2B	TBC1 domain family, member 2B	0.68
1570482_at	NA	NA	0.67
222413_s_at	MLL3	myeloid/lymphoid or mixed-lineage leukemia 3	0.66
208806_at	CHD3	chromodomain helicase DNA binding protein 3	0.65

Probe ID	Gene Symbol	Gene Name	LFC
235952_at	NA	NA	0.64
1558719_s_at	NA	NA	0.64
211986_at	AHNAK	AHNAK nucleoprotein	0.63
230403_at	NA	NA	0.63
244623_at	KCNQ5	potassium voltage-gated channel, KQT-like subfamily, member 5	0.62
235472_at	FUT10	fucosyltransferase 10 (alpha (1,3) fucosyltransferase)	0.62
217104_at	ST20	suppressor of tumorigenicity 20	0.62
242245_at	NA	NA	0.61
207108_s_at	NIPBL	Nipped-B homolog (Drosophila)	0.61
212472_at	MICAL2	microtubule associated monoxygenase, calponin and LIM domain containing 2	0.61
227415_at	DGKH	diacylglycerol kinase, eta	0.61
235585_at	NA	NA	0.60
221695_s_at	MAP3K2	mitogen-activated protein kinase kinase kinase 2	0.60
221103_s_at	WDR52	WD repeat domain 52	0.60
218854_at	DSE	dermatan sulfate epimerase	0.60
213159_at	PCNX	pecanex homolog (Drosophila)	0.59
211928_at	DYNC1H1	dynein, cytoplasmic 1, heavy chain 1	0.59
226203_at	NA	NA	0.58
212256_at	GALNT10	UDP-N-acetyl-alpha-D-galactosamine:polypeptide N-acetylgalactosaminyltransferase 10 (GalNAc-T10)	0.57
225980_at	C14orf43	chromosome 14 open reading frame 43	0.57
222771_s_at	MYEF2	myelin expression factor 2	0.57
225033_at	LOC286167	hypothetical LOC286167	0.57
242635_s_at	NAPEPLD	N-acyl phosphatidylethanolamine phospholipase D	0.56
236471_at	NFE2L3	nuclear factor (erythroid-derived 2)-like 3	0.56
238778_at	MPP7	membrane protein, palmitoylated 7 (MAGUK p55 subfamily member 7)	0.56

Table S4.10 Top 50 probe sets down-regulated by treatment with 1 μM bicalutamide. Probe ID is identifier for probe set from Affymetrix HGU133 Plus 2.0 GeneChip®. Values shown are Log_2 fold-changes (LFC of 1 = 2-fold change).

Probe ID	Gene Symbol	Gene Name	LFC
213139_at	SNAI2	snail homolog 2 (Drosophila)	-1.57
209348_s_at	MAF	v-maf musculoaponeurotic fibrosarcoma oncogene homolog (avian)	-1.50
220786_s_at	SLC38A4	solute carrier family 38, member 4	-1.34
221419_s_at	NA	NA	-1.18
230543_at	USP9X	ubiquitin specific peptidase 9, X-linked	-1.18
223169_s_at	RHOU	ras homolog gene family, member U	-1.06
205883_at	ZBTB16	zinc finger and BTB domain containing 16	-0.97
228854_at	NA	NA	-0.91
222449_at	PMEPA1	prostate transmembrane protein, androgen induced 1	-0.86
228790_at	FAM110B	family with sequence similarity 110, member B	-0.86
221959_at	FAM110B	family with sequence similarity 110, member B	-0.85
204560_at	FKBP5	FK506 binding protein 5	-0.79
1553645_at	CCDC141	coiled-coil domain containing 141	-0.77
243641_at	NA	NA	-0.73
236168_at	NA	NA	-0.69
238474_at	NUP43	nucleoporin 43kDa	-0.68
217875_s_at	PMEPA1	prostate transmembrane protein, androgen induced 1	-0.68
231880_at	FAM40B	family with sequence similarity 40, member B	-0.65
235445_at	NA	NA	-0.65
209854_s_at	KLK2	kallikrein-related peptidase 2	-0.63
219856_at	C1orf116	chromosome 1 open reading frame 116	-0.63
1554152_a_at	OGDH	oxoglutarate (alpha-ketoglutarate) dehydrogenase (lipoamide)	-0.63
223168_at	RHOU	ras homolog gene family, member U	-0.62
230333_at	NA	NA	-0.62
231232_at	NA	NA	-0.60

Probe ID	Gene Symbol	Gene Name	LFC
207891_s_at	UCHL5IP	UCHL5 interacting protein	-0.60
219653_at	LSM14B	LSM14B, SCD6 homolog B (S. cerevisiae)	-0.59
220606_s_at	C17orf48	chromosome 17 open reading frame 48	-0.58
215034_s_at	TM4SF1	transmembrane 4 L six family member 1	-0.58
240757_at	CLASP1	cytoplasmic linker associated protein 1	-0.57
207993_s_at	CHP	calcium binding protein P22	-0.57
1555733_s_at	AP1S3	adaptor-related protein complex 1, sigma 3 subunit	-0.56
230397_at	NA	NA	-0.55
238848_at	OTUD4	OTU domain containing 4	-0.55
226553_at	TMPRSS2	transmembrane protease, serine 2	-0.55
240038_at	NA	NA	-0.55
243750_x_at	C21orf70	chromosome 21 open reading frame 70	-0.55
227332_at	LOC100129022	hypothetical protein LOC100129022	-0.55
212105_s_at	DHX9	DEAH (Asp-Glu-Ala-His) box polypeptide 9	-0.54
231343_at	LOC647131	hypothetical LOC647131	-0.54
1553565_s_at	DDAH1	dimethylarginine dimethylaminohydrolase 1	-0.54
210339_s_at	KLK2	kallikrein-related peptidase 2	-0.54
224840_at	FKBP5	FK506 binding protein 5	-0.53
210233_at	IL1RAP	interleukin 1 receptor accessory protein	-0.53
240690_at	NA	NA	-0.52
225604_s_at	GLIPR2	GLI pathogenesis-related 2	-0.52
238495_at	NA	NA	-0.52
240572_s_at	LOC374443	CLR pseudogene	-0.52
1556082_a_at	NA	NA	-0.51
210783_x_at	CLEC11A	C-type lectin domain family 11, member A	-0.51

Table S4.11 Top 50 probe sets up-regulated by treatment with 5 μM chlorambucil. Probe ID is identifier for probe set from Affymetrix HGU133 Plus 2.0 GeneChip®. Values shown are Log_2 fold-changes (LFC of 1 = 2-fold change). Requirement for LFC ≥ 0.5 omitted some values from the top 50 list.

Probe ID	Gene Symbol	Gene Name	LFC
235801_at	NA	NA	0.88
207247_s_at	ZFY	zinc finger protein, Y-linked	0.85
242691_at	NA	NA	0.77
222309_at	C6orf62	chromosome 6 open reading frame 62	0.76
210756_s_at	NOTCH2	Notch homolog 2 (Drosophila)	0.73
235924_at	NA	NA	0.70
212730_at	DMN	desmuslin	0.69
227476_at	NA	NA	0.68
212256_at	GALNT10	UDP-N-acetyl-alpha-D-galactosamine:polypeptide N-acetylgalactosaminyltransferase 10 (GalNAc-T10)	0.66
208633_s_at	MACF1	microtubule-actin crosslinking factor 1	0.66
221103_s_at	WDR52	WD repeat domain 52	0.64
214752_x_at	FLNA	filamin A, alpha (actin binding protein 280)	0.63
228502_at	NA	NA	0.62
211986_at	AHNAK	AHNAK nucleoprotein	0.62
223027_at	SNX9	sorting nexin 9	0.62
235472_at	FUT10	fucosyltransferase 10 (alpha (1,3) fucosyltransferase)	0.61
212523_s_at	KIAA0146	KIAA0146	0.60
201510_at	ELF3	E74-like factor 3 (ets domain transcription factor, epithelial-specific)	0.60
238744_at	NA	NA	0.60
220739_s_at	CNNM3	cyclin M3	0.60
232095_at	NA	NA	0.59
227229_at	VPS53	vacuolar protein sorting 53 homolog (S. cerevisiae)	0.59
229842_at	ELF3	E74-like factor 3 (ets domain transcription factor, epithelial-specific)	0.58
208830_s_at	SUPT6H	suppressor of Ty 6 homolog (S. cerevisiae)	0.58
222771_s_at	MYEF2	myelin expression factor 2	0.58

Probe ID	Gene Symbol	Gene Name	LFC
1563649_at	NA	NA	0.58
212076_at	MLL	myeloid/lymphoid or mixed-lineage leukemia (trithorax homolog, Drosophila)	0.58
212472_at	MICAL2	microtubule associated monoxygenase, calponin and LIM domain containing 2	0.57
223581_at	ZNF577	zinc finger protein 577	0.57
218522_s_at	MAP1S	microtubule-associated protein 1S	0.57
1569133_x_at	ARSK	arylsulfatase family, member K	0.56
203061_s_at	MDC1	mediator of DNA damage checkpoint 1	0.55
1558105_a_at	NA	NA	0.55
1558277_at	ZNF740	zinc finger protein 740	0.55
208989_s_at	FBXL11	F-box and leucine-rich repeat protein 11	0.53
211928_at	DYNC1H1	dynein, cytoplasmic 1, heavy chain 1	0.53
240574_at	NA	NA	0.53
206540_at	GLB1L	galactosidase, beta 1-like	0.52
232667_at	NA	NA	0.52
1554887_at	NA	NA	0.51
201073_s_at	SMARCC1	SWI/SNF related, matrix associated, actin dependent regulator of chromatin, subfamily c, member 1	0.50
226158_at	KLHL24	kelch-like 24 (Drosophila)	0.50

Table S4.12 Top 50 probe sets down-regulated by treatment with 5 μM chlorambucil. Probe ID is identifier for probe set from Affymetrix HGU133 Plus 2.0 GeneChip®. Values shown are Log_2 fold-changes (LFC of 1 = 2-fold change). Requirement for LFC ≥ 0.5 omitted some values from the top 50 list.

Probe ID	Gene Symbol	Gene Name	LFC
232964_at	WBSCR19	Williams Beuren syndrome chromosome region 19	-0.97
243495_s_at	NA	NA	-0.95
231152_at	INO80D	INO80 complex subunit D	-0.95
214336_s_at	COPA	coatomer protein complex, subunit alpha	-0.91
214668_at	C13orf1	chromosome 13 open reading frame 1	-0.87
217544_at	LOC729806	similar to hCG1725380	-0.83
1566115_at	NA	NA	-0.80
76897_s_at	FKBP15	FK506 binding protein 15, 133kDa	-0.79
212105_s_at	DHX9	DEAH (Asp-Glu-Ala-His) box polypeptide 9	-0.77
241816_at	C14orf106	chromosome 14 open reading frame 106	-0.76
235179_at	ZNF641	zinc finger protein 641	-0.73
223169_s_at	RHOU	ras homolog gene family, member U	-0.71
202547_s_at	ARHGEF7	Rho guanine nucleotide exchange factor (GEF) 7	-0.71
236985_at	NA	NA	-0.70
238474_at	NUP43	nucleoporin 43kDa	-0.66
1554029_a_at	TTC37	tetratricopeptide repeat domain 37	-0.65
205966_at	TAF13	TAF13 RNA polymerase II, TATA box binding protein (TBP)-associated factor, 18kDa	-0.65
238336_s_at	DNAJC21	DnaJ (Hsp40) homolog, subfamily C, member 21	-0.64
214592_s_at	SNAPC5	small nuclear RNA activating complex, polypeptide 5, 19kDa	-0.63
215046_at	C2orf67	chromosome 2 open reading frame 67	-0.63
242349_at	HECTD1	HECT domain containing 1	-0.63
231500_s_at	BOLA2	bolA homolog 2 (E. coli)	-0.62
205448_s_at	MAP3K12	mitogen-activated protein kinase kinase kinase 12	-0.62
223661_at	NUCKS1	nuclear casein kinase and cyclin-dependent kinase substrate 1	-0.61
228790_at	FAM110B	family with sequence similarity 110, member B	-0.60

Probe ID	Gene Symbol	Gene Name	LFC
232613_at	PBRM1	polybromo 1	-0.60
209136_s_at	USP10	ubiquitin specific peptidase 10	-0.59
1555733_s_at	AP1S3	adaptor-related protein complex 1, sigma 3 subunit	-0.56
231343_at	LOC647131	hypothetical LOC647131	-0.56
230098_at	PHF20L1	PHD finger protein 20-like 1	-0.55
209754_s_at	TMPO	thymopoietin	-0.55
223888_s_at	LARS	leucyl-tRNA synthetase	-0.53
219927_at	FCF1	FCF1 small subunit (SSU) processome component homolog (S. cerevisiae)	-0.53
240690_at	NA	NA	-0.53
235588_at	ESCO2	establishment of cohesion 1 homolog 2 (S. cerevisiae)	-0.52
223481_s_at	MRPL47	mitochondrial ribosomal protein L47	-0.52
1554520_at	LOC283861	hypothetical locus LOC283861	-0.51
1564381_s_at	NA	NA	-0.51
231640_at	LYRM5	LYR motif containing 5	-0.51
210733_at	TRAM1	translocation associated membrane protein 1	-0.51
1556082_a_at	NA	NA	-0.51
211022_s_at	ATRX	alpha thalassemia/mental retardation syndrome X-linked (RAD54 homolog, S. cerevisiae)	-0.51
213747_at	AZIN1	antizyme inhibitor 1	-0.50
1555106_a_at	CTDSPL2	CTD (carboxy-terminal domain, RNA polymerase II, polypeptide A) small phosphatase like 2	-0.50

Table S4.13 Top probe sets up-regulated by treatment with DMSO, relative to 6 hr untreated sample. Probe ID is identifier for probe set from Affymetrix HGU133 Plus 2.0 GeneChip®. Values shown are Log_2 fold-changes (LFC of 1 = 2-fold change). Requirement for LFC ≥ 0.5 omitted other values.

Probe ID	Gene Symbol	Gene Name	LFC
217544_at	LOC729806	similar to hCG1725380	0.78
231933_at	MARCH8	membrane-associated ring finger (C3HC4) 8	0.65
238336_s_at	DNAJC21	DnaJ (Hsp40) homolog, subfamily C, member 21	0.62
215339_at	NKTR	natural killer-tumor recognition sequence	0.57
205637_s_at	SH3GL3	SH3-domain GRB2-like 3	0.56
231343_at	LOC647131	hypothetical LOC647131	0.52
228937_at	C13orf31	chromosome 13 open reading frame 31	0.51
240690_at	NA	NA	0.51
231035_s_at	OTUD1	OTU domain containing 1	0.50

Table S4.14 Top probe sets down-regulated by treatment with DMSO, relative to 6 hr untreated sample. Probe ID is identifier for probe set from Affymetrix HGU133 Plus 2.0 GeneChip®. Values shown are Log_2 fold-changes (LFC of 1 = 2-fold change). Requirement for LFC ≥ 0.5 omitted other values.

Probe ID	Gene Symbol	Gene Name	LFC
207247_s_at	ZFY	zinc finger protein, Y-linked	-0.83
235729_at	ZNF514	zinc finger protein 514	-0.81
1563571_at	LOC285463	hypothetical protein LOC285463	-0.74
235801_at	NA	NA	-0.72
240574_at	NA	NA	-0.71
1554103_at	NA	NA	-0.68
227720_at	ANKRD13B	ankyrin repeat domain 13B	-0.62
1569552_at	PTPN18	protein tyrosine phosphatase, non-receptor type 18 (brain-derived)	-0.62
1557170_at	NEK8	NIMA (never in mitosis gene a)- related kinase 8	-0.60
213758_at	COX4I1	cytochrome c oxidase subunit IV isoform 1	-0.59
209386_at	TM4SF1	transmembrane 4 L six family member 1	-0.58
219996_at	ASB7	ankyrin repeat and SOCS box-containing 7	-0.51
241352_at	NA	NA	-0.51
226419_s_at	SFRS1	splicing factor, arginine/serine-rich 1	-0.50
1557701_s_at	POLH	polymerase (DNA directed), eta	-0.50

Table S4.15 Top probe sets up-regulated by 6 hr incubation in fresh media relative to cells isolated at treatment time. Probe ID is identifier for probe set from Affymetrix HGU133 Plus 2.0 GeneChip®. Values shown are Log_2 fold-changes (LFC of 1 = 2-fold change). Requirement for LFC ≥ 0.5 omitted other values.

Probe ID	Gene Symbol	Gene Name	LFC
1558148_x_at	FLJ90757	hypothetical protein LOC440465	0.63
211833_s_at	BAX	BCL2-associated X protein	0.61
201340_s_at	ENC1	ectodermal-neural cortex (with BTB-like domain)	0.60
212901_s_at	CSTF2T	cleavage stimulation factor, 3' pre-RNA, subunit 2, 64kDa, tau variant	0.56
225831_at	LUZP1	leucine zipper protein 1	0.53
224387_at	COMMD5	COMM domain containing 5	0.52

Table S4.16 Top probe sets down-regulated by 6 hr incubation in fresh media relative to cells isolated at treatment time. Probe ID is identifier for probe set from Affymetrix HGU133 Plus 2.0 GeneChip®. Values shown are Log_2 fold-changes (LFC of 1 = 2-fold change). Requirement for LFC ≥ 0.5 omitted some values from the top 50 list.

Probe ID	Gene Symbol	Gene Name	LFC
239493_at	LOC100127893	similar to ribosomal protein L7	-1.06
1569664_at	NA	NA	-0.82
226444_at	NA	NA	-0.81
239091_at	NA	NA	-0.79
205841_at	JAK2	Janus kinase 2 (a protein tyrosine kinase)	-0.77
239014_at	CCAR1	cell division cycle and apoptosis regulator 1	-0.76
220946_s_at	SETD2	SET domain containing 2	-0.72
1568817_at	NA	NA	-0.71
229246_at	FLJ44342	hypothetical LOC645460	-0.71
240105_at	NA	NA	-0.70
1556678_a_at	NA	NA	-0.70
232740_at	MCM3APAS	minichromosome maintenance complex component 3 associated protein antisense	-0.69
229899_s_at	C20orf199	chromosome 20 open reading frame 199	-0.68
221015_s_at	CDADC1	cytidine and dCMP deaminase domain containing 1	-0.68
219171_s_at	ZNF236	zinc finger protein 236	-0.67
230241_at	NA	NA	-0.66
1570227_at	NA	NA	-0.66
228506_at	NSMCE4A	non-SMC element 4 homolog A (S. cerevisiae)	-0.65
210425_x_at	GOLGA8A	golgi autoantigen, golgin subfamily a, 8A	-0.64
239372_at	NA	NA	-0.63
228047_at	RPL30	ribosomal protein L30	-0.61
208798_x_at	GOLGA8A	golgi autoantigen, golgin subfamily a, 8A	-0.61
239653_at	NA	NA	-0.61
221103_s_at	WDR52	WD repeat domain 52	-0.59
218978_s_at	SLC25A37	solute carrier family 25, member 37	-0.58

Probe ID	Gene Symbol	Gene Name	LFC
238299_at	NA	NA	-0.57
236887_at	KIN	KIN, antigenic determinant of recA protein homolog (mouse)	-0.57
225949_at	NRBP2	nuclear receptor binding protein 2	-0.57
225496_s_at	SYTL2	synaptotagmin-like 2	-0.57
1556035_s_at	ZNF207	zinc finger protein 207	-0.57
203788_s_at	SEMA3C	sema domain, immunoglobulin domain (Ig), short basic domain, secreted, (semaphorin) 3C	-0.56
227383_at	LOC727820	hypothetical protein LOC727820	-0.56
215029_at	NA	NA	-0.56
205122_at	TMEFF1	transmembrane protein with EGF-like and two follistatin-like domains 1	-0.56
235288_at	NA	NA	-0.55
224336_s_at	DUSP16	dual specificity phosphatase 16	-0.54
1554161_at	SLC25A27	solute carrier family 25, member 27	-0.53
1561961_at	DKFZp686A1627	putative PHD finger protein 2 pseudogene	-0.53
207105_s_at	PIK3R2	phosphoinositide-3-kinase, regulatory subunit 2 (beta)	-0.53
212980_at	USP34	ubiquitin specific peptidase 34	-0.52
221778_at	JHDM1D	jumonji C domain containing histone demethylase 1 homolog D (S. cerevisiae)	-0.52
1563259_at	NA	NA	-0.52
222040_at	LOC728844	hypothetical LOC728844	-0.51
230742_at	RBM5	RNA binding motif protein 5	-0.51
236224_at	RIT1	Ras-like without CAAX 1	-0.51
212913_at	C6orf26	chromosome 6 open reading frame 26	-0.50
206038_s_at	NR2C2	nuclear receptor subfamily 2, group C, member 2	-0.50

Table S4.17 Probe sets more greatly up-regulated by 5 μM 11β treatment than by 5 μM 11β-dimethoxy treatment. Probe ID is identifier for probe set from Affymetrix HGU133 Plus 2.0 GeneChip®. Values shown are Log_2 fold-changes (LFC of 1 = 2-fold change). For these probe sets, the difference in expression level between 11β and 11β-dimethoxy (di) is greater than ~1.74-fold (ΔLFC ≥ 0.8), p-val for 11β (relative to DMSO) < 0.05, and 11β LFC ≥ 0.5. Gray cells indicate p-val ≥ 0.05.

Probe Set ID	Gene Symbol	Gene Name	11β	Di
221577_x_at	GDF15	growth differentiation factor 15	3.48	2.08
209383_at	DDIT3	DNA-damage-inducible transcript 3	3.46	1.71
215209_at	SEC24D	SEC24 related gene family, member D (S. cerevisiae)	2.75	1.36
225956_at	C5orf41	chromosome 5 open reading frame 41	2.35	1.42
242088_at	KLHL24	kelch-like 24 (Drosophila)	2.34	1.26
203725_at	GADD45A	growth arrest and DNA-damage-inducible, alpha	2.19	1.22
210587_at	INHBE	inhibin, beta E	2.16	0.53
219270_at	CHAC1	ChaC, cation transport regulator homolog 1 (E. coli)	2.02	0.90
202766_s_at	FBN1	fibrillin 1	2.02	0.98
238320_at	TncRNA	trophoblast-derived noncoding RNA	2.01	0.87
223195_s_at	SESN2	sestrin 2	1.97	0.95
1554980_a_at	ATF3	activating transcription factor 3	1.85	0.43
203438_at	STC2	stanniocalcin 2	1.78	0.78
207001_x_at	TSC22D3	TSC22 domain family, member 3	1.76	0.85
221085_at	TNFSF15	tumor necrosis factor (ligand) superfamily, member 15	1.74	0.30
201925_s_at	CD55	CD55 molecule, decay accelerating factor for complement (Cromer blood group)	1.68	0.25
213672_at	MARS	methionyl-tRNA synthetase	1.62	0.80
216985_s_at	STX3	syntaxin 3	1.60	0.44
202146_at	IFRD1	interferon-related developmental regulator 1	1.57	0.53
218651_s_at	LARP6	La ribonucleoprotein domain family, member 6	1.54	0.31
202284_s_at	CDKN1A	cyclin-dependent kinase inhibitor 1A (p21, Cip1)	1.47	0.16
212907_at	SLC30A1	solute carrier family 30 (zinc transporter), member 1	1.45	0.54

Probe Set ID	Gene Symbol	Gene Name	11β	Di
213629_x_at	MT1F	metallothionein 1F	1.37	0.44
237054_at	ENPP5	ectonucleotide pyrophosphatase/phosphodiesterase 5 (putative function)	1.36	0.45
1553622_a_at	FSIP1	fibrous sheath interacting protein 1	1.32	0.46
208935_s_at	LGALS8	lectin, galactoside-binding, soluble, 8	1.32	0.36
208933_s_at	LGALS8	lectin, galactoside-binding, soluble, 8	1.30	0.48
201236_s_at	BTG2	BTG family, member 2	1.29	0.30
1559517_a_at	SPIRE1	spire homolog 1 (Drosophila)	1.28	-0.07
213112_s_at	SQSTM1	sequestosome 1	1.28	0.34
1558846_at	PNLIPRP3	pancreatic lipase-related protein 3	1.22	0.35
224336_s_at	DUSP16	dual specificity phosphatase 16	1.19	0.36
226675_s_at	MALAT1	metastasis associated lung adenocarcinoma transcript 1 (non-protein coding)	1.16	0.27
220622_at	LRRC31	leucine rich repeat containing 31	1.08	0.08
221841_s_at	KLF4	Kruppel-like factor 4 (gut)	1.03	0.17
208328_s_at	MEF2A	myocyte enhancer factor 2A	1.01	0.17
1555606_a_at	GDPD1	glycerophosphodiester phosphodiesterase domain containing 1	0.96	0.12
226404_at	RBM39	RNA binding motif protein 39	0.94	0.12
204286_s_at	PMAIP1	phorbol-12-myristate-13-acetate-induced protein 1	0.86	-0.04
203504_s_at	ABCA1	ATP-binding cassette, sub-family A (ABC1), member 1	0.85	-0.04
215719_x_at	FAS	Fas (TNF receptor superfamily, member 6)	0.69	-0.60
205386_s_at	MDM2	Mdm2 p53 binding protein homolog (mouse)	0.58	-0.24
237737_at	LOC727770	similar to ankyrin repeat domain 20 family, member A1	0.57	-0.25
203409_at	DDB2	damage-specific DNA binding protein 2, 48kDa	0.55	-0.25

Table S4.18 Probe sets more greatly down-regulated by 5 μM 11β treatment than by 5 μM 11β-dimethoxy treatment. Probe ID is identifier for probe set from Affymetrix HGU133 Plus 2.0 GeneChip®. Values shown are Log_2 fold-changes (LFC of -1 = 2-fold change). For these probe sets, the difference in expression level between 11β and 11β-dimethoxy (Di) is greater than ~1.74-fold (ΔLFC ≥ 0.8), p-val for 11β (relative to DMSO) < 0.05, and 11β LFC ≤ 0.5. Gray cells indicate p-val ≥ 0.05.

Probe Set ID	Gene Symbol	Gene Name	11β	Di
220302_at	MAK	male germ cell-associated kinase	-0.50	0.38
226811_at	FAM46C	family with sequence similarity 46, member C	-0.64	0.34
204560_at	FKBP5	FK506 binding protein 5	-0.67	0.36
204826_at	CCNF	cyclin F	-0.92	0.07
228252_at	PIF1	PIF1 5'-to-3' DNA helicase homolog (S. cerevisiae)	-0.94	-0.04
208937_s_at	ID1	inhibitor of DNA binding 1, dominant negative helix-loop-helix protein	-1.07	-0.25
231892_at	C9orf100	chromosome 9 open reading frame 100	-1.13	-0.30
1554101_a_at	TMTC4	transmembrane and tetratricopeptide repeat containing 4	-1.22	-0.16
229310_at	KLHL29	kelch-like 29 (Drosophila)	-1.22	-0.33
1554036_at	ZBTB24	zinc finger and BTB domain containing 24	-1.47	-0.50
207038_at	SLC16A6	solute carrier family 16, member 6 (monocarboxylic acid transporter 7)	-1.60	-0.52
227048_at	LAMA1	laminin, alpha 1	-1.70	-0.48
226064_s_at	DGAT2	diacylglycerol O-acyltransferase homolog 2 (mouse)	-2.14	-1.32

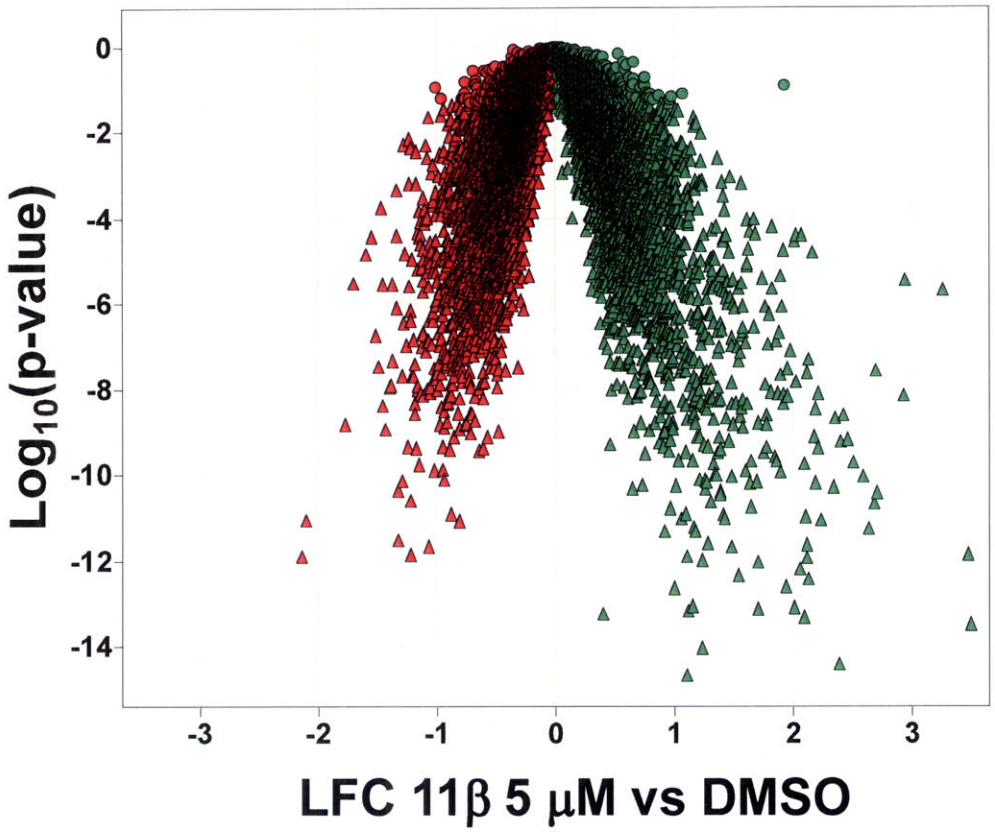

Figure S4.1 Volcano plot for 5 μM 11β compared to DMSO. Each point is a probe set, displayed as the relationship between the Log_2 fold change (LFC 1 = 2-fold change) on the x-axis and the Log_{10} of the p-value. Green points are up-regulated relative to DMSO, while red points are down-regulated. Circles are points with p-value ≥ 0.05, while triangles have p-value < 0.05. As such, significance of comparison increases as points approach the bottom of the graph while magnitude change increases as they spread from the center, creating what looks like a volcano.

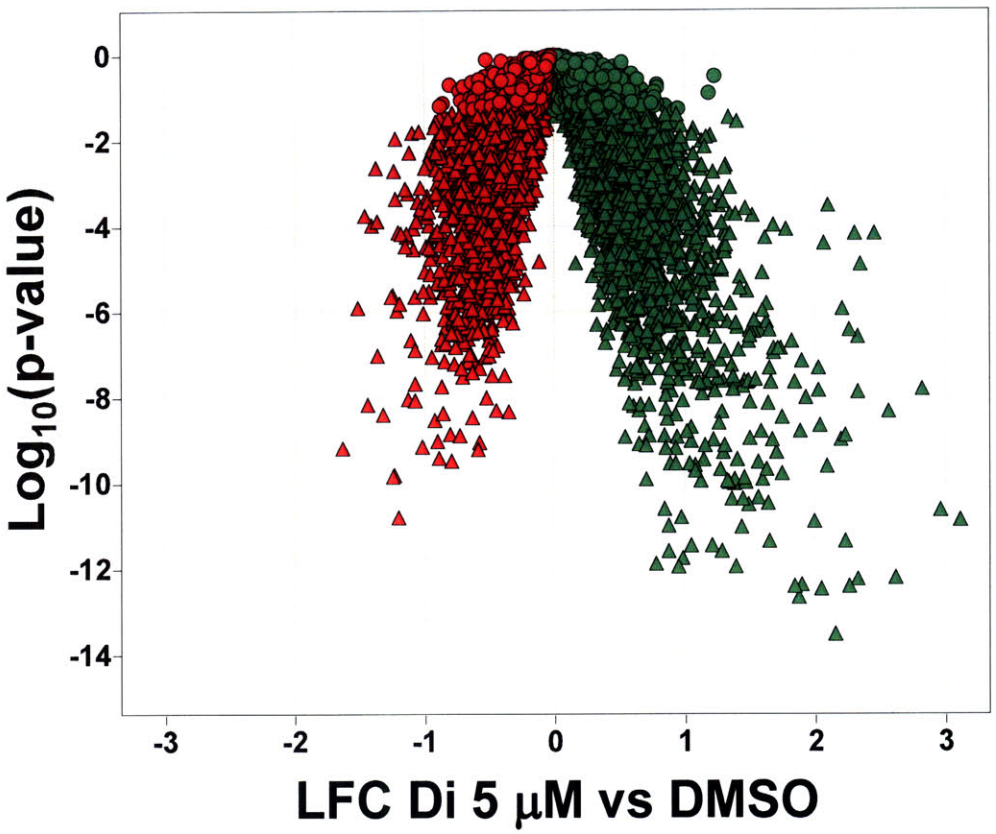

Figure S4.2 Volcano plot for 5 μM 11β-dimethoxy compared to DMSO. Each point is a probe set, displayed as the relationship between the Log_2 fold change (LFC 1 = 2-fold change) on the x-axis and the Log_{10} of the p-value. Green points are up-regulated relative to DMSO, while red points are down-regulated. Circles are points with p-value ≥ 0.05, while triangles have p-value < 0.05. As such, significance of comparison increases as points approach the bottom of the graph while magnitude change increases as they spread from the center, creating what looks like a volcano.

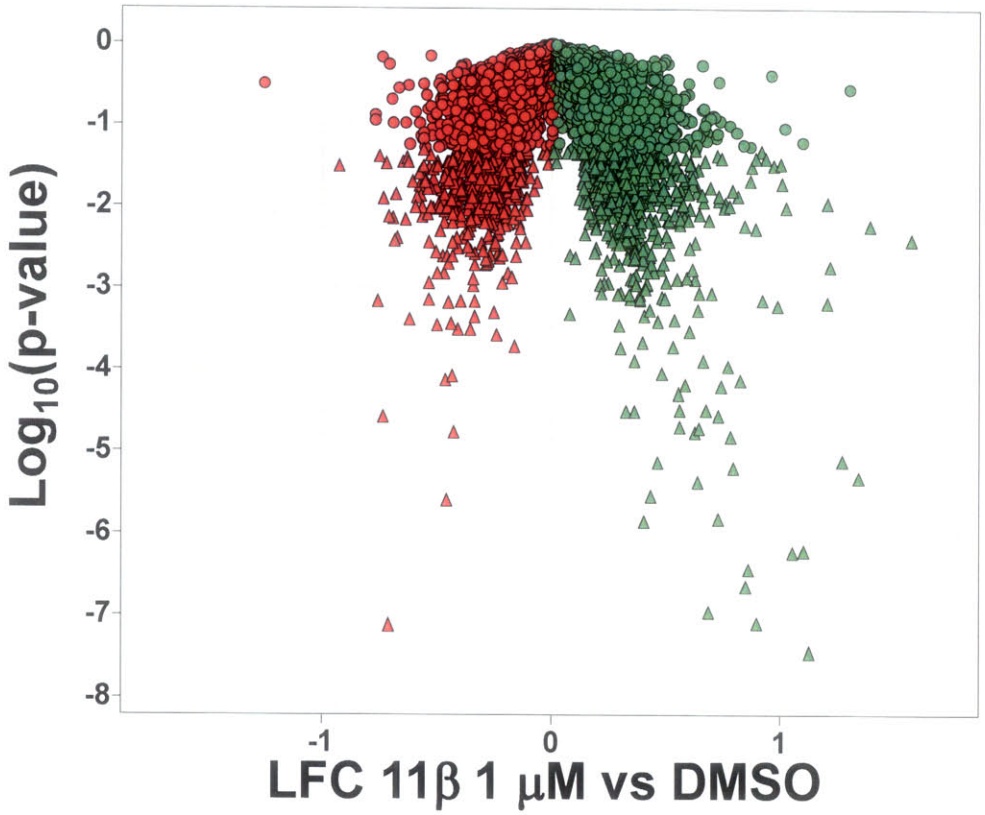

Figure S4.3 Volcano plot for 1 μM 11β compared to DMSO. Each point is a probe set, displayed as the relationship between the Log_2 fold change (LFC 1 = 2-fold change) on the x-axis and the Log_{10} of the p-value. Green points are up-regulated relative to DMSO, while red points are down-regulated. Circles are points with p-value ≥ 0.05, while triangles have p-value < 0.05. As such, significance of comparison increases as points approach the bottom of the graph while magnitude change increases as they spread from the center, creating what looks like a volcano.

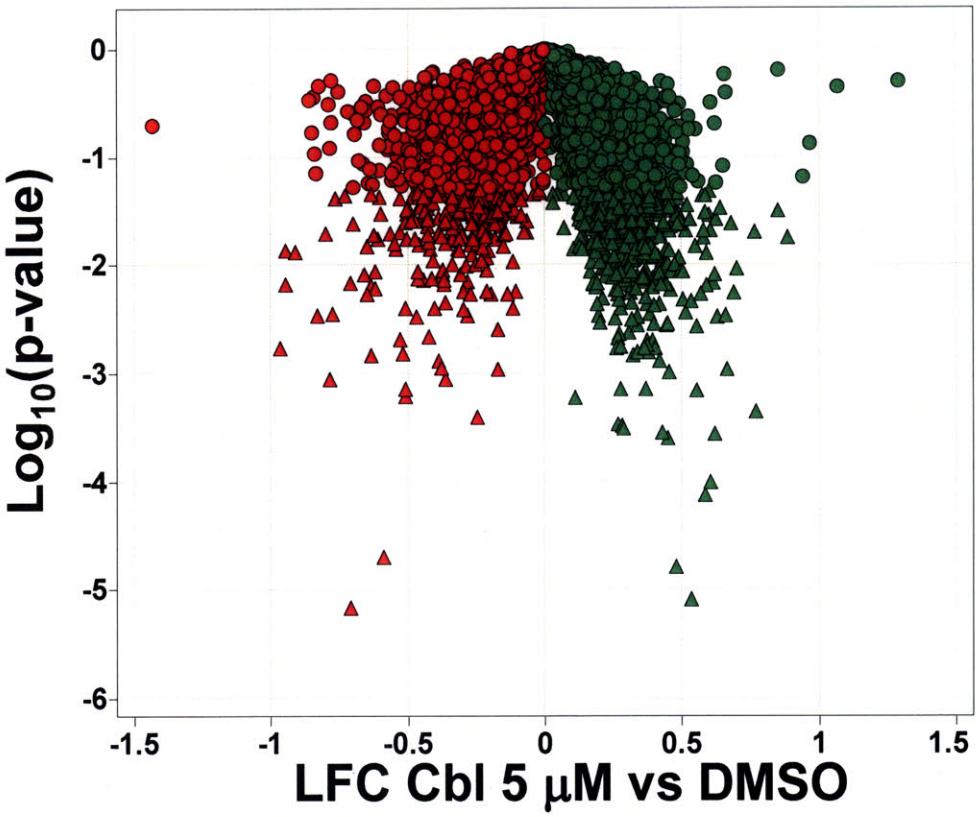

Figure S4.4 Volcano plot for 5 μM chlorambucil (Cbl) compared to DMSO. Each point is a probe set, displayed as the relationship between the Log_2 fold change (LFC 1 = 2-fold change) on the x-axis and the Log_{10} of the p-value. Green points are up-regulated relative to DMSO, while red points are down-regulated. Circles are points with p-value ≥ 0.05, while triangles have p-value < 0.05. As such, significance of comparison increases as points approach the bottom of the graph while magnitude change increases as they spread from the center, creating what looks like a volcano.

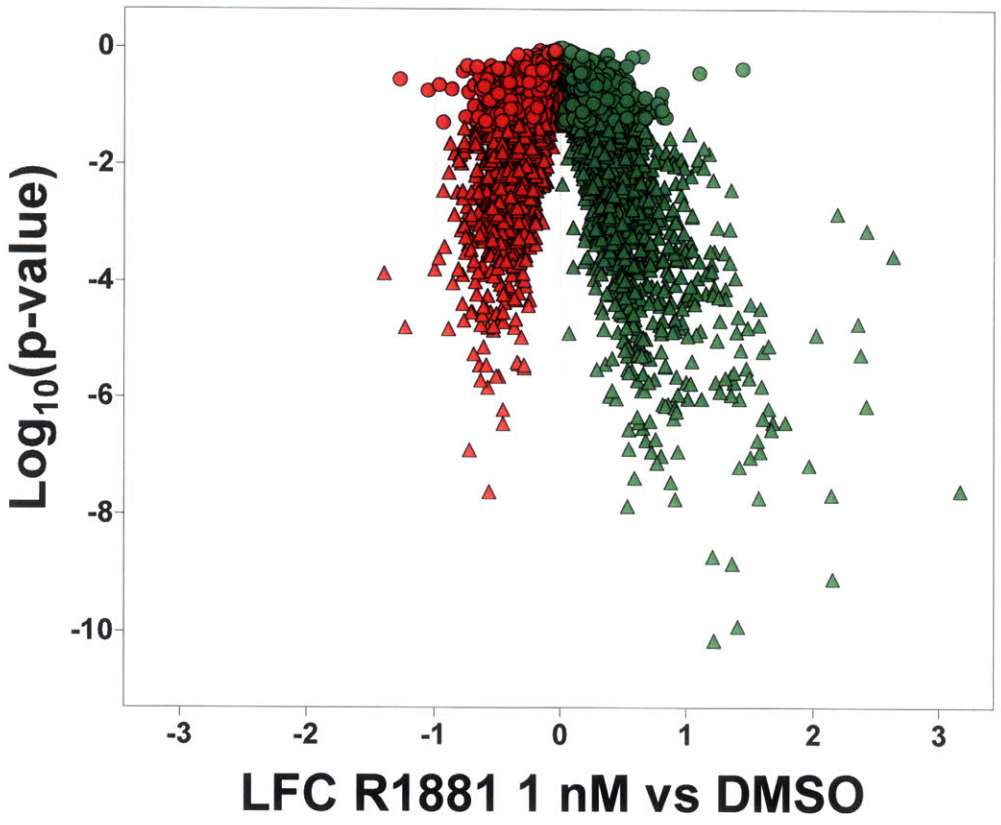

Figure S4.5 Volcano plot for 1 nM R1881 compared to DMSO. Each point is a probe set, displayed as the relationship between the Log_2 fold change (LFC 1 = 2-fold change) on the x-axis and the Log_{10} of the p-value. Green points are up-regulated relative to DMSO, while red points are down-regulated. Circles are points with p-value ≥ 0.05, while triangles have p-value < 0.05. As such, significance of comparison increases as points approach the bottom of the graph while magnitude change increases as they spread from the center, creating what looks like a volcano.

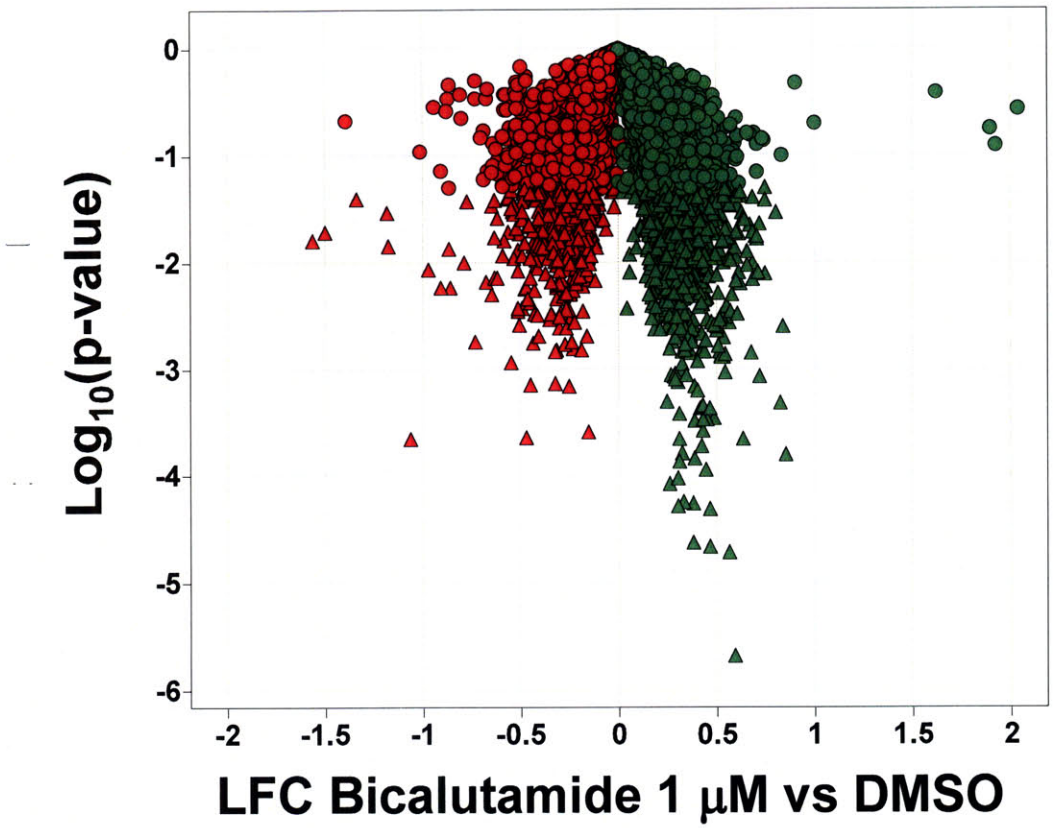

Figure S4.6 Volcano plot for 1 μM bicalutamide compared to DMSO. Each point is a probe set, displayed as the relationship between the Log_2 fold change (LFC 1 = 2-fold change) on the x-axis and the Log_{10} of the p-value. Green points are up-regulated relative to DMSO, while red points are down-regulated. Circles are points with p-value ≥ 0.05, while triangles have p-value < 0.05. As such, significance of comparison increases as points approach the bottom of the graph while magnitude change increases as they spread from the center, creating what looks like a volcano.

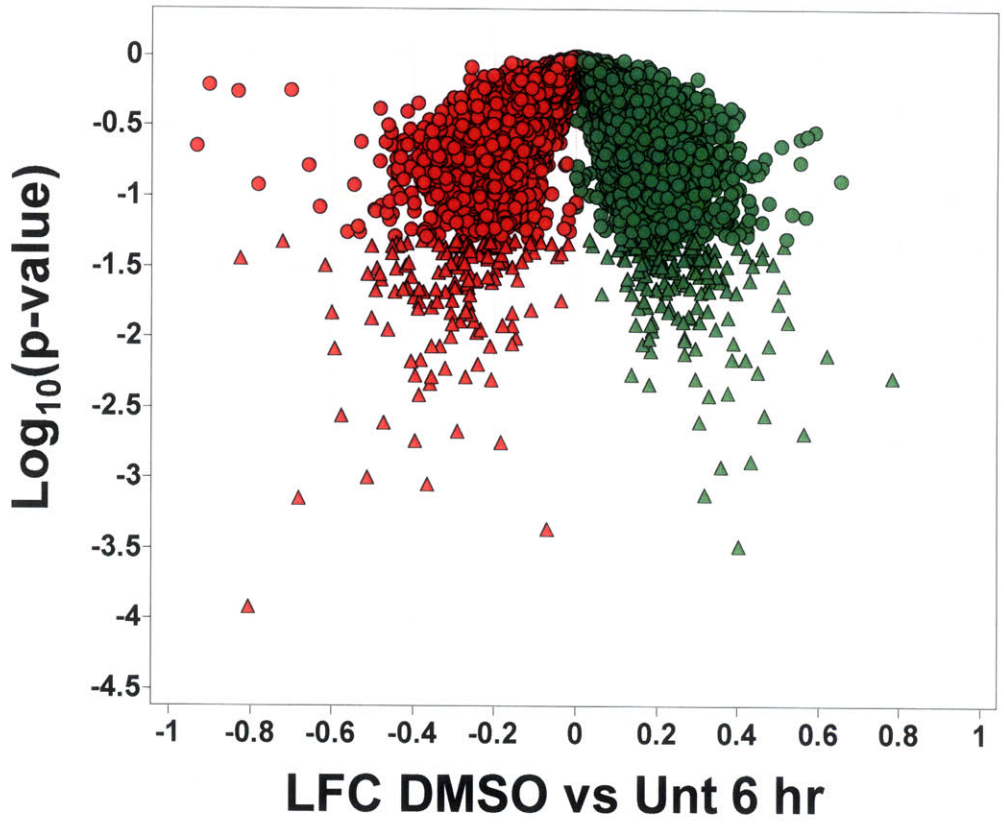

Figure S4.7 Volcano plot for DMSO compared to 6 hr untreated sample. Each point is a probe set, displayed as the relationship between the Log_2 fold change (LFC 1 = 2-fold change) on the x-axis and the Log_{10} of the p-value. Green points are up-regulated relative to DMSO, while red points are down-regulated. Circles are points with p-value ≥ 0.05, while triangles have p-value < 0.05. As such, significance of comparison increases as points approach the bottom of the graph while magnitude change increases as they spread from the center, creating what looks like a volcano.

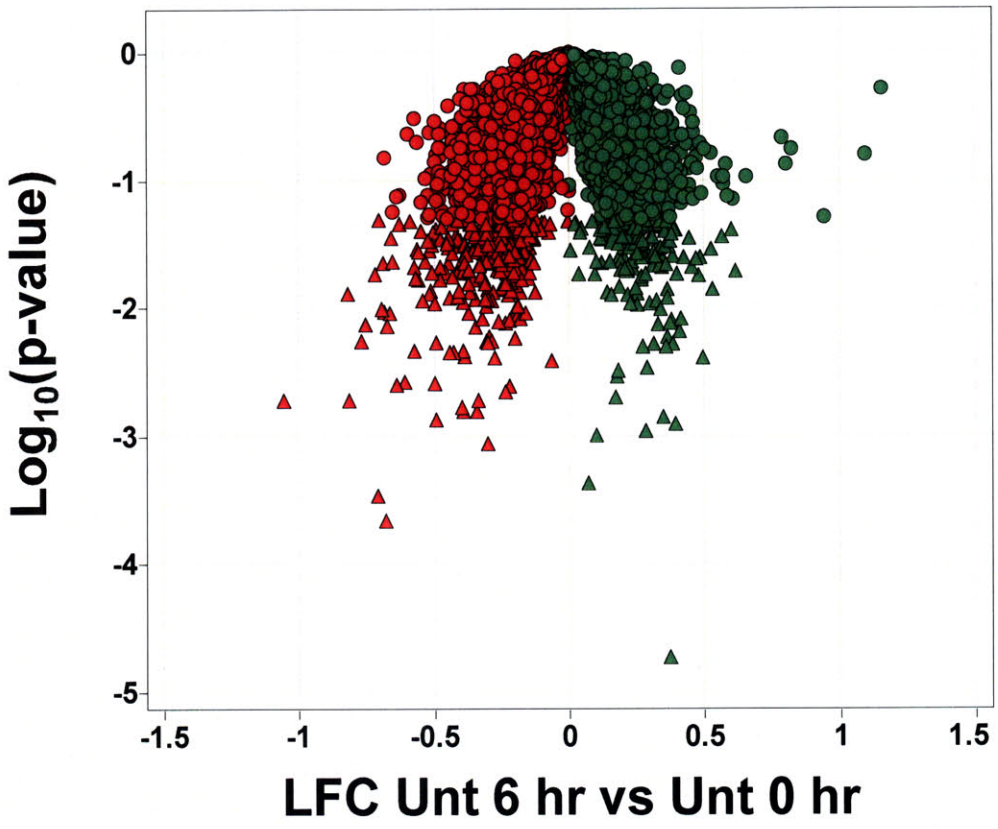

Figure S4.8 Volcano plot for 6 hr untreated sample compared to sample collected at treatment time. Each point is a probe set, displayed as the relationship between the Log_2 fold change (LFC 1 = 2-fold change) on the x-axis and the Log_{10} of the p-value. Green points are up-regulated relative to DMSO, while red points are down-regulated. Circles are points with p-value ≥ 0.05, while triangles have p-value < 0.05. As such, significance of comparison increases as points approach the bottom of the graph while magnitude change increases as they spread from the center, creating what looks like a volcano.

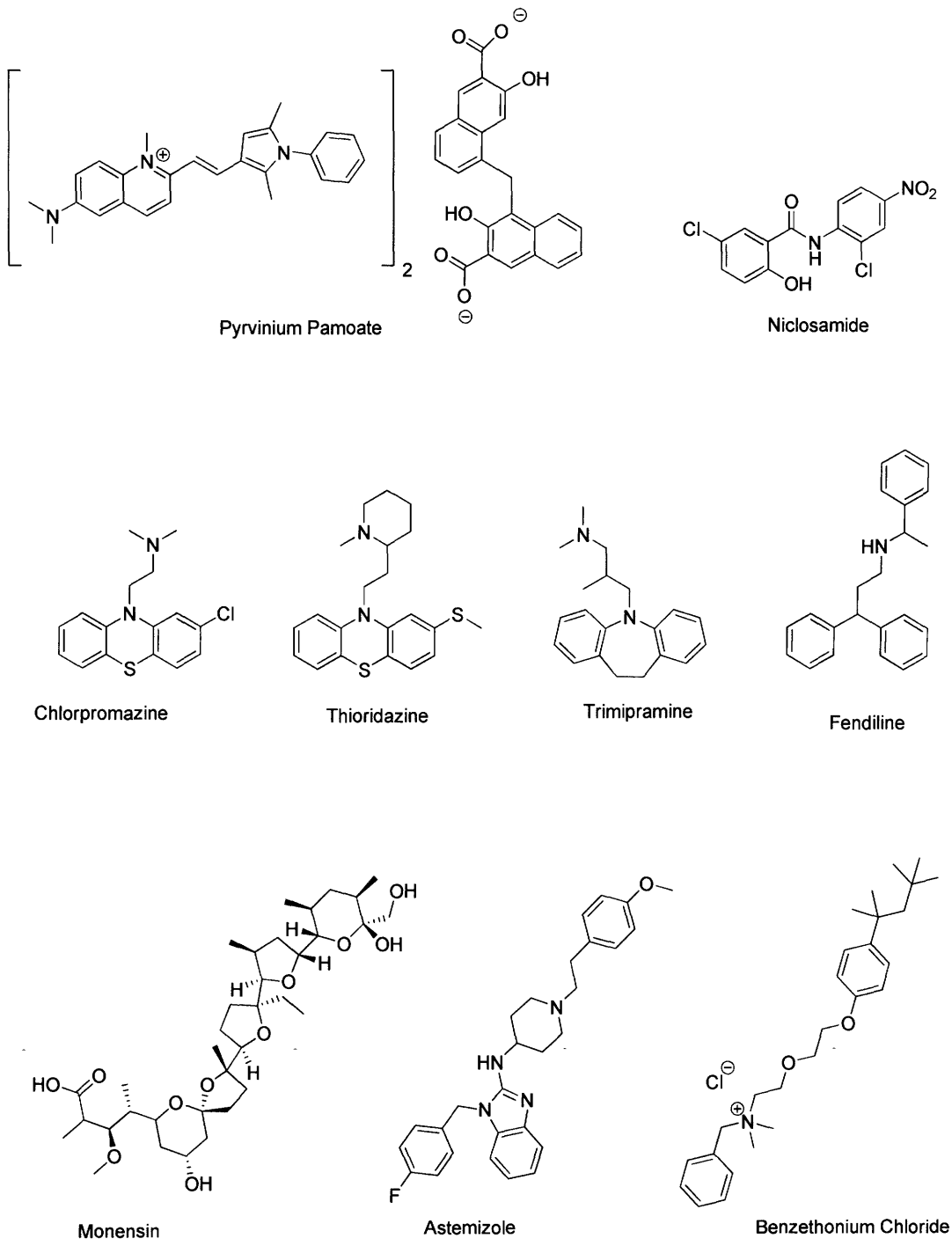

Figure S4.9 Structures of compounds identified by CMAP analysis as inducing similar transcriptional profile as 5 μM 11β.

References

Belfi, CA, Chatterjee, S, Gosky, DM, Berger, SJ & Berger, NA 1999, "Increased sensitivity of human colon cancer cells to DNA cross-linking agents after GRP78 up-regulation." *Biochemical and Biophysical Research Communications*, vol. 257, no. 2, pp. 361-8.

Benjamini, Y & Hochberg, Y 1995, "Controlling the False Discovery Rate: A Practical and Powerful Approach to Multiple Testing." *Journal of the Royal Statistical Society. Series B (Methodological)*, vol. 57, no. 1, pp. 289-300.

Berger, M, Strecker, HJ & Waelsch, H 1956, "Action of chlorpromazine on oxidative phosphorylation of liver and brain mitochondria." *Nature*, vol. 177, no. 4522, pp. 1234-5.

Berridge, MJ 1993, "Inositol trisphosphate and calcium signalling." *Nature*, vol. 361, no. 6410, pp. 315-25.

Breckenridge, DG, Germain, M, Mathai, JP, Nguyen, M & Shore, GC 2003, "Regulation of apoptosis by endoplasmic reticulum pathways." *Oncogene*, vol. 22, no. 53, pp. 8608-18.

Bush, KT, Goldberg, AL & Nigam, SK 1997, "Proteasome Inhibition Leads to a Heat-shock Response, Induction of Endoplasmic Reticulum Chaperones, and Thermotolerance." *J. Biol. Chem.*, vol. 272, no. 14, pp. 9086-9092.

Calfon, M, Zeng, H, Urano, F, Till, JH et al. 2002, "IRE1 couples endoplasmic reticulum load to secretory capacity by processing the XBP-1 mRNA." *Nature*, vol. 415, no. 6867, pp. 92-96.

Chatterjee, S, Hirota, H, Belfi, CA, Berger, SJ & Berger, NA 1997, "Hypersensitivity to DNA cross-linking agents associated with up-regulation of glucose-regulated stress protein GRP78." *Cancer Research*, vol. 57, no. 22, pp. 5112-6.

Chen, M, Chen, L & Chai, KX 2006, "Androgen regulation of prostasin gene expression is mediated by sterol-regulatory element-binding proteins and SLUG." *The Prostate*, vol. 66, no. 9, pp. 911-20.

Chen, X, Ding, Y, Liu, C, Mikhail, S & Yang, CS 2002, "Overexpression of glucose-regulated protein 94 (Grp94) in esophageal adenocarcinomas of a rat surgical model and humans." *Carcinogenesis*, vol. 23, no. 1, pp. 123-130.

Colgan, SM, Tang, D, Werstuck, GH & Austin, RC 2007, "Endoplasmic reticulum stress causes the activation of sterol regulatory element binding protein-2." *The International Journal of Biochemistry & Cell Biology*, vol. 39, no. 10, pp. 1843-51.

Corbett, EF, Oikawa, K, Francois, P, Tessier, DC et al. 1999, "Ca2+ Regulation of Interactions between Endoplasmic Reticulum Chaperones." *J. Biol. Chem.*, vol. 274, no. 10, pp. 6203-6211.

DiPaola, RS & Aisner, J 1999, "Overcoming bcl-2- and p53-mediated resistance in prostate cancer." *Seminars in Oncology*, vol. 26, no. 1 Suppl 2, pp. 112-116.

Fawcett, TW, Martindale, JL, Guyton, KZ, Hai, T & Holbrook, NJ 1999, "Complexes containing activating transcription factor (ATF)/cAMP-responsive-element-binding protein (CREB) interact with the CCAAT/enhancer-binding protein (C/EBP)-ATF composite site to regulate Gadd153 expression during the stress response." *The Biochemical Journal*, vol. 339 (Pt 1), pp. 135-41.

Fernandez, PM, Tabbara, SO, Jacobs, LK, Manning, FCR et al. 2000, "Overexpression of the glucose-regulated stress gene GRP78 in malignant but not benign human breast lesions." *Breast Cancer Research and Treatment*, vol. 59, no. 1, pp. 15-26.

Fornace, AJ, Alamo, I & Hollander, MC 1988, "DNA damage-inducible transcripts in mammalian cells." *Proceedings of the National Academy of Sciences of the United States of America*, vol. 85, no. 23, pp. 8800-8804.

Fribley, A, Zeng, Q & Wang, C 2004, "Proteasome Inhibitor PS-341 Induces Apoptosis through Induction of Endoplasmic Reticulum Stress-Reactive Oxygen Species in Head and Neck Squamous Cell Carcinoma Cells." *Mol. Cell. Biol.*, vol. 24, no. 22, pp. 9695-9704.

Gazit, G, Lu, J & Lee, AS 1999, "De-regulation of GRP stress protein expression in human breast cancer cell lines." *Breast Cancer Research and Treatment*, vol. 54, no. 2, pp. 135-46.

Gentleman, R, Carey, V, Bates, D, Bolstad, B et al. 2004, "Bioconductor: open software development for computational biology and bioinformatics." *Genome Biology*, vol. 5, no. 10, p. R80.

Ghosh, T, Bian, J, Short, A, Rybak, S & Gill, D 1991, "Persistent intracellular calcium pool depletion by thapsigargin and its influence on cell growth." *J. Biol. Chem.*, vol. 266, no. 36, pp. 24690-24697.

Goldstein, JL, Rawson, RB & Brown, MS 2002, "Mutant mammalian cells as tools to delineate the sterol regulatory element-binding protein pathway for feedback regulation of lipid synthesis." *Archives of Biochemistry and Biophysics*, vol. 397, no. 2, pp. 139-48.

Guardavaccaro, D, Corrente, G, Covone, F, Micheli, L et al. 2000, "Arrest of G1-S Progression by the p53-Inducible Gene PC3 Is Rb Dependent and Relies on the

Inhibition of Cyclin D1 Transcription." *Mol. Cell. Biol.*, vol. 20, no. 5, pp. 1797-1815.

Halleck, MM, Holbrook, NJ, Skinner, J, Liu, H & Stevens, JL 1997, "The molecular response to reductive stress in LLC-PK1 renal epithelial cells: coordinate transcriptional regulation of gadd153 and grp78 genes by thiols." *Cell Stress & Chaperones*, vol. 2, no. 1, pp. 31-40.

Harding, HP, Novoa, I, Zhang, Y, Zeng, H et al. 2000, "Regulated translation initiation controls stress-induced gene expression in mammalian cells." *Molecular Cell*, vol. 6, no. 5, pp. 1099-108.

Harper, JW, Adami, GR, Wei, N, Keyomarsi, K & Elledge, SJ 1993, "The p21 Cdk-interacting protein Cip1 is a potent inhibitor of G1 cyclin-dependent kinases." *Cell*, vol. 75, no. 4, pp. 805-16.

Heemers, H, Maes, B, Foufelle, F, Heyns, W et al. 2001, "Androgens stimulate lipogenic gene expression in prostate cancer cells by activation of the sterol regulatory element-binding protein cleavage activating protein/sterol regulatory element-binding protein pathway." *Molecular Endocrinology (Baltimore, Md.)*, vol. 15, no. 10, pp. 1817-28.

Hillier, SM 2005, "Novel genotoxins that target estrogen receptor- and androgen receptor- positive cancers : identification of DNA adducts, pharmacokinetics, and mechanism." Retrieved April 7, 2009, from http://dspace.mit.edu/handle/1721.1/32480

Hillier, SM, Marquis, JC, Zayas, B, Wishnok, JS et al. 2006, "DNA adducts formed by a novel antitumor agent 11{beta}-dichloro in vitro and in vivo." *Mol Cancer Ther*, vol. 5, no. 4, pp. 977-984.

Horton, JD, Goldstein, JL & Brown, MS 2002, "SREBPs: activators of the complete program of cholesterol and fatty acid synthesis in the liver." *The Journal of Clinical Investigation*, vol. 109, no. 9, pp. 1125-31.

Irizarry, RA, Hobbs, B, Collin, F, Beazer-Barclay, YD et al. 2003, "Exploration, normalization, and summaries of high density oligonucleotide array probe level data." *Biostatistics (Oxford, England)*, vol. 4, no. 2, pp. 249-64.

Kaufman, RJ 1999, "Stress signaling from the lumen of the endoplasmic reticulum: coordination of gene transcriptional and translational controls." *Genes & Development*, vol. 13, no. 10, pp. 1211-33.

Koumenis, C, Naczki, C, Koritzinsky, M, Rastani, S et al. 2002, "Regulation of protein synthesis by hypoxia via activation of the endoplasmic reticulum kinase PERK

and phosphorylation of the translation initiation factor eIF2alpha." *Molecular and Cellular Biology*, vol. 22, no. 21, pp. 7405-16.

Lamb, J 2007, "The Connectivity Map: a new tool for biomedical research." *Nat Rev Cancer*, vol. 7, no. 1, pp. 54-60.

Lamb, J, Crawford, ED, Peck, D, Modell, JW et al. 2006, "The Connectivity Map: Using Gene-Expression Signatures to Connect Small Molecules, Genes, and Disease." *Science*, vol. 313, no. 5795, pp. 1929-1935.

Lamb, J, Ramaswamy, S, Ford, HL, Contreras, B et al. 2003, "A mechanism of cyclin D1 action encoded in the patterns of gene expression in human cancer." *Cell*, vol. 114, no. 3, pp. 323-34.

Lange, Y & Steck, T 1994, "Cholesterol homeostasis. Modulation by amphiphiles." *J. Biol. Chem.*, vol. 269, no. 47, pp. 29371-29374.

Lee, A, Iwakoshi, NN & Glimcher, LH 2003, "XBP-1 regulates a subset of endoplasmic reticulum resident chaperone genes in the unfolded protein response." *Molecular and Cellular Biology*, vol. 23, no. 21, pp. 7448-59.

Lee, K, Tirasophon, W, Shen, X, Michalak, M et al. 2002, "IRE1-mediated unconventional mRNA splicing and S2P-mediated ATF6 cleavage merge to regulate XBP1 in signaling the unfolded protein response." *Genes & Development*, vol. 16, no. 4, pp. 452-66.

Li, C & Wong, WH 2001, "Model-based analysis of oligonucleotide arrays: Expression index computation and outlier detection." *Proceedings of the National Academy of Sciences of the United States of America*, vol. 98, no. 1, pp. 31-36.

Lodish, H & Kong, N 1990, "Perturbation of cellular calcium blocks exit of secretory proteins from the rough endoplasmic reticulum." *J. Biol. Chem.*, vol. 265, no. 19, pp. 10893-10899.

Lodish, H, Kong, N & Wikstrom, L 1992, "Calcium is required for folding of newly made subunits of the asialoglycoprotein receptor within the endoplasmic reticulum." *J. Biol. Chem.*, vol. 267, no. 18, pp. 12753-12760.

MacDonald, ML, Lamerdin, J, Owens, S, Keon, BH et al. 2006, "Identifying off-target effects and hidden phenotypes of drugs in human cells." *Nat Chem Biol*, vol. 2, no. 6, pp. 329-337.

Marciniak, SJ, Yun, CY, Oyadomari, S, Novoa, I et al. 2004, "CHOP induces death by promoting protein synthesis and oxidation in the stressed endoplasmic reticulum." *Genes & Development*, vol. 18, no. 24, pp. 3066-77.

Marquis, JC, Hillier, SM, Dinaut, AN, Rodrigues, D et al. 2005, "Disruption of gene expression and induction of apoptosis in prostate cancer cells by a DNA-damaging agent tethered to an androgen receptor ligand." *Chemistry & Biology*, vol. 12, no. 7, pp. 779-87.

McCullough, KD, Martindale, JL, Klotz, LO, Aw, TY & Holbrook, NJ 2001, "Gadd153 sensitizes cells to endoplasmic reticulum stress by down-regulating Bcl2 and perturbing the cellular redox state." *Molecular and Cellular Biology*, vol. 21, no. 4, pp. 1249-59.

McDonnell, TJ, Troncoso, P, Brisbay, SM, Logothetis, C et al. 1992, "Expression of the Protooncogene bcl-2 in the Prostate and Its Association with Emergence of Androgen-independent Prostate Cancer." *Cancer Res*, vol. 52, no. 24, pp. 6940-6944.

Moncur, JT, Park, JP, Memoli, VA, Mohandas, TK & Kinlaw, WB 1998, "The "Spot 14" gene resides on the telomeric end of the 11q13 amplicon and is expressed in lipogenic breast cancers: implications for control of tumor metabolism." *Proceedings of the National Academy of Sciences of the United States of America*, vol. 95, no. 12, pp. 6989-94.

Nelson, PS, Clegg, N, Arnold, H, Ferguson, C et al. 2002, "The program of androgen-responsive genes in neoplastic prostate epithelium." *Proceedings of the National Academy of Sciences of the United States of America*, vol. 99, no. 18, pp. 11890-11895.

Ngan, S, Stronach, EA, Photiou, A, Waxman, J et al. "Microarray coupled to quantitative RT-PCR analysis of androgen-regulated genes in human LNCaP prostate cancer cells." *Oncogene*.

Obeng, EA, Carlson, LM, Gutman, DM, Harrington, WJ et al. 2006, "Proteasome inhibitors induce a terminal unfolded protein response in multiple myeloma cells." *Blood*, vol. 107, no. 12, pp. 4907-4916.

Pandini, G, Genua, M, Frasca, F, Vigneri, R & Belfiore, A 2009, "Sex steroids upregulate the IGF-1R in prostate cancer cells through a nongenotropic pathway." *Annals of the New York Academy of Sciences*, vol. 1155, pp. 263-7.

Prozialeck, WC & Weiss, B 1982, "Inhibition of calmodulin by phenothiazines and related drugs: structure-activity relationships." *The Journal of Pharmacology and Experimental Therapeutics*, vol. 222, no. 3, pp. 509-16.

Radhakrishnan, A, Ikeda, Y, Kwon, HJ, Brown, MS & Goldstein, JL 2007, "Sterol-regulated transport of SREBPs from endoplasmic reticulum to Golgi: Oxysterols block transport by binding to Insig." *Proceedings of the National Academy of Sciences*, vol. 104, no. 16, pp. 6511-6518.

Rao, RV, Castro-Obregon, S, Frankowski, H, Schuler, M et al. 2002, "Coupling Endoplasmic Reticulum Stress to the Cell Death Program. An Apaf-1 Independent Intrinsic Pathway." *J. Biol. Chem.*, vol. 277, no. 24, pp. 21836-21842.

Rouault, JP, Falette, N, Guéhenneux, F, Guillot, C et al. 1996, "Identification of BTG2, an antiproliferative p53-dependent component of the DNA damage cellular response pathway." *Nature Genetics*, vol. 14, no. 4, pp. 482-6.

Rozen, S & Skaletsky, HJ 2000, *Bioinformatics Methods and Protocols: Methods in Molecular Biology* S Krawetz & S Misener (eds), Humana Press, Totowa, NJ.

Shuda, M, Kondoh, N, Imazeki, N, Tanaka, K et al. 2003, "Activation of the ATF6, XBP1 and grp78 genes in human hepatocellular carcinoma: a possible involvement of the ER stress pathway in hepatocarcinogenesis." *Journal of Hepatology*, vol. 38, no. 5, pp. 605-14.

Smyth, G 2005, "limma: Linear Models for Microarray Data," in *Bioinformatics and Computational Biology Solutions Using R and Bioconductor*,pp. 397-420.

Song, MS, Park, YK, Lee, J & Park, K 2001, "Induction of Glucose-regulated Protein 78 by Chronic Hypoxia in Human Gastric Tumor Cells through a Protein Kinase C-{epsilon}/ERK/AP-1 Signaling Cascade." *Cancer Res*, vol. 61, no. 22, pp. 8322-8330.

Tong, M & Tai, HH 2000, "Induction of NAD(+)-linked 15-hydroxyprostaglandin dehydrogenase expression by androgens in human prostate cancer cells." *Biochemical and Biophysical Research Communications*, vol. 276, no. 1, pp. 77-81.

Wang, X, Lawson, B, Brewer, J, Zinszner, H et al. 1996, "Signals from the stressed endoplasmic reticulum induce C/EBP-homologous protein (CHOP/GADD153)." *Mol. Cell. Biol.*, vol. 16, no. 8, pp. 4273-4280.

Weinbach, EC & Garbus, J 1969, "Mechanism of action of reagents that uncouple oxidative phosphorylation." *Nature*, vol. 221, no. 5185, pp. 1016-8.

Weiss, B, Prozialeck, W, Cimino, M, Barnette, MS & Wallace, TL 1980, "Pharmacological regulation of calmodulin." *Annals of the New York Academy of Sciences*, vol. 356, pp. 319-45.

Wu, Y, Fabritius, M & Ip, C 2009, "Chemotherapeutic sensitization by endoplasmic reticulum stress: increasing the efficacy of taxane against prostate cancer." *Cancer Biology & Therapy*, vol. 8, no. 2, pp. 146-52.

Xu, LL, Shanmugam, N, Segawa, T, Sesterhenn, IA et al. 2000, "A novel androgen-regulated gene, PMEPA1, located on chromosome 20q13 exhibits high level expression in prostate." *Genomics*, vol. 66, no. 3, pp. 257-63.

Yabe, D, Brown, MS & Goldstein, JL 2002, "Insig-2, a second endoplasmic reticulum protein that binds SCAP and blocks export of sterol regulatory element-binding proteins." *Proceedings of the National Academy of Sciences of the United States of America*, vol. 99, no. 20, pp. 12753-8.

Yang, H, Chen, D, Cui, QC, Yuan, X & Dou, QP 2006, "Celastrol, a Triterpene Extracted from the Chinese "Thunder of God Vine," Is a Potent Proteasome Inhibitor and Suppresses Human Prostate Cancer Growth in Nude Mice." *Cancer Res*, vol. 66, no. 9, pp. 4758-4765.

Yang, H, Shi, G & Dou, QP 2007, "The Tumor Proteasome Is a Primary Target for the Natural Anticancer Compound Withaferin A Isolated from "Indian Winter Cherry"." *Mol Pharmacol*, vol. 71, no. 2, pp. 426-437.

Yang, T, Espenshade, PJ, Wright, ME, Yabe, D et al. 2002, "Crucial step in cholesterol homeostasis: sterols promote binding of SCAP to INSIG-1, a membrane protein that facilitates retention of SREBPs in ER." *Cell*, vol. 110, no. 4, pp. 489-500.

Ye, J, Rawson, RB, Komuro, R, Chen, X et al. 2000, "ER stress induces cleavage of membrane-bound ATF6 by the same proteases that process SREBPs." *Molecular Cell*, vol. 6, no. 6, pp. 1355-64.

Yoshida, H, Matsui, T, Yamamoto, A, Okada, T & Mori, K 2001, "XBP1 mRNA Is Induced by ATF6 and Spliced by IRE1 in Response to ER Stress to Produce a Highly Active Transcription Factor." *Cell*, vol. 107, no. 7, pp. 881-891.

Zhijin Wu, Rafael A . Irizarry, Robert Gentleman, Francisco Martinez-Murillo & Forrest Spencer 2008, "A Model-Based Background Adjustment for Oligonucleotide Expression Arrays."

Zinszner, H, Kuroda, M, Wang, X, Batchvarova, N et al. 1998, "CHOP is implicated in programmed cell death in response to impaired function of the endoplasmic reticulum." *Genes & Development*, vol. 12, no. 7, pp. 982–995.

Kyle David Proffitt
proffitt@mit.edu

Department of Chemistry
77 Massachusetts Ave.
Room 56-670
Cambridge, MA 02139
Tel: (617) 253-5772

EDUCATION

Massachusetts Institute of Technology, Cambridge, Mass.
Doctor of Philosophy Candidate: Biological Chemistry 2009 Expected
University of South Carolina (Honors College), Columbia, S.C.
Bachelor of Science in Chemistry; GPA 3.735/4.0 2002

RESEARCH EXPERIENCE

Massachusetts Institute of Technology **Cambridge, Mass.**
Departments of Chemistry and Biological Engineering 2002-Present
Advisor: Dr. John M. Essigmann
Proposed Thesis Title: "*Interaction of the Novel DNA Damaging Anticancer Agent 11β with the Androgen Receptor*"

- Demonstrated that the molecule 11β can cause AR phosphorylation, nuclear localization, and binding at the PSA promoter, while also inhibiting the N/C terminal interaction and activation of androgen-regulated genes caused by dihydrotestosterone
- Performed genome-wide analysis of transcription, identifying new effects of this compound on genes related to cell cycle progression, cholesterol biosynthesis, and unfolded protein response
- Synthesized a control compound with identical structure but with 10-fold reduced AR binding affinity to test for AR-dependent toxicity
- Gained proficiency in techniques of Western blotting, RT-PCR, mammalian cell culture, mouse xenograft models, siRNA, DNA microarray, molecular biology, and transcriptional reporter assays

University of South Carolina **Columbia, S.C.**
Department of Chemistry 2002
Advisor: Advisor: Dr. Brian A. Salvatore
Honors Thesis Title: "*Toward the Development of Synthetic Peptide Ion Channels*"

HONORS

MIT National Cancer Institute Training Grant (2003-2006)
MIT Presidential Fellow (2002)
Phi Beta Kappa (2002)
Golden Key National Honor Society (2002)
Harper Award: Highest GPA in Chemistry at USC (2002)

PROFESSIONAL AFFILIATIONS

American Association for Cancer Research
American Chemical Society

MANUSCRIPTS & PRESENTATIONS

Proffitt, K.D.; Essigmann, J.M.; Croy, R.G. Involvement of the Androgen Receptor in Toxicity of the DNA Damaging Agent 11β toward Prostate Cancer Cells. *In Preparation.*

Proffitt, K.D.; Fuangthong, M.; Fry, R.C.; Essigmann, J.M.; Croy, R.G. The Anticancer Agent 11β Elicits a Robust Transcriptional Response Including Altered Expression of Genes Involved in Cell Cycle Control, Cholesterol Biosynthesis, and the Unfolded Protein Response in Prostate Cancer Cells. *In Preparation.*

Kyle Proffitt, John C. Marquis, A. Nicole Dinaut, John M. Essigmann, Robert G. Croy, "Role of the Androgen Receptor in Toxicity of the Novel Anticancer Compound 11β," American Association for Cancer Research National Meeting, Washington, DC, March, 2006, Abstract #567.

Kyle Proffitt, Shawn M. Hillier, Mayuree Fuangthong, Rebecca Fry, John M. Essigmann, Robert G. Croy, "Interaction of the Novel DNA Damaging Anticancer Agent 11β with the Androgen Receptor," American Association for Cancer Research, Translational Cancer Medicine Series, Singapore, November 2007, Abstract #A22.